Keep Dementia in Mind, but Forget Memory Formation: Plasticity of the N-Methyl-D-Aspartate Receptor in Erythroid Cells and its Potential for the Treatment of Sickle Cell Anemia

---

Dissertation
zur
Erlangung der naturwissenschaftlichen Doktorwürde
(Dr. sc. nat.)
vorgelegt der
Mathematisch-naturwissenschaftlichen Fakultät
der
Universität Zürich
Von

Pascal Hänggi
von
Nunningen SO

Promotionskomitee

Prof. Dr. Max Gassmann (Vorsitz)
Dr. Jeroen Goede (Leitung der Dissertation)
Prof. Dr. David Nadal
Prof Dr. Ingolf Bernhardt
Dr. Anna Bogdanova
Dr. Oliver Speer
Dr. Markus Schmugge-Liner

Zürich, 2015

Table of contents

2. List of Abbreviations

ABD	Agonist-binding domain
AKT	Protein kinase B
BFU-e	Burst-forming unit-erythroids
BMP-4	Bone morphogenic protein-4
Ca^{2+}	Calcium
Ca^{2+}-CaM	Ca^{2+}-calmodulin
CaM K	Ca^{2+}/calmodulin-dependent protein kinase
CaM KII	CaM kinase II
CFU-e	Colony-forming unit-erythroids
CFU-GEMM	Colony-forming unit-granulocyte, erythrocyte, monocyte/macrophage, megakaryocyte
CREB	Cyclic-AMP response element binding protein
CTA	Clinical trial approval
CTD	Carboxyl-terminal domain
DAG	Diacylglycerol
DAPK-2	Death associated protein kinase-2
EPCs	Erythroid precursor cells
Epo	Erythropoietin
EpoR	Erythropoietin receptor
ER	Endoplasmic reticulum
Flt-3	Fms-like kinase-3
FOG-1	Friend of GATA-1
GCs	Glucocorticoids
GM-CSF	Colony-stimulating factor
Hb	Hemoglobin
HDAC	Histone deacetylase

HU	Hydroxyurea
IGF-1	Insulin-like growth factor-1
IL	Interleukin
IP_3	Inositol(1,4,5)P_3
JAK2	Janus kinase 2
Klf-1	Krüppel-like factor-1
k_{off}	Dissociation rate constant
NSCC	Non-selective cation channel
NMDAR	N-methyl-D-aspartate receptor
NO	Nitric oxide
NTD	Amino-terminal domain
PI3-kinase	Phosphatidylinositol 4,5-bisphosphate 3-kinase
PIP_2	Phosphatidylinositol 4,5-bisphosphate
PKC	Protein kinase C
PLC-ɣ1	Phospholipase C ɣ1
PoC	Proof of concept
Pu.1	Putative oncogene Spi-1
RBCs	Red blood cells
SCD	Sickle cell disease
STAT-5	Signal Transducer and Activator of Transcription-5
TDM	Transmembrane domain
TFs	Transcription factors
TRPC	Transient receptor potential channel
VCAM-1	Vascular cell-adhesion molecule-1
VDAC	Voltage-dependent anion channel

2. Summary

This project was based on a pilot study indicating that N-methyl-D-aspartate receptors (NMDARs) are expressed in rat erythroid precursor cells (EPCs) and present in both, circulating rat and human red blood cells (RBCs). Furthermore, assessment of this receptor's activity in RBCs of sickle cell disease (SCD) patients revealed that calcium (Ca^{2+}) overload is likely to be due to the pathological up-regulation of receptor abundance and activity in them. The present study was focused on the characterization of NMDARs on the molecular and functional level during erythropoietic maturation. EPCs of healthy humans and SCD patients were studied *ex vivo*. These findings were then bridged with the data obtained from the NMDARs in mature RBCs. The data revealed the changes in the NMDAR subunit composition mirrored by the change of the functional properties during differentiation. Functional NMDARs were shown to be required for survival of the erythroid precursor cells. They prevented cells from undergo apoptosis. In particular, this protecting effect was present at the proerythroblastic stage. Furthermore, no significant difference was observed in the expression of NMDAR subunits during differentiation of the precursor cells of healthy humans and SCD patients. However, in the circulating RBCs of asymptomatic patients, the number of active receptors exceeded that in cells of healthy donors by 5 to 10-fold. Inhibition of the receptors with pore-targeting antagonist Memantine substantially reduced the dehydration of RBCs and decreased the risk of sickle cell transformation. At the same time, EPCs of SCD patients were less sensitive to Memantine than proerythroblasts of healthy humans. These results suggested that inhibition of the NMDARs in RBCs of SCD patients may be beneficial. The reduction of Ca^{2+} uptake could decrease dehydration, increase RBC life span, and reduce the risk of thrombosis. Based on these findings, a clinical trial in which Memantine is to be used for treatment of a small cohort of patients is in preparation.

3. Zusammenfassung

Das Projekt basiert auf einer Pilotstudie die zeigte, dass N-methyl-D-aspartat Rezeptoren in erythropoietischen Zellen von Ratten und Menschen zu finden sind. Zudem wurde festgestellt, dass Patienten mit einer erhöhten intrazellulären Kalzium Konzentration in den Erythrozyten eine gesteigerte Aktivität der Rezeptoren aufweisen. Das Ziel der vorliegenden Arbeit war es, die Zusammensetzung und die Eigenschaften der Rezeptoren während der Erythropoiese von gesunden Probanden und Sichelzellenanämie-Patienten zu untersuchen. Die Ergebnisse wurden anschliessend mit den Daten über die Struktur und die Funktion des Rezeptors aus den roten Blutkörperchen verknüpft.

Die Ergebnisse zeigten, dass sich die Zusammensetzung der Rezeptoruntereinheiten während der Differenzierung der Erythrozyten verändert. Es konnte gezeigt werden, dass die N-methyl-D-aspartat Rezeptoren vor allem für das Überleben der Proerythroblasten und der basophilen Erythroblasten entscheidend sind. Ebenfalls wurde gezeigt, dass sich die Rezeptorexpression während der Erythropoiese in gesunden Probanden nicht massgeblich von Sichelzellenanämie-Patienten unterscheidet. Nichtsdestotrotz wurde klar beobachtet, dass in roten Blutkörperchen von Patienten die Anzahl von aktiven Rezeptoren fünf bis zehn mal grösser ist als im Vergleich zu gesunden Probanden. Die Inhibition dieser aktiven Rezeptoren mit dem Antagonisten Memantin bewirkte eine Reduktion der Dehydration und die damit assoziierte typischen Verformung der Erythrozyten. Gleichzeitig wurde gezeigt, dass die erythropoietischen Vorläuferzellen von Patienten, im Gegensatz zu den Zellen von gesunden Probanden, weniger sensitiv auf Rezeptorantagonisten reagieren.

Diese Ergebnisse legen nahe, dass sich die Inhibition dieser N-methyl-D-aspartat Rezeptoren in Erythrozyten positiv auf den Kalziumspiegel der roten Blutkörperchen auswirkt und damit nicht nur die Lebensdauer der Zellen, sondern auch die gesundheitliche Situation der Patient erheblich verbessert werden kann. Basierend auf diesen Resultaten ist eine klinische Studie mit den Rezeptorantagonisten Memantin als neue Therapie für Sichelzellenanämie in Planung.

4. Introduction

Red blood cells (RBCs) are responsible for oxygen transport in multiple invertebrate species and all vertebrates. [1] In humans, erythrocytes deliver oxygen highly efficient from the lungs to the hypoxic periphery. On the way back to the lungs, erythrocytes transport carbon dioxide as bicarbonate. In addition, RBCs have recently shown to play an active role in the regulation of vascular tone. In mammals, unlike other species, mature RBCs are deprived of essential organelles, including nucleus, endoplasmic reticulum (ER), and mitochondria. This terminal transformation of erythroid precursor cells (EPCs) occurs at the final stage of their differentiation, namely before reticulocytes are released into the circulation. Despite the inability to synthesize new proteins, these remarkable cells are able to tolerate stressful conditions such as shear stress, oxidative stress, and resist to a rather broad range of pH and osmolality change. [2] They can rapidly adapt to a harsh environment, which would seriously damage most other cells in the body. The adaption to those stress conditions is mediated by the release of several hormones (such as catecholamines, insulin, and erythropoietin), inflammatory factors, and gasotransmitters. These signals are sensed by the erythrocytes and trigger adjustments in cell volume, metabolic rate, production of free radicals (radical oxygen species: ROS) and antioxidants including nitric oxide (NO). Finally, those adjustments can modulate the oxygen carrying capacity of hemoglobin (Hb).

Recent studies revealed the presence of N-methyl-D-aspartate receptors (NMDARs) in membranes of rat and human RBCs making these cells responsive to changes in glutamate and glycine concentrations. [3-5] These ligand-gated ion channels exhibit a high permeability to Ca^{2+} ions. NMDARs are voltage, pH, mechano-sensitive and require both, glutamate and glycine for full activation. A change in any of these factors may generate Ca^{2+}-driven signals in erythroid cells. The number of NMDAR in circulating RBCs of rats and humans is low (4-30 per cell on average), which does not allow to investigate the subunit composition of the receptor, but enabling receptor activity measurements, however.

As most of the receptors, NMDARs appeared to be highly abundant in the Epo-dependent human erythroleukemia cell line UT7. [6] These data suggested that the NMDAR-driven signaling might be actively involved in the differentiation of erythroid cells. Thus, EPCs are the cells to choose for studies of the origin and diverse

physiological roles of any channels including the NMDA receptors in the formation of RBCs and their adaptation to varieties of conditions when in the circulation.

4.1. *Ex vivo* erythropoiesis systems

In adult humans around 10^{10} erythrocytes are produced and released into the circulation every hour. [7] Prenatal hematopoiesis appears first with precursor cells in the yolk sac, followed by the blood formation in the fetal liver and the spleen. During the prenatal development the bone marrow takes progressively over the entire RBCs production. Postnatal, the hematopoiesis occurs in the columna vertebralis, pelvis, sternum, ribs, tibia, and femur. While in adults, erythrocyte formation only takes place in the pelvis, cranium, vertebrae, and sternum. [8] Due to the poor accessibility of the EPCs for research, several *ex vivo* cell culture systems were developed within the past years. This made it much easier to study the process of erythropoietic maturation. [9-11] These systems include isolation of $CD34^+$ cells and the differentiation under humanized *in vitro* cell culture conditions as described elsewhere. [3,5,9] EPCs undergo gradual transformation from CD34 expressing burst-forming unit-erythroids (BFU-e) to enucleated reticulocytes representing a robust and reproducible *ex vivo* erythropoietic maturation system (**Figure. 1A, B**).

These differentiation steps correspond to most of the stages that pluripotent stem cells undergo within the bone marrow where a relatively small number of pluripotent stem cells generate all the different lineages of hematopoietic cells. In the erythroid lineage, the multipotential myeloid stem cells differentiate into BFU-e and further differentiate into the rapidly proliferating colony-forming unit-erythroids (CFU-e) (**Figure 1A**). CFU-e cells undergo three to five cell divisions before they differentiate into proerythroblasts, basophilic erythroblasts, and polychromatic erythroblasts. Morphologically erythroblasts at various differentiation stages differ from each other in their hemoglobin content and the size of their nucleus (**Figure 1A, 1B**). [12] Polychromatic erythroblasts, which are still capable for proliferation, are turning into orthochromatic erythroblasts. They undergo enucleation and lose other cell organelles during the differentiation to reticulocytes. The latter are released into the circulation where they turn into mature erythrocytes within the next few days. Complex processes associated with

differentiation of EPCs are coordinated by growth factors, hormones, and miRNAs. These signals are sensed by receptors, transcription factors, cofactors, second messengers and target proteins. [7,13]

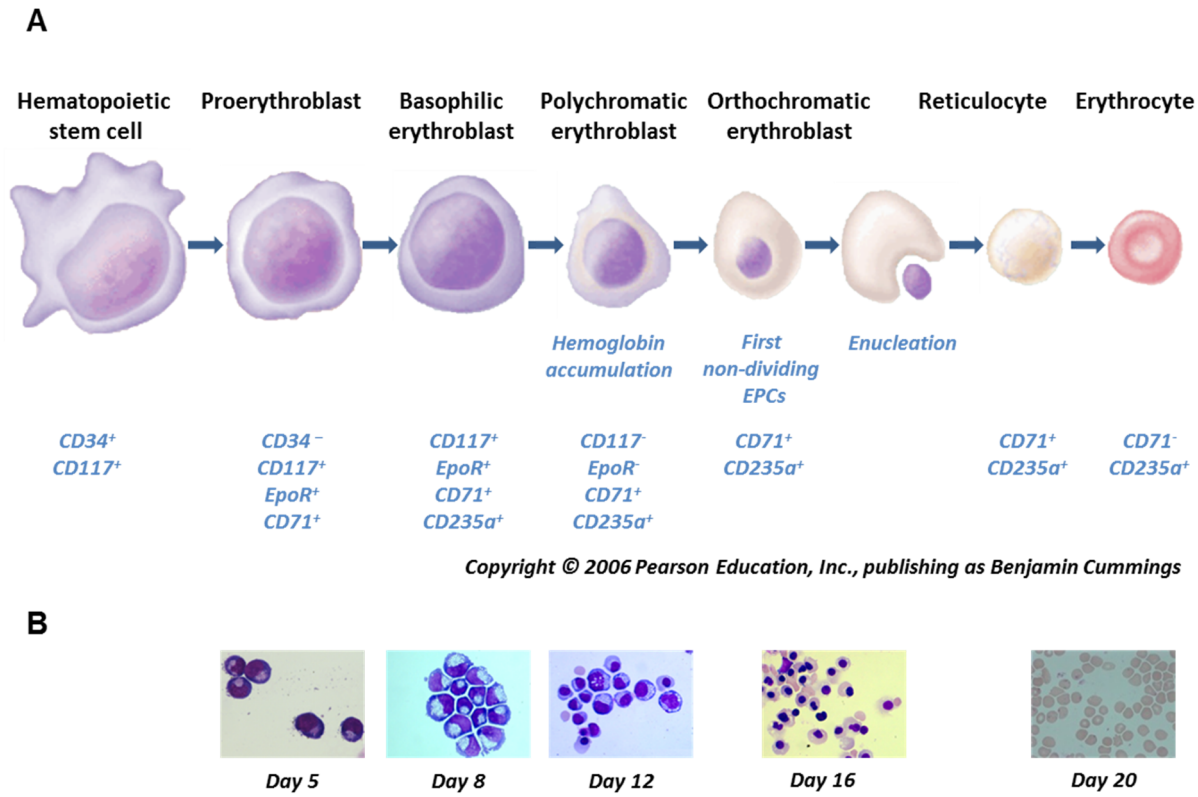

Figure 1A: Erythropoietic maturation with expression of selected receptors and membrane-bound proteins (adapted from Spivak JL, 2005. [14]). Hematopoietic stem cells (HSC) ($CD34^+$ and $CD117^+$) differentiate gradual to CFU-GEMM ($CD38^+$ and $CD34^+$) and to the most immature BFU-e ($CD34^+$, $CD117^+$, $CD71^+$, and low EpoR expression) from the erythroid linage. BFU-e further differentiate to CFU-e ($CD34^-$, $CD117^+$, $CD71^+$, and high EpoR expression) and proerythroblasts ($CD117^+$, $CD71^+$, and $EpoR^+$). Only HSC and proerythroblasts are shown. During proceeding maturation proerythroblasts differentiated to basophilic erythroblasts ($CD117^+$, $EpoR^+$, $CD71^+$, and $CD235a^+$), polychromatic erythroblasts ($CD117^-$, $EpoR^-$, $CD71^+$, $CD235a^+$, and hemoglobin accumulation), and the first non-dividing EPC-type polychromatic erythroblasts ($CD71^+$ and $CD235a^+$). After enucleation reticulocytes ($CD71^+$ and $CD235a^+$) differentiate to fully mature erythrocytes ($CD71^-$ and $CD235a^+$). **B: *Ex vivo* erythropoietic maturation**. Mononuclear cells ($CD34^+$) were isolated from peripheral blood samples, cultured and differentiated in a 2-phase liquid system up to 21 days until they reached the stage of enucleated and mature erythrocytes. Detailed protocol is described elsewhere. [3,5,15]

At various stages differentiation of erythroid cells is controlled by the downstream signaling cascades of a number of receptors. Those receptors found to be essential and sufficient to drive *ex vivo* erythropoiesis are listed in **Table 1**.

Table 1: Selection of downstream signaling cascades during erythropoietic maturation [13,16,17]

Differentiation stage/cell type	Markers expressed	Factors required	Receptors involved	*Ex vivo* erythropoiesis system equivalents
LT-HSC (long-term hematopoietic stem cell)		Wnt, Notch-L (Jagged 1 and 2, Delta1), Shh and BMP-4, SCF, Tpo, IGF-2, FGF-1 Glutamate?	CD117 (c-Kit), MPL, Flt3, IL receptors, Notch, Frizzled, BMP-R, NMDAR?	
ST-HST (Short-term hematopoietic stem cell)	IL-7R$^-$, c-mp1$^+$	SCF, IL-6, Flt3L, G-CSF, Tpo, IL-1, IL-11, IL-12, LIF (?) Glutamate?	CD117 (c-Kit), Flt3R, LR6, MLP, IL11R, NMDAR? (UT7/Epo)	
CMP (common myeloid precursor) or CFU-GEMM	CD34$^+$, CD38$^+$, IL-3Rα, CD45RA$^-$	Epo, SCF, IL-6, IGF-1, Tpo, IL-9, IL-3, Epo, TNFα, Glutamate?	EpoR, c-Kit, IL3R, IL6R, IGF-R, c-MPL, EpoR, IL3R, NMDAR? (UT7/Epo)	
BFU-E	CD71$^+$, CD117$^+$			Flt-3 Ligand, SCF, IL-3, IL-6, dexamethasone, estradiol
Erythroblasts	CD71$^+$, CD235a$^+$			Epo, IL-3, SCF, glutamate/glycine
Reticulocytes		Glutamate	NMDAR	Glutamate/glycine
RBCs		Glutamate	NMDAR	

Table legend: SCF stem cell factor, BMP-4 bone morphogenic protein, CSF colony-stimulating factor, Tpo thrombopoietin, EpoR erythropoietin receptor, IL interleukin, IGF-1/2 insulin-like growth factor 1/2, Flt3L Fms-related tyrosine kinase 3 ligand, Shh sonic hedgehog, Wnt Wingless, FGF fibroblast growth factor, MPL thrombopoietin receptors/myeloproliferative leukemia protein or CD110
Receptor (Ligand): Notch (Jagged/Delta), c-Kit (SCF), Frizzled (WNT proteins), Flt3R (Flt3L), IGFR (IGF2), FGFR (FGF), gp130/IL6R (IL6), β-chain/IL3R (IL3), c-MPL (Tpo), G-CSF-R/CD114 (CSF), EpoR (Epo)

In the first step a 100-1000-fold expansion of CD34$^+$ cells is achieved in the presence of IL-3, IL-6, SCF, Flt3L, dexamethasone, and estradiol in the culturing medium. Within the first five days most of cells reach the proerythroblastic stage. Within the next ~15 days, the cells undergo further differentiation steps, turning from proerythroblasts into basophilic, polychromatic, and orthochromatic erythroblasts and finally to enucleated reticulocytes in the presence of SCF, IL-3, and erythropoietin (Epo). In the culture media, both glutamate and glycine are present along with other essential amino acids. Whether glutamate and/or glycine are involved in proliferation and differentiation of

EPCs is unknown. To answer this question the information on temporal expression pattern and the subunit composition of the receptor is required. The channel properties including the current amplitude, deactivation time and ion preferences are determined by the subunit composition. Most of the receptor subtypes are showing high Ca^{2+} selectivity and their activation results in Ca^{2+} uptake.

The presence of NMDAR in erythroid cells therefore would imply that glutamate release within bone marrow and the erythroblastic islands triggers induction of Ca^{2+}-sensitive signaling pathway(s). Extracellular Ca^{2+} was reported to be required to support survival, proliferation and differentiation of EPCs. [18,19] However, molecular mechanisms of Ca^{2+}-dependent signaling have not yet been identified and the molecular identity of Ca^{2+} transport pathways, including ion channels, remains largely unknown. In the following, chapters the current state of research in the field are presented in more detail. They will cover some aspects of regulation of erythropoiesis, updates of ion channels in erythroid cells in health and diseases, and finally, some insights into the NMDAR properties and their possible physiological role.

4.2. Receptors in erythroid cells and their role in erythropoiesis

Most of the findings on the role of Ca^{2+} in control of erythropoiesis cover erythropoietin receptor-driven erythropoiesis. Therefore, these differentiation stages are covered below in more detail. [20,21] Epo (humoral erythropoietic factor 'hémopoïétine') was discovered to stimulate erythropoiesis in rabbits after bleeding in 1905 by Paul Carnot and Clotilde Deflandre. [22] Following the Epo gene identification in 1985 the first recombinant Epo was licensed and produced by Amgen Inc., Thousand Oaks, USA. Since then, Epo has been used both to treat anemia and illegally to improve sport performance, particularly by endurance athletes. At present Epo is viewed as a pleiotropic glycoprotein hormone that interacts with homodimeric (classical) and most probably also heterodimeric (non-classical) receptors in multiple locations. [23] However, its main function in concordance with other growth factors (Tpo, SCF, IL-3, and IL-6, see **Table 1**) is associated with stimulation of erythrocyte production. Even after 70

years of intensive research, the mechanism of erythropoiesis is still hiding many secrets including the role of amino acids in it. [24]

4.2.1. Erythropoietin and erythropoietin receptor

Erythropoietin and its homodimeric erythropoietin receptor (EpoR) are the main hormonal regulators of erythrocyte production. Each receptor subunit consists of a single transmembrane domain. The EpoR dimerizes upon the interaction with Epo and triggers several signaling cascades essential for cell survival, proliferation, and differentiation. [25,26] The highest expression levels of EpoR was shown in CFU-e and proerythroblasts (up to 1100 receptors per cells) decreasing steadily thereafter. [27,28] It was long believed that reticulocytes and mature RBCs are completely deprived of the EpoR and therefore insensitive to the plasma-borne Epo. However, recent data suggest that the circulating RBCs, particularly reticulocytes, may retain several copies of the receptor. [29] These retaining receptors are most likely involved in regulation of clearance of young RBCs, a process known as neocytolysis. [30,31]

4.2.2. Epo-activated signaling pathways and calcium

The dimerized receptor undergoes auto-phosphorylation of tyrosine residues within the cytosolic domain. These steps are followed by activation of Janus kinase 2 (JAK2), Signal Transducer and Activator of Transcription 5 (STAT5), RAS, phosphatidylinositol 4,5-bisphosphate 3-kinase (PI3-kinase), and Ca^{2+} channels (**Figure 2**). [26] Thus, Ca^{2+} uptake is initiated by Epo binding its receptor. **Table 2** summarizes Ca^{2+}-dependent processes involved at various stages of differentiation, proliferation and protection from apoptosis.

Table 2: Ca^{2+}-dependent processes during erythropoietic maturation

Process	Target regulation	Physiological role	Erythropoiesis
Metabolism	Mitochondria Glycolytic enzymes	Transmembrane potential, reactive oxygen species generation, oxidative phosphorylation efficiency	Epo stimulates oxidative phosphorylation ([32])
Cell cycle (proliferation)	c-fos, c-Jun expression (Ca^{2+} ?) cyclin D expression (CaM K), CDK2 and CDK4 (CaM K) nuclear translocation of transcription factors ([33])	Stimulation of proliferation G1->S phase in cell cycle ([34])	Proliferation of erythroid precursor cells
Cell fate (differentiation) Apoptosis	c-myb expression, Hemoglobin/β-globin production CREB and NFAT phosphorylation (CaM-calcineurin) Ca^{2+}-sensitive endonuclease	Differentiation	Differentiation Apoptosis
Proteolysis	Ca^{2+}-dependent proteases (μ-calpain)	Multiple targets (cytoskeleton, metabolic proteins, ion transporters, signaling proteins…) ([35-37]) → Differentiation	Differentiation
Signaling	PKC-α ([38]) calciueurin	Differentiation	Differentiation
Iron metabolism	Transferrin endocytosis and iron uptake (Ca^{2+}-CaM)	Hemoglobin synthesis	Ca^{2+}-CaM is required to support Fe uptake into erythroid precursors ([39])
Epo-driven signaling cascades	Opening of TRP channels IP3-kinase → PLC → DAG cascade (Ca^{2+}-CaM)	Differentiation	Differentiation

References are given in brackets ().

One of the pathways, which is essential for erythropoiesis, is the JAK2 signaling cascade. [40] After the trans-phosphorylation of JAK2, the kinase phosphorylates the tyrosine residues of the EpoR. STAT5 binds to the phosphorylated EpoR and gets phosphorylated by JAK2. The transcription factor then dissociates from the receptor, dimerizes, and translocates to the nucleus. [26]

A second downstream pathway of the EpoR is the Ras cascade. The binding of the cytoplasmic adaptor protein Grb2 and the Ras guanine nucleotide exchange factor SOS, leads to the translocation of SOS and the associated activation of Shc/Ras/Mitogene-activated kinase (MAPK) pathway. [26,41-43]

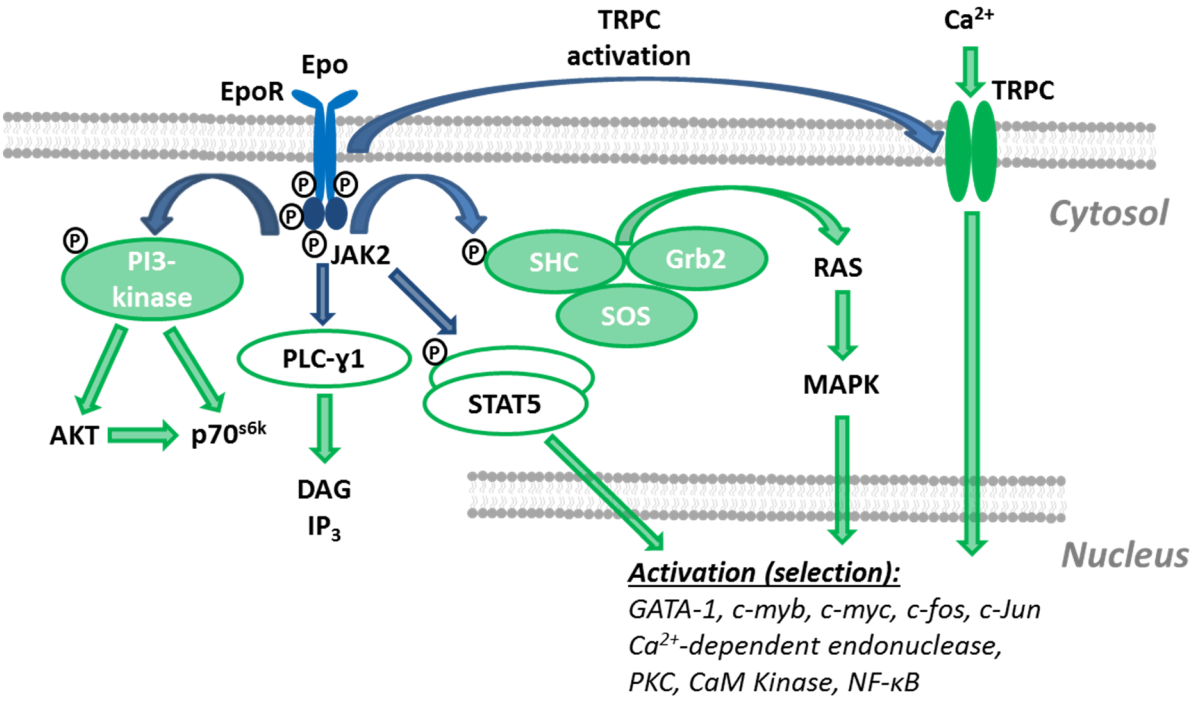

Figure 2: Schematic overview of the major erythropoietin signaling pathways in erythroid cells. After Epo-EpoR binding, dimerization, and tyrosine phosphorylation, the JAK2 tyrosine kinase gets activated and induces (blue arrows) several downstream pathways including MAPK pathway, STAT5, PLC-ɣ1, PI3-kinase, and transient receptor potential channel (TRPC) activation (green arrows).

A third pathway which gets activated by Epo is the PI3-kinase pathway: [44] PI3-kinase generates phosphatidylinositol 3-phosphate, phosphatidylinositol 3,4-bisphosphate, and phosphatidylinositol (3,4,5)-trisphosphate. [45] Theses second messengers activate the serine/threonine-specific protein kinase B (AKT) and $p70^{s6k}$ which mediate mRNA transcription and translation by phosphorylation of ribosomal proteins. [26,46,47] Binding of Epo to its receptor in EPCs results in activation of several other signaling cascades and turns on a variety of transcription factors (TFs). One of these signaling cascades is initiated by the activation of the phospholipase C-ɣ1 (PLC-ɣ1). [26] PLC-ɣ1 triggers cleavage of phosphatidylinositol 4,5-bisphosphate (PIP_2) to diacylglycerol (DAG) and inositol(1,4,5)P_3 (IP_3). Binding of IP_3 to its receptor causes a release of Ca^{2+} from endoplasmic reticulum (ER), followed by the activation of downstream Ca^{2+}-sensitive cytosolic targets, including classic and novel protein kinase C (PKC) isoforms and Ca^{2+}-calmodulin-sensitive processes. [44,45,48] Release of Ca^{2+} from the ER storage was shown to control apoptosis of $CD34^{+}$-derived EPCs. [49] This occurs partially due to the mitochondrial Ca^{2+} overload as well as via the regulation of Ca^{2+}-calmodulin- (Ca^{2+}-CaM) dependent death associated protein kinase-2 (DAPK-2). [21] The Ca^{2+}-CaM

complex can interact with 4.1R protein, a major structural element of the cytoskeleton in erythrocyte. This interaction causes the binding of 4.1R protein to the anion transport protein band 3 and the transmembrane protein glycophorin C. Thereby, Ca^{2+} and its signaling cascades are taking part in RBC membrane biogenesis during terminal erythroid differentiation. [50] Ca^{2+}-CaM binding to the CaM kinase II (CaM KII) results in phosphorylation of IP3-kinase, which in turn phosphorylate multiple targets including IP_3 to IP_4. Ca^{2+}-signaling originating from the ER regulates amongst other cellular processes, the regulation of the expression of the transient receptor potential channel 3 and 6 (TRPC). [51] These channels were shown to be involved in regulation of the intracellular Ca^{2+} in precursor cells during erythropoietic maturation. [18] After the Epo-Epo receptor dependent activation, the channels cause the required Ca^{2+} influx in CFU-e cells and proerythroblasts. [52,53]

4.2.3. Growth factors and membrane-bound proteins

Besides the Epo-Epo receptor interaction, several other interactions of cytokines and growth factors with membrane-bound receptors are essential for erythropoietic maturation. The expression of surface receptors and membrane-bound proteins are quite specific for the different stages of maturation (**Figure 1**).

Although the antigen CD34 is regularly used to identify hematopoietic stem cells, its function is still not fully understood. This glycoprotein is only expressed in erythroid cells until BFU-e stage; it contributes to self-renewal and inhibits differentiation of early stage EPCs. [54] SCF binds to the c-kit receptor (CD117) and promotes proliferation and self-renewal of $CD34^+$ cells, CFU-e cells, proerythroblasts, and basophilic erythroblasts by induction of Myc. [55,56] Similar to the Epo-EpoR signaling, the binding of SCF to CD117 promotes dimerization of the receptor subunits and autophosphorylation of the receptor. Moreover, the activated c-kit receptor has a highly similar downstream signaling cascade, which includes PLC-ɣ, PI-3 kinase, Grb2, and the MAPK pathway. [55,57,58] Both signaling pathways have synergetic effects, are potentially Ca^{2+}-dependent, and are required for erythropoiesis. Nonetheless, the interaction of Epo and SCF signaling is not fully understood. [59,60]

The transferrin receptor protein 1 (CD71) is expressed in EPCs during the whole erythropoietic maturation. CD71 expression is highest in basophilic, polychromatic,

and orthochromatic erythroblasts and decrease in reticulocytes. CD71 is essential for the uptake of the iron-transferrin complex. [61] The heavily glycosylated glycophorin A (CD235a) provides erythroid cells with hydrophilic surface. The surface expression of CD2351a increases in proerythroblasts and remains high even in mature erythrocytes. [62] Interleukin-3 (IL-3), Granulocyte macrophage colony-stimulating factor (GM-CSF), and SCF contribute to the early differentiation steps from a colony-forming unit-multipotential myeloid stem cell (CFU-GEMM) cell to a BFU-e and CFU-e cell. [13,20,63,64] Another factor that triggers self-renewal of BFU-e over terminal differentiation is the bone morphogenic protein-4 (BMP-4), which induces the expression of Smad5, SCL/Tal-1, and GATA-2. This member of the TGF-β family is essential for the stress-induced erythropoiesis and enhanced production of erythrocytes by increasing the number of BFU-e cells. [65-67] Thrombopoietin is neither limited to megakaryocyte differentiation nor platelets production. [68,69] Together with Fms-like tyrosine kinase-3 (Flt-3) ligand, thrombopoietin are important for maintenance of common myeloid progenitors and CFU-GEMM. [70,71] Insulin and insulin-like growth factor-1 (IGF-1) are required for the differentiation of BFU-e and CFU-e and they stimulate the maturation of polychromatic erythroblasts. [72-74] This overlapping expression stage with the EpoR, might suggest some interaction with the Epo signaling pathway, but the exact mechanism of possible co-regulation remains unclear. Even less is known about the role of Fas ligand receptor in erythroid cells. The receptor of the tumor necrosis factor family is a known trigger of caspase activation and apoptosis in other cell types. However, recent studies imply that in the EPCs, the Fas ligand induce positive signals for erythropoietic maturation. [75]

While the early stages of terminal erythropoietic maturation (BFU-e cells to polychromatic erythroblasts) is highly Epo-dependent, the later differentiation stages are integrin-dependent. The interaction of integrin with the extracellular matrix protein fibronectin is required for the last cell divisions of polychromatic erythroblasts and triggers enucleation of reticulocytes. [13,76] Furthermore glucocorticoids (GCs) stimulate the stress-induced erythropoiesis by increasing the number of CFU-e cells and protect the BFU-e cells. [13] GCs enhance the expression of the transcription factors involved in self-renewal of BFU-e cells (Myb and LMO-2) and impair GATA-1 expression, which promotes terminal differentiation. [77,78]

4.3. Transcriptional and posttranscriptional regulation of erythropoietic maturation

Several transcription factors (TFs) involved in erythropoietic maturation have been described extensively in the literature. Some of them maintain the self-renewal of the erythropoietic cells, while others induce the various differentiation steps. Nevertheless, analogue to the functions of growth factors and their complex interplay, the transcriptional regulation with all of the posttranscriptional modifications are only partially understood.

4.3.1. Transcriptional regulation

The regulation and the complex interplay of transcription factors, cofactors, miRNAs, and post-translational histone modifications have been studied for years. The number of crucial transcriptional regulators is relatively small, but arrangement with various cofactors and the mechanism of how those multiprotein complex regulate gene expression is far less understood (**Figure 3**).

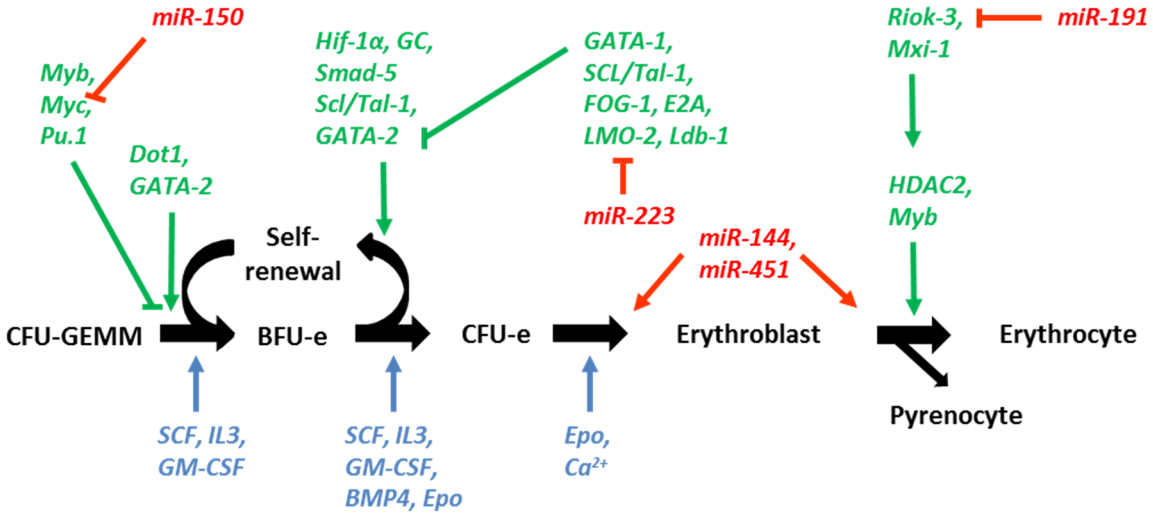

Figure 3: Transcriptional and posttranscriptional regulation of the erythropoietic maturation (adapted from Hattangadi *et al.* [13]). Selection of transcription factors, DNA-binding factors (both in green), microRNAs (in red), and growth hormones/factors (in blue) which influence erythroid maturation. The pentameric complex of GATA-1, LMO-2, SCL/Tal-1, Ldb-1, and E2A triggers terminal maturation, while the GATA-2 variant of this complex activates c-kit transcription and self-renewal. At various stages, microRNAs (miRs) trigger the self-renewal of EPCs or differentiation, including the enucleation and formation of the condensed nucleus embedded in a cytoplasmic layer (pyrenocyte), respectively. [12]

Two of the best studied TFs involved in erythropoiesis are GATA-1 and GATA-2. The two homologues zinc-finger domains of those TFs bind to the DNA consensus sequence ((A/T)GATA(G/A)) in many erythroid genes, including the genes of band 3 protein, globins, and EpoR. GATA-2 is expressed in early EPCs and contributes to the expansion and cell survival of those cells. [79] If GATA-2 expression is high and GATA-1 is low, the terminal maturation of EPCs is blocked and early EPCs proliferation is increased. Next to GATA-2 the proto-oncogene c-Myb and putative oncogene Spi-1 (Pu.1) block terminal differentiation and promote self-renewal of early EPCs. Furthermore, for the differentiation of pluripotent hematopoietic stem cells in to erythroid linage, the relative ration of Pu.1 and GATA-2 is crucial. Low expression of GATA-2 and high expression of Pu.1 lead to the formation of myeloid precursor cells, while only high GATA-2 and low Pu.1 expression results in EPCs formation.

In the course of switching from self-renewal of BFU-e cells to induction of terminal erythropoiesis GATA-2, c-Myb, and Pu.1 need to be down-regulated while GATA-1 and several cofactors need to be up-regulated. [79-82] The increased expression of GATA-1 leads together with the co-regulators SCL/Tal-1, E2A, and LIM domain containing factors LMO-2 and Ldb-1, to the formation of a major activating complex for terminal maturation. LMO-2 and Ldb-1 act in this complex as bridging factors between the DNA binding SCL/Tal-1 and GATA-1. It has been assumed that the zinc-finger protein friend of GATA (FOG-1) contributes to erythropoiesis in a GATA-1 independent and GATA-1 dependent manner. The repressor complex is formed by binding of FOG-1 and Gfi-1b to GATA-1. In contrast to the activation complex, less is known about the composition and the mechanism of the action of the GATA-1 repressor complex, which enables the down-regulation of GATA-2. [2,13,79,82] The CACC consensus binding sites for the zinc finger protein Krüppel-like factor-1 (Klf-1) are often located closely to the GATA binding sites in erythroid genes. The interaction of GATA-1 and Klf-1 promotes gene expression. One of the target genes is the β-globin. In Klf-1 knock-out mice embryonic erythropoiesis (ε- and ζ-globin) occurs normally, but they suffer from a lethal β-globin deficiency. Klf-1 deficient mice show, besides the β-globin deficiency, up-regulated ɣ-globin expression. This indicates that Klf-1 is required for terminal erythropoiesis, hemoglobin switch, and especially β-globin expression. [2,83-86]

Besides the balance between self-renewal, proliferation, and differentiation, cell survival is another crucial factor of successful erythopoietic maturation. The transcription factor STAT5 is essential to prevent apoptosis of EPCs. Upon binding to

the activated EpoR, STAT5 gets phosphorylated and activated. The dimerized STAT5 translocates to the nucleus and up-regulates the expression of the antiapoptotic gene Bcl-x. [79,87]

4.3.2. MicroRNAs

During the entire erythropoietic maturation, microRNAs (miRs) are important regulators of differentiation, proliferation, and enucleation. The small non-coding RNA molecules can silence genes by interfering with their mRNA (**Figure 3**). For example, at the early stage of CFU-GEMM cells, the down-regulation of miR-150 is a trigger for differentiation towards erythropoietic linage by reducing the Myb expression. [88] During further maturation of CFU-e cells to erythroblasts, the down-regulation of miR-223 is critical for the enhanced expression of the zinc finger domain containing LMO-2 and terminal differentiation. [89] The expression of majority of miRs is down-regulated during normal erythropoiesis. Two exceptions are the miR-144 and miR-451. They are transcriptional targets of GATA-1 and are highly up-regulated during terminal differentiation and chromatin condensation. [90] Another crucial regulator for terminal maturation is miR-191. The miR-191 inhibits the expression of Riok3 and Mix1, two genes essential for chromatin condensation and enuclation. In EPCs over-expressing miR-191 enuclation was abundant. [28] There are several additional microRNAs that are involved in the regulation of erythropoietic maturation, but to determine the exact mechanism further investigation is needed. [13]

4.3.3. Epigenetic modifications during differentiation and enuclation

Mature mammalian RBCs are enucleated. For this enucleation during erythropoiesis, chromatin condensation is required. By the interaction with a macrophage, the orthochromatic erythroblast extrudes his nucleus and divides asymmetrically into a reticulocyte, containing most of the cytoplasm, and the condensed nucleus embedded in a cytoplasmic layer (pyrenocyte). [12] While reticulocytes get released into the circulation and further differentiate to erythrocytes, pyrenocytes get degraded by macrophages. This asymmetric cell division enables an enrichment of reticulocytes with hemoglobin. Condensation and inactivation of the nucleus appears in all vertebrates, but the enuclation is limited to mammals. [12,13,91,92]

Crucial for enucleation is the completed chromatin condensation. Depending on the acetylation status of the histones (H3 and H4), chromatin can occur in an open (euchromatin) and a closed (heterochromatin) conformation. [12,93] The switch from euchromatin to heterochromatin is mainly regulated by histone deacetylases (HDAC). If the histones get deacetylted by a HDAC, both the chromatin shifts to its closed conformation and the polymerase complex can no longer bind, thereby the genes are getting silenced. [12] HDAC function is precisely regulated by the Ca^{2+} signal exchange between the ER and the nuclear compartment. The activation of the inositol 3 phosphate receptors within the ER membrane leads to phosphorylation of HDACs mediated by nuclear Ca^{2+}-calmodulin-sensitive kinases (CaM Ks). [94] In erythropoiesis, several HDAC isoforms (HDAC1, HDAC2, and HDAC3) have been identified that induce terminal differentiation, regulate the globin switch, and cause chromatin condensation, respectively. When BFU-e differentiate to CFU-e, GATA-1 suppresses GATA-2 by binding to a HDAC1 containing complex and down-regulates its expression. [12,95] The HDAC3 complex represses the ɣ-globin expression and contributes to the switch from fetal to adult hemoglobin. [96] In polychromatic erythroblasts, the HDAC2 complex induces the chromatin condensation and triggers the terminal differentiation to orthochromatic erythroblasts. [12,97]

4.3.4. Stress-induced erythropoiesis

Hematocrit and erythrocyte production is under precise regulation by Epo. In healthy adults, Epo concentrations are relatively low (20-50 mU/L), but under stress conditions, an enhanced Epo release triggers production of new red blood cells. This Epo-mediated increase of erythrocytes production is limited by a fixed number of divisions (3 to 5 cell divisions) of the CFU-e, proerythroblasts, basophilic, and polychromatic erythroblasts. Under conditions of severe chronic anemia, the Epo-mediated increase is not sufficient and enhanced Epo-independent formation of BFU-e and CFU-e is required. [13,98]

4.4. Ion homeostasis and ion channels

Considerably fewer studies have been focusing on the identification and characterization of the physiological role of ions and ion channels in erythroid cells. Transient receptor potential cation channels (TRPCs) have been studied in EPCs in more detail by Miller and colleagues. [99,100] By now, TRPCs remain the only channels studied during erythropoiesis, including their expression patterns, functions, or interactions. Although a number of other channels - including Gardos channels, non-selective cation channels (NSCC), voltage-dependent anion channels (VDAC) and several others - have been reported in mature red cells, none of them were studied in the EPCs and their physiological function remain largely unclear. [101] In this section more emphasis will therefore be given to the literature on ion channels in mature RBCs. As no *de novo* protein synthesis occurs in enucleated circulating RBCs, all of these channels are obviously expressed in not yet released erythroid cells, at least during the late differentiation stages.

4.4.1. Ion homeostasis and cell hydration

The changes in cell ion content and cell volume occur in a variety of differentiating cells. Especially in EPCs are those changes during the transformation from BFU-e to the orthochromatic erythroblasts easy to follow (**Figure 1A, B**). Cell volume and hydration in erythroid cells are mainly determined by cation concentration (Na^+, K^+, Ca^{2+}, and Mg^{2+}). Various ion channels and electroneutral ion transporters control this homeostasis in erythrocytes, including the K^+-Cl^- and Na^+-K^+-$2Cl^-$ co-transporters, the Na^+/H^+ exchanger, the gradient-forming Na^+,K^+-ATPase, and plasma membrane Ca^{2+} pump. [102,103] However, acute dehydration of RBCs may result from the activation of Ca^{2+}-sensitive K^+ channel (Gardos channel, KCNN4, K(Ca)3.1). Anion concentration (Cl^-, HCO_3^-, hemoglobin, and 2,3-BPG) is pretty fixed, with a strong increase of hemoglobin concentration in reticulocytes and red blood cells, respectively (Donnan effect). Mutations in the anion exchanger (band 3 protein) however, are believed to be associated with an increase in cation permeability and abnormalities in cell ion and water content *e.g.* in patients with cryohydrocytosis. [104,105] Disturbances in cell volume regulation lead to the compromised hemorheology and premature clearance of RBCs. [106] Dehydration of erythrocytes has particularly fatal consequences in patients

with SCD, as it promotes irreversible sickle cell transformation. [107,108] Dehydrated erythrocytes have a much higher probability for hemoglobin S (HbS) polymer formation and cell adhesion. [109,110]

In contrast to erythrocytes, there is less known about ion homeostasis in EPCs. Mainly K^+-Cl^- co-transporters and TRPCs have been studied during erythropoietic maturation. K^+-Cl^- co-transporters are taking part in regulation of cell volume, [111,112] and TRPCs are essential for the regulation of Ca^{2+} signaling during the EPC differentiation. [49,96]

4.4.1.1. Calcium

Calcium is a master-regulator of multiple processes in any living cell. [113] Relative small changes in the intracellular Ca^{2+} or its re-distribution between the intracellular compartments are sensed by numerous Ca^{2+} sensors. [114] In contrast to other ions, there is a large concentration gradient between free intracellular Ca^{2+} (20-50 nM) and extracellular Ca^{2+} (~2 mM). Furthermore, the divalent ion is essential for several cellular processes, including gene transcription and regulation of cell survival (**Figure 4**). [113]

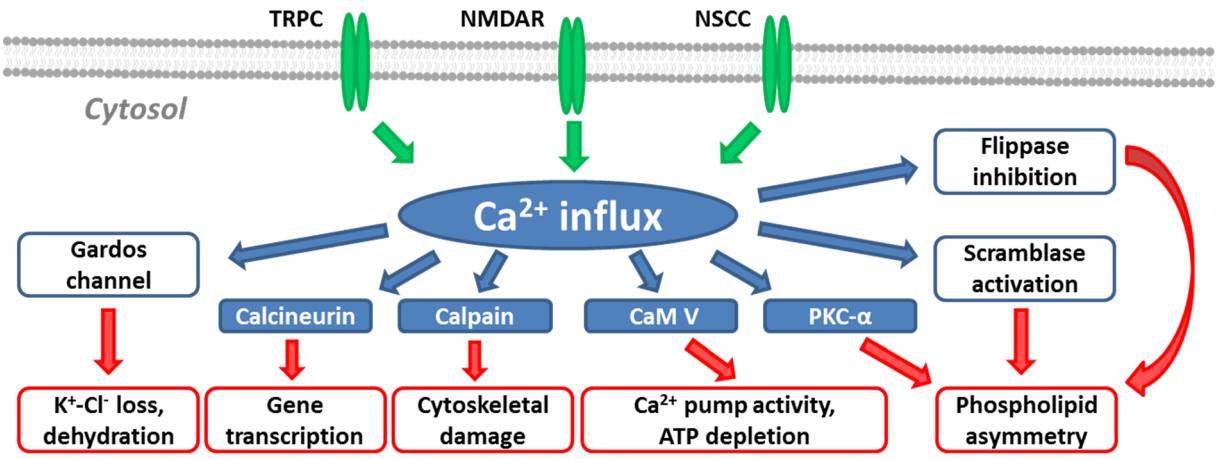

Figure 4: Schematic overview of Ca^{2+} signaling in erythroid cells and effects of enhanced Ca^{2+} influx. The Ca^{2+} influx through ion channels (TRPC, NMDAR, and non-selective cation channel (NSCC)) (in green) leads to activation of a variety of proteins (in blue). Enhanced intracellular Ca^{2+} influx can trigger several processes (in red), which can induce the removal of the RBC from the circulation or even hemolysis.

Calmodulin is one of the intracellular Ca^{2+} sensors. After the binding of Ca^{2+}, the messenger protein can interact with hundreds of different proteins. [113,115] These interactions can lead from gene expression to the regulation of apoptosis. [115] Ca^{2+} signaling can appear very locally within a cell, and the intracellular Ca^{2+} concentration

can increase by 100-fold over 10 nm. [116,117] In the dendritic spine, the localization of Ca^{2+} signaling produces an increase of intracellular Ca^{2+} concentration up the 1 µM within a few milliseconds. [113,118-120] In contrast to almost any other cell type, the release of intracellular Ca^{2+} from organelles such as mitochondria or endoplasmic reticulum, is due the lack of those compartments marginal.

During the erythropoietic maturation, Ca^{2+} signaling is one of the major regulators for cell survival, proliferation, and differentiation. Two of the essential proteins of this signaling cascade are the protein phosphatase-calcineurin and the serine/threonine-specific protein kinase Ca^{2+}/calmodulin-dependent protein kinase (CaM K). [33,121] The inhibition of CaM KIV causes the differentiation of hematopoietic stem cells to myeloid cells over erythroid cells. [122] On the other hand, over-activation of Ca^{2+} signaling in the non-hematopoietic tissues surrounding erythroblastic islands leads to apoptosis. [121] Besides the co-regulation of various transcription factors, including *c-myb* and *c-fos*, Ca^{2+}-signaling triggers the activation of hemoglobin synthesis, the endothelial NO-synthase, and the type I adenylylcyclase. [121,123,124] These findings indicate that precise regulation of intracellular Ca^{2+} in erythroid cells as well as in adjacent non-hematopoietic cells are crucial for successful erythropoiesis.

4.4.1.2. Potassium

Transmembrane Na^+/K^+ gradient in human EPCs and in mature red blood cells is mediated by the Na^+,K^+-ATPase, [125,126] whereas passive K^+ loss occurs via several types of ion channels (TRPCs, Gardos channels, non-selective cation channels [101,127,128]) and co-transporters (such as the Na^+-K^+-$2Cl^-$ co-transporter and K^+-Cl^- co-transporter [129-132]). These transporters and channels are responsible for the maintenance of the steady state intracellular potassium levels. The expression levels and the activity of these proteins vary, depending on the differentiation state, cell age and various pathologies. [106,111,112] A number of factors, including intracellular Ca^{2+}, pH, cell volume changes, shear stress, oxidative stress, and Hb oxygenation, control their activity precisely.

Nonetheless in the pathophysiology of SCD at least two of those proteins exhibit enhanced expression or activity. In patients the hyper-activation of the Gardos channel and the K^+-Cl^- co-transporter lead to cell dehydration, further deoxygenation, and facilitated sickling of RBCs. [133] Whereas the K^+-Cl^- co-transporter is particularly up-regulated in the RBCs, forming medium density fraction, abnormally high activity of the

Gardos channel is more pronounced in the cells forming dense fraction on Percoll/Ficoll gradient. [134,135]

4.4.1.3. Sodium

Low intracellular Na^+ levels are maintained by the Na^+,K^+-ATPase. A fraction of high density irreversible sickled erythrocytes exhibits an abnormal high sodium concentration. [136] The exact mechanism and the significance of high Na^+ concentration in a subpopulation are still not fully understood. Some studies have shown alteration in cation permeability and the impaired activity contributes to increased intracellular Na^+ levels. [108,137,138] Nevertheless, in the pathophysiology of sickle cell anemia, Ca^{2+} and K^+ are much more important.

4.4.2. Ion channels in erythroid cells

There is still an ongoing discussion about the role of ion channels in mature RBCs. The presence of a variety of ion channels has been demonstrated on a molecular and function level. However, their physiological role in precursors, and in particular in circulating RBCs, remains obscure. Researchers argue if these channels are just relics of differentiation or if they are take actively part in the regulation of ion homeostasis. [52,100,101,139-145] Pathophysiological conditions associated with malfunction of these ion channels indicate that they are required for survival, differentiation, and proliferation of erythroid cells. [52,100,101,141,142,146-148]

4.4.2.1 Gardos channel and dehydration

Gardos channels received particular attention in RBCs of patients with SCD. These channels were chosen as a potential pharmacological target for treatment of the hereditary disorder. [149-151] Activation of Gardos channels by enhanced intracellular Ca^{2+} levels result in a transient shrinkage of cells, due to the net loss of K^+-Cl^- and water. The dehydration triggers the irreversible polymerization of the deoxygenated HbS. This process is responsible for the characteristic changes in cells morphology of erythrocytes known as sickling. [135,144,152] Therefore, inhibition of the Gardos channel was suggested to be a beneficial pharmacological strategy for the treatment of SCD. The inhibitor Senicapoc (ICA-17043, 2,2-bis(4-fluorophenyl)-2-phenylacetamide) entered the phase II trial and was shown to reduce hemolysis in patients, but it did not

affect the frequency of pain crisis. [149] The physiological function of the Gardos channels in healthy RBC is currently unclear, but is probably related to the upstream up-regulation of Ca^{2+}, as activation of this channel requires a local increase in free Ca^{2+} from 20-50 nmol l^{-1} above 150 nmol l^{-1}. [101,153]

4.4.2.2. Voltage-dependent anion channel

The Voltage-dependent anion channel (VDAC) has been described first and studied intensively as a mitochondrial protein. [101,154,155] Later, the presence in the plasma membrane of human B-lymphocytes and RBCs was shown. [101,156-158] In artificial membrane systems, VDACs were still open in the range of from -10 mV to +10 mV. [156] With a resting membrane potential of RBCs (around -10 mV) the channel should remain in the open conformation, but it is actually inactive under physiological conditions. This indicates a different gating and activation mechanism in the erythrocyte membrane compared to artificial systems. [101] Moreover, Ca^{2+} and reactive oxygen species (ROS) influence the function of VDAC, but the exact mechanisms of its physiological regulation in erythroid cells remain unknown. [154]

4.4.2.3. Peripheral benzodiazepine receptor complex

Another receptor of the VDAC conductive pathway present in erythrocytes is the peripheral benzodiazepine receptor. Just like most of the channels in the RBC membrane, these receptors are dormant under physiological conditions but get activated in cells infected by *Plasmodium falciparum*. [159] The maxi-anion channel contributes to a band 3-independet anion transport. [143,148,159] Two proteins of this peripheral benzodiazepine receptor complex are the translocator protein and the adenine nucleotide transporter. They interact with VDAC and might be involved in the regulation of apoptosis. [101,160]

4.4.2.4. Transient receptor potential cation channels

During erythropoietic maturation, the temporary rise of intracellular Ca^{2+} is essential for differentiation and proliferation. [18,19,161] It has been demonstrated that Epo stimulates a dose-dependent increase in free intracellular Ca^{2+} levels by modulating the TRPC. TRPCs are non-selective, voltage-independent cation channels with the highest permeability to Ca^{2+} ions. [52,53,140,162-165] A complex interplay of different proteins and the receptor is needed to change the conformation in the open state. The activated

EpoR-PLCɣ complex interacts directly with several sites of the TRPCs. Next to PLCɣ, activated IP_3-receptor is needed for full activation of the receptor and induces the enhanced Ca^{2+} influx in EPCs. [52] Together with EpoRs, TRPCs are relevant during the first stage of maturation up to the stage of basophilic erythroblasts (**Figure 2**).

4.4.2.5. Small conductance chloride channel

Even less is known about the Zinc-sensitive small conductance chloride channel. The channel might contribute to the basal conductance and the regulation of cell volume. Typical properties of these channels are long opening, followed by long closing intervals and a conductance of 5 pS. [148,166]

4.5. The N-methyl-D-aspartate receptor

N-methyl-D-aspartate receptors (NMDARs) have been studied intensively since they were first discovered in neurons in the late 70s in spinal cord of a frog. [167,168] As they appeared to be of pivotal importance in synaptic transmission, electrophysiology, pharmacology, and molecular biology of these receptors were mainly studied by researchers in basic and clinical neuroscience. Within the past decades, these receptors were characterized in a variety of non-neuronal tissues as well. [169] In 2010, Makhro *et al*. [4] from our laboratory showed the presence of functional NMDARs in rat erythrocytes for the first time. Earlier these receptors were found in cells originating from the hematopoietic lineage (lymphocytes, platelets, macrophages, and megakaryocytes). [170-174] This discovery created great curiosity about their relevance in human erythroid cells and if they could possibly be involved in the pathophysiology of red blood cell-related disorders.

4.5.1. Properties, structure, and downstream signaling cascade of the N-methyl-D-aspartate receptors

Together with the AMPA and kainate receptors, the voltage-dependent NMDARs belong to the family of ionotropic glutamate receptors. [175-182] The heteromeric ion channels are composed of four subunits (**Figure 5**).

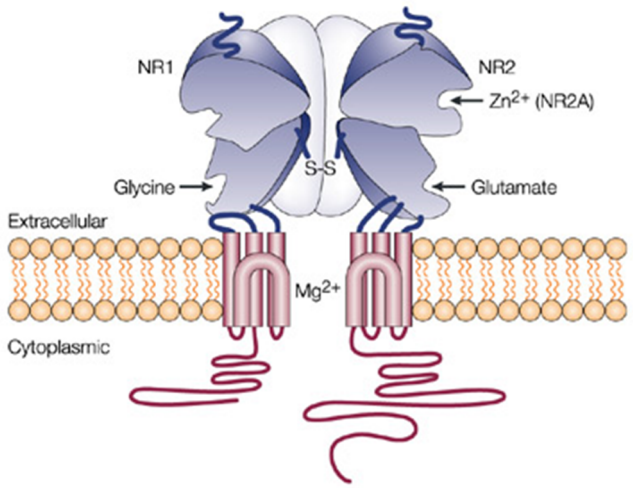

Figure 5: Model of the N-methyl-D-aspartate receptor (by Witt *et al*. [183]). The tetrameric channel requires for full activation glutamate and glycine. The naturally occurring antagonist Mg^{2+} can block the Ca^{2+} influx in a voltage-dependent manner. The different NMDAR subunits have several binding sites for allosteric modulators *e.g.* GluN2A for Zinc.

By now, seven different subunit types have been described. There are the glycine or D-serine binding subunits GlunN1 and GluN3 (A-B) and the L-glutamate or N-methyl-D-aspartate binding subunits GluN2 (A-D). [167,184-187] Some subunits have additional splicing variants and isoforms. Such as from the GluN1 subunit eight functional splicing variants have been described so far. [188-191] These subunits variants are highly pH-dependent and may therefore function as a pH sensor. [180,192-194] For full activation of classical NMDARs, L-glutamate and glycine binding subunits are required. However, recently NMDARs composed of glycine binding subunits (GluN1 and GluN3) only have also been described. [192,195,196] In neuronal cells, the presynaptic release of glutamate is taking the function of a neurotransmitter, while glycine acts as a modulator. [197] The pharmacological and electrophysiological properties of NMDARs highly depend on their subunit composition. [198,199] NMDARs containing GluN2A-B subunits have high conductance and fast decay time while GluN2C-D show low conductance and slow deactivation. [196,200-211] GluN3 (A-B) subunits exhibit dominate negative properties, referring to their current response and permeability to divalent ions. [192,195,212-220] Intensive structural and functional studies during the last years have led to better understanding of the subunit assembly. All subunits are encoded by seven

different genes and their length varies from 900 to 1480 amino acids. The different sizes of the subunits are mainly attributed to the variations in intracellular carboxyl-terminal domain (CTD). This domain is coupled to the downstream signaling pathway. [199,221] NMDAR subunits are structured in four domains: the amino-terminal domain (NTD), the agonist-binding domain (ABD), the transmembrane domain (TDM) and the CTD. The NTD is composed of two clamshell-like regions and is taking part in allosteric modulation and subunit assembly. The ABD is made of the segments (S1 and S2) that are binding either glutamate or glycine. The TMD is formed of three transmembrane helices and one re-entrant pore loop, which is responsible for the selectivity to ions. Depending on the subunit composition, NMDARs have a different permeability of Ca^{2+} Na^{+}, K^{+}, and Cs^{+} ions. [222] They have the highest permeability for Ca^{2+} and Na^{+} ions. [177,178,188,199,202,221,223-225] Analogue to conductance and deactivation time, NMDARs have subunit-dependent sensitivity to magnesium block. [178,179,226-228] Di-heteromeric channels containing GluN1 together with GluN2A or GluN2B have a lower half-maximal inhibitory concentration than NMDAR containing GluN2C or GluN2D. These characteristics are primarily controlled by one amino acid in the M3 transmembrane region. [221,229] Besides magnesium, there are several endogenous modulators of NMDAR, such as Zn^{2+}, H^{+}, and polyamines. [180,189,198,207,230] GluN3A or GluN3B containing receptors show, beside the lower conductance a reduced sensitivity to Mg^{2+} as well. [212,217,231] Apart from agonist or antagonist binding, phosphorylation and dephosphorylation of the CTD are a crucial mechanism for the regulation of NMDARs. Varieties of different kinases are interacting with the CTD and trigger the downstream signaling cascade. The PDZ-binding domains of GluN2 subunits can interact with several membrane-associated guanylate kinase scaffolding proteins, such as SAP-102 and PSD-95. [232-237] Several other kinases - including protein kinase A, protein kinase C, and Ca^{2+}/calmodulin-dependent protein kinase - are participating in the NMDAR trafficking. Further downstream the cascade, NMDAR signaling affects the MAPK and cyclic-AMP response element binding protein (CREB) mediated pathway and regulates multiple gene activation and cell survival. [221,238]

4.5.2. Plasticity and function in neuronal cells

The NMDAR is involved in a lot of molecular and functional processes from memory formation to inflammation. [199] Expression patterns for the different NMDAR subunits change greatly during the development from embryonic to adult brain. [221] While expression of the GluN1 isoforms is pronounced and ubiquitous in the brain, GluN2 and GluN3 subunits expression is more likely to be associated with specific development stages, areas, and functions of the receptor. [239-241] This plasticity of NMDAR is not limited to the development stage. Alterations in the number and activity of receptors in adult neurons may occur within minutes. Relatively little is known about the regulation of this subtype plasticity. [221] Besides the subunit composition, the function of NMDARs is highly influenced by the localization. Activation of synaptic NMDARs triggers neuronal cells survival by activation of CREB and inhibition of pro-apoptotic genes. In contrast to that activation of extrasynaptic NMDARs causes dephosphorylation of CREB, inactivation of the serine/threonine kinase ERK1/2, and triggers cell death by mitochondrial dysfunction. [238,242] NMDARs contribute decisively to the long term potentiation, synaptic plasticity, learning, memory formation, and neuronal communication. [221]

4.5.3. Pathophysiology and the potential as a drug target in neuronal cells

Since the receptor is crucial for neuronal development and memory formation, it is associated with several neuronal disorders and damages. [242] In Alzheimer's disease it has been shown that a constant over-activation of extrasynaptic NMDARs and a decreased GluN2B expression are affecting the progress of the disease. [243,244] In the brain of patients with Parkinson's disease, location of the GluN2B-containing receptor shifts from the synaptic to the extrasynaptic site, and the GluN2A levels get up-regulated. [242,245] In Alzheimer's and Huntington's diseases, an increase in extrasynaptic NMDAR activity has been described by Gladding and Raymond. [246] In contrast to these neurodegenerative disorders, schizophrenia is associated with a decrease in NMDAR activity. [247] During both acute and chronic alcohol/cocaine abuse, alteration in the receptor expression and properties occur as well. [248-250] Taken together, over-stimulation of the NMDARs leads to sever increased intracellular Ca^{2+}

levels, which causes excitotoxicity, while under-stimulation can cause cognitive dysfunction. This turns the use of the NMDAR as a drug target into a balancing act. The NMDAR modulators D-serine and glycine are used to stimulate the receptors in patients with schizophrenia [251] and multiple synthetic blockers (competitive and non-competitive antagonists) were designed to compensate for the hyper-activation of the NMDARs in the brain. [197,252] In addition to the receptor channel pore and glycine/glutamate binding sites, the receptors containing GluN2A and 2B subunits are equipped with several binding sites for allosteric modulators, including Zinc, ifenprodil, and polyamines (**Figure 5**). Even through these extracellular allosteric modulatory binding sites offer novel opportunities for therapy approaches, many compounds have failed in clinical trials because of their side effects. The most promising candidates are those with subunit selectivity (*e.g.* GluN2B subunit), reversible channel blockers (*e.g.* Memantine), and activity–dependent blockers. [197]

4.5.4. Keep dementia in mind - Memantine

Over-activation of NMDARs is associated with a variety of neurodegenerative disorders, such as dementia, Huntington's, and Parkinson diseases. [253-255] Therefore, NMDARs have been of interest as a promising drug target for years. Unfortunately, attempts to use NMDARs antagonists in multiple clinical trials have often failed because of their deleterious and repressive side effects. [253,256,257] One of the inhibitors with approval in the US and in Europe is Memantine (1-amino-3,5-dimethyl-adamantane) (**Figure 6**). It is clinically used for the treatment of moderate to severe forms of Alzheimer's disease. [183,254,258] Originally, Memantine was synthesized as a precursor molecule for a compound (N-arylsulfonyl-N'-3,5-dimethyladamantylurea) to lower blood sugar levels by Eli Lilly. [255,259] Nine years later, in 1972, Merz and Co. reported that Memantine may be used for the treatment of diseases of the central nervous system and they filed a patent. [255,260,261] After another ten years of research several groups showed that the therapeutic effects of the compound were caused from the NMDAR antagonism. [262-266] Besides the pathological over-activation present in various diseases, exceeding inhibition also affects the glutamate-mediated synaptic transmission, thereby critically affecting cognitive function, memory formation, and synaptic plasticity. [257] Compared to the other non-competitive NMDAR antagonists as

dizocilpine ((5S,10R)-(+)-5-Methyl-10,11-dihydro-5H-dibenzo[a,d] cyclohepten-5,10imine), the open channel blocker Memantine has special binding properties: the binding site of Memantine is at the asparagine-residues in the M2 loop region of GluN1 and GluN2 subunits. The channel needs to be open to bind and block the NMDAR. After the agonist dissociates from its binding site, the receptor gets deactivated and Memantine remains partial trapped inside the channel pore. The naturally occurring NMDAR antagonist Mg^{2+} has a highly similar mechanism of action. [254] The advantage of Memantine over the other open channel blockers is mainly based on its pharmacological properties and not the partial trapping: it has a low affinity and a fast dissociation rate constant (k_{off}) of around 0.2 s^{-1}. Furthermore, the affinity is NMDAR subunit specific and the degree of inhibition depends on agonist concentration. At a high agonist concentration and receptor activity, the probability of a Memantine molecule staying inside the channel pore increases. [255] As a result, Memantine does not affect normal synaptic transmission under physiologically conditions, but inhibits receptors only when pathological over-activated. [254] Furthermore pharmacokinetics of Memantine contributes to its clinical efficiency and the oral application improves the compliance. The bioavailability is almost 100% and plasma levels reach the peak concentration three to eight hours after the intake. It is eliminated mainly by the kidneys as uncharged substance with a total clearance of 170 ml/min/1.73 m^2 (glomerular filtration rate at normal kidney function). Cytochrome P450 interactions have not been described so far and the half-life is between 60-100 hours. [254,267]

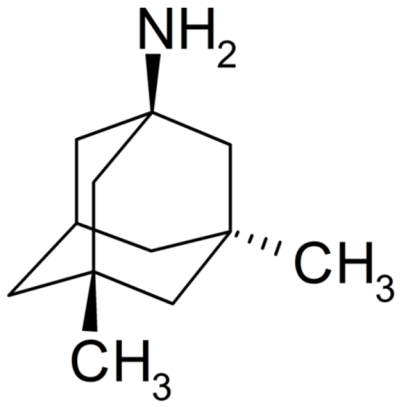

Figure 6: Structure of Memantine. Structure of the non-competitive channel blocker Memantine with the same binding site inside the pore loop as magnesium.

Memantine got the approval for the treatment of mild to severe Alzheimer's disease in Europe (2002) and the US (2003) after successful clinical trials demonstrated the neuroprotective efficacy. [255,257,268] Usually, it is administrated at 10-20 mg per day, which results in concentrations of < 1 µM in the cerebrospinal fluid. Those levels are

far below the effective level at any other target (low off-target toxicity). [183,265,269,270] Because of the pharmacological properties and the neuroprotective effects, Memantine was used as a potential candidate for clinical trials in both neurodegenerative and psychiatric disorders. Even in child and adolescent psychiatry studies for the off-label use have been performed, including the fields of autism spectrum disorder, attention deficit hyper-activity syndrome, and obsessive compulsive disorder. [271,272]

4.5.5. Forget memory formation - NMDARs in non-excitable tissues as potential drug targets

Although NMDARs are mostly studied in neuronal cells, it has been shown that the receptors are present in several other tissues, including osteoclasts and osteoblasts as well as in kidney tissue. [169,273,274] Furthermore, functional NMDARs were reported to be present in various cells originating from hematological lineages, such as leucocytes, platelets, and red blood cells. [3,172,275]

The presence of NMDARs was shown in rat erythrocytes in 2010 by our laboratory, [4] while Eaton *et al*. [276] have already demonstrated in the 1970s that sickle cell erythrocytes exhibit elevated Ca^{2+}. These two findings laid the foundation for the study of the NMDAR in SCD patients' erythrocytes. As enhanced Ca^{2+} influx is a major trigger in the pathophysiology of sickle cell anemia, the possible involvement of NMDAR in Ca^{2+} homeostasis, the potential as a novel drug target, and the preclinical safety-assessment of Memantine, making it a candidate for clinical trials to treat SCD will be one of the main parts of this study. Therefore the following chapters will cover some aspects of sickle cell anemia, its pathophysiology, epidemiology, and therapeutic strategies for its treatment.

4.6. Sickle cell anemia

Sickle cell anemia is one of the most common inherited disorders worldwide. [277] The physician James Herrick [278] described the typically sickle-shaped red blood cells

(Figure 7) for the first time in 1910. In 1942, Linus Pauling and colleagues [279] introduced the term molecular disease for SCD. Thirteen years, later Vernon Ingram [280] showed that a single point mutation in the hemoglobin gene is responsible for the devastating disease. However, even after decades of intensive research, no sufficient therapy for this severe disease has been developed. [277]

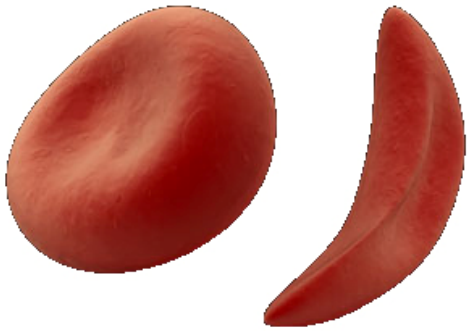

©2013 Georgia Regents University

Figure 7: Typical sickle-shape erythrocyte. Red blood cells of a sickle cell anemia patient.

As gene therapy is not available and bone marrow transplantation is expensive, finding a potential target that may relieve the symptoms of SCD offers great opportunities for the development of new therapeutic strategies. Especially, if the new treatment would be a drug, that is already on the market for several years (new indication/off-label use).

4.6.1. Genotypes and phenotypes of sickle cell anemia

The term “sickle cell anemia” includes all genotypes with at least one HbS gene. Next to the most common homozygous HbS/S genotype, there are several other genotypes (most common listed in **Table 3** [277,281]). The different genotypes and mutations affect severity of the disease. Furthermore it has been shown that there is heterogeneity in both the manifestation and the progress of SCD. [282] Several polymorphisms have been linked to the severity and complications (such as polymorphism in the promoter of the ɣ-globin or in the *BCL11A* gene). [283,284] Even less characterized than the influence of polymorphisms are the effects of environmental factors on the SCD progression.

Table 3, Most common genotypes of sickle cell anemia

Genotype	Phenotype	Characteristics
HbS/S	Severe	Most common form, β6Glu>Val/β6Glu>Val
Severe HbS/β^{+} thalassemia	Severe	Highest prevalence in Eastern Mediterranean and India, small amount of HbA,
HbS/β^{0} thalassemia	Severe	Highest prevalence in Eastern Mediterranean and India
HbS/O Arab	Severe	Relatively rare, present in north Africa and Middle East, β6Glu>Val/β121Glu>Lys
HbS/D Punjab	Severe	Highest prevalence in Northern India, β6Glu>Val/β121Glu>Gln
HbC/S Antilles	Severe	Very rare, β6Glu>Lys/β6Glu>Val, β23Val-Ile
HbS/C	Moderate	25-30% of all cases in Africa, β6Glu>Val/β6Glu>Lys
Moderate HbS/β^{+} thalassemia	Moderate	Highest prevalence in Eastern Mediterranean
HbA/S Oman	Moderate	Very rare double mutation, β^{A}/β6Glu>Val/β121Glu>Lys
Mild HbS/β^{++} thalassemia	Mild	16-30% HbA present
HbS/HbE	Mild	Highest prevalence in South East Asia, β6Glu>Val/β26Glu>Lys
HbS/HPFH	Mild	Large deletions in β-globin

4.6.2. Pathophysiology

A mutation in the β-globin gene causes the monogenic disorder. The 17th nucleotide is exchanged from thymine to adenine, leading to the replacement of a glutamic acid by a hydrophobic valine. [285] During deoxygenation of erythrocytes, the hydrophobic pockets are exposed to each other and the polymerization of β1- and β2-globin chains is initiated. The probability to induce irreversible polymerization of HbS in a RBC depends on the cell volume, the HbS concentration, the amount of fetal hemoglobin (HbF), and the extent of deoxygenation. The HbS polymers promote further dehydration, endothelial dysfunction, impair cytoskeletal stability, and decrease cell flexibility. [277,285,286]

Accumulation of sickled erythrocytes leads to a variety of severe pathophysiological processes and complications. Two of the main triggers of all complications are hemolysis and vaso-occlusion. They can lead to such complications as acute chest syndrome, pulmonary hypertension, acute pain crisis, leg ulceration, priapism, renal damage, and stroke. [277,287] Next to the rigid and sickled erythrocytes, inflammation is the second factor that drives vaso-occlusion. The inflammatory meditated aggregation of RBCs and leucocytes leads to an enhanced RBC-leucocyte-endothelial adhesion, resulting in vascular obstruction. [288-290] The episodic occlusion mainly affects the microcirculation and leads to ischemia and endothelial dysfunction after reperfusion. [277] The tissue damage produces oxidative stress and a further release of inflammatory cytokines that increases expression of adhesion molecules and the vaso-occlusion. [286] The consequence of those repetitive vaso-occlusion crises can

provoke, among others, acute chest syndrome or fat embolization in lung and bone marrow. [277,282] Enhanced hemolysis in SCD patients leads not only to chronic anemia, oxidative stress, and fatigue, it also affects the progressive vasculopathy. [277,291-293] Free hemoglobin is another factor which has an important role in the pathophysiology. The potent NO binder hemoglobin, disrupts not only the cytoskeleton, it decreases NO, and produces free radicals (ROS). [294] Furthermore, free iron increases ROS production (H_2O_2 and hydroxyl radicals), that further decreases NO bioavailability and therefore inhibits the NO-signaling in endothelial cells. [295,296] As NO acts as a vasodilator, inhibits platelets activation, and suppresses the transcriptional expression of adhesion molecules (such as spectrins and vascular cell-adhesion molecule-1 (VCAM-1)); the depletion of NO is crucial for the progression of SCD. Furthermore, during hemolysis, the substrate for NO production (arginine) is depleted by the release of the enzyme arginase. [297-300]

4.6.3. Cell heterogeneity

RBC heterogeneity is more pronounced in sickle cell anemia patients than in healthy subjects. [301] Blood of patients is enriched with both very dense and low-density RBCs. Part of this difference is due to the low activity of K^+-Cl^- co-transporter in low density RBCs and the high activity in dense RBCs. [132,302] In contrast, in healthy cells, reticulocytes along with old cells are found in the dense RBC fraction, suggesting that young RBCs are prone to dehydration. [303] The mechanism of the rapid dehydration assumes the activation of either K^+-Cl^- co-transporter or the Gardos channel and an enhanced Ca^{2+} influx into to young cells.

4.6.4. Epidemiology

Over 275'000 children are born with the HbS mutation every year and millions of people are affected worldwide. [304-306] Besides the genetic advantage in malaria-endemic regions, migration is the second factor for the global distribution of SCD. [277] In 1954, A.C. Allison [307] suggested for the first time that HbS carrier have a survival advantage after a *Plasmodium falciparum* infection. By now, the hypothesis of a balanced polymorphism has been confirmed in various studies. [308-310] High frequency of the HbS

allele appears in three regions in Africa (Senegal, Benin, and Bantu) and the Arab-India region (**Figure 8**). [287]

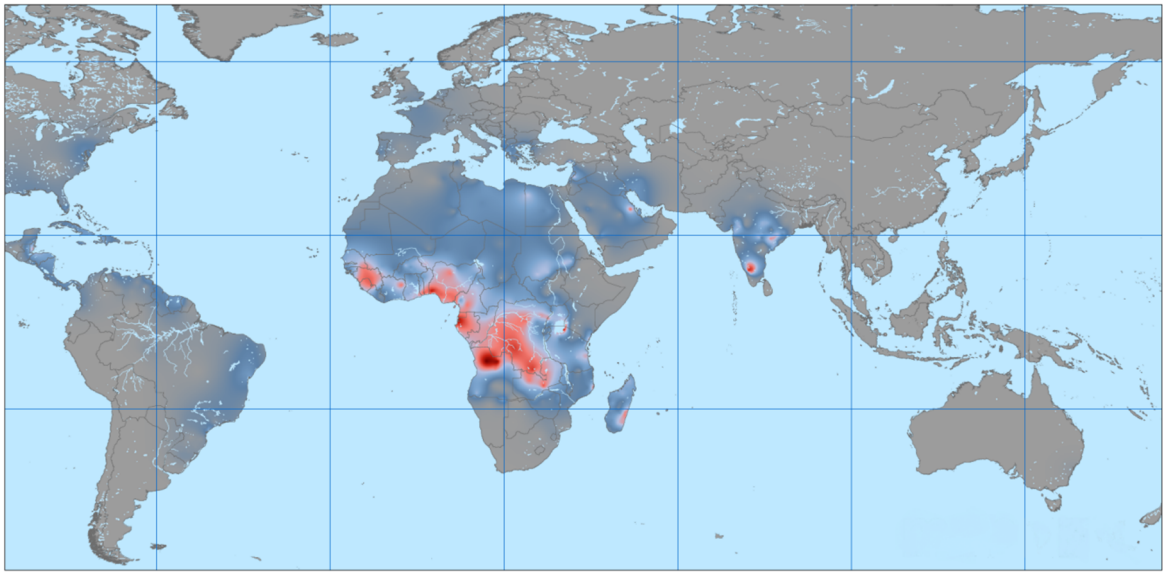

Figure 8: Map of the estimated sickle cell allele frequency [315] (©2010 Malaria Atlas Project). Distribution of the sickle cell allele (HbS) frequency. Due to migation, the HbS/S frequency is further increased during the next decades in Europe and North America.

About 80% of all births with HbS/S worldwide have been born in the sub-Saharan region. [277,311] The number of affected births in the US (around 1800) and in Europe (around 1300) every year has been increasing steadily over the past years, and SCD gets more and more attention. [305,306,312-314]

4.6.5. Therapeutic strategies

Even after intensive years of research, there is still no therapy on the market that targets specifically the pathophysiology of SCD. By now, blood transfusion and iron chelation, the treatment with hydroxyurea, and the management of the complications are the main therapeutic options.

4.6.5.1. Blood transfusion and iron chelation

Blood transfusion is one of the major therapeutic options for acute and chronic complications in SCD (**Table 4**). [277] Besides the reduction of the HbS percentage and

the anemic condition, transfusions can improve health conditions and prolong the patient's life span. [277,316] Iron chelation and erythocytapheresis have increased the efficacy of transfusion and reduced the risks of complications. [316] Iron overload is one major complication in SCD patients with sporadic and frequent blood transfusions: [317] Intermittent transfusions and increased hemolysis are the causes of this iron overload. In contrast to thalassemia major patients, SCD patients tend to show a lower risk for iron overload because of the different transfusion schemata and decreased basal iron levels. [318] Furthermore, through hemolysis, a substantial amount of the iron gets extracted via urine (15 mg/d). [318-320] If Iron accumulation occurs it affects mainly the liver and can lead to cirrhosis. [321,322] To avoid the adverse effects of iron overload under transfusion therapy, iron chelators, such as Deferiprone or Deferoxamine are used additionally. [323,324] Alloimmunisation to erythrocyte antigens is the other main complication of transfusion therapy. [325] Blood group genotyping for better antigen-matched erythrocytes will probably decrease alloimmunisation in the near future. [316,325-327]

Table 4. Indication for blood transfusion [277]

Acute transfusion	Repetitive transfusion
Acute chest syndrome	Recurrent acute chest syndrome
Acute exacerbation of anemia	Progressive organ damage
Stroke or multiorgan failure	Stroke prevention
Pre-operative	Failure of Hydroxyurea treatment

4.6.5.2. Hydroxyurea

Hydroxyurea (HU) is still the only drug approved in the US and Europe for SCD treatment. Although the complete mechanism of action is still not fully understood yet, it has been shown that HU up-regulates HbF and thereby reduces the hemoglobin polymerization. The cytotoxic drug inhibits the ribonucleotide reductase and arrests the cell cycle in the G1-S phase. [328,329] Compared to other cytotoxic drugs, HU has a much lower toxicity with short-term myelosuppression as the main adverse effect. [330] It has been demonstrated in several studies and meta-analyses that HU reduces the frequency of pain crises, hospitalization, and transfusions. But there are two major concerns with HU: the long-term toxicity is not yet fully understood and HU has not been efficient enough in all SCD patients. [110,282,287,330-333]

4.6.5.3. Management of complications

Sickle cell anemia and irreversible sickled erythrocytes lead to a wide range of complications, morbidity and a higher mortality. [277,282,334] Vaso-occlusion and acute pain crises are the most frequent complications and causes of hospitalizations. The management of acute pain crisis is quite limited and opiate analgesia is mainly used. [335-337] Acute chest syndrome is caused by vaso-occlusion, fat embolism, and infarction in the lung. Besides acute pain crises, acute chest syndrome causes second most hospitalization. [338] During the alveolar pulmonary infiltration, respiratory failure occurs and can lead to death. [339] Transfusions, bronchodilators, and antibiotics are used to treat those patients. [340] Elevated pulmonary artery systolic pressure and pulmonary hypertension can be observed 20-30% of patients, which increase the risk of death significantly. [341] Several approaches have been used in clinical trials for pulmonary hypertension, including phosphodiesterase-5 inhibitors, prostaglandin analogues, and endothelin receptor antagonists. [277] Another cardiopulmonary risk factor for high mortality is diastolic dysfunction. Preventive echocardiographic screenings to assess the risk factors is recommended in adult SCD patients. [342] Especially in developed countries, infection increases morbidity and mortality of children with SCD. Antibiotic prophylaxis and vaccination against *H influenza* or *S pneumonia* can reduce the risk of death in children. [277,343] Neurological complications and strokes are mostly associated with vaso-occlusive events in the distal internal carotid and middle cerebral arteries. They occur in 7-8% of all children with SCD. [277,344] Regularly blood transfusions (reduction of HbS to < 30%) and preventive transcranial doppler screenings reduce this frequency significantly. [345] The physiological conditions occurring in the kidneys (low pH, high osmolality, and low oxygen partial pressure highly) favor induction of sickling and lead to vaso-occlusive crises, papillary necrosis, and renal complications. [277,346] Sickle cell anemia manifests itself with plenty of other complications, including priapism, leg ulcers, and retinitis proliferans. Taken all of these complications together, SCD causes chronic organ damage and reduces the patient's life span. Therefore several general and specific therapeutic approaches have been used for the management and treatment (selection is listed in **Table 5**). Despite all of the efforts and progress made during the last years, there is still a strong need for new, efficient, and inexpensive therapies.

Table 5. Therapeutic approaches for the treatment of sickle cell anemia [277,287,347]

Target or complication	Approach	Examples
Inflammatory response	Corticosteroids, phospholipase A2 inhibitors	Dexamethasone, varespladib
Blood rheology	Inhibition of adhesion, inhibition of endothelin receptors	Bosentan, GMI-1070, Poloxamer-188, herparin, sulfasalazine
Tissue damage	Reduce oxidative stress	N-acetyl cysteine, glutamnie
HbF	Increase of HbF	Pomalidomide, Decitabine, butyrate
Dehydration (RBC)	Cation channel inhibition	Senicapoc, magnesium, zinc, dipyridamole
Nitric oxide	Increase NO	Nitric oxide, arginine, sildenafil, statins
Priapism	Adrenergic agonists	Phosphodiesterase-5 inhibitors, Finasteride
Retinitis proliferans	Screening and laser photocoagulation	-
Hyposplenism	Screening, prophylaxis	Prophylactic antibiotics
General	Stem-cell transplantation, gene therapy	-

5. Aim and Publications

5.1. Aim of the work

The main focus of the study was to characterize the expression and the function of NMDAR in erythropoietic precursor cells of both healthy subjects and sickle anemia patients. After the *ex vivo* erythropoiesis system was established, the mRNA expression pattern (*GRIN* genes) and the protein expression (GluN) of the NMDAR subunits was studies first. Nonetheless, it was crucial to verify the expression pattern during erythropoietic maturation of the NMDAR on functional level as well. Therefore the second part of the study was focused on the function of NMDARs in erythroid cells and the validation of the expression pattern on the functional level by measuring NMDA induced whole-cell currents and NMDA mediated Ca^{2+} influx.

The three key findings of the work are:

(i) Characterization of the temporal expression pattern for the *GRIN* genes in differentiating EPCs and monitoring the function of the NMDARs in the erythroid precursor cells of healthy humans and SCD patients;

(ii) Assessment of the impact of the NMDAR on the regulation of intracellular Ca^{2+} and the functional plasticity of the receptor during erythropoietic maturation, including inter-individual variability in the receptor expression pattern;

(iii) Safety assessment for the use of the NMDAR antagonist Memantine for the treatment of sickle cell anemia.

5.2. N-methyl-D-aspartate receptors in human erythroid precursor cells and in circulating red blood cells contribute to the intracellular calcium regulation

Asya Makhro*, Pascal Hänggi*, Jeroen S. Goede, Jue Wang, Andrea Brüggemann, Max Gassmann, Markus Schmugge, Lars Kaestner, Oliver Speer, and Anna Bogdanova.

* Asya Makhro and Pascal Hänggi contributed equally to this work.

Am J Physio Cell Physiol. 305: C1123-C1138, 2013
Submitted 31 January 2013; accepted in final from 16 September 2013

Am J Physiol Cell Physiol 305: C1123–C1138, 2013.
First published September 18, 2013; doi:10.1152/ajpcell.00031.2013.

N-methyl-D-aspartate receptors in human erythroid precursor cells and in circulating red blood cells contribute to the intracellular calcium regulation

Asya Makhro,[1,4]* Pascal Hänggi,[1,2,4]* Jeroen S. Goede,[3,4] Jue Wang,[5] Andrea Brüggemann,[6] Max Gassmann,[1,4] Markus Schmugge,[2,4,7] Lars Kaestner,[5] Oliver Speer,[2,4,7] and Anna Bogdanova[1,4]

[1]*Institute of Veterinary Physiology, Vetsuisse Faculty, University of Zurich, Zurich, Switzerland;* [2]*Division of Hematology, University Children's Hospital, Zürich, Switzerland;* [3]*University Hospital Zurich, Division of Hematology, Zurich, Switzerland;* [4]*Zurich Center for Integrative Human Physiology, University of Zurich, Zurich, Switzerland;* [5]*Institute for Molecular Cell Biology, Medical Faculty, Saarland University, Homburg/Saar, Germany;* [6]*Nanion Technologies, München, Germany; and* [7]*Children's Research Center, University Children's Hospital, Zürich, Switzerland*

Submitted 31 January 2013; accepted in final form 16 September 2013

Makhro A, Hänggi P, Goede JS, Wang J, Brüggemann A, Gassmann M, Schmugge M, Kaestner L, Speer O, Bogdanova A. *N*-methyl-D-aspartate receptors in human erythroid precursor cells and in circulating red blood cells contribute to the intracellular calcium regulation. *Am J Physiol Cell Physiol* 305: C1123–C1138, 2013. First published September 18, 2013; doi:10.1152/ajpcell.00031.2013.—The presence of *N*-methyl-D-aspartate receptor (NMDAR) was previously shown in rat red blood cells (RBCs) and in a UT-7/Epo human myeloid cell line differentiating into erythroid lineage. Here we have characterized the subunit composition of the NMDAR and monitored its function during human erythropoiesis and in circulating RBCs. Expression of the NMDARs subunits was assessed in erythroid progenitors during ex vivo erythropoiesis and in circulating human RBCs using quantitative PCR and flow cytometry. Receptor activity was monitored using a radiolabeled antagonist binding assay, live imaging of Ca^{2+} uptake, patch clamp, and monitoring of cell volume changes. The receptor tetramers in erythroid precursor cells are composed of the NR1, NR2A, 2C, 2D, NR3A, and 3B subunits of which the glycine-binding NR3A and 3B and glutamate-binding NR2C and 2D subunits prevailed. Functional receptor is required for survival of erythroid precursors. Circulating RBCs retain a low number of the receptor copies that is higher in young cells compared with mature and senescent RBC populations. In circulating RBCs the receptor activity is controlled by plasma glutamate and glycine. Modulation of the NMDAR activity in RBCs by agonists or antagonists is associated with the alterations in whole cell ion currents. Activation of the receptor results in the transient Ca^{2+} accumulation, cell shrinkage, and alteration in the intracellular pH, which is associated with the change in hemoglobin oxygen affinity. Thus functional NMDARs are present in erythroid precursor cells and in circulating RBCs. These receptors contribute to intracellular Ca^{2+} homeostasis and modulate oxygen delivery to peripheral tissues.

NMDA receptors; calcium; red blood cells; erythroid precursors

INTRACELLULAR CALCIUM IS A regulator of multiple processes in mammalian red blood cells (RBCs; Ref. 6). Functions of key glycolytic enzymes are calcium sensitive (e.g., Refs. 2, 36, 75). Increase in the intracellular calcium to 1 μM and more causes activation of Ca^{2+}-dependent K^+ channels (Gardos channels), loss of KCl from the cells, cell shrinkage, and dehydration (37). Along with the changes in cell volume and cation content, accumulation of Ca^{2+} was shown to facilitate intercellular adhesion (60). Upregulation of the intraerythrocytic Ca^{2+} results in activation of calpain and promotes cleavage of cytoskeletal proteins (actin, spectrin, ankyrin, and band 4.1 protein) as well band 3 protein and the plasma membrane Ca^{2+} pump (PMCA; Ref. 6). Thus the cell membrane becomes destabilized in RBCs upon Ca^{2+} overload. The changes in rheology associated with cell dehydration and proteolysis of cytoskeletal proteins are followed by the alteration of hemodynamics. Uncontrolled Ca^{2+} accumulation upon treatment of RBCs with Ca^{2+} ionophore A23187 was reported to cause phosphatidylserine (PS) exposure to the outer membrane leaflet (16). This process may contribute to enhanced RBC clearance by macrophages in patients with a number of diseases. Apart of PS exposure, high intracellular Ca^{2+} may promote oxidative stress due to the activation of NADPH oxidase and nitric oxide synthase in its uncoupled mode (20, 51). Whereas extracellular Ca^{2+} concentration in the plasma reaches 1.8 mM, the intracellular free Ca^{2+} level is precisely controlled and does not exceed 50–100 nM in healthy human RBCs (64). This impressive transmembrane gradient is maintained by an active Ca^{2+} extrusion via the PMCA and low passive permeability of the RBC plasma membrane for Ca^{2+} which is mainly mediated by ion channels (28). PMCA in RBCs has been well characterized, whereas our knowledge on the ion transport systems mediating Ca^{2+} uptake in human RBCs is rather limited. Among the transport systems contributing to Ca^{2+} uptake into human RBCs are several classes of cation channels (28). An increase in Ca^{2+} "leak" and the concomitant elevation of intracellular Ca^{2+} concentrations are typical for RBCs of patients with phosphofructokinase deficiency (75), thalassemia (7), and sickle cell disease (7, 70). The importance of electrogenic Ca^{2+} uptake pathway (P_{sickle}) in promoting sickle cell transformation upon deoxygenation has been acknowledged (8, 70, 72). The molecular identity of the nonselective cation channels, including those mediating P_{sickle}, remains unknown.

Recently, we have reported the presence of *N*-methyl-D-aspartate receptors (NMDARs) in the plasma membrane of rat RBCs and in the human erythroid precursor cell (EPC) line UT-7/Epo (38). These receptors are ligand-gated, nonselective cation channels showing a 10-fold preference for Ca^{2+} over Na^+ or K^+ (12).

These receptors are comprised of four subunits of which eight different isoforms coded by independent genes have been described (68). Subunits NR1 and NR3A and B are binding glycine or D-serine whereas NR2A, B, C, and D interact with glutamate and its homologues homocysteine, homocysteic acid

* A. Makhro and P. Hanggi contributed equally to this work.

Address for reprint requests and other correspondence: A. Bogdanova, Institute of Veterinary Physiology, Vetsuisse Faculty, and Zurich Center for Integrative Human Physiology (ZIHP), Univ. of Zurich, Winterthurerstrasse 260,, CH-8057 Zurich, Switzerland (e-mail: annab@access.uzh.ch).

(HCA), or NMDA. Subunit composition defines gating properties and ion preferences of the channel, as well as its affinity to the agonists and antagonists. Whereas channels composed of NR1-NR2A/B generate large currents and deactivate quickly, the channels built up by the NR1-NR2D generate smaller currents and are slow-deactivating (10). Physiological role of the "inhibitory" NR3 subunits making the receptors in the brain glutamate insensitive are not well defined (52). Local expression pattern vary within the brain (21, 40). Apart of that in the brain NMDARs have been shown to be expressed in a number of nonneuronal tissues including the bone and the kidney (42, 57). Subunit composition, physiological function, and regulation of activity of these "atypical glutamate receptors" in megakaryocytes (19, 24) and in rat RBCs (38) have been reported. In rat RBCs activation of the NMDARs by administration of agonists triggered Ca^{2+} accumulation whereas exposure of the cells to antagonists on the contrary reduced the intracellular Ca^{2+} levels (38). Furthermore, activation of the receptor by glutamate, NMDA, or HCA triggered opening of the Gardos channel followed by cell shrinkage as well as activation of the endothelial nitric oxide synthase (38).

Herein we report the presence of NMDARs in membranes of EPCs and circulating RBCs of healthy human subjects. We characterize subunit composition of the receptor and explore its function and contribution to the maintenance of intracellular Ca^{2+} homeostasis and in regulation of hemoglobin oxygen affinity.

DESIGN AND METHODS

Human subjects. Our subject pool consisted of 36 adult subjects (Caucasians, both genders, median age 32.5; range 25–49) with no history of hematological disorders. Five to ten milliliters of venous heparinized blood were obtained after informed, written consent, in accordance with the Declaration of Helsinki, at the Divisions of Hematology of the University Hospital and the Children's Hospital Zurich as well as at the Medical Faculty, Saarland University, Homburg/Saar, Germany and processed immediately. The Institutional Ethics Board of the University Hospital in Zurich and that of the Canton of Zurich as well as the Ethics committee of the medical association of the Saarland approved the study protocol.

RBC purification for flow cytometry and quantitative real-time PCR. Blood was washed three times with 10 ml of PBS containing 2 mM EDTA and separated in a Ficoll-Hypaque gradient (GE Healthcare, Glattbrug, Switzerland) to remove mononuclear cells and platelets. Reticulocytes were then filtered through a leuco-depletion filter (Purecell Neo; Pall, Basel, Switzerland). The leuco-depleted reticulocytes were washed and resuspended in PBS/EDTA. The purity grade of reticulocytes was assessed by an automated blood cell analyzer (Sysmex Digitana, Horgen, Switzerland), as well as by flow cytometry for surface expression of CD45 with fluorescence-labeled antibodies (Becton Dickinson, Rotkreuz, Switzerland). In addition, depletion of leukocytes and platelets and enrichment of late EPCs and reticulocytes were analyzed by quantitative real-time PCR (qPCR). The pan-leukocyte marker CD45 was used as a white blood cell (WBC) marker, and mRNAs encoding hemoglobin subunits were chosen to detect late EPCs and reticulocytes.

Ex vivo hematopoiesis. EPCs were cultured using a two-phase liquid system as described elsewhere (41, 42). At phase I mononuclear cells were isolated from peripheral blood according to the protocol provided by the GE Healthcare producing Ficoll-Paque PLUS and seeded in StemSpan SFEM Medium supplemented with a cytokine mix supplements CC100 StemSpan (StemCell Technologies, Grenoble, France) and penicillin/streptomycin. Cells were maintained in phase I medium at a density of $0.1–1 \times 10^6$ cells/ml for 5 days. Thereafter, nonadherent cells were reseeded in StemSpan SFEM Medium with 2% penicillin/streptomycin, 20 ng/ml SCF, 1 U/ml Epo, 5 ng/ml IL-3, 2 μM dexamethasone, and 1 μM β-estradiol and maintained in it for 6, 12, or 18 days.

mRNA isolation and qPCR. Total RNA was purified from cells by the TRIzol/glycogen/osopropanol. GRIN1, GRIN2A, GRIN2C, GRIN2D, GRIN3A, GRIN3B, and CD45 mRNAs, as well as control GAPDH mRNA, were quantified using the TaqMan Gene Expression Kits acquired from Applied Biosystems (Rotkreuz, Switzerland). The following primers were used: Hs02758991_g1 Gapdh: GTCCCCATCCCAACTCAGCCCCCAA; Hs00609557_m1 Grin1: TCATCTCCAGCCAGGTCTACGCCAT; Hs00168219_m1 Grin2a: GGAATGGGAAAAGGTGGGCAAGTGG; Hs00168230_m1 Grin2b: TGGGAAAGGGTGGGGAAGTGGAAAG; Hs01016626_m1 Grin2c: TGGCTTTCAGCAGGGGCATCTACAG; Hs00367969_m1 Grin2d: CAGCTCAAGGCAGGGAAGCTGGACG; Hs00370290_m1 Grin3a: ACATGACCCCAAGTTACATCATCCT; and Hs00367969_m1 Grin3b: GCTTCTTGGCACGGTTCCTGGCCAA.

Flow cytometry for detection of NMDAR abundance and distribution in EPCs. Staining of EPCs for the NMDAR subunit-specific antibodies was performed as follows. Cells were washed once with working solution (PBS supplemented with 0.1% BSA) and centrifuged for 30 s at 3,000 rpm. The supernatant was discarded and the cells resuspended in working solution and fixed with 0.05% glutaraldhyde solution prepared in PBS for 9 min. Cells were washed twice, supernatant was discarded, and cells were resuspended in Tween solution (working solution supplemented with 0.1% of NaN_3 and 0.1% of Tween20) to permeabilize them. Before the primary antibody was added, the EPCs were washed once and resuspended in working solution.

After incubation with primary antibodies for 15 min in the darkness at room temperature, the cells were washed once and exposed to the allophycocyanin-conjugated secondary antibodies for 15 min in the darkness. The following antibodies were used: IgG1 mouse anti human Anti-CD45 PerCP, clone 2D1 (BD, San Jose, CA) as a marker of WBCs; IgG2a mouse anti-human CD71, clone M-A712 FITC-conjugated (BD) as a marker of reticulocytes; anti-NMDAε3 (NR2C), goat polyclonal IgG, no. sc-1470; anti-NMDAε4 (NR2D), mouse monoclonal IgG, no. sc-178221; anti-NR3A (NR3A), goat polyclonal IgG no. sc-51160; and anti-NR3B, goat polyclonal IgG, no. sc-55731. All primary antibodies against the NMDAR subunits used were provided by Santa Cruz Biotechnology (Dallas, TX) and used at a final concentration of 0.2 μg/ml. Allophycocyanin-cojugated AffiniPure F(ab')2 Fragment Donkey Anti-Goat IgG, Code 705–136-147, and allophycocyanin-cojugated AffiniPure F(ab′)2 Fragment Goat Anti-Mouse IgG, Code 155–136-146 were used as secondary antibodies at 1:625 and 1:2500 dilutions, respectively.

Stained cells were washed once with the working solution supplemented with 1% formaldehyde and resuspended in an appropriated volume of the working solution, and fluorescence intensity was measured using the BD Biosciences FACSCalibur flow cytometer (BD Biosciences). Cells stained with the secondary antibodies alone were used as a negative control. Data were analyzed by using FCS express software (De Novo Software, Los Angeles, CA). All chemicals were provided by Sigma-Aldrich (St. Louis, MO).

Fractionation of RBCs on Percoll density gradient. Fractionation of RBCs into light (L), medium (M), and dense (D) fractions was performed in 90% isotonic Percoll solution prepared by mixing a 90-ml aliquot of sterile Percoll (GE Healthcare; density 1.130 g/ml) with 10 ml × 10 PBS (Sigma-Aldrich) and 11 ml × 1 PBS (Sigma-Aldrich). Blood or RBC suspension was prefiltered on cellulose filter to remove WBCs, platelets were as described elsewhere (5), and 1.0–1.5 ml was overlaid then over 12.5 ml isotonic Percoll and centrifuged using Sorvall RC 5C plus centrifuge equipped with a SM-24 rotor at 4°C for 30 min at 45,000 *g*. The obtained L, M, and D fractions of RBCs were collected and washed three times with the

incubation medium containing the following (mM): 145 NaCl, 4 KCl, 10 glucose, 10 Tris·HCl, 0.1 EDTA, and 0.1% BSA (pH 7.4 at room temperature). Therefore, the obtained RBCs were used for detection of the number of [^{3}H]MK-801 binding sites or for fluorescence live imaging. The amount of reticulocytes in L, M, and D fractions was 18.1 ± 8.2, 1.5 ± 4, and 0.89 ± 0.08% respectively, with mean reticulocyte counts of 1.9 ± 0.6%. Mean cell volume (MCV) of cells in fractions was 103.6 ± 1.9, 90.9 ± 0.7, and 82.6 ± 1.5 fl for the L, M, and D fraction, respectively, mean MCV being 86.5 ± 1.4 fl (means ± SD; Sysmex Digitana, Horgen, Switzerland).

Percoll solutions of lower density (82–86% Percoll) were used to monitor rapid changes in volume occurring within the M fraction containing the majority of mature RBCs in response to the NMDAR stimulation. Final ion composition in Percoll solution was adjusted to 145 mM NaCl, 5 mM KCl, 20 mM HEPES (pH 7.4 at room temperature), 10 mM glucose, and 2 mM $CaCl_2$. Control samples were agonists free. Stimulation of the NMDARs was performed by supplementation of Percoll solution with 200 μM of 1:1 NMDA-glycine mixture. Washed RBCs (0.5 ml packed cells per 12 mM of Percoll solution) were added to the Percoll solution, mixed with it and centrifuged for 2 min at 48,000 *g* at room temperature. Due to the interindividual variability in basal cell density and in the amplitude of responses, Percoll density was slightly adjusted for each of five healthy subjects tested to achieve better separation of the M fraction. In four out of five donors, the agonists-induced changes in RBC density developed within 2 min and were reversed already after 5 min of stimulation. In one subject the volume changes prevailed even 15 min after the onset of exposure to the agonists.

NMDAR activity measurements in circulating RBCs. Changes in the intracellular Ca^{2+} levels in RBCs caused by exposure to the NMDAR agonists or antagonists were monitored in L, M, and D fractions by means of microfluorescent live imaging using fluo-4 AM (Molecular Probes, Eugene, OR) as a marker (31). Loading of RBCs with the fluorescent dye (1–5 μM) was performed for 30 min at room temperature in the darkness. During loading, the cells were resuspended in the incubation medium supplemented with 0.1% BSA and 2 mM $CaCl_2$ to a density of ~4×10^6 cells/ml. Thereafter, the cells were placed in an imaging chamber and allowed to settle for 10 min. In experiments in which kinetics of responses of individual cells to the NMDA agonists and antagonists was monitored over time, the coverslip serving as a bottom of the imaging chamber was coated with polylysine to immobilize the cells. A series of images (bright field and fluorescent images excited at center wavelength of 480 nm with a half-width of 25 nm and a 510-nm longpass emission filter to reach maximal detection efficiency) were taken with a ×100 objective using Axiovert 200M microscope (Carl Zeiss, Jena, Germany). At least five images were taken before the addition of agonists or antagonists and used to calculate baseline levels of fluorescence. Solvent (incubation medium) addition was performed in control samples.

Calibration was performed using cells resuspended in calcium buffer containing 20–200 nM free Ca^{2+} (a set of $CaCl_2$-EGTA mixtures) in the presence of Ca^{2+} ionophore A23187 (10 μM) and the Ca^{2+} pump blocker sodium orthovanadate (4 mM). These cells were addressed to as calcium-clamped cells.

Analysis of the obtained images was performed using CellFinder program developed by Dr. M. Makhinya (Computer Vision Lab; ETH Zurich). This software was designed to detect the cell projection area as an indicator of cell volume, the average fluorescent intensity within this area corrected for the background fluorescence, and anisotropy (a longest to shortest diameter ratio).

Radiolabeled antagonist binding assay was used as an alternative approach to assess the number of active receptors per cell. [^{3}H]MK-801 is a specific NMDAR antagonist interacting with the channel pore of active receptors exclusively (18). The number of [^{3}H]MK-801 binding sites per cell in the absence or in the presence of a 200-fold excess of nonlabeled MK-801 was assessed for evaluation of specific and nonspecific binding.

Washed RBCs were incubated with [^{3}H]MK-801 (20 Ci/mmol; American Radiolabeled Chemicals) at a concentration of 5×10^{-7} mmol/ml (1 h, room temperature) in the presence of 300 μM NMDA and 100 μM Gly. Thereafter the cells were fractioned according to their density on 90% Percoll gradient (45,000 *g*, 30 min). L, M, and D fractions were collected, washed three times in *buffer 1* containing the following (in mM): 145 NaCl, 5 KCl, 10 glucose, 0.1 EDTA, 10 Tris·HCl (pH 7.4 room temperature) supplemented with 0.1% BSA, and lysed. One part of packed RBCs was mixed with 30 parts of lysis buffer containing 25 mM NaH_2PO_4 and 1 mM EDTA (pH 7.0 at 0°C) and incubated on ice for 30 min. Thereafter, RBC membranes were precipitated (45,000 *g* for 30 min at 4°C) and the amount of [^{3}H]MK-801 bound to the membranes was assessed using Packard 1600 TR liquid scintillation analyzer. The number of [^{3}H]MK-801 binding sites per cell was then calculated using the following equation:

$$N_{NR} = \frac{A_{cells}}{A_{sp}(MK-801) * N_A * N_{cells}}$$

N_{NR} is a number of NMDARs per cell, A_{cells} denoted activity of bound [^{3}H]MK-801 after nonspecific binding is subtracted [Bq] and A_{sp} stands for specific activity of the [^{3}H]MK-801 in [Bq/mmol], N_A is the Avogadro constant (6.022×10^{23} mol^{-1}), and N_{cells} are the amount of cells in the sample.

Whole cell currents were measured using a NPC-16 Patchliner (Nanion, Munich, Germany). The "pipette" solution contained the following (in mM): 50 KCl, 10 NaCl, 60 KF, 20 EGTA, and 10 HEPES (pH adjusted to 7.2 by KOH), while the bath solution contained the following (in mM): 140 NaCl, 4 KCl, 1 $MgCl_2$, 2 $CaCl_2$, 5 glucose, and 10 HEPES (pH adjusted to 7.4 by NaOH). NMDA, glycine, and MK-801 were added as indicated in the experiments. The pipette resistance was in the range of 3–5 MΩ, and the seal resistance was between 800 MΩ and 5 GΩ at a holding potential of −40 mV. Measurements were performed with fresh RBC samples from three healthy donors within 2–3 h after blood withdrawal.

pH measurements in RBCs and in RBC lysates. Shifts in the intracellular pH were monitored over 10 min using microfluorescence live imaging. RBC were washed three times in isotonic buffer containing the following (in mM): 15 NaCl, 5 KCl, 10 glucose, 20 HEPES-imidazol buffer, 0.1 EDTA, and 0.1% BSA. The cells were centrifuged and resuspended in the same buffer supplemented with 2 mM $CaCl_2$ and 2 μM of pH-sensitive fluorescent dye BCECF-AM and incubated for 45 min at 37°C in the darkness to achieve optimal dye loading. Some samples were supplemented with 50 μM of MIA during loading with the dye. The kinetics of the changes in BCECF fluorescence in response to the treatment with 300 μM of 1:1 NMDA-glycine mixture were recorded at 488-nm excitation and 535-nm emission wavelengths using Axiovert 200M fluorescent microscope (Zeiss). The images were taken in time laps mode at ×100 magnification at a constant rate of 1 frame per min. The obtained data were analyzed using CellFinder software. Fluorescent intensities were normalized to those at time zero (first frame) and expressed as changes compared with the readouts obtained for nontreated cells to correct for the BCECF photobleaching.

Calcium-induced changes in pH were monitored in fresh hemoglobin solution obtained by lysing 10 μl of packed RBCs in 5 ml of distilled water. Final hemoglobin concentration obtained that way was ~0.25 μM. Sodium chloride concentration was then adjusted to 150 mM, and 2,3-diphosphglycerate pentasodium salt (2-mM final concentration; Sigma) was added to it. These solutions were supplemented with various $CaCl_2$ doses (0–200 μM), and pH was measured at 37 ^{0}C using glass pH electrode of the ABL 700 blood analyzer (Radiometer). Thereafter, oxygen dissociation curves were recorded from these cell lysates as described below.

Hemoglobin oxygen dissociation curves. Oxygen affinity of hemoglobin was assessed using Hemox analyzer (TCS Scientific, New

Hope, PA). Measurements were performed in Ca^{2+}-clamped cells, in intact RBCs resuspended in buffer containing 2 mM $CaCl_2$, and in RBC lysates. Ten microliters of packed RBCs were added to 5 ml of buffer in the presence or absence of NMDAR agonists NMDA (300 μM) and glycine (100 μM). Oxygen dissociation curves were recorded at 30 or 37°C and P_{50} calculated from them using Hemox Analytical Software (HAS). Similar recordings were performed in cell lysates [10 μM of cells lysed in 5 ml H_2O supplemented with 150 mM NaCl, 2 mM 2,3-diphosphoglycerate (2,3-DPG), and various concentrations of $CaCl_2$] obtained as stated above after pH detection.

Statistical analysis. The obtained data were analyzed using GraphPad Instat v.3.0 (GraphPad Software,) and presented as means ± SE. Statistical significant differences were assessed using normality test followed by either one-way ANOVA test (when distribution was normal) or Kruskal-Wallis test (when normality of distribution cannot be confirmed) with the Bonferroni or Dunn's posttest correspondingly (accepted at $P < 0.05$).

RESULTS

Expression of the NMDAR subunits in erythroid progenitors during erythropoiesis. The number of functional NMDAR heterotetramers in the immortalized human erythroid cell line UT-7/Epo was estimated to be~350,000 copies per cell (38). We have then performed characterization of the expression pattern of NMDAR subunits during ex vivo erythropoiesis derived from peripheral stem cells and in circulating human RBCs. Subunit speciation of the NMDARs in human EPCs during their differentiation was monitored in the course of transformation from pluripotent precursor (*day 0*) cells through the proerythroblast (*day 6*) and basophilic and polychromatic erythroblast (*day 12*) stages to normoblasts and enucleated reticulocytes (*day 18*). Differentiation stages were verified morphologically (Fig. 1, *A–C*) as well as by expression of CD71 (Fig. 2). We have detected transcripts of the genes

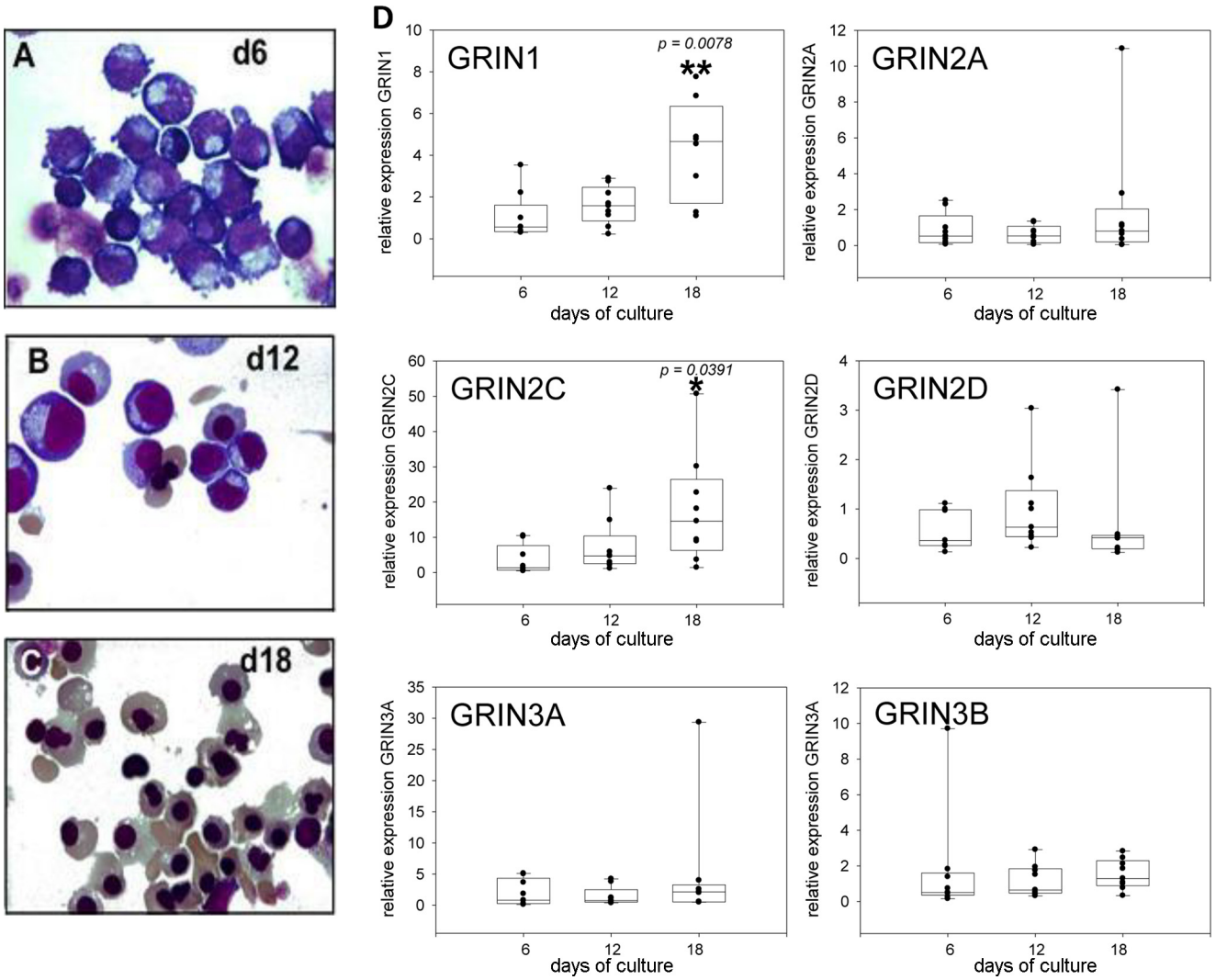

Fig. 1. Peripheral blood-derived erythroid cultures express *N*-methyl-D-aspartate receptor (NMDAR) subunits. Representative cytospins of erythroid cells on *day 6* (d6, *A*), *12* (d12, *B*), and *18* (d18, *C*). Cytospins were stained with May Grünwald Giemsa, and images were acquired with a Zeiss Axioskop2 microscope equipped with a Zeiss Plan-Apochromat ×63/1.4 oil immersion objective lens and a Zeiss AxioCam MRc digital camera. Images were recorded using Zeiss AxioVision AC release 4.5.0 software. *D*: relative amounts of the GRIN gene transcripts in erythroid precursor cells (EPCs) harvested at *day 6*, *12*, and *18* measured by TaqMan quantitative PCR. Values are represented as box plots of 9 erythroid cultures, each started with cells from a different donor. An overall comparison indicated significant increase in expression of GRIN1 and GRIN2C between the *days 6* and *18* in culture. *$P = 0.0391$; **$P = 0.0078$.

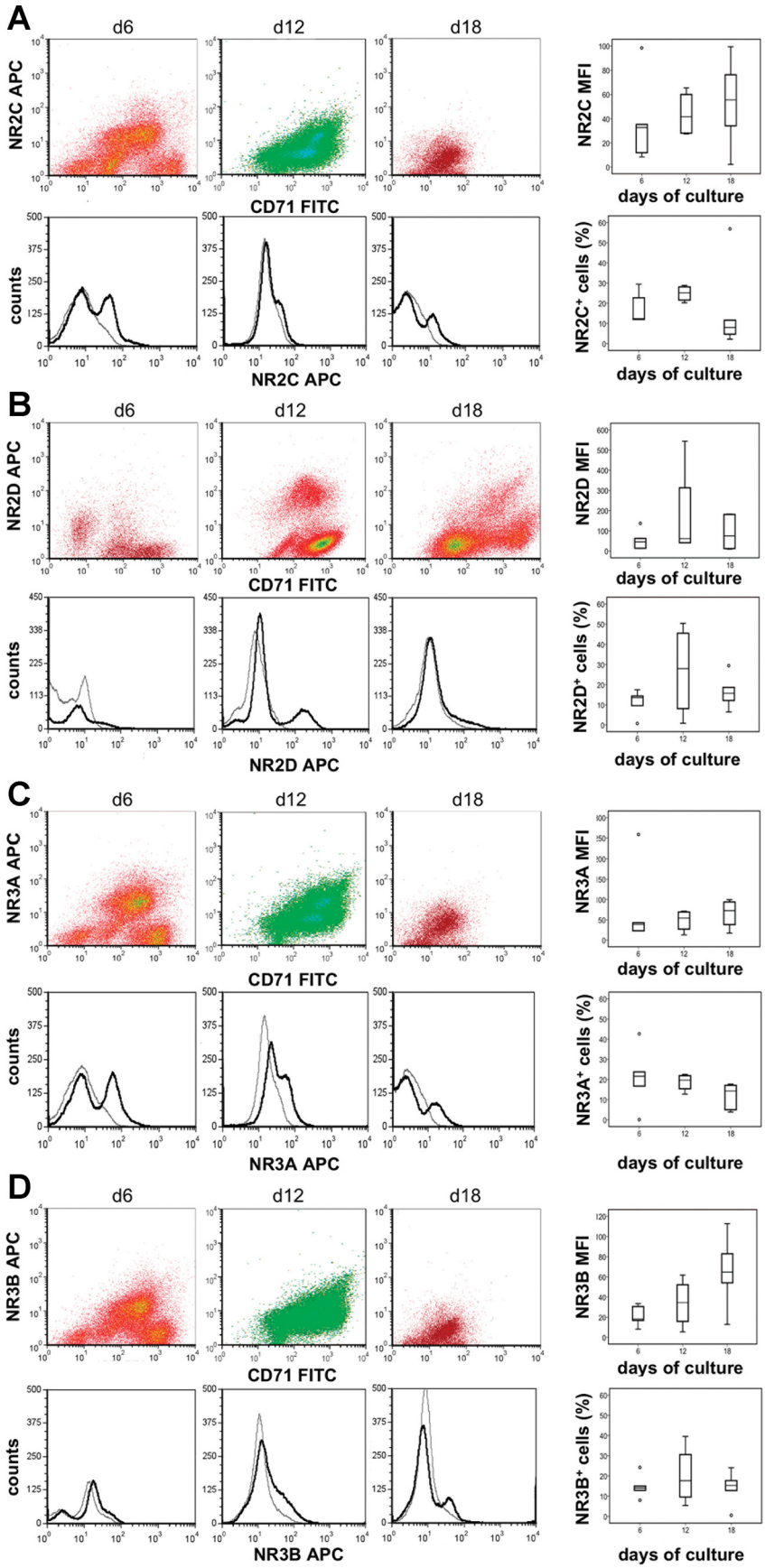

Fig. 2. Changes of protein levels of NMDAR subunits during erythropoiesis. Peripheral blood-derived erythroid cultures were analyzed by flow cytometry on *day 6* (d6), *12* (d12), and *18* (d18) after seeding. NMDAR subunit expression at various EPC differentiation states was assessed. Surface expression of CD71 (CD71 FITC) was used as a marker of EPCs in the presented dot blots. The number of cells expressing NMDAR subunits are shown as histograms. Grey plots show the signal obtained from staining with secondary APC-conjugated antibodies alone, and black plots show specific anti-NR-APC signal. The geometric mean fluorescence intensity (MFI) and the fraction of cells showing specific anit-NR-APC signal were analyzed from 60'000 cells each measurement and represented as box plots for the subunits NR2C (*A*), NR2D (*B*), NR3A (*C*), and NR3B (*D*). Values are represented as box plots of 9 erythroid cultures, each started with cells from a different donor ($n = 9$).

Table 1. *Expression of NMDAR subunits in WBCs*

Gene	ID*	Protein	ΔCt	ΔΔCt (fold mRNA expression compared with EPCs)
GRIN1	2902	NR1	19.8 ± 1.6	7.0
GRIN2A	2903	NR2A	15.8 ± 1.9	11.2
GRIN2B	2904	NR2B	18.8 ± 1.4	(Not expressed in EPCs)
GRIN2C	2905	NR2C	15.6 ± 1.8	0.7
GRIN2D	2906	NR2D	12.0 ± 0.9	11.0
GRIN3A	116443	NR3A	18.3 ± 2.3	1.0
GRIN3B	116444	NR3B	17.3 ± 1.6	10.8

Values are ± SE for 3 cultures, each started with cells from a different donor ($n = 3$). EPC, erythroid precursor cell. Relative amounts of transcripts of *N*-methyl-D-aspartate receptor (NMDAR) subunits were detected by TaqMan quantitative PCR. White blood cells (WBCs; predominantly monocytes) were obtained from mononuclear cells in culture and separated from the hematopoietic stem cells (HSC) at *day 3* of culturing as "adherent cell fraction." Individual values were normalized to GAPDH (ΔCt), and the individual fold change compared with the median ΔCt values of erythropoiesis at *day 6* was calculated (expΔΔCt, fold change in mRNA expression). Comparison with the values for mRNA expression in HSCs at *day 3* was not possible as too few cells were available at that time. GRIN2B expression in HSCs was fixed to 40 cycles. *NCBI gene ID.

GRIN1, GRIN2A, GRIN2C, GRIN2D, GRIN3A, and GRIN3B encoding NMDAR subunits NR1, NR2A, 2C, and 2D and NR3A and 3B in EPC at various stages of erythropoiesis (Fig. 1; Table 1). Relative expression of GRIN1 and GRIN2C mRNA increased substantially from *day 6* to *day 18* in culture ($P < 0.05$; Fig. 1*E*). A tendency to increased expression of GRIN2A, GRIN3A, and GRIN3B mRNA over 18 days in culture was detected but was not statistically significant (Fig. 1*E*). Maximal expression of GRIN2D mRNA was found in cells after 12 days in culture, whereas in 18-day-old cells the expression levels dropped to the values similar to those detected at *day 6* (Fig. 1*G*). No transcripts of GRIN2B were detected at any differentiation stage. In peripheral RBCs we were not able to detect any GRIN transcripts, indicating that those were eliminated during erythrocyte maturation (data not shown).

Protein levels of subunits NR2C, 2D, 3A, and 3B were measured using flow cytometry (Fig. 2). The number of erythroid cells in culture expressing NMDAR subunits varied between 10 and 30%. The number of erythroid cells expressing NR2C and NR2D increased during the basophilic and polychromatic cell stages and decreased again once cells matured towards normoblasts and reticulocytes (Fig. 2, *A* and *B*). However, the number of copies for these subunits was rather stable throughout the culture period as follows from the mean fluorescence intensity levels (Fig. 2, *A* and *B*). The subunit NR3A appeared to be expressed by an increasing proportion of cells throughout erythropoiesis; however, its expression decreased slightly (Fig. 2*C*). The number of cells expressing NR3B remained stable during the erythropoietic culture, whereas its expression increased slightly (Fig. 2*D*). Specifically during ex vivo differentiation, the GRIN2D levels of the median subunit per cell remained relatively unchanged from *day 6* (proerythroblast) with 186,000 (41,000–320,000) to *day 12* (basophilic erythroblast) with 140,000 (18,300–540,000) subunits per cell. Towards *days 18–24* in culture (polychromatic- and normoblast, and also reticulocytes), expression of the NR2D subunit dropped to 120,000 (4,100–240,000) subunits per cell. Thus the stable expression of GRIN2D mRNA during differentiation from myeloid progenitor towards the basophilic/polychromatic erythroblast was mirrored by a stable expression in GRIN2D protein levels. During differentiation towards erythrocytes the transcripts appear to become degraded, as they are not detected anymore, whereas NR2D protein is retained although at much lower levels (data not shown).

The importance of functional NMDARs in EPCs in the course of differentiation was explored. The kinetics of changes in the intracellular Ca^{2+} levels in EPCs in response to stimulation of the NMDARs with a mixture of NMDA and glycine (300 μM each) in the absence or presence of 50 μM MK-801 were monitored using fluorescence microscopy. Administration of NMDA/glycine to the cells at *day 12* resulted in acute increase in the intracellular Ca^{2+} levels as shown in Fig. 3*A*.

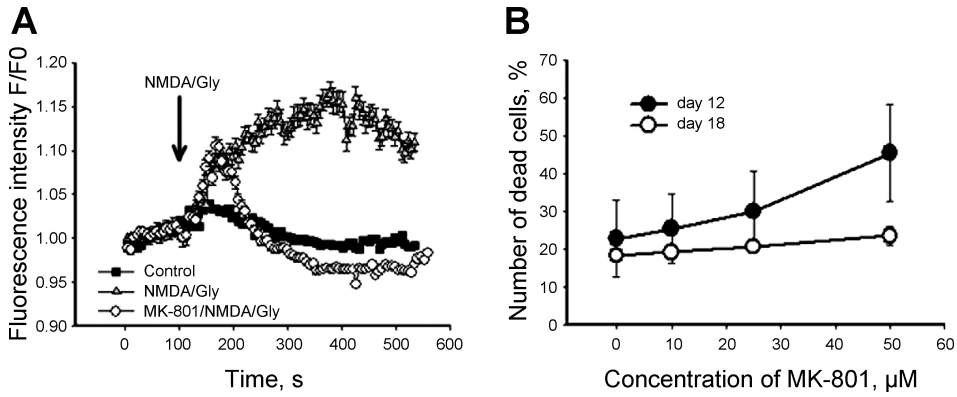

Fig. 3. NMDAR function in EPCs. *A*: cells on *day 12* were loaded with 3 μM fluo-4 AM for 45 min at 37°C in cell culture medium and thereafter fluorescence recordings were initiated using Axiovert 200M microscope in time-lapse mode at a frequency of one frame in 7 s. Cells were stimulated with 300 μM of NMDA/glycine 1 min after the onset of recordings and the changes in fluorescence followed for 10 min. Some cells were pretreated with 50 μM of MK-801 for 45 min before the imaging procedure. The antagonist was present in the cell culture medium during the imaging. The number of cells analyzed was 542 for control nontreated group (closed squares), 511 for the NMDA/Glycine-stimulated group (grey triangles), and 494 for the cells pretreated with MK-801 before the stimulation with antagonists (open circles). *B*: cells at *day 12* (closed circles) or at *day 18* (open circles) were exposed to various concentrations of MK-801 for 24 h and cellular viability was assessed thereafter using flow cytometry (FacsCalibur; BD). Nuclear staining of propidium iodide was used as a marker of cell death.

Whenever MK-801 was present in the incubation medium before the receptor activation, the response was biphasic. A transient and incomplete Ca^{2+} accumulation during the first 30 s upon NMDA/glycine addition was followed by a decrease in the intracellular Ca^{2+} significantly below the levels observed in control nontreated cells. On *day 18*, EPCs lost their sensitivity to NMDA/glycine and stimulation of the receptors did not result in any acute significant changes in the intracellular calcium along with higher intercellular variability in the intracellular Ca^{2+} levels and responsiveness to the stimulation (data not shown). The effects of long-term exposure on the EPCs to different concentrations of the pore blocking NMDAR antagonist MK-801 were explored. In line with the data on NMDA/Gly-sensitivity of the intracellular Ca^{2+} levels, exposure of EPCs at *day 12* to *50* μM MK-801 for 24 h resulted in significant increase of mortality whereas the cells at *day 18* were antagonist resistant (Fig. 3*B*).

NMDAR expression pattern in WBCs. To evaluate the impact of potential contaminations of myeloid progenitors in our culture systems and that of WBCs in our RBCs preparations, we used CD45 as a marker of myeloid and WBCs (45). We were unable to detect myeloid cells in our culture system after *day 6*. No WBCs were detected in purified RBCs, as shown previously (3). We have assessed the expression GRIN transcripts in adhesive WBCs separated at *day 2* from our erythroid culture. These cell preparations contained predominantly monocytes. Expression of GRIN1 in this myeloid cell population exceeded that in erythroid cells at *day 6* of the erythropoietic culture by 4.4-fold, that of GRIN2A by 6.5-fold, and that of GRIN2D by 9.8-fold whereas GRIN2C was 50% lower in WBCs than in erythroid progenitors (Table 1). Compared with erythropoietic cultures at *day 18*, WBCs expressed 0.6-fold less GRIN1, 3.8-fold more GRIN2A, 0.06-fold less GRIN2C, and 10.8-fold more GRIN2D compared with the levels in basophilic and polychromatic erythroblasts (Table 1).

These findings provided further evidence for the absence of myeloid cells or WBCs in erythroid cell culture. Expression profiles for NMDAR subunits GRIN1, GRIN2C, and GRIN3A in differentiated erythroid cells differed substantially from those in WBCs. Furthermore, WBCs appeared to express GRIN2B subunit whereas in erythroid cells the GRIN2B transcripts remained below detection level at any time in culture (Table 1).

NMDAR activity and intracellular Ca^{2+}concenrtation. In the following set of experiments, the activity of NMDAR was assessed in circulating RBCs. Changes in the intracellular calcium levels in RBCs upon treatment with agonists NMDA, glutamate, and HCA are shown in Fig. 4*A*. Increase in the intracellular Ca^{2+} levels, which was induced within minutes of exposure to the agonists, could be blocked by the pore-blocking antagonist interacting with the open receptor channel MK-801 (Fig. 4, *A* and *B*). Responses of individual cells to the NMDAR stimulation varied substantially (Fig. 4*C*). However, despite pronounced intercellular variability, the majority of cells responded to the treatment with the NMDAR agonists with acute Ca^{2+} uptake.

NMDAR-induced whole cell currents in RBCs. Calcium uptake following activation of the NMDAR was associated with an increase in whole cell currents across the RBC plasma membranes (Fig. 5). Changes in membrane conductance were assessed using automated patch clamp platform Patchliner (Nanion). Similar to the observations obtained using microfluorescence live imaging (Fig. 4*C*), sensitivity of the cells to agonists and antagonists varied markedly between individual cells. An increase in currents associated with exposure to the NMDA-glycine mixture was observed in 29.4% of cells. Currents induced by the treatment of cells with agonists could be blocked by the treatment of cells with MK-801. Examples of the NMDA-sensitive currents are shown in Fig. 5, *A* and *C*, and statistical analysis of the findings in responding cells is given in Fig. 5*E*. The appearance of the current-voltage (*I-V*) curves changes when the NMDAR is activated (green line in Fig. 5*D*) or when it is blocked (blue line in Fig. 5*D*). To relate the current traces to the other data in the paper the slope of the *I-V* curves was analyzed in the physiological relevant range between −30 and 0 mV (Fig. 5*D*). At stimulated NMDAR, the whole cell conductance is significantly increased compared with naïve RBCs (green column vs. red column in Fig. 5*E*). When the RBCs with activated NMDARs are treated with MK-801 to block NMDAR activity, the whole cell conductance is significantly decreased (green column vs. blue column in Fig. 5*E*).

NMDAR abundance in RBC fractions of high medium and low density. In the next sets of experiments RBCs were separated into fractions according to their density using Percoll density gradient centrifugation. D, M, and L fractions were isolated as shown in Fig. 6*A*. The basal activity of the receptor and total number of the functional NMDAR units was measured in each fraction using two independent approaches: radioactive antagonist binding assay and agonists/antagonists-induced changes in the intracellular calcium levels. Basal receptor activity was evaluated as the cells were allowed to interact with [^{3}H]MK-801 in plasma and then fractioned on Percoll gradient. The number of binding sites for radiolabeled antagonist per cell obtained that way reflected the number of NMDARs active in plasma-borne RBCs. The values for the [^{3}H]MK-801 binding to "activated" cells were obtained in the presence of saturating concentrations of NMDA in plasma and hence represented the total number of receptors. As shown in the Fig. 6*B*, the number of active receptors interacting with [^{3}H]MK-801 was maximal in the L fraction enriched with reticulocytes and young cells (see DESIGN AND METHODS). In this fraction, no further activation of the receptor could be caused by glutamate/NMDA supplementation of plasma. In contrast to that, the receptors in M and D fractions, although significantly lower in number, could be further activated by addition of agonist to plasma (Fig. 6*B*).

These experimental settings could give rise to artefacts due to the WBCs contamination (average of 5.6, 4.9, and 1.4 per 1,000 cells in the L, M, and D fractions; Ref. 45). To avoid the overestimation of the receptor activity in RBCs, we have used an alternative approach monitoring the agonist-induced Ca^{2+} uptake in individual RBCs of L, M, and D fractions isolated from blood of three healthy individuals by microfluorescence live imaging. Receptor activity in RBCs of these donors was assessed by [^{3}H]MK-801 binding and presented in the right panel of Fig. 6 (in red for *donor 1*, in green for *donor 2*, and in blue for *donor 3*). The observations obtained by means of microfluorescence imaging were in agreement with the ones generated using radiolabeled antagonist binding assay. Maximal amount of "responding" RBCs of each individual donor was present in the L fraction (Fig. 7*A*). Maximal amplitude of NMDA-induced Ca^{2+} uptake was recorded in the least dense

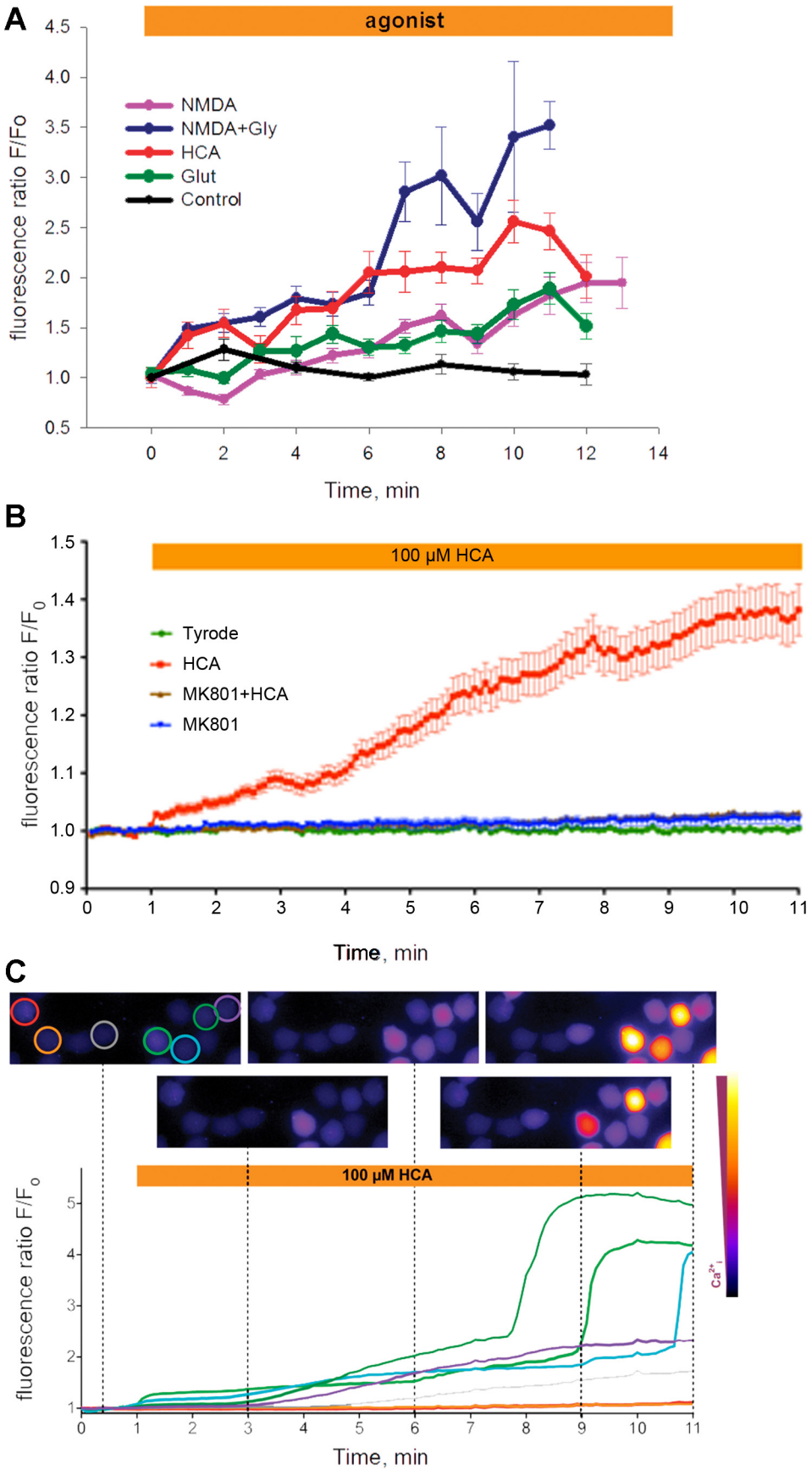

Fig. 4. Changes in the intracellular Ca^{2+} levels in red blood cells (RBCs) exposed to agonists and antagonist of NMDARs. *A*: an increase in the intracellular Ca^{2+} in response to administration of 100 μM NMDA, 100 μM NMDA + 100 μM glycine, 100 μM glutamate, or 50 μM homocysteic acid (HCA) was observed. Data are means of 34–80 single cell recordings ± SE. The orange bar on top of each panel schematically indicates the duration of exposure to the agonists. *B*: sensitivity of the HCA-induced Ca^{2+} uptake by RBCs to the NMDAR antagonist MK-801 (50 μM). Pretreatment with antagonist for 10 min abolished the effects of subsequent exposure to HCA. The green trace represents the average Ca^{2+}-sensitive fluorescent signal recordings for 444 unstimulated control HBA RBCs in Tyrode's solution. The red trace shows the F/F_o ratio for RBCs stimulated with NMDAR agonist HCA (100 μM) 1 min after the start of the recordings averaged from 776 single cell recordings. Preincubation of the cells with NMDAR antagonist MK-801 (100 μM) administered 10 min before the onset of the recordings did not affect the basal intracellular Ca^{2+} levels during 20 min of exposure (blue trace, average of 775 individual cell recordings), but effectively inhibited the HCA-sensitive Ca^{2+} influx, as depicted by the brown trace (average of 742 individual cell recordings). Each curve shows data from 9 independent measurements of 3 healthy donors ± SE. (*C*) A selection of traces from individual cells. The images above the diagram exemplify the original fluorescent images of cells at the time points indicated by the dotted lines. The false color coding scale is shown next to the original tracks of the changes in fluorescence intensity over time. The colors of traces correspond to those of the circles marking the individual cells in the leftmost image. The tremendous cell-to-cell variation is obvious in both the images and the traces.

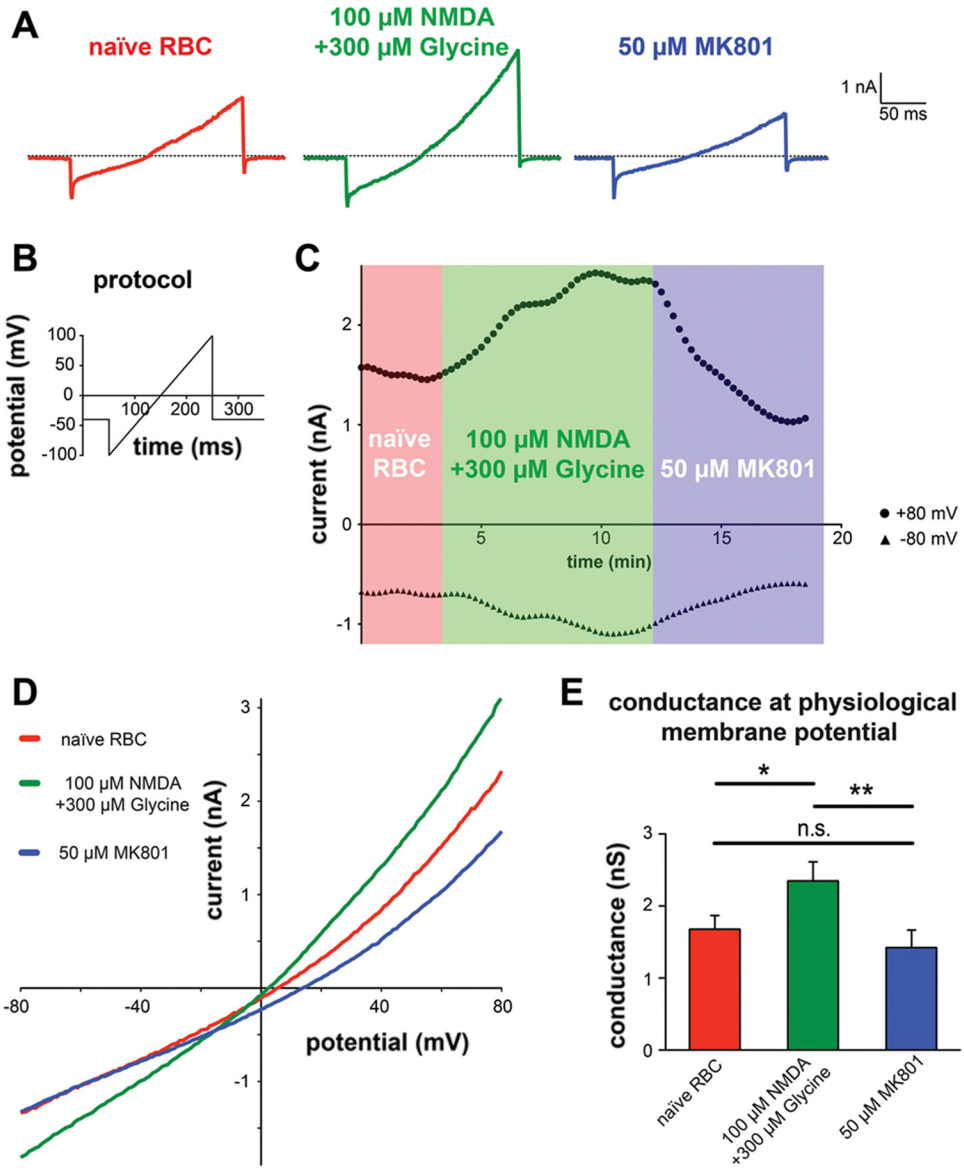

Fig. 5. Whole cell currents of RBC under activation and blocking of the NMDARs. Measurements as shown in *A* were performed on 56 gigasealed RBCs. However, for an observation period of 15–20 min only 34 cells were stable enough to allow analysis. 29% of the analyzed RBCs were classified as "responders." Similar in size fraction of responding cells was obtained in Ca^{2+} imaging experiments and when the number of NR2D subunits was assessed using flow cytometry. Responding cells were the RBCs showing an increase in conductance with the application of NMDA (100 μM) and glycine (300 μM) and a decrease when MK-801 was added. *A*: original current traces of an RBC under the conditions presented above the traces as a response to the voltage protocol given in *B*. The current-time (*I-t*) diagram in *C* depicts the temporal distribution of the currents at +80 and −80 mV over the experimental course starting with naïve RBC, application of NMDA and glycine for NMDAR activation and finally MK801 for NMDAR block as indicated. The current traces in *A* correspond to the time points at 2, 10, and 18 min, respectively in *C*. *D*: current-voltage (*I-V*) curves of the responding RBCs under the conditions indicated (data are mean of 10 measurements). The slope of the curves in the range between −30 and 0 mV was analyzed by linear regression and the results are presented in *E*, revealing significant differences in the whole cell conductance at the physiologically relevant membrane potential for the different experimental conditions. Significance was tested by comparing the slopes using a 2-way ANOVA test and is expressed as $*P < 0.05$, $**P < 0.01$, and n.s., $P > 0.05$.

fraction of RBCs of *donor 2*. Transient Ca^{2+} accumulation in RBCs was associated with a transient shrinkage of cells that could be caused by the activation of Gardos channel. Medium density fraction of the *donor 2* was also rich in responding RBCs and showing a transient reduction in cell volume in response to the NMDAR stimulation (Fig. 7*B*, *middle*).

We used Percoll density gradient to assess the amount of cells changing their volume in response to the NMDAR stimulation in the M fraction to which majority of RBCs belong (Fig. 6*A*). The density of Percoll solution used in these experiments was adjusted to resolve the changes in the M fraction. As shown in Fig. 7*D*, most of the cells forming M fraction migrated downwards in Percoll gradient 2 min after the onset of stimulation with 300 μM of 1:1 NMDA/glycine mixture. This increase in RBC density was transient and could not be detected 5 min after the onset of exposure to the NMDAR agonists in four out of five donors. Cells of the fifth donor remained dehydrated even after 15 min of exposure to the agonists. No volume changes were observed in RBCs of all donors suspended in nominally Ca^{2+}-free Percoll solution containing 0.1 mM EDTA supplemented with NMDA and glycine (data not shown).

In fraction D (Fig. 7*C*), the cells remained largely insensitive to the agonist treatment and showing modest transient increase in the intracellular Ca^{2+}. The obtained data revealed vast interindividual and intercellular variation in the number of functional receptor units and the amplitude of responses to the NMDAR agonists. Among typical morphological characteristics of responding cells are big volume (cell surface projection) and low density as L fraction is enriched with responding cells. Medium fraction also contains some of the responders, whereas D fraction is largely deprived of them.

The impact of NMDAR activation state on Gardos channel function. The following experiments were performed to assess the possible influence of NMDA-sensitive Ca^{2+} uptake on K^+ transport across the RBC membrane. Ouabain-resistant chloride-independent K^+ (^{86}Rb) influx was assessed at room temperature, as was the case for Ca^{2+} imaging presented in Fig. 7.

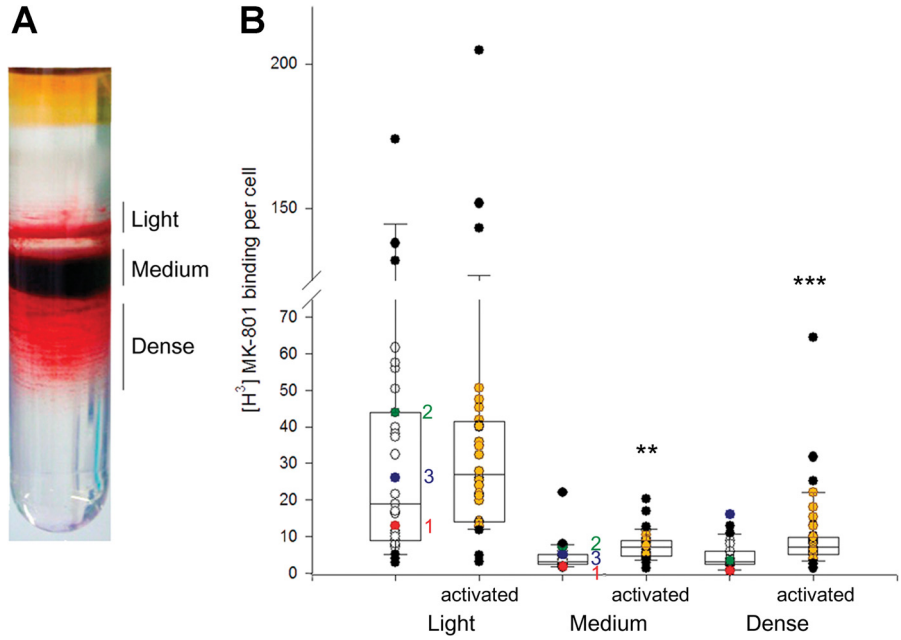

Fig. 6. Activity and abundance of the NMDAR units in light (L), medium (M), and dense (D) RBC fractions. Cells were incubated with radiolabeled [^{3}H]MK-801 in the absence or presence of saturating concentrations of NMDA (300 μM) and glycine (100 μM) added to plasma (activated cells, orange dots). Thereafter, the cells were separated according to their density into L, M, and D fractions on Percoll gradient as shown in *A*. *B*: presents binding of radio-labeled MK-801 to the activated NMDARs was then determined in RBCs in L, M, and D fractions. Non-specific binding was assessed in the presence of 200-fold excess of non-labeled MK-801 and subtracted from the obtained values. Thus the number of active NMDARs was obtained. Values obtained in plasma were shown as "basal receptor activity" in nonstimulated RBCs. Upon stimulation with agonists all receptors in cells were activated and therefore binding of [^{3}H]MK-801. Thus the number of [^{3}H]MK-801 binding sites within activated cells reflected total number of receptors in cells forming L, M, and D fractions. The measurements were performed in blood samples per cell collected from 31 healthy human subjects. Data are presented as box and whisker plots in which each dot represent a value obtained for an individual subject. Specifically marked in red (*1*), green (*2*), and blue (*3*) are the number of active receptors in blood samples of donors blood of which was used to generate data shown in Fig. 7. In L, M, and D fractions distribution of values for individual donors did not show normal Gaussian distribution and statistical analysis of the data was performed using nonparametric Kruskal-Wallis test with Dunn's posttest (**$P < 0.01$, and ***$P < 0.0001$ compared with the basal activity of the NMDAR in corresponding fraction).

No density fractioning was performed before flux measurements. As shown in Table 2, treatment of RBCs suspended in Ca^{2+}-containing but not in nominally Ca^{2+}-free incubation medium with 50 μM memantine caused reduction in unidirectional K^+ influx. Administration of 100 μM NMDA triggered the activation of clotrimazol-sensitive Ca^{2+}-dependent K^+ influx. In nonactivated cells, Gardos channels remained quiescent.

Effect of the NMDAR activation on hemoglobin oxygen affinity. The effect of the intracellular Ca^{2+} on oxygen binding to hemoglobin was tested. Intracellular free Ca^{2+} concentration was clamped as cells were treated with Ca^{2+} ionophore A23187, and extracellular concentration of free calcium ions was adjusted to 10–200 nM by using an EGTA-$CaCl_2$ buffer system. Oxygen dissociation curves were then measured and P_{O_2} required to achieve hemoglobin oxygen saturation of 50%, P_{50}, was assessed for the calcium-clamped RBCs. Calcium levels in clamped RBCs were assessed using microfluorescence imaging. As shown in Fig. 8, the fluorescent signal intensity of fluo-4 follows linearly the changes in the intracellular Ca^{2+} within the 10- to 200-nM interval (Fig. 8*A*). Intraerythrocytic Ca^{2+} levels in intact and NMDA-stimulated cells lies within this concentration range (triangle symbols). Oxygen affinity of Ca^{2+}-clamped cells drops (P_{50} increases from 2.28 ± 0.01 to 4.1 ± 0.27 kPa) as intracellular Ca^{2+} increased from 20 to 200 nM (Fig. 8*C*). Exposure of RBCs in suspension to 300 μM NMDA-100 μM glycine mixture was also associated with an increase in P_{50} (Fig. 8, *B* and *D*).

Acute transient RBC shrinkage triggered by exposure to the NMDAR agonists results in transient increase in the intracellular levels of 2,3-DPG and ATP due to the cytosolic water loss. Additional experiments were performed to explore if this factor contributed to a decrease in hemoglobin oxygen affinity. Oxygen dissociation curves were monitored in RBCs suspended in the medium containing 100 mM KCl/50 mM NaCl medium or in the presence of clotrimazol. The effect of NMDA/glycine on P_{50} was less pronounced but still preserved in both conditions, (3.04 ± 0.65 kPa in control vs. 3.16 ± 0.04 kPa in depolarizing high KCl medium, $P = 0.011$).

The effect of NMDAR agonists on the intracellular pH was assessed microscopically using proton-sensitive fluorescent dye BCECF-DA. Treatment of RBCs with NMDA/glycine resulted in a modest transient decrease in pH-dependent BCECF fluorescence indicating transient intracellular acidification (Fig. 8*F*). The signal we reported was underestimated as shrinkage following the NMDAR activation caused concentration of the fluorescent dye. This acidification reaction monitored in bicarbonate-free medium was insensitive to the inhibitor of Na^+/H^+ exchanger methyl isobutyl amiloride applied at the concentration of 50 μM. The ability of Ca^{2+} to cause the proton release from hemoglobin was explored as RBC lysates (Hb concentration of 0.25 μM, equilibrated with ambient air) were exposed to various concentrations of Ca^{2+}. Cell lysates prepared in 150 mM NaCl solution showed no changes in pH in response to Ca^{2+} administration. However, dose-dependent acidification was observed if cell lysates were exposed to Ca^{2+}

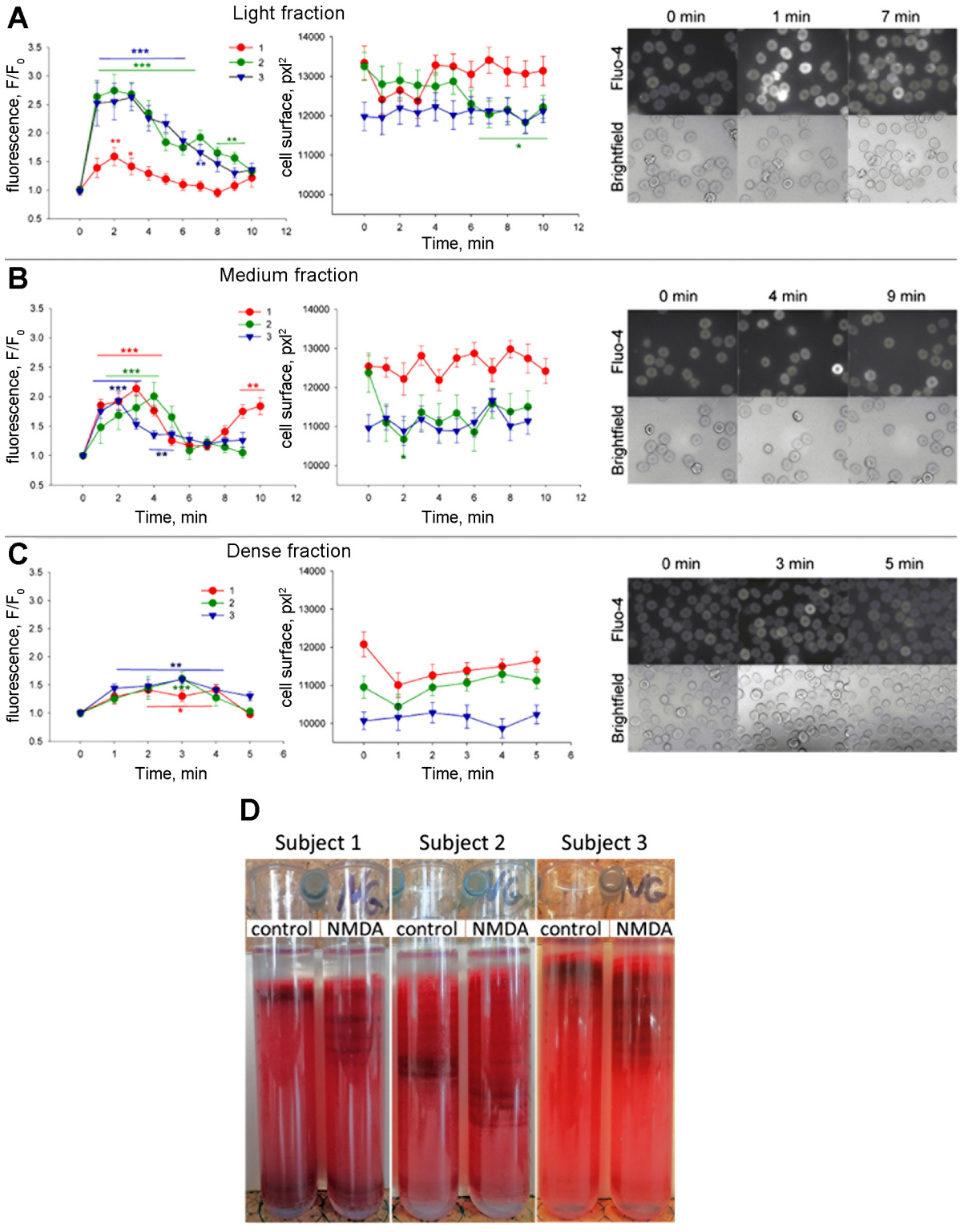

Fig. 7. Kinetics of Ca^{2+} uptake and volume changes in response to NMDAR activation in L, M, and D fractions. Intracellular calcium levels were assessed in RBCs forming L (*A*), M (*B*), and D (*C*) fractions after their separation on Percoll density gradient using fluorescent live cell imaging. The experiments were performed using blood of *subjects 1* (red), *2* (green), and *3* (blue). The values of [^{3}H]MK-801 binding obtained for RBCs of these subjects are highlighted in corresponding colors in Fig. 6. Presented in the left panels are quantification of Fluo-4 fluorescence intensity F upon stimulation with glutamate (300 μM) and glycine (100 μM) normalized to that at time zero in agonist-free medium (F_o). *Middle*: changes in cell projection area in the bright field images over the period of stimulation with the NMDAR agonists. The numbers of cells used for analysis varied from 13 to 35. Data are presented as mean ± SE. *Right*: representative fluorescent images at 3 points in time (before, 1, and 6 min after the stimulation) for the cells in L, M, and D fractions obtained from blood of subject 2 (green plots). Kruskal-Wallis test was performed to follow the changes in Ca^{2+} levels and cell surface (a marker of volume) after the receptor activation. *$P < 0.05$, ** and **$P < 0.01$ and ***$P < 0.001$ compared with time zero. *D*: shift of RBCs within the M fraction down the Percoll density gradient in response to 2 min of stimulation with 300 μM of 1:1 NMDA/glycine mixture in *donors 1*, *2*, and *3*.

Table 2. *Effects of NMDA and memantine on the unidirectional ouabain-insensitive Cl^- -independent K^+ ($^{86}Rb^+$) influx in Ca^{2+}-containing and Ca^{2+}-free medium*

Treatment	1.8 mM Ca^{2+}, mmol·l_{cells}^{-1}·h^{-1}	Ca^{2+}-free, mmol·l_{cells}^{-1}·h^{-1}
Control	0.0134 ± 0.0017	0.0176 ± 0.0029
Memantine	0.0056 ± 0.0012*	0.0162 ± 0.0015
Clotrimazol	0.0158 ± 0.0016	NA
NMDA	0.0201 ± 0.0017*	0.0160 ± 0.0008
NMDA-memantine	0.0102 ± 0.0059	0.0168 ± 0.0028
NMDA-clotrimazol	0.0126 ± 0.0023	NA

Values are means ± SE. *$P < 0.05$, in one-way ANOVA analysis with Dunnett multiple comparison posttest; NA, not assessed.

in the presence of 2 mM 2,3-DPG (Fig. 9). Exposure of 2,3-DPG alone to Ca^{2+} did not result in the changes in pH (Fig. 9). Oxygen binding to hemoglobin within RBC lysates was tested in the presence of 2,3-DPG and various concentrations of Ca^{2+}. As shown in Fig. 9 Ca^{2+}-induced proton release was associated with a dose-dependent rightward shift in oxygen binding curve, the effect observed in Ca^{2+}-loaded or NMDA-glycine stimulated RBCs (Fig. 8). Similar to that of pH, oxygen binding to hemoglobin in lysates remained calcium-insensitive in the absence of 2,3-DPG (data not shown).

DISCUSSION

Following up on our earlier observations on the presence of NMDARs in rat RBCs and in human myeloid cell line differentiating into erythroid progeny, UT-7/EPO (38), we have demonstrated that NMDAR subunits are expressed in human EPCs. Circulating human RBCs retain a limited number of functional receptor units compared with the EPCs. Mammalian RBCs may therefore be added to the list of cells possessing NMDARs along with neurons and a number of nonneuronal cells and tissues (22, 57). Expression of the GRIN transcripts coding for the NMDAR subunits was changing dynamically during erythropoiesis, as did the protein abundance. NMDARs appear to be essential for survival, particularly at the early stages of differentiation of precursor cells during erythropoiesis. Subunit composition of the erythroid receptors differed substantially between the erythroid progeny and WBCs.

Calcium uptake was reported to be of key importance for promoting differentiation and proliferation of EPCs at the stages of burst-forming units erythroid (BFU-E) colony-forming units erythroid (CFU-E; Refs. 43, 56). Increase in the intracellular Ca^{2+} is an integral part of signaling pathway activated by binding of erythropoietin to its receptor (44). Our data suggest that glutamate released from megakaryocytes (63)

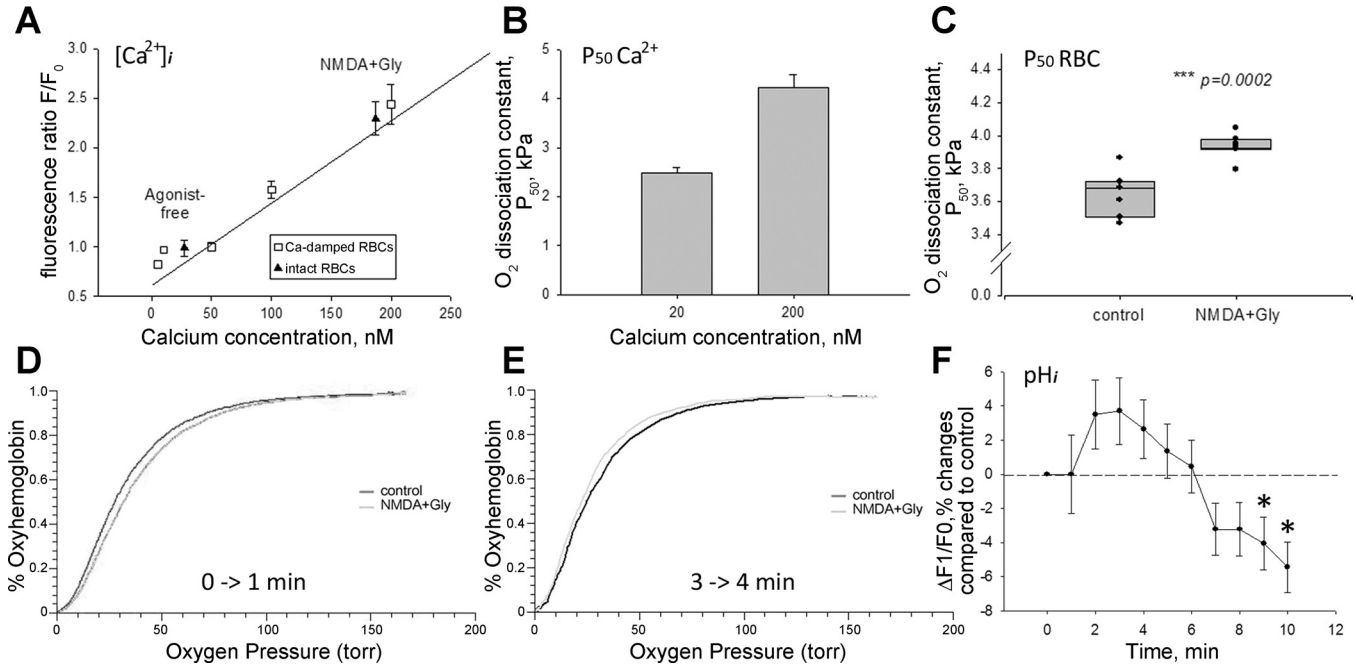

Fig. 8. Ca^{2+} sensitivity of hemoglobin oxygen affinity. Intracellular Ca^{2+} concentration in RBCs was clamped using A23187 and EGTA-$CaCl_2$ buffer to 5–200 nM. *A*: efficacy of clamping of intracellular Ca^{2+}, which was monitored as the change in fluorescence intensity of fluo-4 (open circles). Fluorescence intensity measured in cells clamped at 50 nM Ca^{2+} was chosen as F_o. Closed triangles show the fluorescence intensity of fluo-4 in native cells in the absence of presence of 300 μM NMDA/100 μM glycine, which were resuspended in buffer containing 1.8 mM $CaCl_2$. *B*: data on P_{50} detection obtained for the blood of one single donor on four occasions. Before the P_{50} detection RBCs were loaded with various concentrations of calcium (clamping at 20 or 200 nM free Ca^{2+}). Oxygen dissociation curves for calcium-clamped cells were recorded at 30°C. *C*: changes in P_{50} caused by exposing RBCs of 7 healthy donors to a mixture of NMDA (300 μM) and glycine (100 μM). Intact RBCs were resuspended in the medium containing 2 mM Ca^{2+} at 37°C and agonists added at the onset of oxygen dissociation curve recording. Each point represents P_{50} of one donor (mean of triple recordings). Also presented are median values with variance shown as whiskers. *D*: rightward shift in oxygen dissociation curve observed 1 min after the onset of stimulation with 300 μM of 1:1 mixture of NMDA/glycine at 37°C. *E*: opposite leftward shift in the same blood sample monitored between the 3d and 4th min of NMDAR stimulation. These reciprocal changes in P50 were associated with the opposite shifts in the intracellular pH over shown in *F*. RBCs of 4 different donors were used for measurements of the intracellular pH by means of microfluorescence live imaging. Due to the technical difficulties imaging was performed at room temperature. Shown are the differences in mean fluorescence intensity between the unstipulated control and cells exposed to the 300 μM of 1:1 mixture of NMDA/glycine. The number of cells analyzed at each time point ranged between 343 and 412. $P < 0.05$ resulting from Mann-Whitney test (normal distribution was not confirmed). ***$P = 0.0002$, *$P < 0.05$.

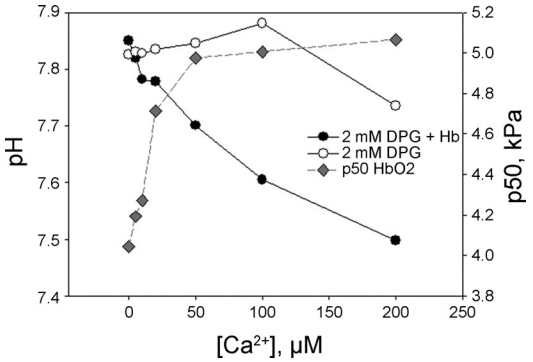

Fig. 9. Dose-dependent Ca^{2+}-induced changes in pH and in P_{50} measured in RBC lysates. Changes of pH and hemoglobin oxygen affinity in RBC lysates in the presence of 2,3-diphosphoglycerate (2,3-DPG). RBCs were lysed in the distilled water, and then NaCl was added to a final concentration of 150 mM with the final hemoglobin concentration 0.25 μM. 2,3-DPG (2 mM) and various concentrations of $CaCl_2$ were added and pH (closed circles) was measured at 37 ^{0}C for each sample in prior to the P_{50} measurements (grey diamonds). The impact of 2,3-DPG-Ca^{2+} interactions into the observed shifts in pH was assessed (open circles). Data shown are means of triplicate measurements form one representative donor. The experiment was repeated with blood of 3 different healthy individuals.

may contribute to the regulation of Ca^{2+} levels in EPCs at *day 12* corresponding to the stage of basophilic and polychromatic erythroblasts (Fig. 3*A*). The number of EPCs possessing NR2C, 2D, and 3A subunits is maximal at this stage (Fig. 2). Accordingly, the cells display high sensitivity to treatment with NMDAR agonists in our ex vivo erythropoietin system (Fig. 3*A*).

Ca^{2+} uptake is inhibited and differentiation and survival of EPCs is compromised in calcium-free medium (43, 56). Similar to that, inhibition of Ca^{2+} uptake by MK-801 in our ex vivo erythropoiesis system resulted in 45.5 ± 12.8% mortality of cells at the stage of basophilic and polychromatic erythroblasts (Fig. 3*B*). Cells at later differentiation stages (normoblasts at *day 18* and enucleated RBCs) are less or not at all damaged by MK-801.

Transient receptor potential channels TRPC2, 3, and 6 were suggested to mediate Ca^{2+} currents in EPCs (23, 67). However, observations on the activation of the TRPC channels by the downstream targets of erythropoietin [e.g., phospholipase C (PLC), and protein kinase C (PKC)] were exclusively reported in nonerythroid channel expressing systems (CHO and HEK cells). Similar to TRPCs, NMDARs were shown to be sensitive to the activation of PLC-inositol-3-phosphate kinase signaling cascade and targets of regulatory PKC-induced phosphorylation (39, 73). Thus both types of ligand-gated channels may coexist in membranes of EPCs (63).

Subunit composition of the erythroid NMDARs. From the data shown in this study, we conclude that human erythroid NMDARs are hetero-tetramers composed of NR1, NR2A, 2C, and 2D and NR3A and 3B subunits. Subunit composition of the erythroid NMDARs differs strikingly from that of the neuronal receptors. As follows from our observations, NR2D and NR2C are most abundant NMDAR subunits in EPCs and, most likely, in circulating RBCs. In the mammalian brain, this subunit shows particularly restricted temporal and spatial expression pattern. Very high levels of expression of NR2D in some areas of embryonic rat brain (precocious midline diencephalic structures and medial geniculate, anteroventral nucleus, and periaqueductal grey zones) drop down dramatically during postnatal period (49). In adult rodent brain, NR2D is only detected in cerebellum and Golgi structures (9, 47) and is highly expressed in motoneurons of the spinal cord (66). In bone marrow and in megakaryoblasts derived from $CD34^+$ precursor cells, the NR2D subunit was found along with NR1 and NR2A (19, 24). Among the characteristic features reported for the NR2D/NR1 heterodimers are reduced Mg^{2+} block, lower ion conductance and slow inactivation (15, 54). However, based on the available data obtained in transfected cells by other groups, one can suggest that the erythroid-specific receptor channels share at least some of these features, such as slow inactivation, since glutamate-binding NR2D subunit is highly abundant in these cells. Calcium accumulations observed upon activation of the receptor activity with glutamate, NMDA, and homocysteic acid that could be blocked by MK-801 (Fig. 4) are in line with this hypothesis (33, 46, 48). However, in erythroid precursors the glycine-binding NR3A and B subunits were highly expressed, whereas the expression of a common NR1 subunit was modest compared with that in the brain (Figs. 1 and 2). These subunits are known as "inhibitory subunits" in the brain as they are glutamate-insensitive but excited by glycine only (35). Currents induced by glycine in NR1/NR3 diheteromers are insensitive to MK-801 or memantine (58). This is not the case for the erythroid NMDARs, as the receptors respond to the pore-targeting antagonists in both EPCs and circulating RBCs. Thus the receptors are either NR1/NR2 heterodimers or are built up of all three subunit subtypes (NR1/NR2C, D/NR3 heterotetramers), although the existence of the latter has been questioned (69). Any speculations on the electrophysiological characteristics of erythroid NMDARs require verification upon detailed investigation.

Receptor function in circulating RBCs of healthy human subjects. NMDARs retained in circulating RBCs remain functional and keep responding to stimulation with glutamate, HCA, or NMDA as well as to the inhibition by MK-801 (Figs. 3–6). Calcium transport through the receptor is electrogenic, putting NMDARs in line with other calcium-transporting ion channels (Fig. 4). The number of such ion channels in RBC is rather limited and their molecular identity often remains unknown (28). Among the TRP channels, only TRPC6 is described in RBC (17). Furthermore, there is biochemical and functional evidence for a $Ca_V2.1$ channel (1, 71). There are numerous electrophysiological reports of Ca^{2+}-permeable channels that can be grouped in two categories: nonselective voltage activated cation channels (NSVAC; e.g., Refs. 4, 29) and receptor-mediated channels (e.g., Refs. 13, 25). Although the *I-V* curve for NSVAC in whole cell conductance mode (55) differs from that shown in Fig. 4*D*, NMDARs and NSVACs have one common property. Both channels share the hysteresis of whole cell current-voltage curves as their opening probability depends on the direction in which membrane potential changes occur (50).

The receptor-activated channels previously described in RBCs share some conductance properties with the channel described in Fig. 5 (13, 25). However, it is premature to make any conclusions on the molecular identity of these channels. Our findings strongly suggest that the currents presented in Fig. 5 are NMDAR mediated. Stimulation of RBCs with NMDA induced an increase in conductance whereas administration of the pore-blocking antagonist suppressed it. Asymmetrical alterations in conductance in response to NMDA treatment

suggest that is it may be channel mediated. The current measured is a superposition of NMDAR-channel current, currents mediated by other ion channels (e.g., those reported elsewhere; Refs. 11, 62), and a leak current. Channel-mediated components show a slight outward rectification and a positive reversal potential (Fig. 5*D*, blue *I-V* curve). Considering the composition of the bath and pipette solutions this could well be chloride channel activity (61). The contribution of the NMDAR channel can be estimated as the difference between putative fully activated channels (Fig. 5*D*, green trace) and the corresponding inhibited channels (Fig. 5*D*, blue trace). In the physiological relevant range between −30 and 0 mV, this difference amounts to a conductance of ~930 pS (Fig. 5*E*). The decreased current at negative membrane potentials in the presence of Mg^{2+} in the bath solution is another indication for the NMDAR identity of the channel (15).

So far channel-mediated Ca^{2+} uptake by RBC was always associated with pathophysiological conditions, such as clot formation (30, 74) or Ca^{2+}-induced clearance (34). To our knowledge, our study is the first one revealing possible physiological role of controlled transient Ca^{2+} uptake following the activation of NMDARs, namely the regulation of oxygen affinity of hemoglobin (Figs. 8 and 9).

Among endogenous regulators of the erythroid NMDAR activity are plasma-borne glutamate, glycine, D-serine, homocysteine, and HCA. The rodent NMDAR EC_{50} for glutamate is 96 ± 20 μM (26), being ~10 μM for HCA (53), and ~40 μM for glycine (38, 58). These data were obtained for the receptors in neurons and in artificial expression systems. These values are close to the EC_{50} for glutamate (88.2 μM) and homocysteic acid (21 μM) reported for the NMDARs in rat RBCs (38). Glutamate concentrations in plasma of healthy human subjects vary substantially depending on physical condition, exercises, gender, diet, and age, making up from 7 ± 1 μM (14) to 255 ± 26 μM (32). Local glutamate and glycine availability in vicinity of RBC membranes may exceed the bulk plasma levels due to high abundance of these amino acids in the cytosol (32). Homocysteine and HCA also contribute to the activation of erythroid NMDARs. Plasma total homocysteine levels ranges from 4.2 to 17.2 μM in healthy human subjects to up to 470 μM in patients with hyper-homocysteinemia (59).

Transient activation of the NMDARs by glutamate released from the exercising muscle (14) or obtained with meal (27) might also contribute to a transient increase in the intracellular Ca^{2+} promoting thereby oxygen release from hemoglobin (Fig. 8). The exact mechanism of a cross talk between calcium levels in RBCs and hemoglobin oxygen affinity remains to be studied in details.

Shrinkage (Fig. 8; Table 2) results in a rapid transient increase in 2,3-DPG levels in the cytosol, which in turn could stabilize hemoglobin in T state and promote oxygen release (Fig. 7, *B* and *D*). However, a shift in oxygen affinity of hemoglobin caused by the stimulation of the NMDARs was preserved in the presence of clotrimazol or in high KCl medium, conditions preventing Ca^{2+}-induced KCl and water loss from RBCs. The obtained data reveal that changes in the intracellular pH result from the shifts in protonation of hemoglobin (Fig. 8). The latter result in the 2,3-DPG-dependent alterations in P_{50} (Figs. 8 and 9). These observations are consistent with earlier reports on an increase in free Ca^{2+} concentration in the cytosol of RBCs undergoing deoxygenation in which hemoglobin gets protonated (65). Conformational changes responsible for these Ca^{2+}-induced changes in oxygen affinity of hemoglobin await further characterization.

Taken together, the obtained findings reveal the presence of functional NMDARs in EPCs and, at much lower levels, in circulating RBCs. The abundance and activity of these receptors in plasma membrane of RBCs and their progenitors are proportional to the intracellular Ca^{2+} levels. Among the downstream targets of Ca^{2+} accumulation are cell volume and hemoglobin oxygen affinity.

ACKNOWLEDGMENTS

We thank Maxim Makhinya for the excellent program CellFinder for intracellular calcium content estimation and morphometric analysis of RBCs he has written for us.

GRANTS

This study was supported by the Swiss National Science Foundation (No. 112 449 and 310030 124970/1 to A. Bogdanova), by Zurich Center for Integrative Human Physiology (cooperative grant to J. Goede, O. Speer, and A. Bogdanova), as well as by Hartmann Müller-Stiftung (to O. Speer and J. Goede). Financial support was provided by the Saarland Graduate School (to J. Wang).

DISCLOSURES

No conflicts of interest, financial or otherwise, are declared by the author(s).

AUTHOR CONTRIBUTIONS

Author contributions: A.M., P.H., J.W., A. Brüggemann, L.K., O.S., and A. Bogdanova performed experiments; A.M., P.H., J.W., A. Brüggemann, L.K., O.S., and A. Bogdanova analyzed data; A.M., P.H., J.S.G., J.W., A. Brüggemann, M.G., M.S., L.K., O.S., and A. Bogdanova interpreted results of experiments; A.M., P.H., J.W., L.K., O.S., and A. Bogdanova prepared figures; A.M., L.K., O.S., and A. Bogdanova drafted manuscript; A.M., J.S.G., A. Brüggemann, M.G., M.S., L.K., O.S., and A. Bogdanova edited and revised manuscript; A.M., P.H., J.S.G., J.W., A. Brüggemann, M.G., M.S., L.K., O.S., and A. Bogdanova approved final version of manuscript; J.S.G., M.S., L.K., O.S., and A. Bogdanova conception and design of research.

REFERENCES

1. **Andrews DA, Yang L, Low PS.** Phorbol ester stimulates a protein kinase C-mediated agatoxin-TK-sensitive calcium permeability pathway in human red blood cells. *Blood* 100: 3392–3399, 2002.
2. **Assouline-Cohen M, Beitner R.** Effects of Ca^{2+} on erythrocyte membrane skeleton-bound phosphofructokinase, ATP levels, and hemolysis. *Mol Genet Metab* 66: 56–61, 1999.
3. **Azzouzi I, Moest H, Winkler J, Fauchere JC, Gerber AP, Wollscheid B, Stoffel M, Schmugge M, Speer O.** MicroRNA-96 directly inhibits gamma-globin expression in human erythropoiesis. *PLoS One* 6: e22838, 2011.
4. **Bennekou P, Kristensen BI, Christophersen P.** The human red cell voltage-regulated cation channel. The interplay with the chloride conductance, the Ca(2+)-activated K(+) channel and the Ca(2+) pump. *J Membr Biol* 195: 1–8, 2003.
5. **Beutler E, West C, Blume KG.** The removal of leukocytes and platelets from whole blood. *J Lab Clin Med* 88: 328–333, 1976.
6. **Bogdanova A, Makhro A, Wang J, Lipp P, Kaestner L.** Calcium in red blood cells-a perilous balance. *Int J Mol Sci* 14: 9848–9872, 2013.
7. **Bookchin RM, Ortiz OE, Shalev O, Tsurel S, Rachmilewitz EA, Hockaday A, Lew VL.** Calcium transport and ultrastructure of red cells in beta-thalassemia intermedia. *Blood* 72: 1602–1607, 1988.
8. **Browning JA, Staines HM, Robinson HC, Powell T, Ellory JC, Gibson JS.** The effect of deoxygenation on whole-cell conductance of red blood cells from healthy individuals and patients with sickle cell disease. *Blood* 109: 2622–2629, 2007.
9. **Cull-Candy SG, Brickley SG, Misra C, Feldmeyer D, Momiyama A, Farrant M.** NMDA receptor diversity in the cerebellum: identification of subunits contributing to functional receptors. *Neuropharmacology* 37: 1369–1380, 1998.

10. **Cull-Candy SG, Leszkiewicz DN.** Role of distinct NMDA receptor subtypes at central synapses. *Sci STKE* 2004: re16, 2004.
11. **Desai SA, Bezrukov SM, Zimmerberg J.** A voltage-dependent channel involved in nutrient uptake by red blood cells infected with the malaria parasite. *Nature* 406: 1001–1005, 2000.
12. **Dingledine R, Borges K, Bowie D, Traynelis SF.** The glutamate receptor ion channels. *Pharmacol Rev* 51: 7–61, 1999.
13. **Duranton C, Huber SM, Lang F.** Oxidation induces a Cl(−)-dependent cation conductance in human red blood cells. *J Physiol* 539: 847–855, 2002.
14. **Durham WJ, Miller SL, Yeckel CW, Chinkes DL, Tipton KD, Rasmussen BB, Wolfe RR.** Leg glucose and protein metabolism during an acute bout of resistance exercise in humans. *J Appl Physiol* 97: 1379–1386, 2004.
15. **Erreger K, Chen PE, Wyllie DJ, Traynelis SF.** Glutamate receptor gating. *Crit Rev Neurobiol* 16: 187–224, 2004.
16. **Foller M, Huber SM, Lang F.** Erythrocyte programmed cell death. *IUBMB Life* 60: 661–668, 2008.
17. **Foller M, Kasinathan RS, Koka S, Lang C, Shumilina E, Birnbaumer L, Lang F, Huber SM.** TRPC6 contributes to the Ca(2+) leak of human erythrocytes. *Cell Physiol Biochem* 21: 183–192, 2008.
18. **Foster AC, Wong EH.** The novel anticonvulsant MK-801 binds to the activated state of the N-methyl-D-aspartate receptor in rat brain. *Br J Pharmacol* 91: 403–409, 1987.
19. **Genever PG, Wilkinson DJ, Patton AJ, Peet NM, Hong Y, Mathur A, Erusalimsky JD, Skerry TM.** Expression of a functional N-methyl-D-aspartate-type glutamate receptor by bone marrow megakaryocytes. *Blood* 93: 2876–2883, 1999.
20. **George A, Pushkaran S, Konstantinidis DG, Koochaki S, Malik P, Mohandas N, Zheng Y, Joiner CH, Kalfa TA.** Erythrocyte NADPH oxidase activity modulated by Rac GTPases, PKC, and plasma cytokines contributes to oxidative stress in sickle cell disease. *Blood* 121: 2099–2107, 2013.
21. **Goebel DJ, Poosch MS.** NMDA receptor subunit gene expression in the rat brain: a quantitative analysis of endogenous mRNA levels of NR1Com, NR2A, NR2B, NR2C, NR2D and NR3A. *Brain Res Mol Brain Res* 69: 164–170, 1999.
22. **Hinoi E, Takarada T, Ueshima T, Tsuchihashi Y, Yoneda Y.** Glutamate signaling in peripheral tissues. *Eur J Biochem* 271: 1–13, 2004.
23. **Hirschler-Laszkiewicz I, Tong Q, Conrad K, Zhang W, Flint WW, Barber AJ, Barber DL, Cheung JY, Miller BA.** TRPC3 activation by erythropoietin is modulated by TRPC6. *J Biol Chem* 284: 4567–4581, 2009.
24. **Hitchcock IS, Skerry TM, Howard MR, Genever PG.** NMDA receptor-mediated regulation of human megakaryocytopoiesis. *Blood* 102: 1254–1259, 2003.
25. **Huber SM, Gamper N, Lang F.** Chloride conductance and volume-regulatory nonselective cation conductance in human red blood cell ghosts. *Pflügers Arch* 441: 551–558, 2001.
26. **Jasek MC, Griffith WH.** Pharmacological characterization of ionotropic excitatory amino acid receptors in young and aged rat basal forebrain. *Neuroscience* 82: 1179–1194, 1998.
27. **Jinap S, Hajeb Glutamate P.** Its applications in food and contribution to health. *Appetite* 55: 1–10, 2010.
28. **Kaestner L.** Cation channels in erythrocytes–historical and future perspective. *Open Biol J* 4: 27–34, 2011.
29. **Kaestner L, Christophersen P, Bernhardt I, Bennekou P.** The non-selective voltage-activated cation channel in the human red blood cell membrane: reconciliation between two conflicting reports and further characterisation. *Bioelectrochemistry (Amsterdam, Netherlands)* 52: 117–125, 2000.
30. **Kaestner L, Tabellion W, Lipp P, Bernhardt I.** Prostaglandin E2 activates channel-mediated calcium entry in human erythrocytes: an indication for a blood clot formation supporting process. *Thromb Haemost* 92: 1269–1272, 2004.
31. **Kaestner L, Tabellion W, Weiss E, Bernhardt I, Lipp P.** Calcium imaging of individual erythrocytes: problems and approaches. *Cell Calcium* 39: 13–19, 2006.
32. **Kiessling K, Roberts N, Gibson JS, Ellory JC.** A comparison in normal individuals and sickle cell patients of reduced glutathione precursors and their transport between plasma and red cells. *Hematol J* 1: 243–249, 2000.
33. **Kutsuwada T, Kashiwabuchi N, Mori H, Sakimura K, Kushiya E, Araki K, Meguro H, Masaki H, Kumanishi T, Arakawa M, Mishina M.** Molecular diversity of the NMDA receptor channel. *Nature* 358: 36–41, 1992.
34. **Lang F, Lang KS, Wieder T, Myssina S, Birka C, Lang PA, Kaiser S, Kempe D, Duranton C, Huber SM.** Cation channels, cell volume and the death of an erythrocyte. *Pflügers Arch* 447: 121–125, 2003.
35. **Low CM, Wee KS.** New insights into the not-so-new NR3 subunits of N-methyl-D-aspartate receptor: localization, structure, and function. *Mol Pharmacol* 78: 1–11, 2010.
36. **Magnani M, Serafini G, Stocchi V.** Effects of Ca^{2+} and lipoxygenase inhibitors on hexokinase degradation in rabbit reticulocytes. *Mol Cell Biochem* 85: 3–7, 1989.
37. **Maher AD, Kuchel PW.** The Gardos channel: a review of the Ca^{2+}-activated K^+ channel in human erythrocytes. *Int J Biochem Cell Biol* 35: 1182–1197, 2003.
38. **Makhro A, Wang J, Vogel J, Boldyrev AA, Gassmann M, Kaestner L, Bogdanova A.** Functional NMDA receptors in rat erythrocytes. *Am J Physiol Cell Physiol* 298: C1315–C1325, 2010.
39. **Mandal M, Yan Z.** Phosphatidylinositol (4,5)-bisphosphate regulation of N-methyl-D-aspartate receptor channels in cortical neurons. *Mol Pharmacol* 76: 1349–1359, 2009.
40. **Masu M, Nakajima Y, Moriyoshi K, Ishii T, Akazawa C, Nakanashi S.** Molecular characterization of NMDA and metabotropic glutamate receptors. *Ann NY Acad Sci* 707: 153–164, 1993.
41. **Migliaccio G, Migliaccio AR, Druzin ML, Giardina PJ, Zsebo KM, Adamson JW.** Long-term generation of colony-forming cells in liquid culture of CD34+ cord blood cells in the presence of recombinant human stem cell factor. *Blood* 79: 2620–2627, 1992.
42. **Migliaccio G, Sanchez M, Masiello F, Tirelli V, Varricchio L, Whitsett C, Migliaccio AR.** Humanized culture medium for clinical expansion of human erythroblasts. *Cell Transplant* 19: 453–469, 2010.
43. **Miller BA, Cheung JY.** Mechanisms of erythropoietin signal transduction: involvement of calcium channels. *Proc Soc Exp Biol Med* 206: 263–267, 1994.
44. **Miller BA, Cheung JY, Tillotson DL, Hope SM, Scaduto RC Jr.** Erythropoietin stimulates a rise in intracellular-free calcium concentration in single BFU-E derived erythroblasts at specific stages of differentiation. *Blood* 73: 1188–1194, 1989.
45. **Minetti G, Egee S, Morsdorf D, Steffen P, Makhro A, Achilli C, Ciana A, Wang J, Bouyer G, Bernhardt I, Wagner C, Thomas S, Bogdanova A, Kaestner L.** Red cell investigations: art and artefacts. *Blood Rev* 27: 91–101, 2013.
46. **Mishina M, Mori H, Araki K, Kushiya E, Meguro H, Kutsuwada T, Kashiwabuchi N, Ikeda K, Nagasawa M, Yamazaki M, Masaki H, Yamakura T, Morita T, Sakimura K.** Molecular and functional diversity of the NMDA receptor channel. *Ann NY Acad Sci* 707: 136–152, 1993.
47. **Misra C, Brickley SG, Farrant M, Cull-Candy SG.** Identification of subunits contributing to synaptic and extrasynaptic NMDA receptors in Golgi cells of the rat cerebellum. *J Physiol* 524: 147–162, 2000.
48. **Misra C, Brickley SG, Wyllie DJ, Cull-Candy SG.** Slow deactivation kinetics of NMDA receptors containing NR1 and NR2D subunits in rat cerebellar Purkinje cells. *J Physiol* 525: 299–305, 2000.
49. **Monyer H, Burnashev N, Laurie DJ, Sakmann B, Seeburg PH.** Developmental and regional expression in the rat brain and functional properties of four NMDA receptors. *Neuron* 12: 529–540, 1994.
50. **Nowak LM, Wright JM.** Slow voltage-dependent changes in channel open-state probability underlie hysteresis of NMDA responses in Mg(2+)-free solutions. *Neuron* 8: 181–187, 1992.
51. **Ozuyaman B, Grau M, Kelm M, Merx MW, Kleinbongard P.** RBC NOS: regulatory mechanisms and therapeutic aspects. *Trends Mol Med* 14: 314–322, 2008.
52. **Paoletti P, Neyton J.** NMDA receptor subunits: function and pharmacology. *Curr Opin Pharmacol* 7: 39–47, 2007.
53. **Patneau DK, Mayer ML.** Structure-activity relationships for amino acid transmitter candidates acting at N-methyl-D-aspartate and quisqualate receptors. *J Neurosci* 10: 2385–2399, 1990.
54. **Qian A, Johnson JW.** Permeant ion effects on external Mg^{2+} block of NR1/2D NMDA receptors. *J Neurosci* 26: 10899–10910, 2006.
55. **Rodighiero S, De Simoni A, Formenti A.** The voltage-dependent non-selective cation current in human red blood cells studied by means of whole-cell and nystatin-perforated patch-clamp techniques. *Biochim Biophys Acta* 1660: 164–170, 2004.
56. **Schaefer A, Magocsi M, Marquardt H.** Signalling mechanisms in erythropoiesis: the enigmatic role of calcium. *Cell Signal* 9: 483–495, 1997.

57. **Skerry TM, Genever PG.** Glutamate signalling in non-neuronal tissues. *Trends Pharmacol Sci* 22: 174–181, 2001.
58. **Smothers CT, Woodward JJ.** Pharmacological characterization of glycine-activated currents in HEK 293 cells expressing N-methyl-D-aspartate NR1 and NR3 subunits. *J Pharmacol Exp Ther* 322: 739–748, 2007.
59. **Stabler SP, Marcell PD, Podell ER, Allen RH, Savage DG, Lindenbaum J.** Elevation of total homocysteine in the serum of patients with cobalamin or folate deficiency detected by capillary gas chromatography-mass spectrometry. *J Clin Invest* 81: 466–474, 1988.
60. **Steffen P, Jung A, Nguyen DB, Muller T, Bernhardt I, Kaestner L, Wagner C.** Stimulation of human red blood cells leads to Ca^{2+}-mediated intercellular adhesion. *Cell Calcium* 50: 54–61, 2011.
61. **Thomas SL, Bouyer G, Cueff A, Egee S, Glogowska E, Ollivaux C.** Ion channels in human red blood cell membrane: actors or relics? *Blood Cells Mol Dis* 46: 261–265, 2011.
62. **Thomas SL, Egee S, Lapaix F, Kaestner L, Staines HM, Ellory JC.** Malaria parasite Plasmodium gallinaceum up-regulates host red blood cell channels. *FEBS Lett* 500: 45–51, 2001.
63. **Thompson CJ, Schilling T, Howard MR, Genever PG.** SNARE-dependent glutamate release in megakaryocytes. *Exp Hematol* 38: 504–515, 2010.
64. **Tiffert T, Bookchin RM, Lew WL.** Calcium homeostasis in normal and abnormal human red cells. In: *Red Cell Membrane transport in Health and Disease*, edited by Bernhardt I, Ellory JC. Berlin, Germany: Springer, 2003, p. 373–405.
65. **Tiffert T, Etzion Z, Bookchin RM, Lew VL.** Effects of deoxygenation on active and passive $Ca^{2}+$ transport and cytoplasmic Ca^{2+} buffering in normal human red cells. *J Physiol* 464: 529–544, 1993.
66. **Tolle TR, Berthele A, Zieglgansberger W, Seeburg PH, Wisden W.** The differential expression of 16 NMDA and non-NMDA receptor subunits in the rat spinal cord and in periaqueductal gray. *J Neurosci* 13: 5009–5028, 1993.
67. **Tong Q, Chu X, Cheung JY, Conrad K, Stahl R, Barber DL, Mignery G, Miller BA.** Erythropoietin-modulated calcium influx through TRPC2 is mediated by phospholipase Cγ and IP3R. *Am J Physiol Cell Physiol* 287: C1667–C1678, 2004.
68. **Traynelis SF, Wollmuth LP, McBain CJ, Menniti FS, Vance KM, Ogden KK, Hansen KB, Yuan H, Myers SJ, Dingledine R.** Glutamate receptor ion channels: structure, regulation, and function. *Pharmacol Rev* 62: 405–496, 2010.
69. **Ulbrich MH, Isacoff EY.** Rules of engagement for NMDA receptor subunits. *Proc Natl Acad Sci USA* 105: 14163–14168, 2008.
70. **Vandorpe DH, Xu C, Shmukler BE, Otterbein LE, Trudel M, Sachs F, Gottlieb PA, Brugnara C, Alper SL.** Hypoxia activates a Ca2+-permeable cation conductance sensitive to carbon monoxide and to GsMTx-4 in human and mouse sickle erythrocytes. *PLoS One* 5: e8732, 2010.
71. **Wagner-Britz L, Wang J, Kaestner L, Bernhardt I.** Protein kinase Calpha and P-type Ca channel CaV2.1 in red blood cell calcium signalling. *Cell Physiol Biochem* 31: 883–891, 2013.
72. **Weiss E, Rees DC, Gibson JS.** Role of calcium in phosphatidylserine externalisation in red blood cells from sickle cell patients. *Anemia* 2011: 379894, 2010.
73. **Xiao Z, Jaiswal MK, Deng PY, Matsui T, Shin HS, Porter JE, Lei S.** Requirement of phospholipase C and protein kinase C in cholecystokinin-mediated facilitation of NMDA channel function and anxiety-like behavior. *Hippocampus*, 2011.
74. **Yang L, Andrews DA, Low PS.** Lysophosphatidic acid opens a Ca(++) channel in human erythrocytes. *Blood* 95: 2420–2425, 2000.
75. **Zancan P, Sola-Penna M.** Calcium influx: a possible role for insulin modulation of intracellular distribution and activity of 6-phosphofructo-1-kinase in human erythrocytes. *Mol Genet Metab* 86: 392–400, 2005.

5.3. Functional plasticity of the N-methyl-D-aspartate receptor in differentiating human erythroid precursor cells

Pascal Hänggi, Vsevolod Telezhkin, Paul J Kemp, Markus Schmugge, Max Gassmann, Jeroen S. Goede, Oliver Speer*, and Anna Bogdanova*

* stands for equal contribution of co-authors

Am J Physio Cell Physiol. 308; C993-C1007, 2015

Submitted 11 December 2014; accepted in final from 17 March 2015

Am J Physiol Cell Physiol 308: C993–C1007, 2015.
First published March 18, 2015; doi:10.1152/ajpcell.00395.2014.

Functional plasticity of the *N*-methyl-D-aspartate receptor in differentiating human erythroid precursor cells

Pascal Hänggi,[1,3,4] Vsevolod Telezhkin,[2] Paul J. Kemp,[2] Markus Schmugge,[4,5,6] Max Gassmann,[1,6] Jeroen S. Goede,[3,6] Oliver Speer,[4,5,6]* and Anna Bogdanova[1,6]*

[1]*Institute of Veterinary Physiology, University of Zurich, Zurich, Switzerland;* [2]*Division of Pathophysiology and Repair, School of Biosciences, Cardiff University, Cardiff, United Kingdom;* [3]*Division of Hematology University Hospital Zurich, Zurich, Switzerland;* [4]*University Children's Hospital, Zurich, Switzerland;* [5]*Children's Research Center, Zurich, Switzerland;* [6]*Zurich Center for Integrative Human Physiology (ZIHP), University of Zurich, Zurich, Switzerland*

Submitted 11 December 2014; accepted in final form 17 March 2015

Hänggi P, Telezhkin V, Kemp PJ, Schmugge M, Gassmann M, Goede JS, Speer O, Bogdanova A. Functional plasticity of the *N*-methyl-D-aspartate receptor in differentiating human erythroid precursor cells. *Am J Physiol Cell Physiol* 308: C993–C1007, 2015. First published March 18, 2015; doi:10.1152/ajpcell.00395.2014.—Calcium signaling is essential to support erythroid proliferation and differentiation. Precise control of the intracellular Ca^{2+} levels in erythroid precursor cells (EPCs) is afforded by coordinated expression and function of several cation channels, including the recently identified *N*-methyl-D-aspartate receptor (NMDAR). Here, we characterized the changes in Ca^{2+} uptake and electric currents mediated by the NMDARs occurring during EPC differentiation using flow cytometry and patch clamp. During erythropoietic maturation, subunit composition and properties of the receptor changed; in proerythroblasts and basophilic erythroblasts, fast deactivating currents with high amplitudes were mediated by the GluN2A subunit-dominated receptors, while at the polychromatic and orthochromatic erythroblast stages, the GluN2C subunit was getting more abundant, overriding the expression of GluN2A. At these stages, the currents mediated by the NMDARs carried the features characteristic of the GluN2C-containing receptors, such as prolonged decay time and lower conductance. Kinetics of this switch in NMDAR properties and abundance varied markedly from donor to donor. Despite this variability, NMDARs were essential for survival of EPCs in any subject tested. Our findings indicate that NMDARs have a dual role during erythropoiesis, supporting survival of polychromatic erythroblasts and contributing to the Ca^{2+} homeostasis from the orthochromatic erythroblast stage to circulating red blood cells.

calcium; differentiation; erythropoiesis; NMDA receptor

EVERY HOUR, APPROXIMATELY 10^{10} new erythrocytes are released into the circulation in an adult human after having undergone a tremendous variety of critical transformations during erythropoiesis. These sequential transformations occur within several days and are controlled by numerous intracellular and extracellular regulatory factors. Erythropoietin (Epo) and Ca^{2+} ions are two of the essential players in signaling cascades that support cell survival, proliferation, and differentiation of EPCs through stages from burst-forming units-erythroid (BFUe) to red blood cells (RBCs) (9, 30, 53, 61). The key role of stage-specific alterations in intracellular Ca^{2+} levels and the underlying changes in activity of Ca^{2+} transport pathways in the EPCs have been reported previously (21, 42, 53). Omission of extracellular Ca^{2+} completely inhibits erythopoietic maturation (44). Given its importance, the molecular identity of ion channels mediating Ca^{2+} uptake by EPCs during the early stages of maturation has been a subject of intensive investigation (11, 15, 42). In human and mouse EPCs, Ca^{2+} influx that is mediated by transient receptor potential channels (TRPCs) contributes to the Epo-Epo receptor (EpoR)-mediated signaling (10, 11, 15, 42, 58). Indeed, Epo regulates, in a concentration-dependent manner, Ca^{2+} influx into already hemoglobinized BFUe-derived EPCs, but not in EPCs at earlier stages of differentiation (24). However, Cheung et al. (8) have reported that Ca^{2+} influx induced by Epo was insufficient to activate Ca^{2+}-sensitive K^+ channels (Gardos channel). This strongly indicates the presence of multiple Ca^{2+} uptake pathways in EPCs during differentiation (52). We have recently reported the presence of *N*-methyl-D-aspartate receptors (NMDARs) in human progenitor cells and have shown that these nonselective, ligand-gated cation channels mediate Ca^{2+} uptake in EPCs (18, 35).

NMDARs are best characterized in neurons, but are not limited to the central and peripheral nervous system alone. Indeed, these receptors have been reported in a variety of cells and tissues, including osteoclasts, megakaryocytes, leucocytes, and RBCs (28, 35, 37, 39, 41). NMDARs are formed of glycine-binding subunits GluN1 and GluN3A/3B, and glutamate-binding subunits GluN2A/2B/2C/2D (12, 46, 59). For full activation, the heteromeric ion channel requires glutamate and the cotransmitters glycine (in the brain) or D-serine (in the spinal cord) (12). Depending on the subunit composition, cation selectivity, deactivation time, conductance, sensitivity to Mg^{2+} inhibition, and pharmacology of the NMDARs vary greatly (6, 46, 50). NMDARs containing GluN2C/2D have a lower conductance and a prolonged decay time (45, 47). Combination of these subunits with GluN3A/B results in a further decrease in the current amplitude, distinct channel properties, and altered pharmacology (6, 7, 34). In contrast, NMDAR containing the GluN2A subunit has a fast decay time and higher conductance (55). Recently, we have shown that expression of the *GRIN2C* (GluN2C) and *GRIN3B* (GluN3B) mRNA levels increased progressively from proerythroblast to orthochromatic erythroblast stage, whereas *GRIN2A* gene, coding for the GluN2A subunit, exhibited a high interindividual variability during maturation (35). This study was designed to characterize the function of the NMDARs expressed in EPCs at various stages of differentiation. Using an ex vivo erythropoietic maturation system, we monitored Ca^{2+} uptake and ionic

* O. Speer and A. Bogdanova contributed equally to this work.

Address for reprint requests and other correspondence: A. Bogdanova, Institute of Veterinary Physiology and Zurich Center for Integrative Human Physiology (ZIHP), Univ. of Zurich, Winterthurerstrasse 260, CH-8057 Zurich, Switzerland (e-mail: annab@access.uzh.ch).

  ISSN 0363-6143.

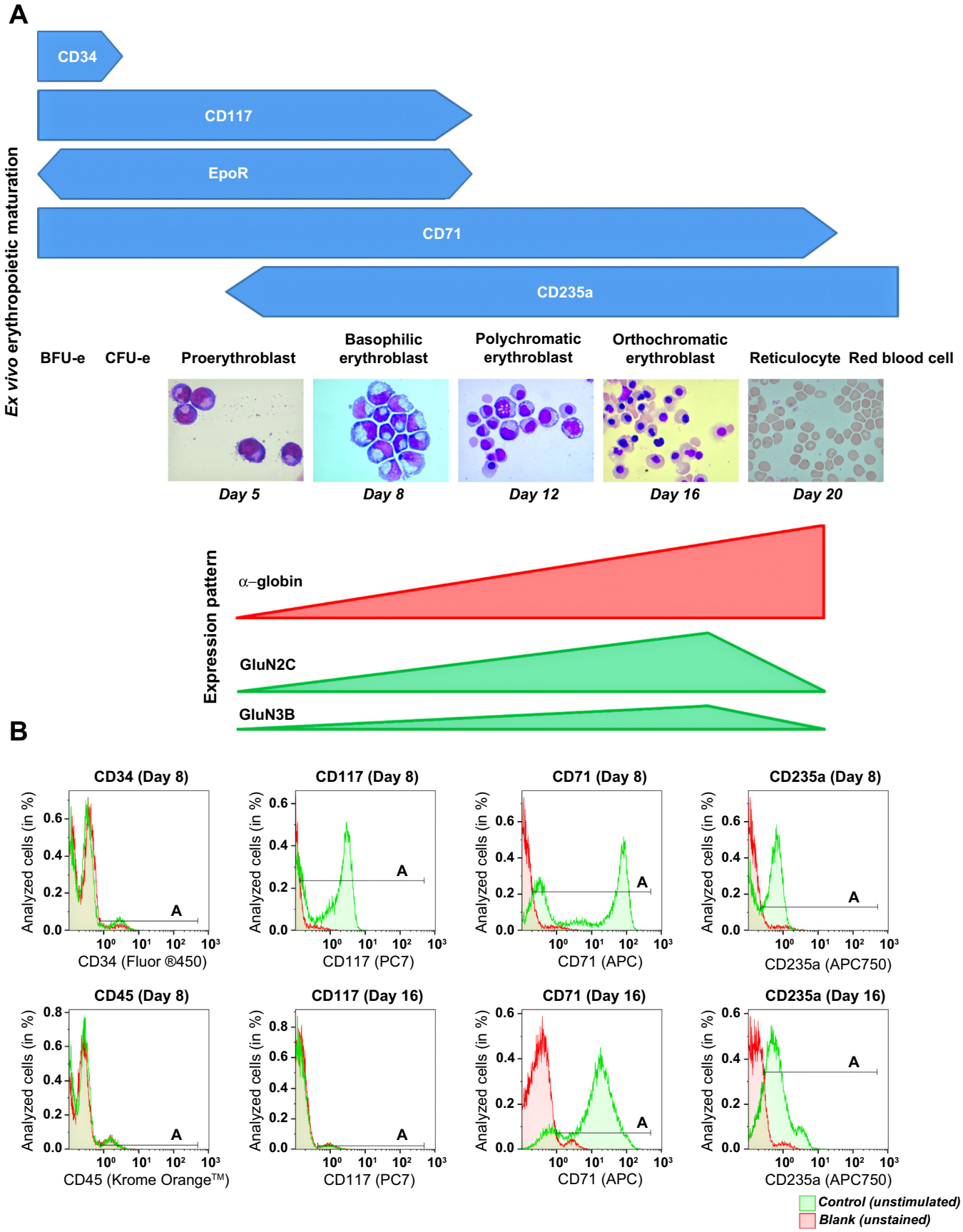
A
CD34
CD117
EpoR
CD71
CD235a
Ex vivo erythropoietic maturation
BFU-e
CFU-e
Proerythroblast
Basophilic erythroblast
Polychromatic erythroblast
Orthochromatic erythroblast
Reticulocyte
Red blood cell
Day 5
Day 8
Day 12
Day 16
Day 20
Expression pattern
α–globin
GluN2C
GluN3B
B
CD34 (Day 8)
CD117 (Day 8)
CD71 (Day 8)
CD235a (Day 8)
Analyzed cells (in %)
CD34 (Fluor ®450)
CD117 (PC7)
CD71 (APC)
CD235a (APC750)
CD45 (Day 8)
CD117 (Day 16)
CD71 (Day 16)
CD235a (Day 16)
CD45 (Krome Orange™)
Control (unstimulated)
Blank (unstained)

Table 1. *Characterization of erythropoietic maturation with specific surface marker*

Day of Maturation	$CD34^+$ Cells (Gate A)	$CD117^+$ Cells (Gate A)	$CD71^+$ Cells (Gate A)	$CD235a^+$ Cells (Gate A)	$CD45^+$ Cells (Gate A)
Day 8	2.30 ± 1.83%	62.72 ± 14.89%	80.04 ± 9.53%	50.06 ± 11.21%	0.08 ± 0.34%
Day 16	0.00 ± 0.01%	0.77 ± 1.45%	83.12 ± 10.12%	69.69 ± 19.63%	0.00 ± 0.01%

The percentage of cells in gate A (see Fig. 1*B*) presented as mean ± SD ($n = 9$ different donors).

currents induced by NMDAR agonists in human basophilic, polychromatic, and orthochromatic erythroblasts derived from isolated mononuclear cells to determine the stage-dependent alterations in NMDAR channel properties which mirrored the switch in subunit expression pattern observed at the transcriptional level (18, 35). Our new findings demonstrate the importance of the NMDAR in protecting the EPCs against apoptosis.

MATERIALS AND METHODS

Human blood samples and isolation of $CD34^+$ and erythropoietic precursor cells. Blood samples were obtained at the University Children's Hospital Zurich, Switzerland, or mononuclear cells were bought as a product from the Welsh blood bank in Cardiff, UK. All blood donors ($n = 16$ donors, both sexes, ages between 18 and 49 yr, Caucasian) provided written informed consent in accordance with the Declaration of Helsinki. Mononuclear cells were isolated from heparinized venous blood on a Ficoll-Paque PLUS gradient according to the protocol provided by GE-Healthcare (Dietikon, Switzerland).

Ex vivo hematopoiesis. Freshly isolated mononuclear cells were cultured in a two-phase liquid system as described elsewhere (35, 40). During the first phase, cells were maintained in StemSpan Serum-Free Medium for expansion of Hematopoietic Cells (SFEM) containing 0.51 mM L-glutamic acid and 0.4 mM glycine supplemented with StemSpan CC100 Cytokine mixture (StemCell Technologies, Grenoble, France) and 2% of penicillin-streptomycin (Sigma-Aldrich). After 4 days in culture, nonadherent cells were reseeded in StemSpan SFEM containing 20 ng/ml stem cell factor, 5 ng/ml interleukin-3, 1 unit Epo (all provided by ProSpec-Tany TechnoGene, Ness-Ziona, Israel) and 2% of penicillin-streptomycin (Sigma-Aldrich).

Morphological characterization. Cell morphology was assessed microscopically after cytocentrifugation (Cytospin 4 Cytocentrifuge, Thermo Fisher Scientific, Reinach, Switzerland) and May-Grünwald-Giemsa staining as described elsewhere (40). Differentiation state of the erythropoietic precursor cells (EPCs) was evaluated with the Axio Imager 2 Research Microscope (Carl Zeiss, Feldbach, Switzerland). Standard morphological appearance of basophilic, polychromatic, orthochromatic erythroblasts and reticulocytes is represented in multiple sources (e.g., Ref. 1).

Flow cytometry. To measure the changes in intracellular Ca^{2+} levels, cells were loaded with 3 μM FLUO-4 AM for 30 min, followed by a further 30 min of treatment with the following anti-human monoclonal antibodies: CD34, (eFluor 450 conjugated, clone 4H11, Ref. 48-0349-42), CD71, (APC conjugated, clone OKT9, Ref. 17-0719) both from eBiosciences (San Diego, CA), and CD117 (PC7 conjugated, clone 104D2D1, PN IM3698), CD235a (APC-Alexa Fluor 750 conjugated, clone KC16, PN A89314), and CD45 (Krome Orangeconjugated, clone J.33, PN A96416) all from Beckman Coulter. Loading with both the fluorescent probe and the antibodies was performed in StemSpan SFEM medium (containing 0.51 mM glutamate and 0.4 mM glycine). Preincubation with the receptor antagonist MK-801 (80 μM) for 30 min also occurred in the cell culture medium in a humidified atmosphere with 5% CO_2 at 37°C. Incubation with FLUO-4 AM, antibodies against the surface markers, and antagonist was performed in cell culture medium to mimic the "physiological conditions" in which basal level of NMDAR activation was maintained. Furthermore, MK-801 can only bind to activated NMDAR. Cell culture medium was replaced by the FACS solution in which cells were washed twice and resuspended before the assessment of fluorescence intensity. FACS solution contained (in mM) 135 NaCl, 5 KCl, 5 HEPES, 10 D-glucose, 2 $CaCl_2$ and was adjusted to pH 7.35 with NaOH. Agonist-induced Ca^{2+} uptake was recorded as response to the administration of 150 μM NMDA and 50 μM glycine (NMDA/GLY) to the cell-containing FACS medium. In a separate set of experiments, apoptotic markers were detected in EPCs pretreated with 500 μM MK-801 or memantine for 12 h in glutamic acid- and glycine-containing StemSpan SFEM. Those markers included caspases 3, 8, 9 and phosphatidylserine. Unstained (blank, red histograms) and unstimulated (control, green histograms) cells were used as controls. All experiments have been performed in triplicate, and 15,000 to 35,000 cells had been analyzed at each occasion. Galios Flow Cytometer software was used for data acquisition and Kaluza 1.2 software (Beckman Coulter) was applied for analysis.

Electrophysiology. Electrophysiological experiments were performed using EPCs obtained from eight donors between *day 7* and *20* of erythropoietic maturation. Nonadherent EPCs were plated down on coverglasses coated with poly-L-lysine solution (0.01% vol/wt in H_2O). Cells were voltage clamped during continuous perfusion at room temperature.

Protocols used elsewhere (14) to record NMDA-induced whole cell currents were adapted for detection of NMDAR activity in EPCs with some modification. The internal solution contained (in mM) 115 *N*-methyl-D-glucamine (NMDG)-HCl, 40 4-(2-hydroxyethyl)-1-piperazineethanesulfonic acid (HEPES), 10 ethylene glycol-bis(β-aminoethyl ether)-*N*,*N*,*N*′,*N*′-tetraacetic acid (EGTA), 2 Na_2ATP, and 0.2 Na_3GTP and pH was adjusted to 7.2–7.25 by HCl titration and osmolality to 280–285 mosmol/kgH_2O. The external solution contained (in mM) 127 NaCl, 20 CsCl, 12 D-glucose, 10 HEPES, 5 $BaCl_2$, 2 $CaCl_2$, with pH adjusted to 7.35 and osmolality to 300–305 mosmol/kgH_2O. Cs^+ and Ba^{2+} were used to reduce K^+ conductance. High concentration of EGTA was applied to bind the residual free Ca^{2+} after depolarization. To record passive membrane currents, standard intracellular solution containing (in mM) 117 KCl, 11 HEPES, 11 EGTA, 10 NaCl, 2 $MgCl_2$, 2 Na_2ATP, 1 $CaCl_2$ adjusted to pH 7.2 with KOH was used. The standard extracellular solution consisted of (in mM) 135 NaCl, 5 KCl, 5 HEPES, 10 D-glucose, 1.5 $CaCl_2$, adjusted to pH 7.35 with NaOH. Junction potential was

Fig. 1. Stage-dependent *N*-methyl-D-aspartate receptor (NMDAR) subunit expression during ex vivo erythropoietic maturation. *A*: differentiation stages of erythroid precursor cells (EPCs) in culture derived from peripheral blood-borne $CD34^+$ cells were analyzed morphologically and by the presence of the differentiation markers (CD34, CD117, CD71, and CD235a) assessed by flow cytometry (56) and matched with the α-globin, *GRIN2C*, and *GRIN3B* transcript abundance during ex vivo erythropoietic maturation (36). EpoR, erythropoietin (Epo)-Epo receptor; BFUe, burst-forming units-erythroid; CFUe, colony-forming units- erythroid. *B*: green histograms (control, unstimulated) showing CD34, CD117, CD71, and CD235a abundance in the EPCs at *days 8* (basophilic erythroblasts) and *16* (orthochromatic erythroblasts) in culture. Horizontal bars indicate the A gate selection. Shown in red are the histograms for the unstained cells (blank). CD45 was used to assess the fraction of white blood cells in erythroid cultures (quantification of the data and statistics are presented in Table 1).

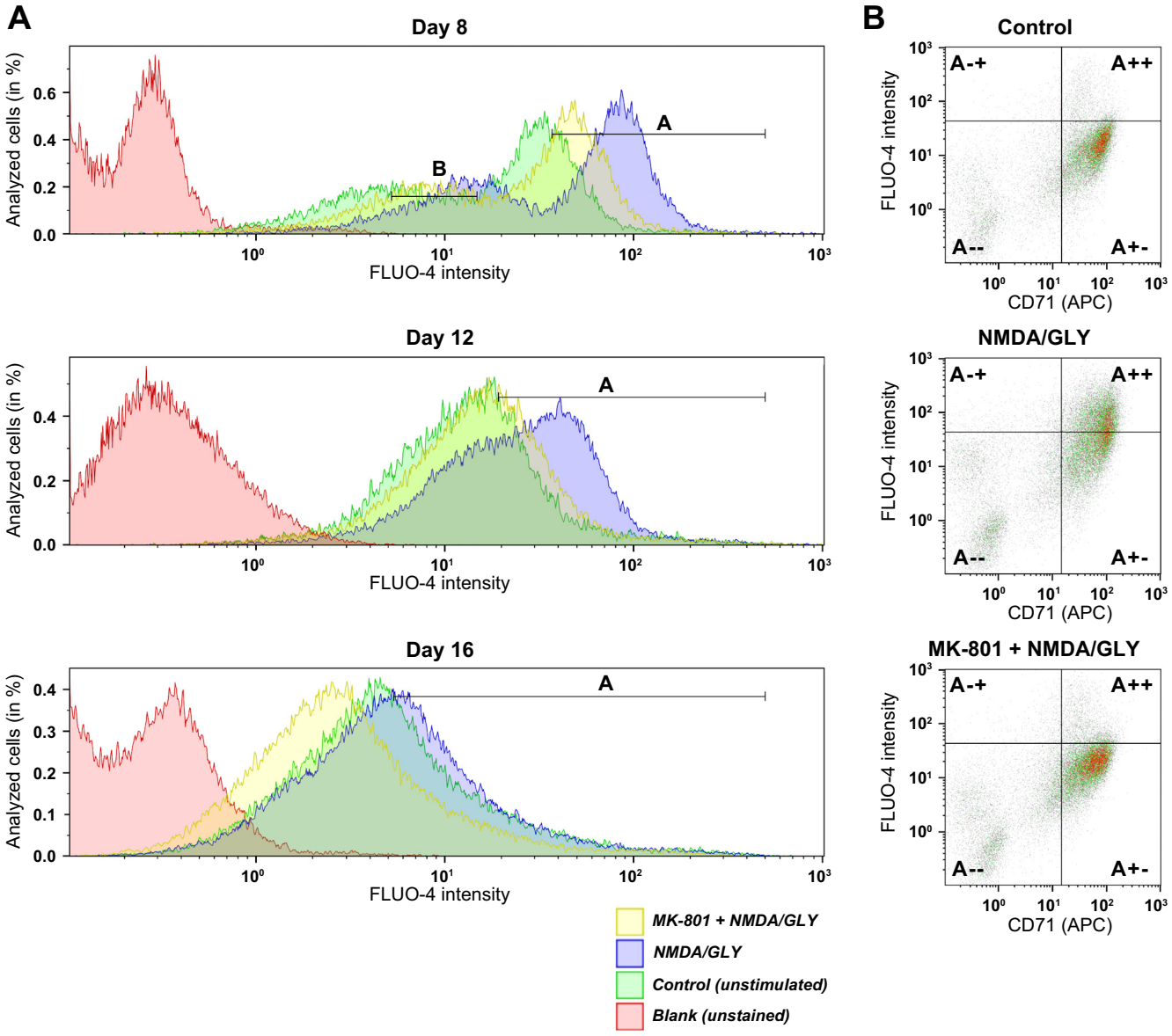
A
Day 8
Analyzed cells (in %)
FLUO-4 intensity
A
B
Day 12
Day 16
B
Control
NMDA/GLY
MK-801 + NMDA/GLY
FLUO-4 intensity
CD71 (APC)
A-+
A++
A--
A+-
MK-801 + NMDA/GLY
NMDA/GLY
Control (unstimulated)
Blank (unstained)

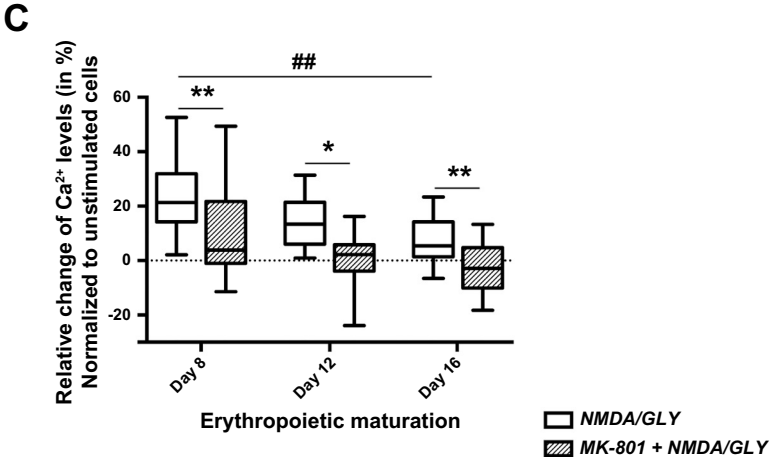
C
Relative change of Ca2+ levels (in %)
Normalized to unstimulated cells
##
**
*
**
Day 8
Day 12
Day 16
Erythropoietic maturation
NMDA/GLY
MK-801 + NMDA/GLY

Table 2. *Ca^{2+} influx upon stimulation with NMDA/GLY in the absence or presence of MK-801 at various differentiation stages*

	Day of Maturation (Gate)							
	Day 8 (Gate A)		Day 8 (Gate B)		Day 12 (Gate A)		Day 16 (Gate A)	
Treatment	FLUO-4 Intensity (Gated Cells)	GMF	FLUO-4 Intensity (Gated Cells)	GMF	FLUO-4 Intensity (Gated Cells)	GMF	FLUO-4 Intensity (Gated Cells)	GMF
Control	18.17 ± 8.19%	11.46	14.66 ± 6.21%	9.25	30.97 ± 7.27%	11.70	59.95 ± 9.73%	4.08
NMDA/GLY	56.06 ± 6.14%	30.83	18.01 ± 2.69%	9.88	60.79 ± 5.88%	21.07	64.71 ± 6.17%	4.46
MK-801 + NMDA/GLY	37.89 ± 7.08%	17.82	16.68 ± 4.82%	9.23	38.94 ± 8.53%	13.39	37.37 ± 7.41%	2.36

Measurements were performed in repetitive erythroid precursor cell EPCs) cultures ($n = 3$) from the same donor. Gating conditions are exemplified in Fig 2*A* and are presented in the table as the mean percentage of cells in the gate ± SD and geometric mean fluorescence (GMF). NMDA, *N*-methyl-D-aspartate; GLY, glycine.

adjusted after seal formation. For single recordings, high-resistance seals (GΩ seals) were formed, and cells were stable for 2–10 min. External and pipette solution (in mM: 117 KCl, 11 HEPES, 10 NaCl, 10 D-glucose, and 1.5 $CaCl_2$) was used to record single-channel activity. The pH was adjusted with NaOH to 7.35. Currents were normalized to the cell capacitance (pA/pF). Patch pipettes were pulled from borosilicate glass (GC100F-15, Harvard Apparatus, Holliston, MA) and fire polished. When filled with this pipette solution, they had tip resistances of between 9 and 12 MΩ in the bath solution. Axopatch 200B amplifier, Digidata 1440A, and pClamp 10.3 were used to acquire and filter (5 kHz) data (Axon CNS, Molecular Devices, Downingtown, PA). Leak current in whole cell recordings was subtracted manually. The electrophysiological properties of the EPC membranes were assessed using a voltage-step protocol, which held the voltage at −70 mV and stepped for 200 ms from −120 mV to +60 mV, in 10-mV increments. Agonist-evoked currents were recorded while holding the membrane at −60 mV. A voltage-step protocol described elsewhere (48) with a sequence of a hyperpolarizing step (−100 mV) and two depolarizing steps (+30 mV and +80 mV) was applied to liberate Mg^{2+} from the pore receptor prior to testing of the effects of pore-targeting NMDA antagonists MK-801 and memantine (48). NMDAR modulators were added at the holding potential of −60 mV. The recordings were performed at the depolarizing step (+100 mV). To ensure fast drug application, a Rapid Solution Changer System was used, which allowed solution changes within 20 ms. All chemicals were purchased from Sigma-Aldrich.

Statistical analysis. Data are presented as means ± SD. Statistical analysis was performed using one-way ANOVA with Bonferroni's multiple comparison test, Kruskal-Wallis with Dunn's post test, or Student's paired *t*-test, as appropriate. For all tests, significance was set at $P < 0.05$.

RESULTS

Ex vivo erythropoietic maturation. Characteristic changes in differentiating EPC cultures were monitored by morphological examination (Fig. 1*A*). In addition, hemoglobin accumulation and the expression of stage-specific markers such as CD34, CD117, CD71, and CD235a were assessed. These differentiation steps were associated with the alteration in the levels of transcripts for the *GRIN* genes (Fig. 1*B*) and corresponding protein abundance of NMDAR subunits (Fig. 1*A*) (18, 35). EPCs are referred to as the dominant (80%) cell type at the specific day as the cell population has never been completely homogeneous. On *day 8* of erythropoietic maturation, 2.3% still expressed CD34, the rest of the EPCs had differentiated to proerythroblasts. White blood cells ($CD45^+$) could not be traced. In all experiments, the proportion of $CD45^+$ cells was <0.01%. After 8 days in culture, the majority of EPCs had differentiated into basophilic erythroblasts with characteristic morphology (large cells with large nuclei with clumped chromatin, no nucleoli seen) and the onset of $CD117^+$ expression. On *day 12*, the majority of the EPCs were smaller in size with further progressing chromatin condensation in the nucleus and low hemoglobinization (Fig. 1*A*). The EPCs expressed CD71 and CD235a and were CD117 negative. These characteristics indicated that at *day 12* the polychromatic erythroblast stage was dominant. On *day 16*, most of the EPCs appeared to be smaller, with highly condensed nuclear and strongly hemoglobinized and expressing CD71 and CD235a and defined as orthochromatic erythroblasts (Fig. 1 and Table 1). Enucleation and reticulocyte formation occurred intensively after *day 17* in culture, with ≥90% of all EPCs losing nucleus by *day 20* as shown in Fig. 1*A*.

NMDA-induced whole cell currents and Ca^{2+} influx in EPCs during differentiation stages. Activity of NMDARs in basophilic, polychromatic, and orthochromatic erythroblasts was determined by monitoring whole cell currents and Ca^{2+} uptake

Fig. 2. Stage-dependent Ca^{2+} influx into the EPCs upon stimulation with NMDA and glycine (GLY) in the absence or absence of MK-801. The size of cell population responding to the stimulation with NMDA/GLY (150 μM/50 μM) with Ca^{2+} uptake was tested in the EPCs derived from nine different donors at *days 8*, *12*, and *16* in culture. Changes in intracellular Ca^{2+} were evaluated with Ca^{2+} indicator FLUO-4. *A*: representative histograms showing fluorescence intensity in unstimulated cells (control, shown in green), cells stimulated with NMDA (150 μM) and glycine (50 μM) (NMDA/GLY, in blue), and stimulated cells in the presence (MK-801 + NMDA/GLY, in yellow) of antagonist MK-801 (60 μM). Blank (unstained) readouts from the cells free from fluorophore are shown in red. At *day 8* of maturation one population of cells with high FLUO-4 intensity (gate A) and one with low FLUO-4 intensity (gate B) were present. At later stages only one population was present (gate A). Quantification of the data is presented in Table 2. *B*: dot plots illustrating relative change of intracellular Ca^{2+} levels in $CD71^+$ cells (gate A+- and gate A++). Presented are the representative readouts from the EPCs at *day 12* in culture in which Ca^{2+}-sensitive fluorescence of FLUO-4 was recorded in unstimulated cells (control), in stimulated (NMDA/GLY) cells, and in stimulated cells in the presence of antagonist (MK-801 + NMDA/GLY). Quantification of the data is presented in Table 3. *C*: Ca^{2+} uptake by the EPCs upon the stimulation with NMDA/GLY on average decreased during maturation from *day 8* to *day 16* in culture (##$P < 0.01$ compared with values for *day 8*). Inhibition of NMDAR by MK-801 resulted in significant reduction of intracellular Ca^{2+} at all stages of maturation (*$P < 0.05$ and **$P < 0.01$ compared with the antagonist-free cells). All experiments were performed in triplicate for each of nine donors used in these experiments. The amount of cells analyzed for each single recording ranged from 15,000 to 35,000. Data were normalized to the values obtained for unstimulated EPCs (dashed line). Box plots show the median and 95% confidence interval.

in a group of healthy human donors that were involved in previous molecular characterization of the receptor (18, 35). Since NMDARs, but not the other ionotropic glutamate receptors, are highly sensitive to *N*-methyl-D-aspartate, we mainly used NMDA for the receptor stimulation. Nonetheless, similar currents were induced by 250 μM glutamate and 50 μM glycine (data not shown).

Ca^{2+} uptake via the NMDAR was recorded in the cells, which were transferred from the glutamate and glycine-containing culture medium to agonist-free culture medium. Thereafter the cells were stimulated with the agonists (NMDA/GLY). The number of EPCs responding to the stimulation with induction of Ca^{2+} uptake (NMDA/GLY) (exemplified in Fig. 2*A* and Table 2) decreased with differentiation of basophilic erythroblasts to polychromatic and orthochromatic erythroblasts (24.9 ± 17.9%, 14.4 ± 9.6%, and 7.8 ± 8.5% of "responding cells" in the population, respectively) (Fig. 2*C*). All cells responded to stimulation with the NMDAR agonists with an increase in the intracellular Ca^{2+}-expressed CD71 (gate A++ in Fig. 2*B* and Table 3). The amplitude of Ca^{2+} uptake in erythroid precursor cells caused by the stimulation with NMDA/GLY reduced with differentiation from basophilic (*day 8*) to orthochromatic (*day 16*) erythroblasts (Fig. 2*C*). In orthochromatic erythroblasts (*day 16*), MK-801 treatment resulted in a modest, but significant decrease in intracellular Ca^{2+} levels (2.5 ± 9.1%) compared with the unstimulated EPCs (dotted line in Fig. 2*C*). Whole cell voltage-clamp recordings were used to verify the data obtained by flow cytometry. At a holding potential of −60 mV, coadministration of NMDA and GLY for 500 ms resulted in induction of currents with characteristics depending on the differentiation stage of the EPCs, as illustrated in Fig. 3*A*. Stimulation of the EPCs in whole cell and single-channel configuration with γ-amino butyric acid (GABA) used as a negative control was without an effect (data not shown).

In basophilic erythroblasts (Fig. 3*A*, *day 8*), stimulation with agonists immediately induced currents with a density of 77.41 ± 31.81 pA/pF (Fig. 3*B*) and a deactivation time of 332.0 ± 149.4 ms (Fig. 3*C*). Desensitization of the channels was observed upon repetitive stimulation with the agonists (Fig. 3*D*). Maturation to polychromatic erythroblasts (Fig. 3*A*, *day 12*) was associated with a decrease in current density to 40.96 ± 25.13 pA/pF (Fig. 3*B*) and prolongation of deactivation to 591.3 ± 206.2 ms (Fig. 3*C*). This tendency persisted with differentiation to orthochromatic erythroblasts (Fig. 3*A*, *day 16*) in which current density declined further to 16.01 ± 7.81 pA/pF (Fig. 3*B*) while deactivation time increased to 1,139.1 ± 382.9 ms (Fig. 3*C*). The number of cells, which were sensitive to agonist stimulation, declined during maturation, from 24.9 ± 13.3% in basophilic erythroblasts to 18.6 ± 9.3% of polychromatic erythroblasts, making up only 8.4 ± 8.6% in orthochromatic erythroblasts. The number of cells responding to the stimulation of NMDARs at various differentiation stages was identical no matter what technique (electrophysiology or flow cytometry) was used for detection of the NMDAR activation (Fig. 3*E*).

Sensitivity of agonist-induced currents to MK-801 and memantine. We have explored the sensitivity of currents induced by the receptor agonists to the potent and selective NMDAR channel blockers MK-801 (60 μM) and memantine (80 μM). As shown in Fig. 3*F*, these noncompetitive antagonists reduced the agonist-sensitive current density significantly. The application of MK-801 decreased the current density mediated by the NMDARs from 62.77 ± 10.42 pA/pF to 42.12 ± 8.51 pA/pF and memantine suppressed the mean current density to 46.82 ± 10.29 pA/pF. Long-term application of NMDA and glycine and repetitive performance of the voltage-step protocol induced deactivation (Fig. 3, *D* and *G*). Further inhibition of current density could be mediated by MK-801 supplementation (Fig. 3*G*).

Activation of single channels after application of NMDA and glycine. The effects of NMDAR activation and the concomitant Ca^{2+} uptake on the activity of ion channels is consistent with the properties of Ca^{2+}-activated K^+ channels and were determined in the cell-attached configuration. The single Ca^{2+}-sensitive K^+ channel currents (Fig. 4*A*) had a current-voltage (*I–V*) relationship resembling the characteristics of Gardos channels (13). The conductance of 23 pS of the channels was determined from the slope of the regression line. This value was similar to the conductance of 18–22 pS reported for the Gardos channels in mature red blood cells (16, 17, 27). Stimulation of reticulocytes with the NMDAR agonists induced a 6.7-fold increase in the product of open state probability (P_{open}) and number (N) of open channels (NP_{open}) (0.64 ± 0.19 vs. 0.09 ± 0.16 in nonstimulated cells) in 8.6 ± 7.4% of cells between *day 17* and *day 20* in culture (Fig. 4, *B* and *C*). The single-channel activity decreased after ~30 s of stimulation with agonists. Removal of the agonists resulted in recovery of the basal channel activity within 2 min. The spontaneous activity of these channels has been previously described by Dyrda et al. (13), and attributed to pressure activation. Further characterization of the Ca^{2+}-sensitive K^+ current was outside the scope of the study.

Interindividual variability of NMDAR activity correlates with the changes in GluN subunit expression levels during maturation. We have monitored interindividual variability in the relative mRNA expression of *GRIN2A* at *day 8* and the relative change of intracellular Ca^{2+} concentration after NMDAR activation that was recorded as a shift in geometric mean fluorescence (GMF). *GRIN2A* expression of individual donors correlated with the amplitude of changes in

Table 3. *Reduction of NMDAR-mediated Ca^{2+} influx after pretreatment with MK-801 in $CD71^+$ cells*

Treatment	Gate A−− (Gated Cells)	Gate A−+ (Gated Cells)	Gate A+− (Gated Cells)	Gate A++ (Gated Cells)
Control	24.53 ± 4.55%	1.01 ± 0.85%	67.82 ± 7.41%	6.64 ± 5.00%
NMDA/GLY	25.77 ± 3.89%	2.42 ± 1.19%	38.65 ± 4.02%*	33.16 ± 5.03%*
MK-801 + NMDA/GLY	29.02 ± 3.81%	1.63 ± 2.25%	60.72 ± 4.49%	8.63 ± 4.83%

The distribution of cells between the quadrants (see Fig. 2*A*) presented as mean % ± SD. *$P < 0.01$, compared with the unstimulated control (Student's paired *t*-test).

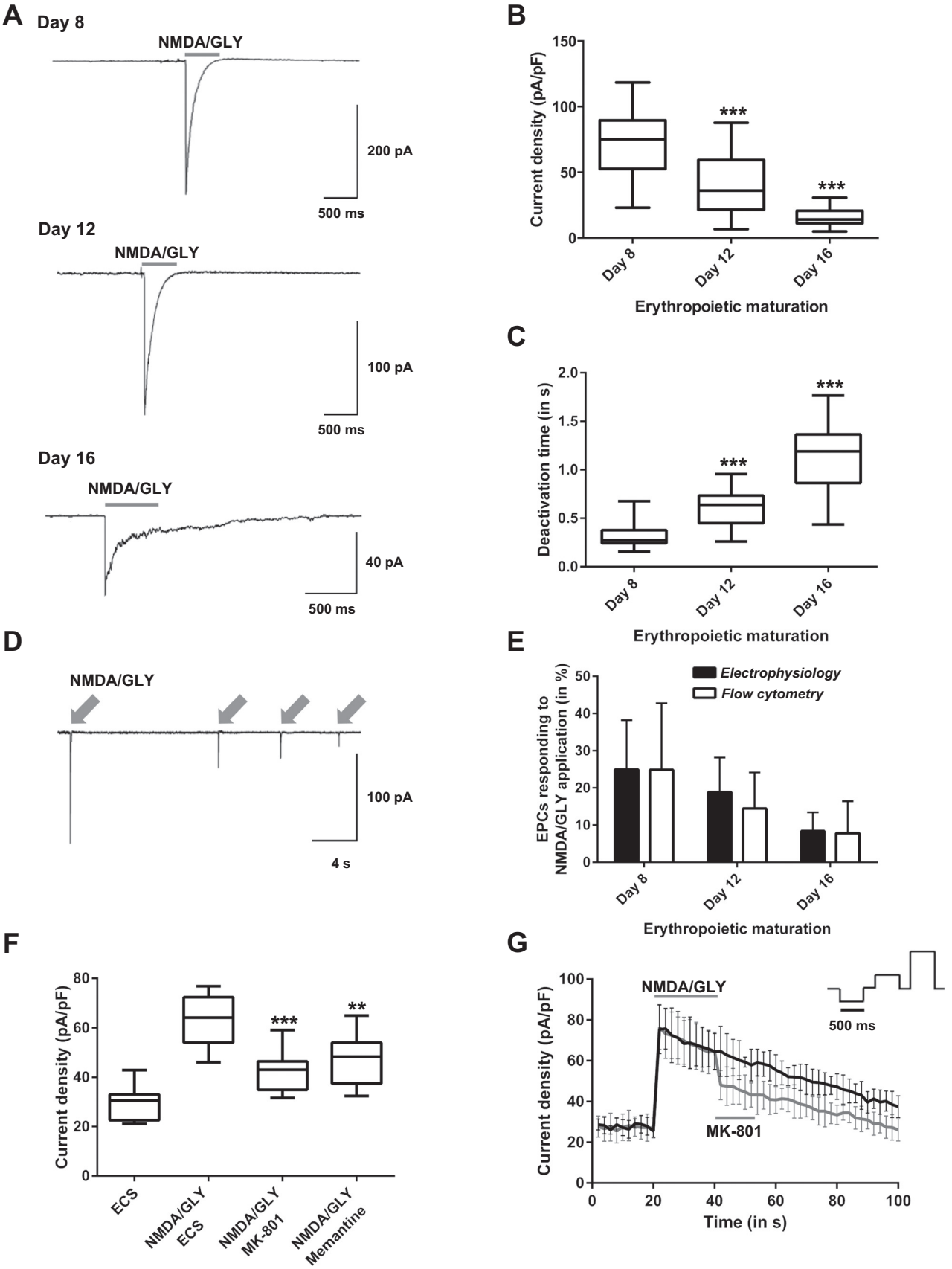
A
Day 8
NMDA/GLY
200 pA
500 ms
Day 12
NMDA/GLY
100 pA
500 ms
Day 16
NMDA/GLY
40 pA
500 ms
B
Current density (pA/pF)
150
100
50
0
***
***
Day 8
Day 12
Day 16
Erythropoietic maturation
C
Deactivation time (in s)
2.0
1.5
1.0
0.5
0.0
***
***
Day 8
Day 12
Day 16
Erythropoietic maturation
D
NMDA/GLY
100 pA
4 s
E
Electrophysiology
Flow cytometry
EPCs responding to NMDA/GLY application (in %)
50
40
30
20
10
0
Day 8
Day 12
Day 16
Erythropoietic maturation
F
Current density (pA/pF)
80
60
40
20
0
***
**
ECS
NMDA/GLY ECS
NMDA/GLY MK-801
NMDA/GLY Memantine
G
Current density (pA/pF)
100
80
60
40
20
0
NMDA/GLY
500 ms
MK-801
0
20
40
60
80
100
Time (in s)

the intracellular Ca^{2+} levels after NMDAR stimulation (Fig. 5*A*).

In basophilic erythroblasts, low levels of the *GRIN2C* and *GRIN3B* transcripts were associated with a prominent increase in the intracellular Ca^{2+} upon NMDAR activation (Fig. 6*A*). Inverse correlation was observed between the upregulation of the *GRIN2C* and *GRIN3B* genes and the amplitude of Ca^{2+} uptake in the EPCs stimulated with the NMDAR agonists during the transformation into polychromatic and orthochromatic erythroblasts (Fig. 6*B*).

Further correlations were detected between the type of NMDA-induced current and the subunit expression pattern. Deactivation time correlated inversely with the relative *GRIN2A* expression levels of individual donors (Fig. 5*C*).

A switch in NMDAR properties from channels with high amplitude and fast decay currents, characteristic of the basophilic erythroblasts, to currents of smaller amplitude and longer deactivation time from polychromatic erythroblast stage onwards, mirrored a switch from the GluN2A to GluN2C/3B in all nine donors (Fig. 6, *B* and *C*).

Alteration in electrophysiological properties during enucleation of erythropoietic cells. Besides the above-mentioned stage-dependent switch in NMDAR properties and the basal intracellular Ca^{2+} levels, alterations in basal electrophysiological properties of the EPC membranes exhibited during enucleation.

Current-voltage relationship within the −120 to +60 mV potential range showed no substantial changes until *day 15* of differentiation. A representative *I–V* curve (current type A) recorded from basophilic and polychromatic erythroblasts showed characteristic lack of voltage dependence within the range of potentials from −90 mV to +30 mV resembling the *I–V* relationship reported for chloride channels reported to be present in RBCs (26, 57) (Fig. 7, *A* and *D*). During enucleation (between *day 16* and *18*), a switch from voltage-independent to two types of voltage-dependent behavior occurred in 82.8 ± 1.01% of cells (Fig. 7, *B–E*). The majority of cells (70.8 ± 3.01%) exhibited a steep increase in conductance during depolarization from −20 mV to +50 mV (current type B), a feature characteristic of certain potassium channel types (25, 26, 57) (Fig. 7, *B* and *D*). In 12.0 ± 2.01% of EPCs a bell-shaped *I–V* relation (type C current) with maximal current density monitored at +30 mV was observed (Fig. 7, *C* and *D*). At *day 18* of differentiation, in 17.2 ± 1.0% of cells the *I–V* relationship (type A current) remained essentially voltage insensitive (Fig. 5*E*). Further in-depth studies are required for detailed characterization and molecular identification of all ion channels contributing to these basal electrophysiological properties.

Treatment of the EPCs with high doses of NMDAR channel pore blockers induces apoptosis. Earlier on, we have shown that high doses of memantine or MK-801 (above 100 or 50 μM, respectively) resulted in cell death, which was particularly pronounced for the early differentiation stages (18, 35). Herein we have extended this observation by analyzing the mechanism of cell death induced by high doses of pore-targeting NMDAR blockers. Incubation of basophilic erythroblasts with 500 μM MK-801 or memantine (the dose toxic for both blockers) for 12 h in the SFEM culture medium induced activation of caspase 3, caspase 8, and caspase 9 in the majority of cells (Fig. 8 and Table 4). Phosphatidylserine exposure was enhanced in EPCs exposed to both NMDAR antagonists (Fig. 8 and Table 5). Hyperactivation of the receptors by additional supplementation of NMDA (500 μM) and glycine (100 μM) to the culture medium caused only modest adverse effects (Table 5).

DISCUSSION

Plasticity of NMDAR and whole cell currents during erythropoiesis. The functional plasticity of the NMDAR during EPC differentiation is the most striking finding of this study. A dynamic switch in the subunit expression patterns was precisely mirrored by changes in the NMDAR channel function. These events contributed to the general remodeling of the membrane reflected by the changes in shape of the *I–V* curves observed in the course of EPC differentiation.

During differentiation from basophilic to polychromatic erythroblasts, the GluN2A subunit of the NMDAR in the cells was substituted by the GluN2C subunit, whereas the expression and abundance of the other subunits, of which GluN2D and 3B subunits were dominating, remained unchanged. The electrophysiological properties of NMDAR in EPCs at any of the stages tested exhibited high similarity to those in their counterparts in neurons (49). Namely, proerythroblasts and basophilic erythroblasts exhibited an NMDAR subtype with high amplitude and fast deactivation kinetics reported for the GluN2A-containing receptors (49). These receptors enable efficient glutamate-induced changes in transmembrane potential and massive short-term Ca^{2+} uptake. At these stages of maturation, EPCs were reported to be particularly dependent on Ca^{2+}-driven signaling. The latter is activated upon binding of erythropoietin to its receptors (42, 43) and engaged in control of a number of other processes of which iron processing in erythroblasts is one of the most important (20). The peak of Epo receptor expression is associated with the highest NMDA-evoked Ca^{2+} influx, fast deactivation time, and high conductance (Fig. 3, *A–C*) (11, 15, 42). Our findings indicate that prolonged exposure to high antagonist concentration en-

Fig. 3. Whole cell currents induced by EPC stimulation with NMDA and glycine. NMDA-induced currents were recorded in whole cell configuration at holding potential −60 mV. *A*: original recordings for the cells exposed to NMDA (150 μM) and GLY (50 μM) at *day 8* (*top*, $n = 64$ cells), *day 12* (*center*, $n = 59$ cells), *day 16* (*bottom*, $n = 47$ cells). *B*: alteration of current density of whole cell currents during erythropoietic maturation (***$P < 0.001$ compared with *day 8*). *C*: alteration of deactivation time during maturation (***$P < 0.001$ compared with *day 8*). *D*: deactivation of whole cell currents upon repetitive application of NMDA and GLY in EPCs at *day 12* in culture. *E*: no significant deviation in percentage of EPCs responding to NMDAR activation recorded using flow cytometry and electrophysiology ($P > 0.05$). EPCs from four different donors were analyzed for patch-clamp techniques (*day 8*, $n = 486$ cells; *day 12*, $n = 458$ cells; *day 16*, $n = 487$ cells) and from nine different donors for flow cytometry. *F*: application of the 60 μM MK-801 or 80 μM memantine reduced the current density significantly immediately after induction of NMDA currents (**$P < 0.01$ and ***$P < 0.001$). *G*: reduced current density after MK-801 (60 μM) application during repetitive voltage steps were applied. Black trace shows current density without antagonist application after NMDAR activation and gray trace shows current density with MK-801 application after NMDAR activation. All data are means ± SD and were recorded at +100 mV.

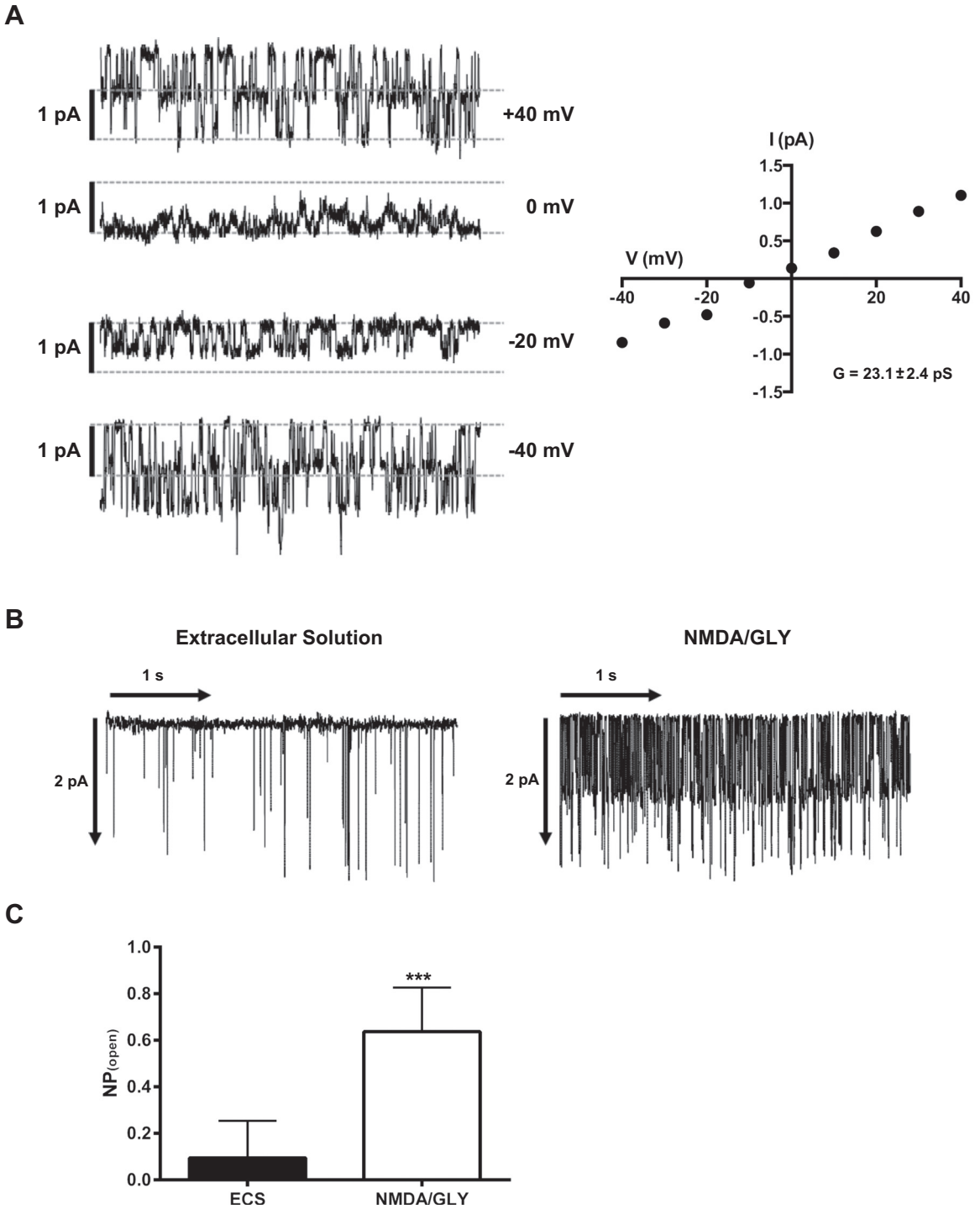

Fig. 4. Activation and deactivation of single channels after NMDAR activation. Single-channel recordings were performed in cell-attached configuration to monitor spontaneous single-channel activity and its alteration in response to the stimulation with 150 μM NMDA and 50 μM glycine. *A*: mean single-channel conductance (*G*) was 23.1 ± 2.4 pS ($n = 4$). *V*, voltage; *I*, current. *B*: single-channel recording before (*left*) and after (*right*) NMDA/GLY application. Holding potential was fixed at −40 mV. *C*: change in open probability and number of open channels (NP_{open}) upon NMDA/GLY application ($n = 96$ cells). ECS, extracellular solution. Data are means ± SD (***$P < 0.001$).

hances phosphatidylserine exposure (Fig. 8). This supports the hypothesis that the maintenance of NMDAR function is crucial for protection against apoptosis in proerythroblasts and basophilic erythroblasts. These observations are in agreement with the earlier studies in which requirement of the extracellular Ca^{2+} for survival and further differentiation of the EPC was postulated (42). Detailed investigation of the molecular mechanisms of involvement of NMDAR in protection of the EPCs from apoptosis was outside the scope of this study. In neural progenitor cells, activation of NMDARs causes transient recruitment of activator protein-1 (AP-1) to the DNA, followed with suppression in proliferation and induction of differentia-

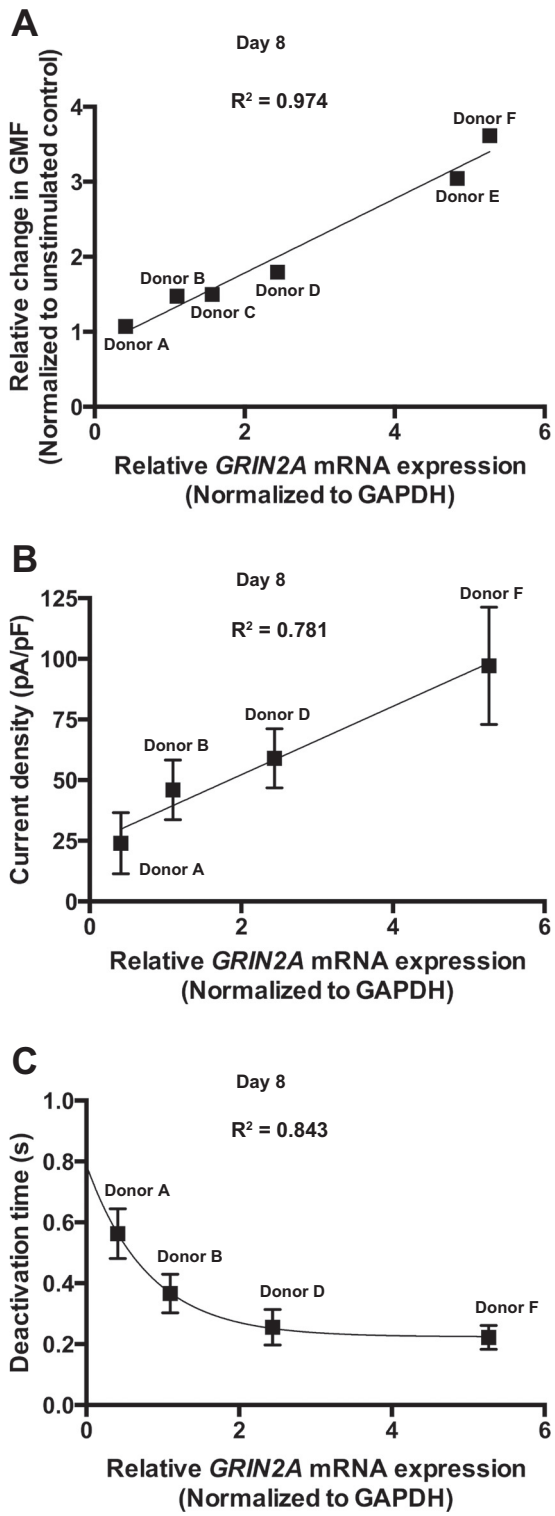

Fig. 5. Donor dependence of Ca^{2+} influx, receptor properties, and *GRIN2A* expression during hematopoiesis. mRNA expression was normalized to GAPDH. *A*: correlation between *GRIN2A* mRNA expression and relative change in geometric mean fluorescence (GMF) in the stimulated EPCs. Correlation coefficient was calculated by the change in GMF triggered by the agonists and the relative mRNA expression from six donors. *B*: correlation of current density and relative *GRIN2A* mRNA expression ($n = 4$). *C*: correlation of deactivation time and relative *GRIN2A* mRNA expression from four donors. Data are means ± SD; linear (*A* and *B*) and exponential (*C*) functions were used for curve fitting.

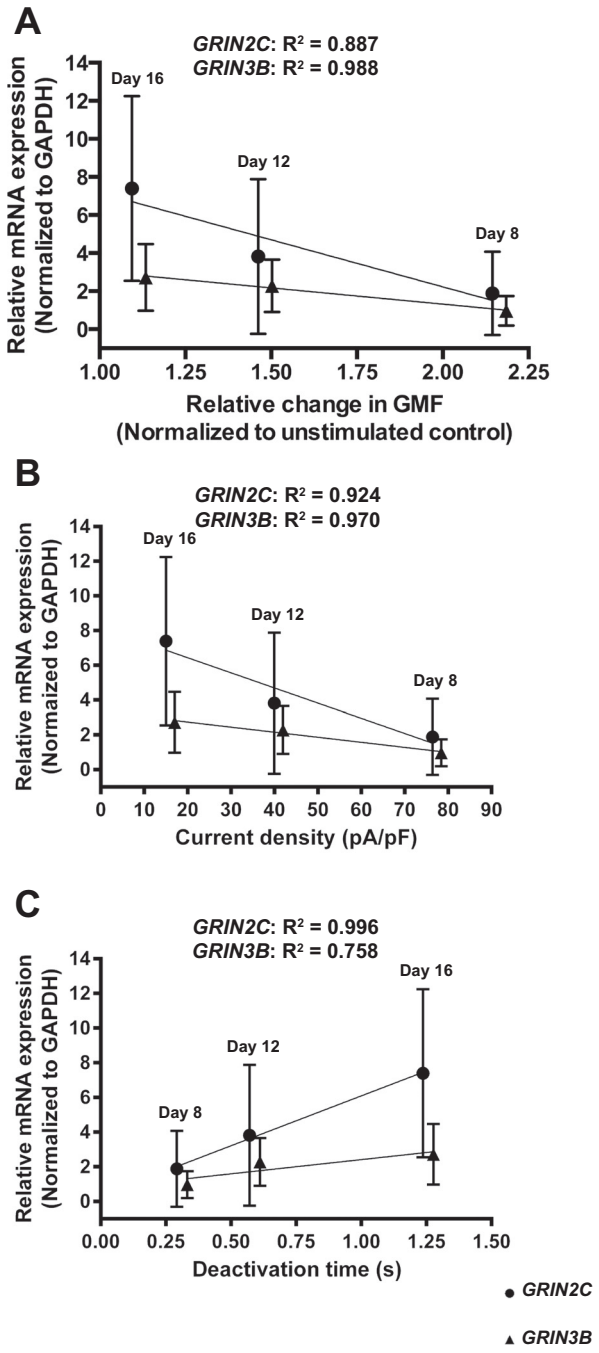

Fig. 6. Stage dependence of Ca^{2+} influx, receptor properties, and *GRIN2C/3B* expression during hematopoiesis. mRNA expression was normalized to GAPDH. *A*: correlation of relative *GRIN2C* and *GRIN3B* mRNA expression ($n = 9$) and relative change in GMF after NMDAR activation ($n = 9$). *B*: correlation of current density and relative *GRIN2C/3B* mRNA expression during erythropoietic maturation ($n = 6$). *C*: correlation of deactivation time and relative *GRIN2C/3B* mRNA expression during erythropoietic maturation ($n = 6$). Data are means ± SD (correlation coefficients see Table 4).

tion (29). In erythroid cells, AP-1 is known to be involved in regulation of proliferation and survival in Epo-dependent erythroid cells via controlling the activity of c-Jun and JunB transcription factors (23, 33).

Our results suggest that NMDARs may contribute to Epo-driven Ca^{2+} signaling along with TRP channels described

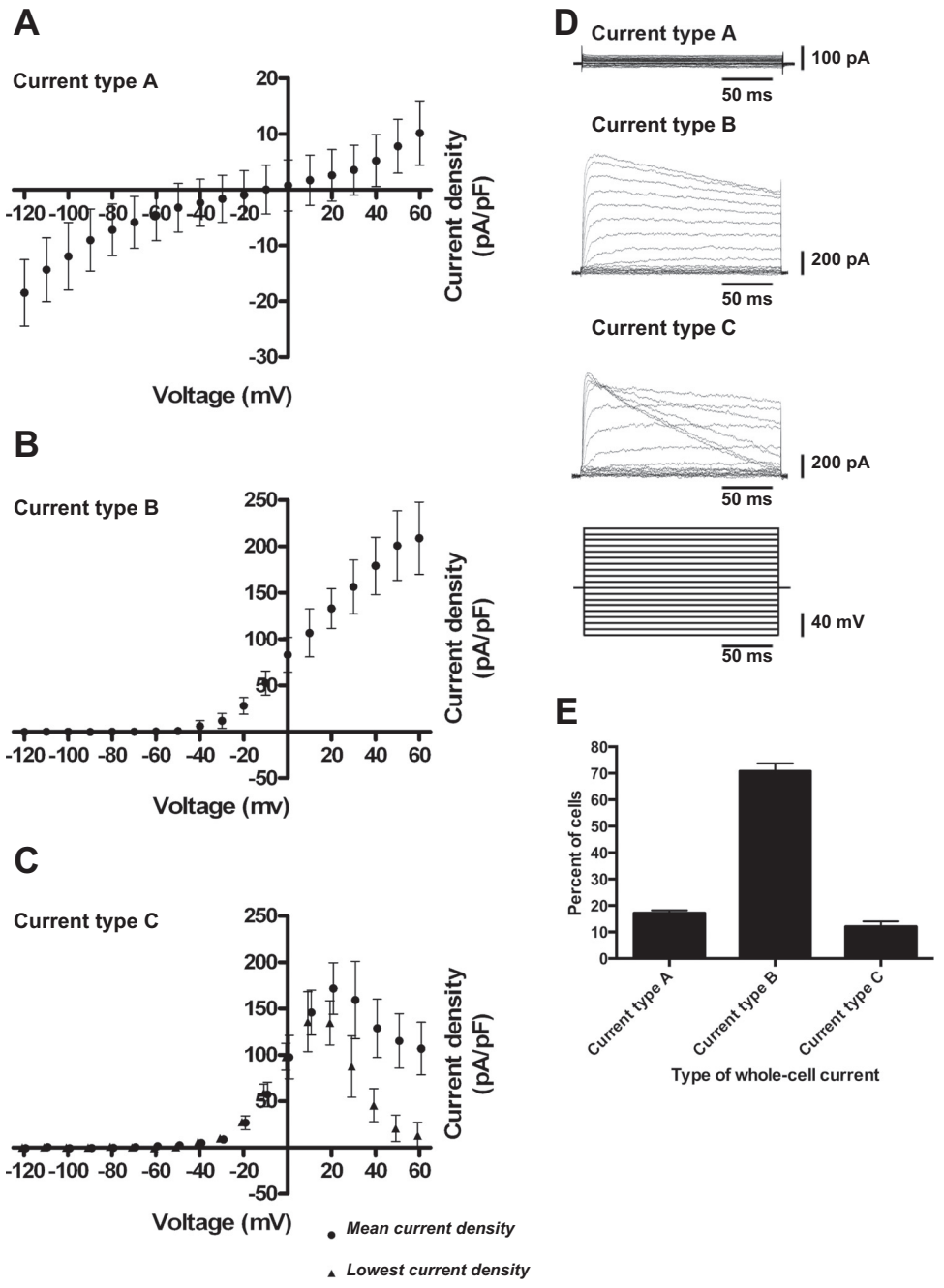

Fig. 7. Alteration in electrophysiological properties during hematopoiesis. Cells were voltage clamped in whole cell configuration during hematopoiesis, and voltage steps (10-mV increments) from −120 mV to +60 mV were applied for 200 ms. Current was normalized to cell capacitance (pA/pF) *A*: frequently observed whole cell currents (type A current, 86 cells) from early and intermediate stages of hematopoiesis (until *day 15*). *B*: frequently observed whole cell currents (type B current, 79 cells) from late stage of erythropoietic maturation (from *day 16* on). *C*: infrequently observed type of whole cell currents (type C current, 8 cells) from late stage (*day 18*). *D*: voltage-step protocol and three examples for the three whole cell current types. *E*: analysis of voltage-current relationship from four different donors at *day 18* of differentiation. Data are means ± SD (n = 76 cells).

earlier (15, 42, 44). Each of these channels mediating Ca^{2+} uptake respond to its own set of stimuli supporting a complex cross-talk between multiple receptors which drive the EPC differentiation process. Further studies are required to characterize the functional and possible physical interaction between these two types of channels.

Maturation to polychromatic and orthochromatic erythroblasts and finally to reticulocytes and RBCs is associated with a gradual replacement of this NMDAR type with the one mediating slowly decaying currents of smaller amplitude (Figs. 3 and 6, *B* and *C*). Induction of expression of the GluN2C subunit, which replaces GluN2A in receptors also containing the GluN2D and GluN3B subunits, coincides with the onset of hemoglobinization [*day 10* in culture according to Wickrema et al. (60) and Fig. 1]. Regulation of exocytosis of transferrin, its receptor recycling, and that of iron uptake by the EPCs in mice, rats, and rabbits is controlled by Ca^{2+}/calmodulin and is bound to sense the changes in Ca^{2+} uptake mediated by the NMDARs (20). Apart from their possible involvement in iron handling at the later stages of EPC differentiation, "slow" NMDARs are best suited for the regulation of basal Ca^{2+} levels. Together with other Ca^{2+}-permeable ion channels, such as voltage-dependent anion channels and voltage-gated calcium channel $Ca_v2.1$, which have been characterized in RBCs (25), these channels contribute to the regulation of cell volume, redox balance control, proteolysis, and O_2 affinity for hemoglobin (5, 18, 35).

Glutamate signaling in the microenvironment of EPCs. Fluctuations of glutamate levels in peripheral blood are mir-

rored by alterations in the activity of erythroid NMDARs. Recently, we have shown that NMDARs in RBCs show a high degree of basal activity when in the circulation (18). Additionally, glutamate levels within the bone marrow may be regulated by controlled secretion of this amino acid from megakaryocytes and macrophages (3, 22, 32, 39). The close association of bone marrow and glutamatergic nerve endings may further contribute to the alterations in glutamate levels promoting erythropoiesis and increasing RBC production. However, the exact range of glutamate levels therein has never been measured. We have shown that hyperactivation of NMDARs in young and mature RBCs, particularly those in sickle cell disease patients, was associated with a transient increase in Ca^{2+}, cell shrinkage, and oxidative burst (18). Prolonged chronic activation of NMDARs in EPCs causes receptor desensitization (Fig. 3*D*) but does not induce apoptosis in precursor cells (Fig. 8). We suggest that the desensitization is essential for cytoprotection as it controls Ca^{2+} uptake. Furthermore, Ca^{2+} oscillations mediated during the activation-deactivation cycles are used for signal transduction by a majority of cells (2, 51). The regulatory mechanisms and the physiological role of NMDARs expressed in EPCs as well as in other hematopoietic progenitors giving rise to leucocytes, and platelets require further investigation (28, 41). The pronounced toxic effect of NMDAR inhibition may be attributed to the importance of these receptors and Ca^{2+} fluxes they mediate for sustaining the EPCs' survival (42), but it more likely represents the off-target action of the receptor blockers at high concentrations (31).

In several studies, the receptors containing GluN2C/2D and GluN3B subunits were shown to have lower sensitivity to the channel pore blockers MK-801 and memantine and to Mg^{2+} block (7, 38, 54). Thus, the reduced efficiency of the pore-targeting MK-801 to inhibit NMDA currents is most likely associated with the unusual subunit compositions of erythroid NMDAR in which GluN1 is underrepresented, whereas GluN3B and 2D were most abundant. The low conductance and slow deactivation time we have observed for NMDARs in polychromatic erythroblasts were shown to be characteristic for the receptor formed by the GluN2C/D and GluN3B subunits (49). Currents mediated by the NMDAR in proerythroblasts showed no plateau phase as it was reported for the NMDAR currents in neuronal cells (4). These findings indicate that an atypical subunit composition and functional pattern of NMDAR in erythroid cells resemble the properties of the receptors described for other nonneuronal tissues (7, 28, 39).

Interindividual variability in quantity and quality of red blood cell production. We have observed marked intercellular and interindividual variability in the expression pattern and abundance of NMDAR subunits in EPCs of healthy humans (Fig. 5, *B* and *C*). However, repetitive measurements per-

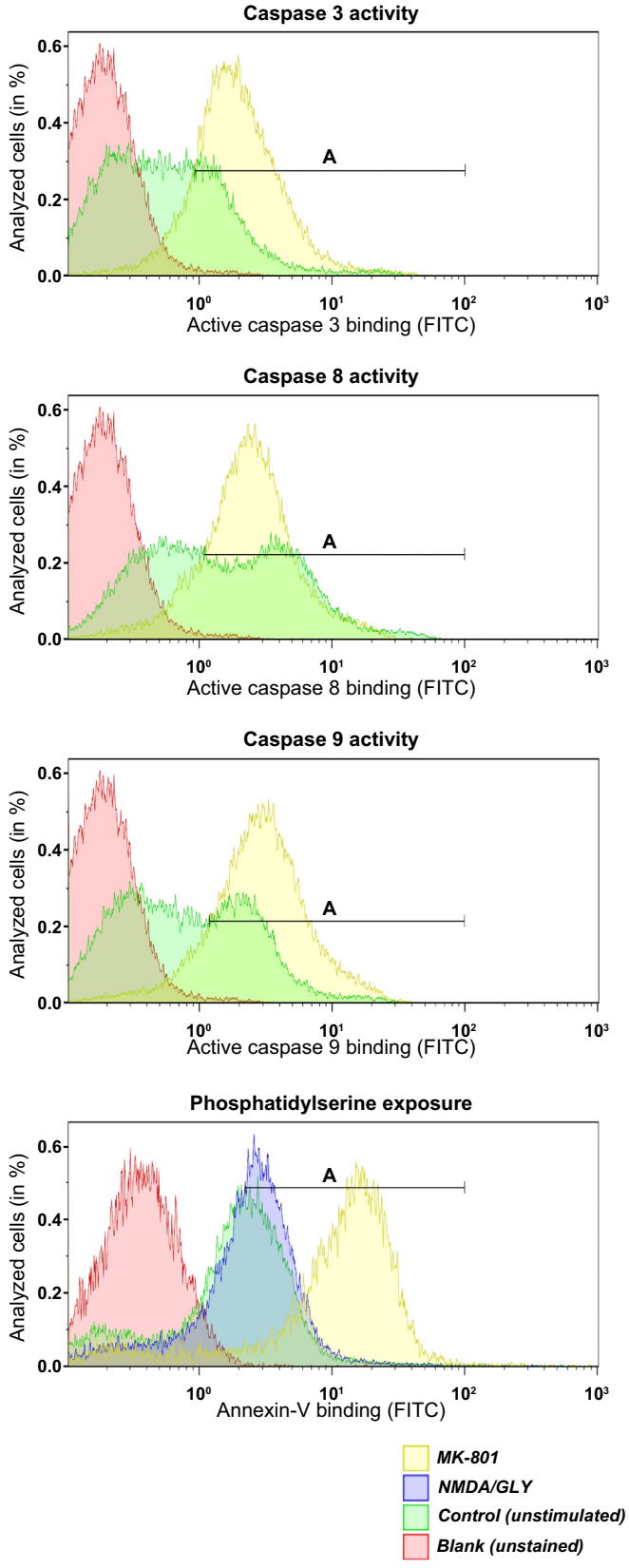

Fig. 8. Downstream activation of caspases and enhanced phosphatidylserine (PS) exposure after long-term blockage of NMDAR in differentiating EPCs. EPCs obtained from three donors and cultured for 12 days were incubated for 12 h at 37°C in the presence of 500 μM MK-801 or memantine or were supplemented with NMDA in addition to the medium-borne agonists (510 μM glutamate and 400 μM glycine). Cells were stained with caspase activity marker or FITC-labeled annexin-V antibody. Caspases 3, 8, and 9 were all upregulated (gate A) after long-term incubation (shown in yellow) with MK-801 and memantine (only MK-801 shown). High concentration of NMDA did not affect caspase activity (data not shown). PS exposure was increased (gate A) after long-term inhibition of NMDAR (only memantine shown). Overactivation of NMDAR (NMDA/GLY) with 500 μM NMDA and 100 μM glycine did not influence annexin-V binding (blue histogram) significantly.

Table 4. *Induction of caspase activity caused by the treatment of the EPCs with 500 μM of MK-801 or memantine*

	Apoptosis Marker					
	Caspase 3 Activity		Caspase 8 Activity		Caspase 9 Activity	
	Gated Cells		Gated Cells		Gated Cells	
Treatment	(Gate A)	GMF	(Gate A)	GMF	(Gate A)	GMF
Control	31.05 ± 7.32%	0.33	49.05 ± 2.60%	0.91	38.63 ± 7.98%	0.47
NMDA/GLY	36.56 ± 10.02%	0.56	53.01 ± 8.92%	1.09	39.91 ± 5.19%	0.53
MK-801	83.95 ± 6.62% †	1.76	79.04 ± 9.15%*	1.94	86.01 ± 8.36% †	2.32
Memantine	74.72 ± 9.19% †	1.59	73.41 ± 8.12%*	1.89	81.56 ± 7.45% †	2.18

The percentage of cells within gate A (Fig. 8) shown as mean ± SD and mean GMF for 3 independent donors. *$P < 0.01$, †$P < 0.001$, compared with nonstimulated control (one-way ANOVA).

formed for NMDARs in EPCs derived from $CD34^+$ cells of the same donor were highly reproducible. Interindividual variability of the *GRIN* gene transcript levels could represent individual genetic, epigenetic, and signaling profiles (19). Intercellular heterogeneity in part reflects heterogeneity of the EPC maturation stages in culture. However, this heterogeneity in NMDAR abundance is persistent in circulating RBCs independent of cell age, suggesting that, despite similar morphology, several subpopulations of RBCs and EPCs are produced representing "glutamate-sensitive" and "glutamate-resistant" cells (18, 35). Expression patterns of *GRIN2A* and *GRIN2C* define the properties of the NMDARs as the levels in *GRIN2A* transcripts in the individual donors are proportional to the peak amplitudes of glutamate-sensitive currents and Ca^{2+} uptake, and are inversely proportional to the deactivation time duration (Figs. 5 and 6).

Based on the finding that enhanced Ca^{2+} influx is a trigger for increased terminal erythropoiesis (15, 42) we have suggested that GluN2A-containing NMDAR contributes to this essential Ca^{2+} uptake. This would imply that the interindividual variability in number of receptors per cell and its subunit composition might have an influence on red blood cell production, properties, and clearance (5). These observations concur with previous reports on the interindividual and inter-cellular variability in sensitivity to NMDAR agonists such as glutamate or homocysteine. The degree of glutamate-sensitivity of RBCs of healthy human individuals may contribute to the quality of stored blood products and the outcome of transfusion (35).

Table 5. *Treatment of the EPCs with supra-pharmacological doses of NMDAR channel pore blockers induced Phosphatidylserine (PS) exposure*

	Apoptosis Marker	
	Phosphatidylserine Exposure	
	Gated Cells	
Treatment	(Gate A)	GMF
Control	44.3 ± 6.88%	0.82
NMDA/GLY	57.4 ± 5.82%	1.42
MK-801	86.3 ± 14.71%*	5.16
Memantine	84.80 ± 15.16%*	5.02

Percentage of cells in gate A (Fig. 8) presented as mean ± SD and mean GMF for 3 donors. *$P < 0.01$ compared with the nonstimulated control (one-way ANOVA).

ACKNOWLEDGMENTS

We thank Dr. Dipak Ramji (University of Cardiff, Cardiff, UK) for providing us with blood samples from the Welsh blood bank.

GRANTS

The study was funded by a cooperative grant from ZIHP (Zurich Center for Integrative Human Physiology), University of Zurich (J. S. Goede, O. Speer, and A. Bogdanova), supported by the Vontobel Foundation (A. Bogdanova) and Hartmann-Müller Stiftung (J. S. Goede and O. Speer), and received funding from the European Community's Seventh Framework Programme (FP7/2007-2013) under grant agreement 602121 (CoMMiTMenT project) to A. Bogdanova.

DISCLOSURES

No conflicts of interest, financial or otherwise, are declared by the author(s).

AUTHOR CONTRIBUTIONS

P.H., P.J.K., M.S., O.S., and A.B. conception and design of research; P.H., V.T., J.S.G., and O.S. performed experiments; P.H., V.T., O.S., and A.B. analyzed data; P.H., V.T., P.J.K., O.S., and A.B. interpreted results of experiments; P.H. prepared figures; P.H., V.T., P.J.K., M.S., M.G., J.S.G., O.S., and A.B. edited and revised manuscript; P.H., V.T., P.J.K., M.S., M.G., J.S.G., O.S., and A.B. approved final version of manuscript; A.B. drafted manuscript.

REFERENCES

1. **Anderson SC, Poulsen KB.** *Anderson's Atlas of Hematology*. New York: Wolters Kluwer Lippincott Willoams and Wilkins, 2014.
2. **Berridge MJ.** Calcium microdomains: organization and function. *Cell Calcium* 40: 405–412, 2006.
3. **Bhangu PS.** 'Pre-synaptic' vesicular glutamate release mechanisms in osteoblasts. *J Musculoskelet Neuronal Interact* 3: 17–29, 2003.
4. **Billups D, Liu YB, Birnstiel S, Slater NT.** NMDA receptor-mediated currents in rat cerebellar granule and unipolar brush cells. *J Neurophysiol* 87: 1948–1959, 2002.
5. **Bogdanova A, Makhro A, Wang J, Lipp P, Kaestner L.** Calcium in red blood cells-a perilous balance. *Int J Mol Sci* 14: 9848–9872, 2013.
6. **Cavara NA, Hollmann M.** Shuffling the deck anew: how NR3 tweaks NMDA receptor function. *Mol Neurobiol* 38: 16–26, 2008.
7. **Chatterton JE, Awobuluyi M, Premkumar LS, Takahashi H, Talantova M, Shin Y, Cui J, Tu S, Sevarino KA, Nakanishi N, Tong G, Lipton SA, Zhang D.** Excitatory glycine receptors containing the NR3 family of NMDA receptor subunits. *Nature* 415: 793–798, 2002.
8. **Cheung JY, Elensky MB, Brauneis U, Scaduto RC Jr, Bell LL, Tillotson DL, Miller BA.** Ion channels in human erythroblasts. Modulation by erythropoietin. *J Clin Invest* 90: 1850–1856, 1992.
9. **Cheung JY, Miller BA.** Molecular mechanisms of erythropoietin signaling. *Nephron* 87: 215–222, 2001.
10. **Cheung JY, Zhang XQ, Bokvist K, Tillotson DL, Miller BA.** Modulation of calcium channels in human erythroblasts by erythropoietin. *Blood* 89: 92–100, 1997.

11. **Chu X, Cheung JY, Barber DL, Birnbaumer L, Rothblum LI, Conrad K, Abrasonis V, Chan YM, Stahl R, Carey DJ, Miller BA.** Erythropoietin modulates calcium influx through TRPC2. *J Biol Chem* 277: 34375–34382, 2002.
12. **Cull-Candy S, Brickley S, Farrant M.** NMDA receptor subunits: diversity, development and disease. *Curr Opin Neurobiol* 11: 327–335, 2001.
13. **Dyrda A, Cytlak U, Ciuraszkiewicz A, Lipinska A, Cueff A, Bouyer G, Egee S, Bennekou P, Lew VL, Thomas SL.** Local membrane deformations activate Ca^{2+}-dependent K^+ and anionic currents in intact human red blood cells. *PloS One* 5: e9447, 2010.
14. **Flores-Hernandez J, Cepeda C, Hernandez-Echeagaray E, Calvert CR, Jokel ES, Fienberg AA, Greengard P, Levine MS.** Dopamine enhancement of NMDA currents in dissociated medium-sized striatal neurons: role of D1 receptors and DARPP-32. *J Neurophysiol* 88: 3010–3020, 2002.
15. **Gillo B, Ma YS, Marks AR.** Calcium influx in induced differentiation of murine erythroleukemia cells. *Blood* 81: 783–792, 1993.
16. **Grygorczyk R, Schwarz W.** Properties of the Ca^{2+}-activated K^+ conductance of human red cells as revealed by the patch-clamp technique. *Cell Calcium* 4: 499–510, 1983.
17. **Grygorczyk R, Schwarz W, Passow H.** Ca^{2+}-activated K^+ channels in human red cells. Comparison of single-channel currents with ion fluxes. *Biophys J* 45: 693–698, 1984.
18. **Hanggi P, Makhro A, Gassmann M, Schmugge M, Goede JS, Speer O, Bogdanova A.** Red blood cells of sickle cell disease patients exhibit abnormally high abundance of *N*-methyl D-aspartate receptors mediating excessive calcium uptake. *Br J Haematol* 167: 252–264, 2014.
19. **Hattangadi SM, Wong P, Zhang L, Flygare J, Lodish HF.** From stem cell to red cell: regulation of erythropoiesis at multiple levels by multiple proteins, RNAs, and chromatin modifications. *Blood* 118: 6258–6268, 2011.
20. **Hebbert D, Morgan EH.** Calmodulin antagonists inhibit and phorbol esters enhance transferrin endocytosis and iron uptake by immature erythroid cells. *Blood* 65: 758–763, 1985.
21. **Hirschler-Laszkiewicz I, Zhang W, Keefer K, Conrad K, Tong Q, Chen SJ, Bronson S, Cheung JY, Miller BA.** Trpc2 depletion protects red blood cells from oxidative stress-induced hemolysis. *Exp Hematol* 40: 71–83, 2012.
22. **Hitchcock IS, Skerry TM, Howard MR, Genever PG.** NMDA receptor-mediated regulation of human megakaryocytopoiesis. *Blood* 102: 1254–1259, 2003.
23. **Jacobs-Helber SM, Wickrema A, Birrer MJ, Sawyer ST.** AP1 regulation of proliferation and initiation of apoptosis in erythropoietin-dependent erythroid cells. *Mol Cell Biol* 18: 3699–3707, 1998.
24. **Jones HM, Edelman P, Pilkington GR, Watts M, Linch DC.** Fc gamma RII, but not erythropoietin or GM-CSF, mediates calcium mobilization in fetal hemopoietic blast cells. *Exp Hematol* 20: 315–319, 1992.
25. **Kaestner L.** Cation channels in erythrocytes - historical and future perspective. In: *Calcium Signalling*. Berlin: Springer, 2012, p. 223–233.
26. **Kaestner L, Bernhardt I.** Ion channels in the human red blood cell membrane: their further investigation and physiological relevance. *Bioelectrochemistry* 55: 71–74, 2002.
27. **Kaestner L, Bollensdorff C, Bernhardt I.** Non-selective voltage-activated cation channel in the human red blood cell membrane. *Biochim Biophys Acta* 1417: 9–15, 1999.
28. **Kalev-Zylinska ML, Green TN, Morel-Kopp MC, Sun PP, Park YE, Lasham A, During MJ, Ward CM.** *N*-methyl-D-aspartate receptors amplify activation and aggregation of human platelets. *Thromb Res* 133: 837–847, 2014.
29. **Kitayama T, Yoneyama M, Tamaki K, Yoneda Y.** Regulation of neuronal differentiation by *N*-methyl-D-aspartate receptors expressed in neural progenitor cells isolated from adult mouse hippocampus. *J Neurosci Res* 76: 599–612, 2004.
30. **Koury MJ, Bondurant MC.** Control of red cell production: the roles of programmed cell death (apoptosis) and erythropoietin. *Transfusion* 30: 673–674, 1990.
31. **Kovacic P, Somanathan R.** Clinical physiology and mechanism of dizocilpine (MK-801): electron transfer, radicals, redox metabolites and bioactivity. *Oxid Med Cell Longev* 3: 13–22, 2010.
32. **Lee YS, Lee SJ, Seo KW, Bae JU, Park SY, Kim CD.** Homocysteine induces COX-2 expression in macrophages through ROS generated by NMDA receptor-calcium signaling pathways. *Free Radic Res* 47: 422–431, 2013.
33. **Liebermann DA, Gregory B, Hoffman B.** AP-1 (Fos/Jun) transcription factors in hematopoietic differentiation and apoptosis. *Int J Oncol* 12: 685–700, 1998.
34. **Low CM, Wee KS.** New insights into the not-so-new NR3 subunits of *N*-methyl-D-aspartate receptor: localization, structure, and function. *Mol Pharmacol* 78: 1–11, 2010.
35. **Makhro A, Hanggi P, Goede JS, Wang J, Bruggemann A, Gassmann M, Schmugge M, Kaestner L, Speer O, Bogdanova A.** *N*-methyl-D-aspartate receptors in human erythroid precursor cells and in circulating red blood cells contribute to the intracellular calcium regulation. *Am J Physiol Cell Physiol* 305: C1123–C1138, 2013.
36. **Makhro A, Hanggi P, Goede JS, Wang J, Bruggemann A, Gassmann M, Schmugge M, Kaestner L, Speer O, Bogdanova A.** *N*-methyl D-aspartate receptors in human erythroid precursor cells and in circulating red blood cells contribute to the intracellular calcium regulation. *Am J Physiol Cell Physiol* 305: C1123–C1138, 2013.
37. **Makhro A, Wang J, Vogel J, Boldyrev AA, Gassmann M, Kaestner L, Bogdanova A.** Functional NMDA receptors in rat erythrocytes. *Am J Physiol Cell Physiol* 298: C1315–C1325, 2010.
38. **McClymont DW, Harris J, Mellor IR.** Open-channel blockade is less effective on GluN3B than GluN3A subunit-containing NMDA receptors. *Eur J Pharmacol* 686: 22–31, 2012.
39. **Merle B, Itzstein C, Delmas PD, Chenu C.** NMDA glutamate receptors are expressed by osteoclast precursors and involved in the regulation of osteoclastogenesis. *J Cell Biochem* 90: 424–436, 2003.
40. **Migliaccio G, Sanchez M, Masiello F, Tirelli V, Varricchio L, Whitsett C, Migliaccio AR.** Humanized culture medium for clinical expansion of human erythroblasts. *Cell Transplant* 19: 453–469, 2010.
41. **Miglio G, Varsaldi F, Lombardi G.** Human T lymphocytes express *N*-methyl-D-aspartate receptors functionally active in controlling T cell activation. *Biochem Biophys Res Commun* 338: 1875–1883, 2005.
42. **Miller BA, Cheung JY, Tillotson DL, Hope SM, Scaduto RC Jr.** Erythropoietin stimulates a rise in intracellular-free calcium concentration in single BFU-E derived erythroblasts at specific stages of differentiation. *Blood* 73: 1188–1194, 1989.
43. **Miller CP, Heilman DW, Wojchowski DM.** Erythropoietin receptor-dependent erythroid colony-forming unit development: capacities of Y343 and phosphotyrosine-null receptor forms. *Blood* 99: 898–904, 2002.
44. **Misiti J, Spivak JL.** Erythropoiesis in vitro. Role of calcium. *J Clin Invest* 64: 1573–1579, 1979.
45. **Misra C, Brickley SG, Wyllie DJ, Cull-Candy SG.** Slow deactivation kinetics of NMDA receptors containing NR1 and NR2D subunits in rat cerebellar Purkinje cells. *J Physiol* 525: 299–305, 2000.
46. **Monyer H, Sprengel R, Schoepfer R, Herb A, Higuchi M, Lomeli H, Burnashev N, Sakmann B, Seeburg PH.** Heteromeric NMDA receptors: molecular and functional distinction of subtypes. *Science* 256: 1217–1221, 1992.
47. **Mullasseril P, Hansen KB, Vance KM, Ogden KK, Yuan H, Kurtkaya NL, Santangelo R, Orr AG, Le P, Vellano KM, Liotta DC, Traynelis SF.** A subunit-selective potentiator of NR2C- and NR2D-containing NMDA receptors. *Nat Commun* 1: 90, 2010.
48. **Nowak L, Bregestovski P, Ascher P, Herbet A, Prochiantz A.** Magnesium gates glutamate-activated channels in mouse central neurones. *Nature* 307: 462–465, 1984.
49. **Paoletti P, Bellone C, Zhou Q.** NMDA receptor subunit diversity: impact on receptor properties, synaptic plasticity and disease. *Nat Rev Neurosci* 14: 383–400, 2013.
50. **Popescu G, Auerbach A.** The NMDA receptor gating machine: lessons from single channels. *Neuroscientist* 10: 192–198, 2004.
51. **Putney JW, Bird GS.** Cytoplasmic calcium oscillations and store-operated calcium influx. *J Physiol* 586: 3055–3059, 2008.
52. **Romero PJ, Romero EA, Mateu D, Hernandez C, Fernandez I.** Voltage-dependent calcium channels in young and old human red cells. *Cell Biochem Biophys* 46: 265–276, 2006.
53. **Schaefer A, Magocsi M, Marquardt H.** Signalling mechanisms in erythropoiesis: the enigmatic role of calcium. *Cell Signal* 9: 483–495, 1997.
54. **Schwartz EJ, Rothman JS, Dugue GP, Diana M, Rousseau C, Silver RA, Dieudonne S.** NMDA receptors with incomplete Mg(2)(+) block enable low-frequency transmission through the cerebellar cortex. *J Neurosci* 32: 6878–6893, 2012.
55. **Siegler Retchless B, Gao W, Johnson JW.** A single GluN2 subunit residue controls NMDA receptor channel properties via intersubunit interaction. *Nat Neurosci* 15: 406–413, S401–S402, 2012.

56. **Spivak JL.** The anaemia of cancer: death by a thousand cuts. *Nat Rev Cancer* 5: 543–555, 2005.
57. **Thomas SL, Bouyer G, Cueff A, Egee S, Glogowska E, Ollivaux C.** Ion channels in human red blood cell membrane: actors or relics? *Blood Cells Mol Dis* 46: 261–265, 2011.
58. **Tong Q, Hirschler-Laszkiewicz I, Zhang W, Conrad K, Neagley DW, Barber DL, Cheung JY, Miller BA.** TRPC3 is the erythropoietin-regulated calcium channel in human erythroid cells. *J Biol Chem* 283: 10385–10395, 2008.
59. **Ulbrich MH, Isacoff EY.** Rules of engagement for NMDA receptor subunits. *Proc Natl Acad Sci USA* 105: 14163–14168, 2008.
60. **Wickrema A, Krantz SB, Winkelmann JC, Bondurant MC.** Differentiation and erythropoietin receptor gene expression in human erythroid progenitor cells. *Blood* 80: 1940–1949, 1992.
61. **Wu H, Liu X, Jaenisch R, Lodish HF.** Generation of committed erythroid BFU-E and CFU-E progenitors does not require erythropoietin or the erythropoietin receptor. *Cell* 83: 59–67, 1995.

5.4. Red blood cells of sickle cell disease patients exhibit abnormally high abundance of N-methyl D-aspartate receptors mediating excessive calcium uptake

Pascal Hänggi*, Asya Makhro*, Jeroen S. Goede, Jue Wang, Andrea Brüggemann, Max Gassmann, Markus Schmugge, Lars Kaestner, Oliver Speer, and Anna Bogdanova.

* Pascal Hänggi and Asya Makhro denotes equal contribution of the authors.

British Journal of Haematology, 2014, 167, 252–264

Received 6 February 2014; accepted for publication 29. May 2014

bjh research paper

Red blood cells of sickle cell disease patients exhibit abnormally high abundance of N-methyl D-aspartate receptors mediating excessive calcium uptake

Pascal Hänggi,[1,2]* Asya Makhro,[2,3]* Max Gassmann,[2,3] Markus Schmugge,[4] Jeroen S. Goede,[1,2]* Oliver Speer[2,4] and Anna Bogdanova[2,3]*

[1]Division of Haematology, University Hospital Zurich, [2]Zurich Centre for Integrative Human Physiology (ZIHP), University of Zurich, [3]Institute of Veterinary Physiology, University Children's Hospital, and [4]Division of Haematology, University Children's Hospital, Zürich, Switzerland

Received 6 February 2014; accepted for publication 29 May 2014

Correspondence: PD Dr Anna Bogdanova, Institute of Veterinary Physiology, and Zurich Centre for Integrative Human Physiology (ZIHP), University of Zurich, Winterthurerstrasse 260, CH-8057 Zurich, Switzerland.
E-mail: annab@access.uzh.ch
*Denotes equal contribution of the authors.

Summary

Recently we showed that N-methyl D-aspartate receptors (NMDARs) are expressed in erythroid precursors (EPCs) and present in the circulating red blood cells (RBCs) of healthy humans, regulating intracellular Ca^{2+} in these cells. This study focuses on investigating the possible role of NMDARs in abnormally high Ca^{2+} permeability in the RBCs of patients with sickle cell disease (SCD). Protein levels of the NMDAR subunits in the EPCs of SCD patients did not differ from those in EPCs of healthy humans. However, the number and activity of the NMDARs in circulating SCD-RBCs was substantially up-regulated, being particularly high during haemolytic crises. The number of active NMDARs correlated negatively with haematocrit and haemoglobin levels in the blood of SCD patients. Calcium uptake via these non-selective cation channels was induced by RBC treatment with glycine, glutamate and homocysteine and was facilitated by de-oxygenation of SCD-RBCs. Oxidative stress and RBC dehydration followed receptor stimulation and Ca^{2+} uptake. Inhibition of the NMDARs with an antagonist memantine caused re-hydration and largely prevented hypoxia-induced sickling. The EPCs of SCD patients showed higher tolerance to memantine than those of healthy subjects. Consequently, NMDARs in the RBCs of SCD patients appear to be an attractive target for pharmacological intervention.

Keywords: red blood cells, calcium, sickle cell disease, N-methyl D-aspartate receptors, memantine.

Sickle cell disease (SCD) is a well-known one-gene disease. A point mutation in position 6 of the beta-globin chain gives rise to polymerization of deoxyhaemoglobin S (HbS), loss of deformability and increase in cell adhesion. Haemolysis, vaso-occlusive and pain crises are hallmarks of this disease. Gene therapy and bone marrow transplantation are the optimal, but rarely available and very expensive treatment strategies for this group of patients (Locatelli *et al*, 2013; Chandrakasan & Malik, 2014). Treatment with hydroxycarbamide (HC), which aims to increase haemoglobin F levels in RBCs, is part of the current standard care (Manwani & Frenette, 2013). This therapy significantly decreases the incidence and severity of pain crises and can be combined with regular blood transfusions. Further management includes symptomatic care, such as iron chelation, antibiotic treatment and psycho-social support. However, not all patients respond equally well to HC treatment. Thus, there is a standing need for novel treatment strategies.

Extensive experimental efforts have resulted in the suggestion of a number of novel potential targets for pharmacological intervention. Inhibition of the Gardos channel with the selective blocker Senicapoc (ICA-17043; Neusentis, Cambridge, UK) was used in a clinical trial aiming to reduce dehydration, which promotes haemoglobin S (HbS) polymerization. (Eaton & Hofrichter, 1990). This strategy alone suppressed haemolysis but failed to decrease the incidence of pain and vaso-occlusive crises (Ataga & Stocker, 2009). Inhibition of the calcium-dependent cysteine protease μ-calpain, was recently suggested as an attractive clinical strategy to reduce proteolysis and thereby suppress premature clearance and lysis of RBCs carrying human haemoglobin S (De Franceschi *et al*, 2013). Further suggestions include protec-

First published online 18 July 2014
doi: 10.1111/bjh.13028

tion of RBCs from oxidative stress by blocking NADPH oxidases (NOXes) which generate superoxide anions and are particularly abundant in the RBCs of SCD patients (George *et al*, 2013). Pathological hyperactivation of Gardos channels, μ-calpain and NOXes in diseased RBCs are not directly triggered by mutated HbS expression. However, all three proteins are known to respond to the up-regulation of the intracellular Ca^{2+} levels which were reported in the RBCs of SCD patients (Bogdanova *et al*, 2013). Furthermore, calcium overload is known to increase the adherence of RBCs to vascular endothelium in SCD patients (Hebbel *et al*, 1980; Mohandas & Evans, 1985). The steady-state passive channel-mediated permeability of red cell membranes for Ca^{2+} in healthy humans is very low (*c.* 50 μmol/($l_{packed\ cells}$•h)). Thus, even a minor increase in Ca^{2+} uptake due to the activation of one or several types of ion channels is associated with a substantial transient increase in intracellular Ca^{2+}. In SCD-RBCs abnormally high Ca^{2+} uptake is mediated by a conductive transport pathway known as P_{sickle}. This pathway is activated by deoxygenation, shear stress and a number of other stimuli (Bookchin & Lew, 1981) and, when activated, results in a 6- to 10-fold increase in intracellular free Ca^{2+} levels (Tiffert *et al*, 2003). The molecular identity of ion channel(s) mediating P_{sickle} remains unknown. Identification and characterization of these channel(s) is of key importance. Inhibition of the P_{sickle} pathway and the consecutive decrease in intracellular Ca^{2+} levels will cause inhibition of Gardos channels, μ-calpain, and NOXes. We have recently shown that N-methyl D-aspartate receptors (NMDARs) are involved in Ca^{2+} uptake by the RBCs of healthy humans (Makhro *et al*, 2013). These ionotropic glutamate receptors are non-selective cation channels requiring glutamate and glycine for their activation. They are known to mediate synaptic Ca^{2+} uptake in the brain (Paoletti *et al*, 2013). This study focuses on the involvement of NMDARs in the control of intracellular Ca^{2+} levels in SCD-RBCs. We have been able to follow the abundance and activity of NMDARs in erythroid precursor cells and in the circulating RBCs of SCD patients. Pathological hyperactivation of the NMDARs monitored in SCD-RBCs resulted in an increase in membrane permeability for Ca^{2+}. Haemolytic crises were associated with further up-regulation in receptor activity. Correlation of NMDAR activity with red cell number and C-reactive protein levels in plasma suggests that NMDAR is an active player in regulating red cell properties and life span in SCD patients.

Subjects and methods

A detailed description of materials and methods is available as a supplementary file.

Patients and healthy subjects

Our subject pool consisted of 16 adult patients (21–44 years old) with symptomatic SCD and 31 age-matched healthy adult subjects with no history of SCD. The group of 16 SCD patients consisted of 9 subjects with HbS/HbS, 3 patients with HbS/HbC, 3 with HbS/β-thalassaemia and one patient with HbS/HbD genotype. All patients experience mild and severe SCD crises, and show chronic haemolytic anaemia and persisting reticulocytosis. Blood samples were collected after obtaining informed consent from the subjects. The study was approved by the Ethics Commission of the Canton of Zurich and was performed in accordance with the declaration of Helsinki. General information on the patients is presented in Table I.

Protein abundance of the GluN1 subunit of the NMDAR in SCD-RBC membranes

Immunoblotting was used to explore the alterations in protein abundance of the GluN1 subunit in membrane fractions obtained from the SCD-RBCs and cells of healthy donors after centrifugation on 90% isotonic Percoll gradient (Lutz *et al*, 1992). Blood or pre-filtered RBC suspension was used for fractionation, and membrane preparation from cells forming the light (L), medium (M) and dense (D) fractions of RBCs was obtained (see Fig 1A). Immunoblotting was performed using mouse monoclonal antibodies against the GluN1 subunit on the NMDAR (#MAB1586 Millipore, Temecula, CA) as well as rabbit polyclonal antibodies against total actin (#A2066, Sigma-Aldrich, St. Louis, MO, USA). Rat cortex lysate was used as a positive control, and total actin as a loading control.

NMDAR activity in SCD-RBCs

The number of active receptors per cell was detected using radiolabelled antagonist binding assay as described earlier (Makhro *et al*, 2013). Blood samples were incubated with [^{3}H]MK-801 (740 GBq/mmol, Perkin Elmer, Boston, MA) with subsequent fractionation on Percoll gradient. The potential impact of white blood cells (WBCs) on the [^{3}H]MK-801 binding assay in RBCs in fractions was assessed, as binding of the radiolabelled antagonist was tested in blood samples with and without filtration through a cellulose column. As filtration resulted in a substantial increase in the number of [^{3}H]MK-801 binding sites due to the shear stress filtration step, it was avoided in cases when basal activity of the erythrocytic NMDARs in plasma was determined. Microfluorescence live imaging was used to confirm the data on receptor activity and abundance obtained using [^{3}H]MK-801 binding assay.

Ca^{2+} uptake through NMDARs as a function of oxygenation of SCD-RBCs

Changes in the intracellular Ca^{2+} levels in RBCs upon treatment with agonists (300 μmol/l of NMDA, glutamate or homocysteine mixed with 100 μmol/l glycine) and/or antagonist

Table I. Clinical characteristics of sickle cell disease patients.

	Patient 1	Patient 2	Patient 3	Patient 4	Patient 5	Patient 6	Patient 7	Patient 8	Patient 9	Patient 10	Patient 11	Patient 12	Patient 13	Patient 14	Patient 15	Patient 16
Age (years)	39	24	44	28	26	37	41	27	38	22	31	24	24	36	35	21
Disease	HbS/HbS	HbS/HbS	HbS/HbS + hom α^+-thal.	HbS/β-thal. minor + het α^+-thal.	HbS/HbC	HbS/HbS	HbS/β-thal. minor	HbS/HbS	HbS/HbS	HbS/HbS	HbS/HbC	HbS/HbD	HbS/HbS	HbS/HbC	HbS/HbS	HbS/HbS
Hb (g/l)	95	91	86	82	105	77	108	80	97	102	104	114	81	119	68	95
Reticulocytes (%)	20·8	12·5	11·9	6·4	6·0	10·7	7·0	32·0	16·8	4·7	4·2	3·83	7·3	4·4	11·4	9·5
MCV (fl)	86·9	92·8	76·6	62·8	80·8	89·2	69·2	96·4	86·0	106·5	81·3	113·6	94·7	74·5	81·1	78·2
LDH (u/l ULN: 420)	979	583	856	582	543	463	642	463	1003	754	419	1094	841	650	887	707
Repeated crisis	Yes	Yes	Yes	Yes	Yes	Yes	Yes	Yes	Yes	Yes	No	No	Yes	Yes	Yes	Yes

Hb, haemoglobin; MCV, men cell volume; LDH, lactate dehydrogenase; ULN, upper limit of normal.
Patients with HbS/HbS: 9.
Patients with HbS/HbC: 3.
Patients with HbS/thal: 3.
Patients with HbS/HbD: 1.

(memantine, 50 μmol/l) of the NMDARs were monitored using the fluo-4 AM dye, as described elsewhere (Makhro *et al*, 2013). RBCs were loaded with 5 μmol/l of the dye for 30 min at room temperature. Incubation medium contained 145 mmol/l NaCl, 5 mmol/l KCl, 1 mmol/l $CaCl_2$, 0·15 mmol/l $MgCl_2$,10 mmol/l Tris-HCl (pH 7·4), 10 mmol/l glucose and 0·1% bovine serum albumin. The effect of hypoxia on cell shape and Ca^{2+} content was tested in the RBCs of SCD patients. The cells were loaded with fluo-4 AM and exposed to 15% O_2 (normoxia) or 0·5% O_2 (hypoxia), 5% CO_2, balanced with N_2 for 10 min, with or without supplementation of the NMDAR antagonist memantine (100 μmol/l) and/or 300 μmol/l NMDA/100 μmol/l glycine mixture. Calcium uptake, cell surface projection and anisotropy as markers of cell volume and sickle cell transformation were then measured microscopically and analysed using CellFinder® (Dr. M. Makhinya, Computer Vision Laboratory, Zürich, Switzerland) as described (Makhro *et al*, 2013).

NMDARs in control of SCD-RBC density, K^+ content and intracellular reduced (GSH) and oxidized (GSSG) glutathione levels

The changes in red cell density upon activation or inhibition of the NMDARs were measured in blood from four selected SCD patients using centrifugation in Percoll density gradient in the presence or absence of NMDA or memantine. Together with mean cell volume (MCV), haematocrit and cell water content, distribution in Percoll gradient was used as an indication of dehydration-rehydration. Changes in the intracellular K^+ content in oxygenated and deoxygenated SCD-RBCs were monitored using flame photometry, and unidirectional chloride-independent K^+ influx was measured using ^{86}Rb as a tracer, as described elsewhere (Makhro *et al*, 2013). The effects of an NMDA/glycine mixture and memantine on the intraerythrocytic GSH:GSSG balance was tested using Ellman's reagent (5,5′-dithio-bis-[2-nitrobenzoic acid]). Proteins were precipitated with 5% trichloroacetic acid and removed; non-protein reduced thiols assessed with or without pre-treatment with glutathione reductase and NADPH, as described elsewhere (Tietze, 1969; Bogdanova *et al*, 2003).

Ex vivo *erythropoiesis and expression of NMDARs in erythroid precursor cells*

Mononuclear cells were isolated from the peripheral blood of healthy people and SCD patients and cultured *ex vivo*, using a 2-phase StemSpan liquid system. After seeding in serum-free expansion medium (SFEM) supplemented with a cytokine mix and penicillin/streptomycin the cells were cultured in it for 5 d. Thereafter non-adherent cells were reseeded and maintained for up to 21 d in StemSpan SFEM with 2% penicillin/streptomycin, 20 ng/ml stem cell factor, 1 u/ml erythropoietin and 5 ng/ml interleukin 3. At day 5, 2 μmol/l dexamethasone and 1 μmol/l β-estradiol were added. During

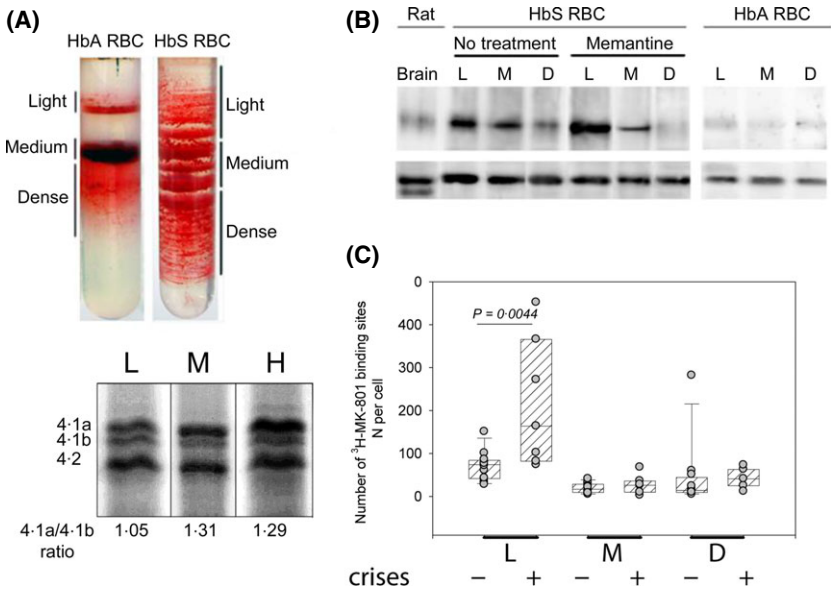

Fig 1. The abundance and activity of NMDARs is altered in the RBCs of SCD patients compared to that in the cells of healthy humans. (A) Separation of RBCs from a healthy donor (HbA) and SCD patient (HbS) into the light (L), medium (M) and dense (D) fractions on Percoll gradient and protein 4·1a/b ratio in cells forming the L, M and D fraction of the SCD patient. (B) Relative abundance of GluN1 subunit protein in the membranes of RBCs forming the L, M and D fraction of a healthy subject (HbA) and a SCD patient (HbS) with or without pre-treatment with memantine (100 μmol/l, 1 h) and in rat cerebellar protein extract. (C) The number of active NMDARs per cell in RBCs of L, M and D fractions of SCD patients during asymptomatic periods and during crises. The means ± SEM for 9 patients are shown. Circles denote individual values. NMDAR, N-methyl D-aspartate receptor; SCD, sickle cell disease; RBCs, red blood cells.

that time the cells progressed from pluripotent cells to proerythroblasts, to basophilic and polychromatic erythroblasts and finally, to normoblasts and enucleated reticulocytes (Makhro *et al*, 2013). High performance liquid chromatography (HPLC) was used to verify globin synthesis in fully differentiated cells. The preferential production of HbA/A2 or HbS in reticulocytes was measured in cells derived from the $CD34^+$ cells using HPLC (Figure S1). Expression of *GRIN* genes was monitored in the course of differentiation of EPCs (at days 6, 12 and 18 in culture) using TaqMan® Gene Expression Kits containing specific primers. Protein levels of NMDAR subunits were assessed in EPCs using flow cytometry. CD45 (Anti-CD45 peridinin chlorophyll [PerCP], clone 2D1, BD, San Jose, CA, USA) was used as a WBC marker and CD71 (clone M-A712 fluorescein isothiocyanate [FITC]-conjugated, BD, San Jose, USA) as reticulocyte marker. Abundance of the NMDAR subunits GluN2C (anti-NMDAε3 (NR2C), goat polyclonal IgG, sc-1470); GluN2D (anti-NMDAε4 (NR2D), mouse monoclonal IgG, sc-178221); GluN3A (anti-NR3A (NR3A), goat polyclonal IgG sc-51160) was measured in EPCs at various stages of differentiation. Stained cells were fixed with 1% formaldehyde and fluorescence intensity was measured using the BD Biosciences FACSCalibur flow cytometer (BD Biosciences, San Jose, USA). Memantine toxicity was probed for the EPCs of healthy donors and SCD patients after 6, 12 or 18 d in culture. Cells were exposed to 0·01–1 mmol/l memantine for 24 h and cell mortality monitored by flow cytometry, using propidium iodide (PI) nuclear staining.

Statistical analysis

The data obtained were analysed using GraphPad Instat v.3·0 (GraphPad Software, Inc., La Jolla, CA) and presented as means ± standard error of the mean (SEM) if not stated otherwise. Statistically significant differences were assessed using a one-way analysis of variance (ANOVA) test with the Bonferroni post-test, when a normal distribution test was passed, or, if normal distribution was not confirmed, with a Kruskal Wallis test with Dunn's *post-test* and accepted at $P < 0{\cdot}05$. Pearson product-moment correlation coefficients were used to assess covariance between the NMDAR activity in RBC fractions and the appearance of blood markers of haemolytic events.

Results

Presence and activity of NMDARs in circulating RBCs of SCD patients during stable periods and in crises

Immunoblotting was used to assess the protein levels of the obligatory GluN1 subunit in membrane fractions prepared from light (L), medium (M) and dense (D) fractions of RBCs of healthy people and SCD patients (Fig 1A). The L fractions of both healthy and SCD-RBCs were enriched with young cells and reticulocytes as follows from cytological estimation using Sysmex (182 ± 82‰ reticulocytes (mean ± standard deviation [SD]) in healthy human samples and 243‰ in the SCD sample shown in Fig 1B) and the

band 4·1a/b ratio (Fig 1A). For SCD-RBCs the L fraction was highly enriched with GluN1 and showed higher receptor activity per cell in RBCs (Fig 1B and Table II). The receptor activity in all fractions of the RBCs of asymptomatic SCD patients exceeded that in cells of healthy donors by 50% and more (Table II). Notably, HC treatment had no effect on the receptor function in SCD-RBCs (Table II). The number of active receptors per cell was similar in RBCs of homozygous HbSS patients and those presented with compound HbS-β thalassaemia (data not shown). Activity of the NMDARs in the L-fraction of SCD-RBCs increased substantially during the crises compared to the asymptomatic values (Fig 1C).

Furthermore, the activity of NMDARs in SCD-RBCs appears to be intimately related to the severity of patients' condition. Up-regulation of the NMDAR activity of mature SCD-RBCs forming the M fraction correlated negatively with haemoglobin and haematocrit levels and positively with plasma lactate dehydrogenase (LDH) and C-reactive protein content (Fig 2). These observations suggest that hyper-activation of NMDARs was associated with onsets of haemolytic events. Furthermore, receptor activity in cells forming fractions L (younger cells) and D (terminally dehydrated cells) correlated positively with neutrophil counts in blood (data not shown). It is noteworthy that all patients studied showed only mild neutrophilia and neutrophil counts did not exceed 12–14 × 10^9/l.

Effect of NMDAR agonists and antagonists on intracellular Ca^{2+} levels, cell volume and ion content

The role of the NMDAR activation state in the maintenance of intracellular Ca^{2+} levels, RBC volume and redox state was explored *ex vivo*.

RBCs of SCD patients loaded with the calcium-sensitive dye fluo-4 AM responded to treatment with the agonists NMDA and glycine (300 and 100 μm respectively), with an acute temporary increase in intracellular Ca^{2+}. Exposure of the SCD-RBCs to memantine (50 μmol/l) caused a modest decrease in Ca^{2+}-sensitive fluorescence (Fig 3A,C, Figures S2 and Supplementary Animated Figures S3-S8). Uptake of Ca^{2+} triggered the activation of Ca^{2+}-sensitive Gardos channels, K^+ loss, and cell shrinkage. Passive K^+ flux through the membranes of SCD-RBCs substantially exceeding that in the RBCs of healthy humans could be further facilitated by the NMDAR agonists, and partially suppressed by the receptor antagonist memantine (Fig 3B). Inhibition or stimulation

Table II. NMDAR activity in light, medium and dense fractions of RBCs of healthy people and SCD patients off or on hydroxycarbamide treatment.

Fraction	Healthy subjects (n = 31)	SCD patients Off-HC (n = 11)	SCD patients On-HC (n = 6)
Light (L)	34·9 ± 7·5	69 ± 11**	72 ± 17**
Medium (M)	4·1 ± 0·7	22 ± 6***	16 ± 3***
Dense (D)	4·3 ± 0·6	30 ± 11***	12 ± 2***

NMDAR, N-methyl D-aspartate receptor; SCD, sickle cell disease; HC, hydroxycarbamide.
**Denotes $P < 0·01$ and ***stands for $P < 0·001$ when compared with healthy control subjects.

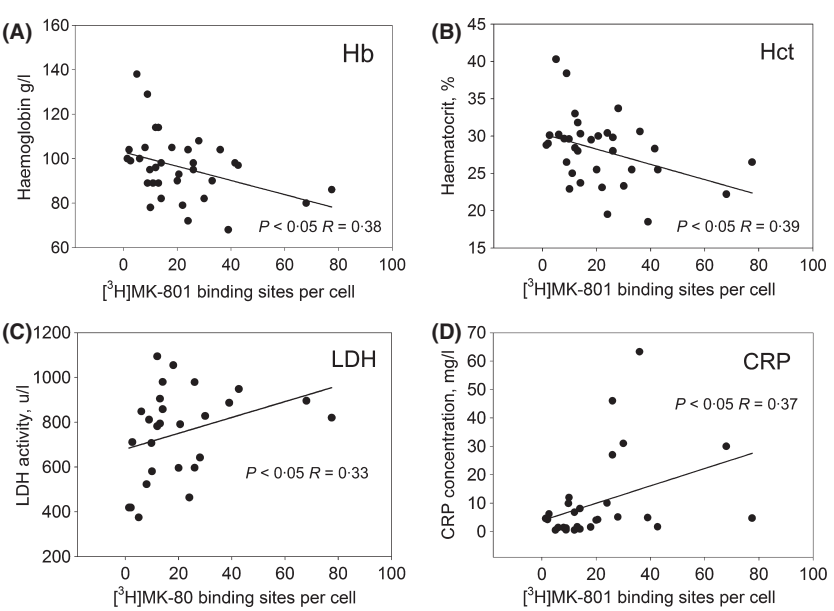

Fig 2. Correlation between the NMDAR activity in the M fraction of SCD-RBCs and markers of haemolysis [haemoglobin (A), haematocrit (B) and lactate dehydrogenase in plasma (C) and inflammation [C-reactive protein (D)]]. Covariance analysis of the receptor activity and the markers of haemolysis and inflammation was performed using Pearson product-moment correlation coefficients for the 34 blood samples taken from 16 patients on different occasions during asymptomatic periods and during haemolytic crises. HB, haemoglobin, Hct, haematocrit; LDH, lactate dehydrogenase; CRP, C-reactive protein.

of the NMDARs resulted in the re-distribution of RBCs in Percoll gradient. Interestingly, the cells containing more receptors underwent dehydration as soon as they were exposed to shear stress while passing through the Percoll, as follows from Fig 1B. These GluN1-enriched cells moved down the Percoll gradient to the D fraction. In line with this observation, filtration of RBCs through the cellulose column was associated with an increase in the NMDAR activity detected using ^{3}H-MK-801 binding assay (data not shown). Dehydration induced by passing through the Percoll gradient could be abolished by the pre-treatment of blood samples with memantine prior to the separation. Memantine-treated cells showed a maximum of GluN1 levels associated with the L fraction, whereas the D fraction was almost deprived of GluN1 (Fig 1B).

Incubation of whole blood from asymptomatic SCD patients with NMDA resulted in further dehydration of cells, which were then shifted down the gradient (Fig 3D). Treatment of blood with memantine, on the other hand, induced re-hydration and a corresponding upward shift within the Percoll gradients (Fig 3D). Monitoring of the kinetics of the morphological responses to the stimulation of the NMDARs in SCD-RBCs in the absence or presence of memantine was performed microscopically. The cells were pre-incubated with saturating concentrations of glutamate and glycine with or without memantine in a Ca^{2+}-free medium. During the recording, Ca^{2+} (final concentration 1.8 mM) was administered to the medium and the changes in cellular morphology monitored over 12 min. The corresponding Supplementary Animated Figures S3-S8, can be viewed online in the supplementary section. These video files show substantial reduction or complete abolishment of echinocytic transformation in the cells pre-treated with memantine before exposure to calcium.

The oxidative stress characteristic of SCD-RBCs was monitored as a four-fold increase in the intracellular oxidized glutathione (GSSG) levels over the GSSG content of RBCs in healthy human subjects. Further accumulation of GSSG was observed upon stimulation of NMDARs in SCD-RBCs with NMDA. Inhibition of the NMDARs with memantine prevented an oxidative burst triggered by NMDA (Fig 3E).

NMDARs and sickle cell transformation caused by deoxygenation

Polymerization of deoxygenated HbS was induced *ex vivo* by equilibration of SCD-RBCs with a humidified gas phase containing 5% CO_2 and 0·5% O_2 in Eschweiler tonometers. These oxygen levels have been recorded in some areas in the brain (Erecinska & Silver, 2001). Cells exposed to a gas phase supplemented with 15% O_2 served as the normoxic control, mimicking pO_2 in human lungs under normoxic conditions (13·3 kPa). At the onset of deoxygenation, the NMDARs in SCD-RBCs were either stimulated with NMDA (300 μmol/l) and glycine (100 μmol/l) or suppressed with memantine (50 μmol/l). Following 2 min of equilibration with the gas phase, the cells were incubated under normoxic or hypoxic conditions for 15 min. Thereafter RBC morphology (Fig 4A–D,F,G and Figure S2), intracellular Ca^{2+} (Fig 4E) and the intracellular ion content (Fig 4H) were assessed.

Deoxygenation of SCD-RBCs resulted in characteristic alterations in cell morphology, including the formation of drepanocytes (indicated with arrows in Fig 4B,C), "holy leaf", and "granular" cells (Figure S2C) and echinocytes (Fig 4 and Figure S2C). Quantitatively, these changes were assessed as an increase in anisotropy (Fig 4G, Figure S2A). Intracellular Ca^{2+} accumulation was induced by deoxygenation, as exemplified in Fig 4B–D and quantified in Fig 4E. Intake of Ca^{2+} triggered loss of K^+ (Fig 4H) and a decrease in cellular projection areas, signifying dehydration and shrinkage (Fig 4F, Fig S2B). The presence of extracellular Ca^{2+} was critical for initiating Ca^{2+}-driven dehydration which in turn facilitated polymerization of deoxy-HbS (Figure S2A). Chelation of the intracellular Ca^{2+} with 1,2-bis(o-aminophenoxy)ethane-N,N,N′,N′-tetraacetic acid (BAPTA) in addition to omission of the extracellular Ca^{2+} further reduced sickling and shrinking of hypoxic SCD-RBCs (Figure S2A).

Polymerization rate of deoxy-HbS is inversely related to the Hb concentration to an extremely high power (Hebbel, 2009). Stimulation of the NMDARs with NMDA and glycine aggravated the morphological changes induced by deoxygenation, including impressive induction of echinocytosis and RBC fragmentation (Fig 4D). Potassium loss from the oxygenated agonists'-treated SCD-RBCs reached its maximum and could not be further stimulated by hypoxia (Fig 4H). Some of the cells were showing signs of irreversible HbS polymerization ("holy leaf" appearance) even under normoxic conditions (Figure S2C). Memantine administration effectively prevented hypoxia-induced sickling and echinocytosis (Fig 4C,G). A decrease in Ca^{2+} uptake by deoxygenated cells was observed upon memantine treatment followed by the suppression of hypoxia-induced K^+ loss and dehydration (Fig 4H and F respectively).

Subunit composition of NMDARs and their expression in erythroid precursor cells of patients (SCD-EPCs)

Previously we explored the expression profile of *GRIN* genes in EPCs derived from healthy human blood (Makhro *et al*, 2013). A similar approach was used to monitor the presence of transcripts of *GRIN* genes and changes in protein levels of all subunits of the NMDARs in SCD-EPCs. Pluripotent mononuclear cells were isolated from the peripheral blood of healthy subjects and patients. These cells were cultured to obtain pro-erythroblasts (day 6), basophilic and polychromatic erythroblasts (day 12) or normoblasts and enucleated reticulocytes (day 18). Expression profiles obtained for the transcripts of *GRIN1, GRIN2A, GRIN2C, GRIN2D, GRIN3A* and *GRIN3B* in SCD-EPCs at each differentiation stage are shown in Fig 5. The expression of *GRIN1* and *GRIN2C* tran-

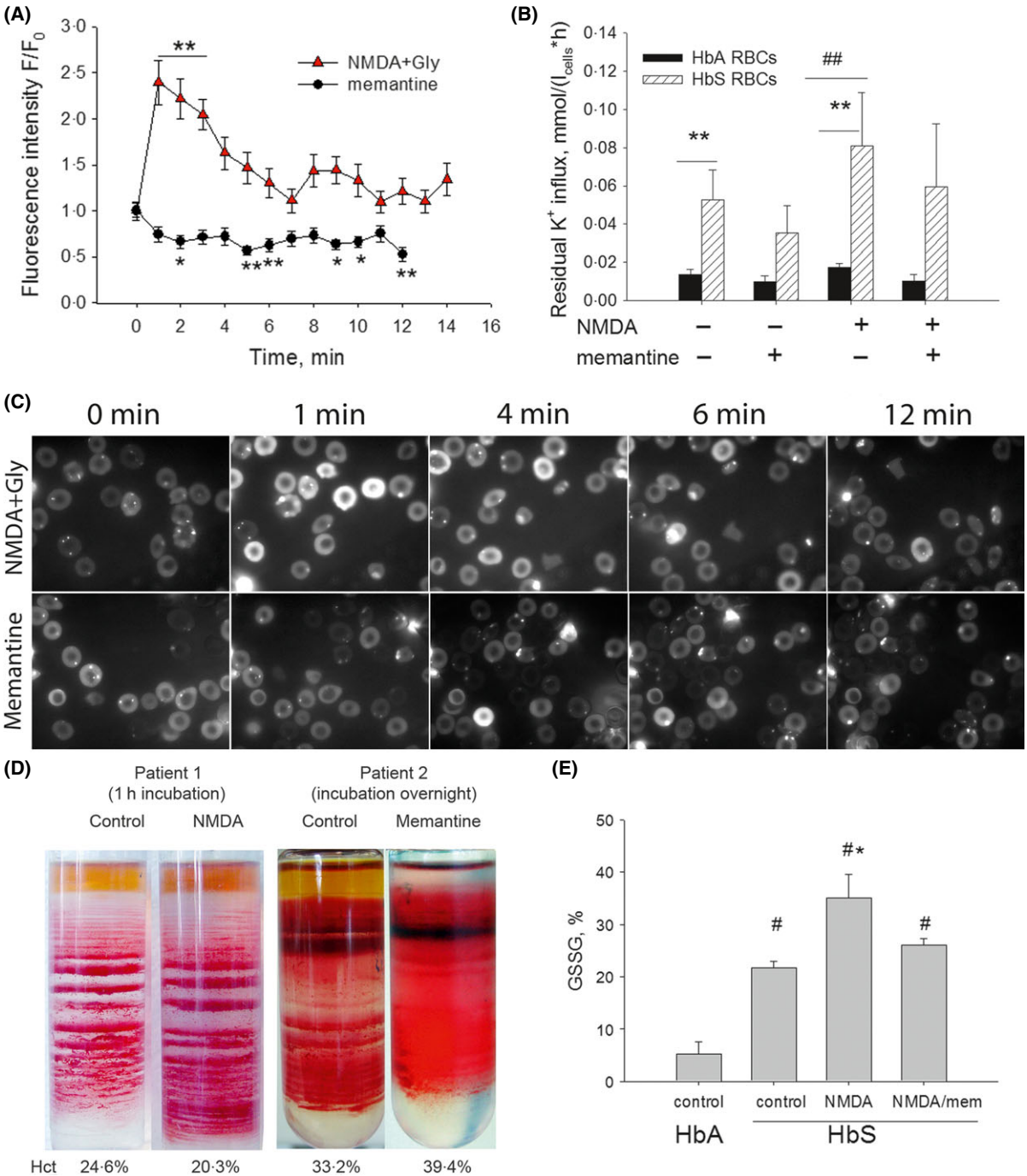

Fig 3. Intracellular Ca^{2+} and oxidized glutathione levels, cell density, and residual K^+ flux in SCD-RBCs upon activation (300 μmol/l glutamate and 100 μmol/l glycine) or inhibition (100 μmol/l memantine) of the NMDARs. (A) Kinetics of changes in the intracellular Ca^{2+} in SCD-RBCs (fluorescence intensity at each time-point (F) normalized to the average signal intensity at time zero (Fo)). Number of cells analysed per time point ranges from 24 to 42. * denotes $P < 0{\cdot}05$ and ** stands for $P < 0{\cdot}01$ when compared to the signal at time zero. (B) Chloride-independent ouabain-insensitive unidirectional K^+ influx into the RBCs of healthy humans and SCD patients. ** indicates $P < 0{\cdot}01$ when fluxes were compared between the HbA and HbS-RBCs under the same conditions. Data are means of six independent experiments ± SD. ## denotes $P < 0{\cdot}01$ for the K^+ fluxes in SCD-RBCs treated with either memantine or NMDA/Gly. (C) Representative experiments showing the alterations in Ca^{2+}-sensitive fluo-4 fluorescent signal intensity in response to NMDA/Gly or memantine treatment quantified in panel A. (D) Distribution of SCD-RBCs in Percoll gradient after pre-treatment of whole blood with either 300 μmol/l NMDA or 100 μmol/l memantine. Numbers below the images indicate the corresponding haematocrit values. (E) Oxidized glutathione (GSSG) content of RBCs exposed to agonists in the presence or absence of memantine for 30 min. # denotes $P < 0{\cdot}05$ compared to the values in the RBCs of healthy humans (HbA-control). *stands for $P < 0{\cdot}05$ compared to control levels in SCD-RBCs (HbS-control). NMDA, N-methyl D-aspartate; SCD, sickle cell disease; RBCs, red blood cells; Gly, glycine.

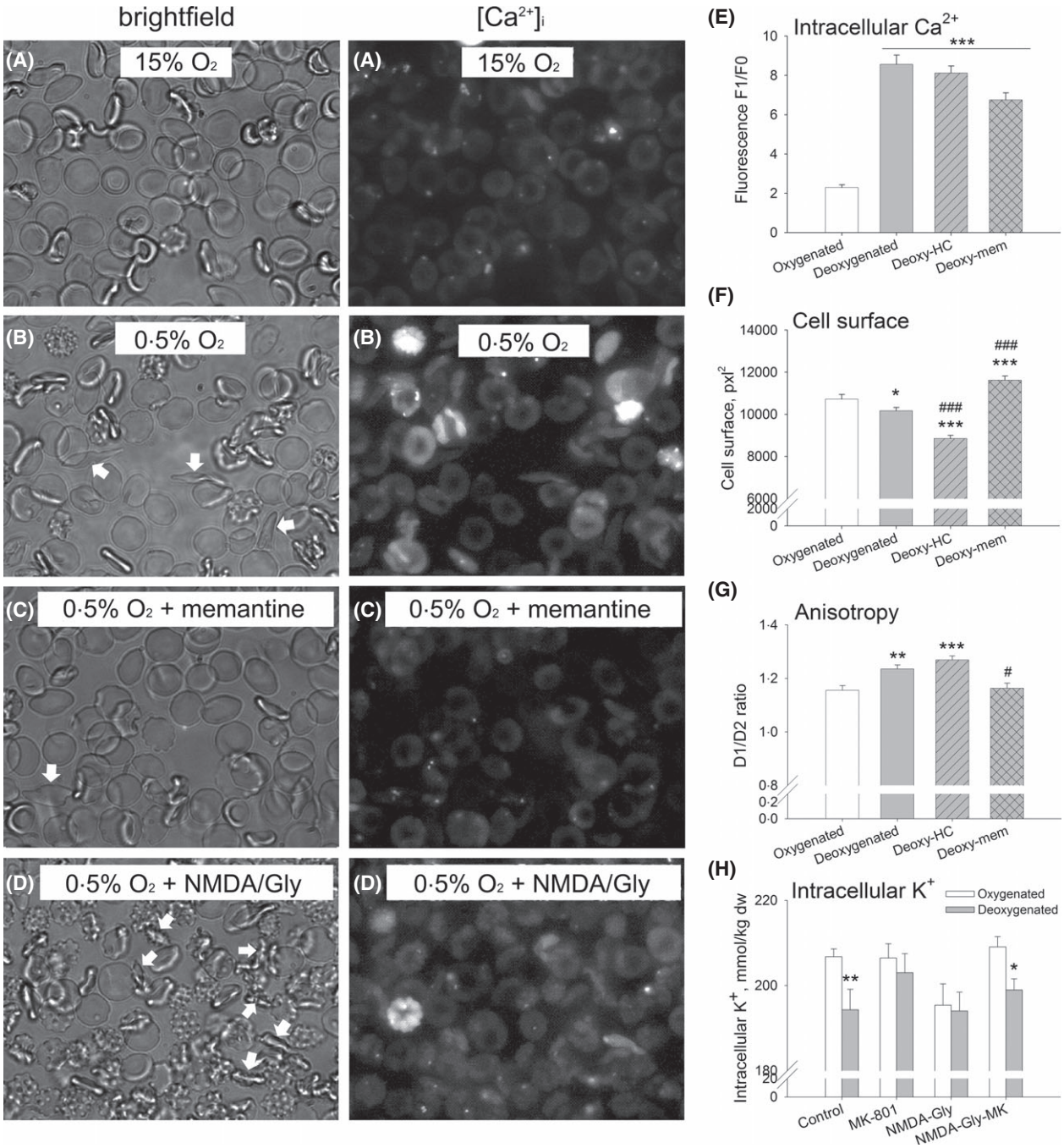

Fig 4. Responses of SCD-RBCs to deoxygenation in the presence of the NMDAR agonists (300 μmol/l NMDA/100 μmol/l glycine) and antagonist (50 μmol/l memantine). RBCs in suspension were exposed to either 15% or 0·5% O_2 in gas phase in Eschweiler tonometers (15 min, 37°C). Shown are (A-D) the representative images of erythrocytes in different conditions, cell morphology and intracellular Ca^{2+} levels; (E) quantification of the changes in the intracellular Ca^{2+} levels; (F) alterations in RBC projection area; (G) changes in anisotropy as a marker of sickle cell transformation in deoxygenated SCD-RBCs and (H) changes in the intracellular K^+ concentration. NMDA, N-methyl D-aspartate; SCD, sickle cell disease; RBCs, red blood cells; Gly, glycine.

scripts in healthy subjects increased progressively during *ex vivo* differentiation. Peak levels of *GRIN2D* transcripts were found at the stage of basophilic and polychromatic erythroblasts (12 d). In SCD-EPCs these stage-dependent variations in expression levels of all *GRIN* genes were blunted. No significant changes in NMDAR transcript levels were detected during differentiation. Compared to healthy controls, relative expression of *GRIN3B* was significantly higher in SCD throughout erythropoiesis. Similar to those in EPCs of healthy humans (Makhro *et al*, 2013), transcripts of *GRIN2B* in EPCs obtained from SCD patients were below the detection threshold at any differentiation stage.

Protein levels per cell and the number of cells expressing GluN2C, 2D, 3A and 3B were assessed in EPCs during differentiation. On average, the percentage of cells expressing the NMDA subunits varied from *c.* 10% for pro-erythroblasts to 20–40% at the later differentiation stages, independent of the presence of the *HBB* E6V mutation (HbS gene) (Fig 6A,C,D, and E). The number of copies of the dominant GluN2D and 3B subunits per cell, expressed as the mean fluorescence intensity, were the highest at the normoblastic stage (Figs 6D and 3B). A tendency towards an increased number of cells expressing GluN3A and 3B subunit in the EPCs of SCD patients was observed at the stage of basophilic and polychromatic erythroblasts (Fig 6E and G). However, this tendency did not reach statistical significance and was not preserved at the normoblastic stage. All in all, the protein levels for all subunits at each differentiation stage tested did not differ between the EPCs of healthy humans and those of SCD patients. This observation suggests that the striking enrichment of the circulating SCD-RBCs with NMDARs resulted from the disturbed clearance of the receptors from reticulocytes.

Sensitivity of the EPCs to memantine exposure was tested as a function of antagonist concentration. As shown in Fig 7, memantine was well-tolerated by both the EPCs of control subjects and those of SCD patents within a pharmacologically relevant concentration range (1–50 μmol/l). At higher concentrations (0·1–1 mmol/l) the highest mortality rate was observed in control EPCs at the pro-erythroblast stage (6 d in culture, Fig 7A). The EPCs of SCD patients showed maximal sensitivity to high doses of memantine only at the stage of polychromatic erythroblasts (12 d in culture, Fig 7B), being generally more tolerant to memantine than the cells of healthy humans. Cell death was accompanied by characteristic changes in morphology, including a high degree of vacuolization and vesiculation (Fig 7C).

Discussion

The present study indicates that an abnormally great abundance of functional NMDARs is characteristic of the circulating RBCs of SCD patients (Fig 1, Table II). Hyperactivation of the NMDARs in RBCs was associated with the severity of haemolytic events, as the number of active receptors in the majority of cells forming M fraction correlated negatively with haemoglobin/haematocrit levels and positively with plasma LDH (Fig 2). Induction of HbS polymerization *in vitro* by exposing the RBCs of SCD patients to low oxygen

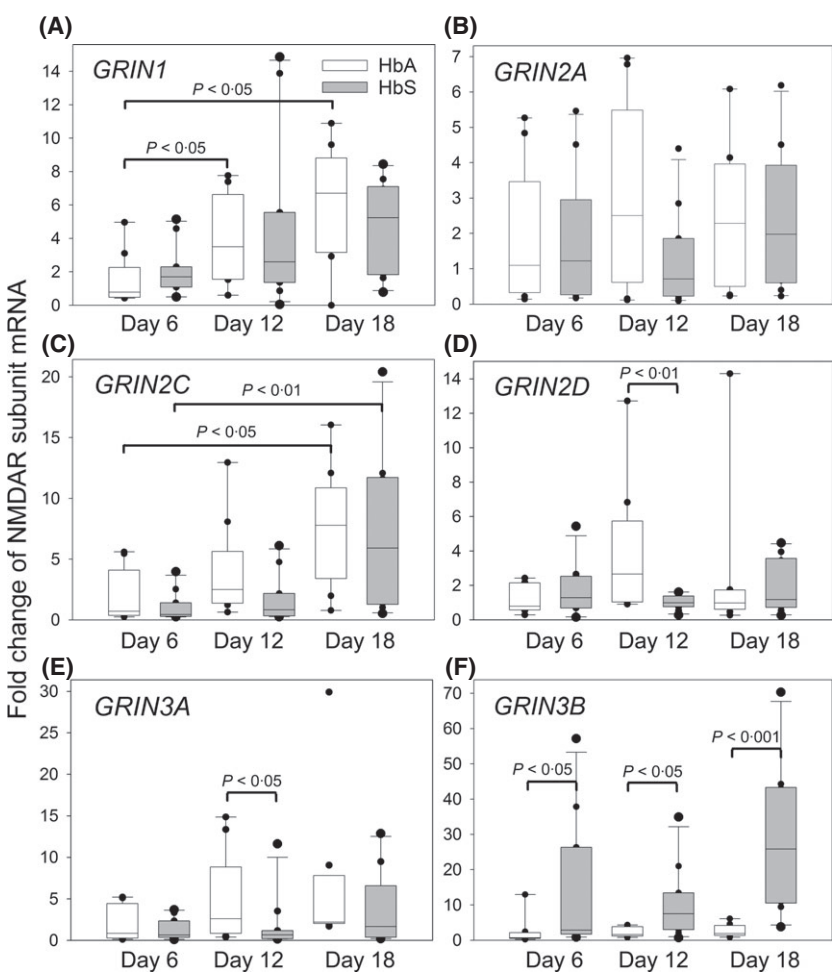

Fig 5. Expression of NMDAR subunits during erythropoiesis**.** (A-F) relative amounts of the different NMDAR isotypes (as indicated). Cells were harvested and analysed at days 6, 12 and 18, transcripts were measured by TaqMan real time polymerase chain reaction. Values are represented as box plots of 9 erythroid cultures from healthy subjects (open boxes, $n = 9$) and 10 erythroid cultures from SCD (grey boxes, $n = 10$), each started with cells from a different donor. An overall comparison indicated significant differences between days of culture only for the expression of *GRIN2C* ($P < 0·05$) and *GRIN1* ($P < 0·05$).

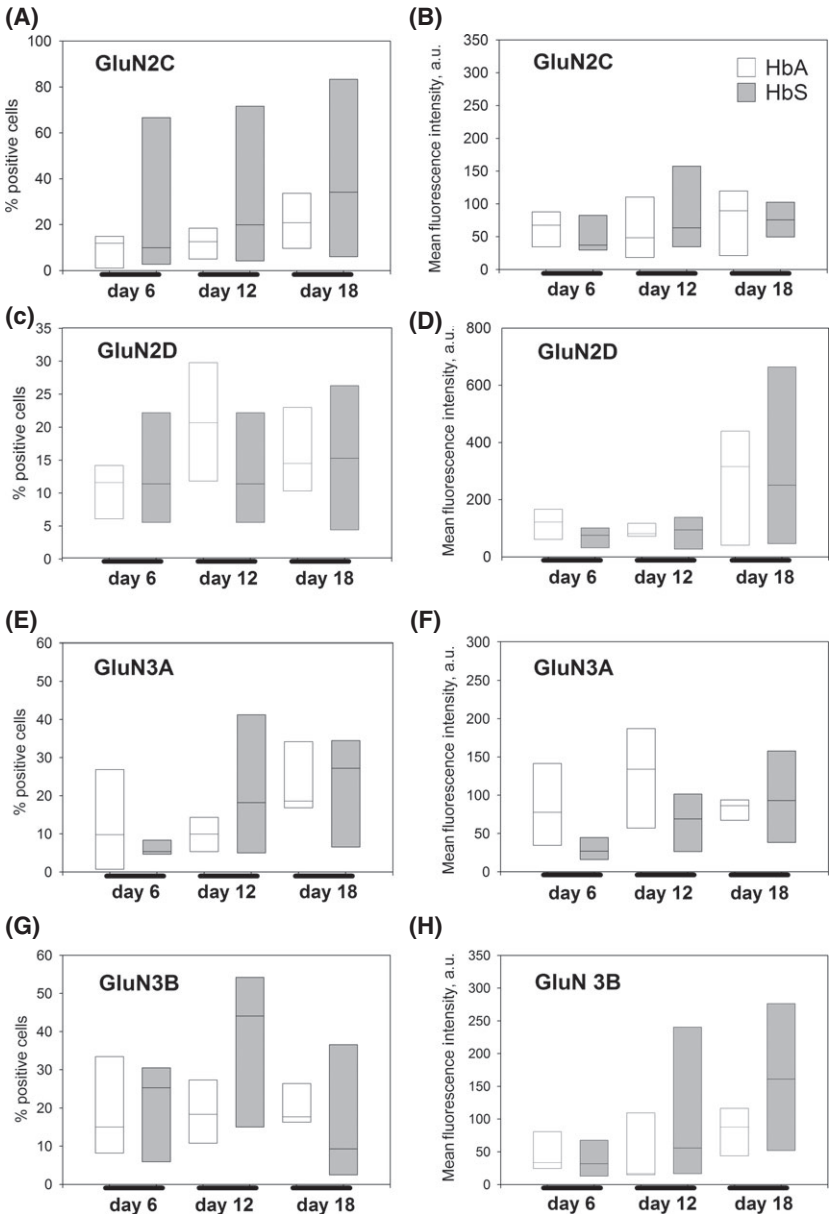

Fig 6. Protein levels of GluN2C, 2D, 3A and 3B in EPCs at various differentiation stages. Shown are the numbers of cells in which fluorescent signal from the corresponding antibodies was detected by means of flow cytometry (A, C, E, G) and the mean intensity of this signal per cell (B, D, F, H). Numbers above boxes represent medians of the corresponding signal in EPC cultures obtained from healthy control subjects. Cells were harvested and analysed at day 6, 12 and 18. Data were obtained from cultures grown from $CD34^+$ cells of four different SCD patients (open boxes) and six healthy subjects (grey boxes). EPCs, erythroid precursors; AU, arbitrary units.

levels revealed that hypoxia-induced Ca^{2+} uptake, dehydration and the polymerization rate itself could be substantially slowed down in the presence of the NMDAR antagonist memantine (Fig 4). Activation of the NMDARs with NMDA and glycine, on the other hand, could induce a complex cell response resembling that occurring during crises, including some sickle cell transformation Ca^{2+} uptake, K^+ and water loss and oxidative stress (Fig 3).

Taken together, all these findings suggest that inhibition of the NMDARs may be beneficial as it hits multiple calcium-sensitive targets, preventing the dehydration, sickling and oxidation associated with haemolytic crises in SCD patients (Bogdanova *et al*, 2013). The design of the present *ex vivo* study did not allow testing for the long-term effects of memantine supplementation on SCD-RBCs, such as changes in calpain activity, or changes in the adherence of SCD-RBCs to the endothelial layer. The lack of active NMDARs in the circulating C57B6 mouse red blood cells was documented by using [^{3}H]MK-801 binding assay (A. Makhro and A. Bogdanova, unpublished observations). This observation limits us to the use of human cells in the future, making mouse models of SCD useless for such a long-term study.

We have previously shown that the number of NMDARs and the amplitude of response to the stimulation of NMDARs in the RBCs of healthy humans is particularly high in the light fraction enriched with reticulocytes and young cells (Makhro *et al*, 2013). Similarly, the number of copies of GluN1 and the number of active receptors assessed as the [^{3}H]MK-801 binding sites per cell is maximal in the upper light fraction of SCD-RBCs (Table II, Fig 1B, C). As reported by Bookchin *et al* (1991), the reticulocytes of SCD patients

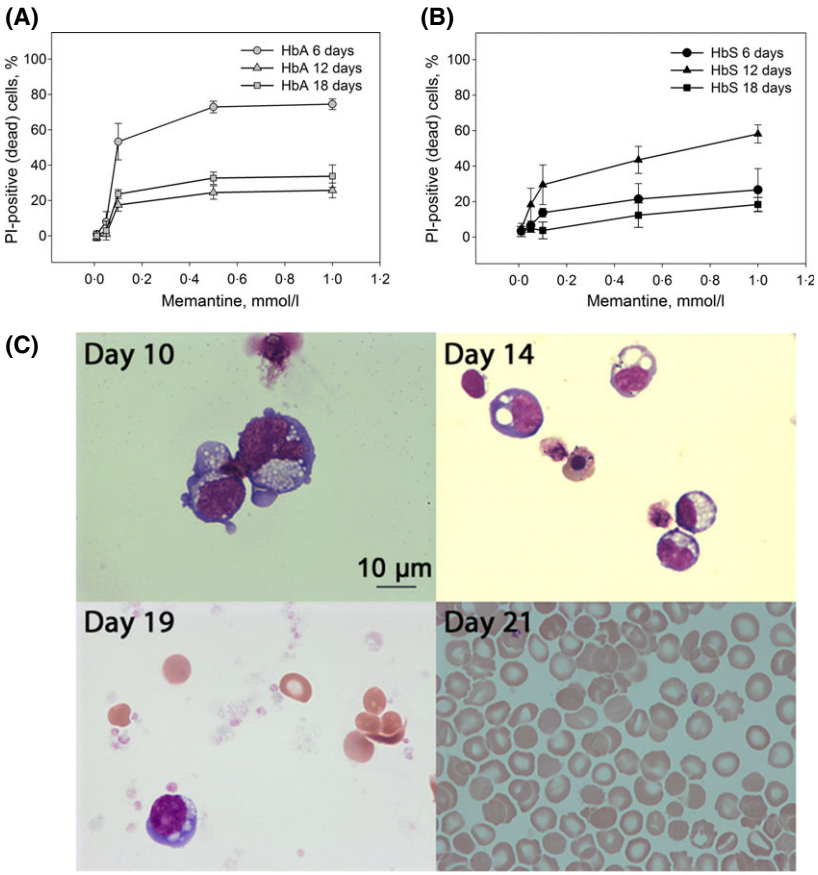

Fig 7. Memantine and MK-801 toxicity studies performed for healthy human-derived EPCs and SCD-EPCs at days 6, 12 and 18 in culture. The EPCs were exposed to memantine added to the culturing medium at concentrations of 10 µmol/l-1 mmol/l for 24 h (A,B). Thereafter the cells were harvested and mortality assessed using propidium iodide staining. Data are the means of four cultures obtained from four independent healthy subjects or HbSS patients ± SD. (C) SCD-EPCs were treated with 0·5 mmol/l MK-801 for 12 h at the various differentiation stages. Vacuolization is present at days 14 and 19 and indicates apoptosis. Cells at the early stage of erythropoiesis (day 10) are less sensitive to MK-801 treatment and mature RBCs (day 21) are completely resistant. SCD, sickle cell disease; EPCs, erythroid precursors.

show maximal susceptibility to dehydration and sickling. This paradoxic predisposition of young cells to premature clearance may be caused at least in part by higher susceptibility to calcium overload resulting from hyperactivation of NMDARs.

Substantial up-regulation of NMDAR abundance and activity in SCD-RBCs was observed in all RBC fractions, being particularly high in the L fraction (Table II). A further increase in the number of active receptors in the L fraction of SCD-RBCs was detected in patients showing symptoms of haemolytic crises manifested as a decrease in haematocrit, and the onset of a pain crisis (Fig 1C). These observations suggest that the greater abundance and activity of NMDARs may be associated with the onset of crises. Dissection of the factors involved in hyperactivation of the NMDARs in RBCs of patients with SCD during the crisis is of key importance. Plasma glutamate and glycine levels are determinants of NMDAR activity in RBCs. Increased levels of glycine and a *c.* 3·5-fold increase in the intraerythrocytic levels of both agonists have been reported for SCD patients during asymptomatic periods (Kiessling *et al*, 2000). No data for plasma amino acid composition during crises are currently available. One can expect that haemolysis would be associated with the release of these excitatory amino acids, resulting in progressive activation of the receptors in RBCs.

Mechanisms that control NMDAR abundance in the RBCs of SCD patients await further in-depth characterization, which is beyond the scope of this study. Although relatively high, the number of receptors per cell in circulating SCD-RBCs is within the 10^2 range and is thus not comparable with that in EPCs, which range from 10^5 to 10^3 receptor copies per cell (Makhro *et al*, 2010, 2013). Terminal stages of EPC differentiation are clearly associated with massive clearance of the receptors from the plasma membrane. Even a slight disturbance in clearance efficiency would result in significant up-regulation of the number of NMDARs remaining in membranes of circulating RBCs. The mechanisms involved in clearance of NMDARs in EPCs have not yet been studied. Unusually high levels of membrane-bound haemoglobin resulting from its higher affinity to the cytosolic domain of band 3 protein may at least partly explain the inclmplete clearance of the receptors (Rotter *et al*, 2010).

The conductive pathway involved in the increased permeability of the membranes of SCD-RBCs to cations, including calcium ions, is known as P_{sickle}. Analysis of the properties and pharmacological profile of P_{sickle} suggests that the current is mediated by more than one channel type. Among the hallmarks of P_{sickle} are activation upon deoxygenation (Browning *et al*, 2007; Vandorpe *et al*, 2010) and filtration (shear stress) (Brain *et al*, 2004), permeability for K^+, Na^+ and Ca^{2+} (Bookchin & Lew, 1981), sensitivity to Zn^{2+} and

stilbene disulfonate (DIDS) (Joiner, 1990; Browning *et al*, 2007), voltage- and pH-dependence (Joiner *et al*, 1993). These properties are shared by NMDARs. We have demonstrated that NMDAR function in the RBCs of SCD patients is oxygen-dependent (Fig 4). Sensitivity to 4,4′- diisothiocyanostilbene-2,2′-disulfonic acid (DIDS) (Tauskela *et al*, 2003) and voltage-dependence were demonstrated in the NMDARs in neurons. Sensitivity of NMDARs to Zn^{2+} appears to be particularly interesting in view of reports that 1 year of zinc sulphate supplementation was found to reduce the incidence of pain crises and infections in SCD patients in several clinical trials (Swe *et al*, 2013). Whether this beneficial action of Zn^{2+} is, at least in part, mediated by suppression of the NMDARs remains to be confirmed.

We have demonstrated the sensitivity of NMDARs in SCD-RBCs to filtration as a manifestation of shear stress (Fig 1B, and text). These receptors have been shown to be mechano-sensitive (Paoletti & Ascher, 1994; Singh *et al*, 2012). Other features of P_{sickle}, such as sensitivity to Gd^{3+}, CO and to a toxin produced by the tarantula spider GsMTx-4 (Vandorpe *et al*, 2010) have not been tested for NMDARs. NMDAR function is known to be highly sensitive to changes in pH, but the optimal pH range for the NMDARs in the brain differs from that of P_{sickle}. These are the indications that Cav2·1 channels and voltage-dependent anion channels (VDACs) may contribute to P_{sickle} along with NMDARs, each responding to a characteristic set of stimuli related to stress and inflammation (Kaestner, 2011).

Our observations clearly show that the inhibition of NMDARs hits multiple targets in RBCs. In addition, memantine has recently been reported to effectively suppress neuropathic pain after surgery (Morel *et al*, 2013). Failure to reduce the number and severity of acute pain episodes was the reason for the negative outcome of several trials in which a Gardos channel blocker, the anti-adhesion drug poloxamer 188, and inhaled nitric oxide were used in treatment of patients with SCD (Gee, 2013). A combination of the prevention of haemolytic crises and reduction in vaso-occlusive events with potential effective pain management makes memantine an attractive candidate for therapy of SCD.

The number of patients with SCD is growing rapidly in Switzerland and other European countries due to the increasing flow of migrants from Africa and Asia to Europe (Schmugge *et al*, 2008). Currently, most of the SCD patients in Switzerland are children. Moreover, when proven efficient in treatment of SCD, calcium-lowering therapy could be extended for treatment of other types of rare hereditary forms of anaemia associated with abnormal intracellular Ca^{2+} levels, such as thalassaemia, phosphofructokinase deficiency and others.

Authorship

P.H. and O.S. performed research shown in Figs 5–7; A.M. produced data for the Figs 1 and 3A,C,D and Table II; A.B. generated data for Figs 3C, 4, and Figures S2 and animation figures; J.S.G. and M.S. provided blood and information on the SCD patients. J.S.G. produced the data shown in Fig 2. All authors contributed to data analysis, discussion and writing of the manuscript.

Acknowledgements

This study was supported by a ZIHP cooperative grant (to J.S.G, O.S. and A.B.), funded by the European Community's Seventh Framework Programme (FP7/2007-2013) under Grant Agreement No. 602121, the CTI/Lyfjos GmbH grant and the Vontobel Foundation (to A.B.), and supported by the Hartmann Müller-Stiftung (to O.S.). The authors state that there is no conflict of interests to disclose. We gratefully acknowledge technical assistance of Nikolay Bogdanov and cordially thank Dr Heather Murray for careful proof-reading and language editing.

Supporting Information

Additional Supporting Information may be found in the online version of this article:

Data S1. Subject and methods**.**

Fig S1. Quantification of HbA, HbF, HbA1C, HbA2 and HbS of the total haemoglobin at reticulocyte stage of erythropoietic maturation (day 21).

Fig S2. The role of intra- and extracellular $Ca2^{+}$ in facilitation of HbS polymerisation and SCD-RBC shrinkage.

Fig S3. Experiment 1 Control: HbSS control 1 BF (bright field)/HbSS control 1 Ca (green channel).

Fig S4. Experiment 2 Control: HbSS control 2 BF (bright field)/HbSS control 2 Ca (green channel).

Fig S5. Experiment 3 Control HbSS control 3 BF (bright field)/HbSS control 3 Ca (green channel).

Fig S6. Experiment 1 Memantine-pretreated cells: HbSS memantine 1 BF (bright field)/HbSS memantine 1 Ca (green channel).

Fig S7. Experiment 2 Memantine-pretreated cells: HbSS memantine 2 BF (bright field)/HbSS memantine 2 Ca (green channel).

Fig S8. Experiment 3 Memantine-pretreated cells: HbSS memantine 3 BF (bright field)/HbSS memantine 3 Ca (green channel).

References

Ataga, K.I. & Stocker, J. (2009) Senicapoc (ICA-17043): a potential therapy for the prevention and treatment of hemolysis-associated complications in sickle cell anemia. *Expert Opinion on Investigational Drugs*, **18**, 231–239.

Bogdanova, A.Y., Ogunshola, O.O., Bauer, C. & Gassmann, M. (2003) Pivotal role of reduced glutathione in oxygen-induced regulation of the Na (+)/K(+) pump in mouse erythrocyte membranes. *Journal of Membrane Biology*, **195**, 33–42.

Bogdanova, A., Makhro, A., Wang, J., Lipp, P. & Kaestner, L. (2013) Calcium in red blood cells-a

perilous balance. *International Journal of Molecular Sciences*, **14**, 9848–9872.

Bookchin, R.M. & Lew, V.L. (1981) Effect of a 'sickling pulse' on calcium and potassium transport in sickle cell trait red cells. *Journal of Physiology*, **312**, 265–280.

Bookchin, R.M., Ortiz, O.E. & Lew, V.L. (1991) Evidence for a direct reticulocyte origin of dense red cells in sickle cell anemia. *Journal of Clinical Investigation*, **87**, 113–124.

Brain, M.C., Pihl, C., Robertson, L. & Brown, C.B. (2004) Evidence for a mechanosensitive calcium influx into red cells. *Blood Cells, Molecules, & Diseases*, **32**, 349–352.

Browning, J.A., Staines, H.M., Robinson, H.C., Powell, T., Ellory, J.C. & Gibson, J.S. (2007) The effect of deoxygenation on whole-cell conductance of red blood cells from healthy individuals and patients with sickle cell disease. *Blood*, **109**, 2622–2629.

Chandrakasan, S. & Malik, P. (2014) Gene Therapy for Hemoglobinopathies: the State of the Field and the Future. *Hematology/oncology Clinics of North America*, **28**, 199–216.

De Franceschi, L., Franco, R.S., Bertoldi, M., Brugnara, C., Matte, A., Siciliano, A., Wieschhaus, A.J., Chishti, A.H. & Joiner, C.H. (2013) Pharmacological inhibition of calpain-1 prevents red cell dehydration and reduces Gardos channel activity in a mouse model of sickle cell disease. *FASEB Journal*, **27**, 750–759.

Eaton, W.A. & Hofrichter, J. (1990) Sickle cell hemoglobin polymerization. *Advances in Protein Chemistry*, **40**, 63–279.

Erecinska, M. & Silver, I. (2001) Tissue oxygen tension and brain sensitivity to hypoxia. *Respiration Physiology*, **128**, 263–276.

Gee, B.E. (2013) Biologic complexity in sickle cell disease: implications for developing targeted therapeutics. *ScientificWorldJournal*, **2013**, 694146.

George, A., Pushkaran, S., Konstantinidis, D.G., Koochaki, S., Malik, P., Mohandas, N., Zheng, Y., Joiner, C.H. & Kalfa, T.A. (2013) Erythrocyte NADPH oxidase activity modulated by Rac GTPases, PKC, and plasma cytokines contributes to oxidative stress in sickle cell disease. *Blood*, **121**, 2099–2107.

Hebbel, R.P. (2009) Chapter 42 Pathobiology of sickle cell disease. In: Hematology. Basic Principles and Practice. (ed. by Hoffma, R., Benz, E.J., Shattil, S.J., Furie, B., Silberstein, L.E., McGlave, P. & Heslop, H.), pp. 565–576. Churchill Livingstone Elsevier, Philadelphia, PA.

Hebbel, R.P., Yamada, O., Moldow, C.F., Jacob, H.S., White, J.G. & Eaton, J.W. (1980) Abnormal adherence of sickle erythrocytes to cultured vascular endothelium: possible mechanism for microvascular occlusion in sickle cell disease. *Journal of Clinical Investigation*, **65**, 154–160.

Joiner, C.H. (1990) Deoxygenation-induced cation fluxes in sickle cells: II. Inhibition by stilbene disulfonates. *Blood*, **76**, 212–220.

Joiner, C.H., Morris, C.L. & Cooper, E.S. (1993) Deoxygenation-induced cation fluxes in sickle cells. III. Cation selectivity and response to pH and membrane potential. *American Journal of Physiology*, **264**, C734–C744.

Kaestner, L. (2011) Cation channels in erythrocytes - historical and future perspective. *The Open Biology Journal*, **4**, 27–34.

Kiessling, K., Roberts, N., Gibson, J.S. & Ellory, J.C. (2000) A comparison in normal individuals and sickle cell patients of reduced glutathione precursors and their transport between plasma and red cells. *Hematology Journal*, **1**, 243–249.

Locatelli, F., Kabbara, N., Ruggeri, A., Ghavamzadeh, A., Roberts, I., Li, C.K., Bernaudin, F., Vermylen, C., Dalle, J.H., Stein, J., Wynn, R., Cordonnier, C., Pinto, F., Angelucci, E., Socie, G., Gluckman, E., Walters, M.C., Rocha, V. & Eurocord, European, B. & Marrow Transplantation, g. (2013) Outcome of patients with hemoglobinopathies given either cord blood or bone marrow transplantation from an HLA-identical sibling. *Blood*, **122**, 1072–1078.

Lutz, H.U., Stammler, P., Fasler, S., Ingold, M. & Fehr, J. (1992) Density separation of human red blood cells on self forming Percoll gradients: correlation with cell age. *Biochimica et Biophysica Acta*, **1116**, 1–10.

Makhro, A., Wang, J., Vogel, J., Boldyrev, A.A., Gassmann, M., Kaestner, L. & Bogdanova, A. (2010) Functional NMDA receptors in rat erythrocytes. *American Journal of Physiology. Cell Physiology*, **298**, C1315–C1325.

Makhro, A., Hanggi, P., Goede, J.S., Wang, J., Brueggemann, A., Gassmann, M., Schmugge, M., Kaestner, L., Speer, O. & Bogdanova, A. (2013) N-methyl D-aspartate (NMDA) receptors in human erythroid precursor cells and in circulating red blood cells contribute to the intracellular calcium regulation. *American Journal of Physiology. Cell Physiology*, **305**, C1123–C1138.

Manwani, D. & Frenette, P.S. (2013) Vaso-occlusion in sickle cell disease: pathophysiology and novel targeted therapies. *Blood*, **122**, 3892–3898.

Mohandas, N. & Evans, E. (1985) Sickle erythrocyte adherence to vascular endothelium. Morphologic correlates and the requirement for divalent cations and collagen-binding plasma proteins. *Journal of Clinical Investigation*, **76**, 1605–1612.

Morel, V., Etienne, M., Wattiez, A.S., Dupuis, A., Privat, A.M., Chalus, M., Eschalier, A., Daulhac, L. & Pickering, G. (2013) Memantine, a promising drug for the prevention of neuropathic pain in rat. *European Journal of Pharmacology*, **721**, 382–390.

Paoletti, P. & Ascher, P. (1994) Mechanosensitivity of NMDA receptors in cultured mouse central neurons. *Neuron*, **13**, 645–655.

Paoletti, P., Bellone, C. & Zhou, Q. (2013) NMDA receptor subunit diversity: impact on receptor properties, synaptic plasticity and disease. *Nature Reviews Neuroscience*, **14**, 383–400.

Rotter, M.A., Chu, H., Low, P.S. & Ferrone, F.A. (2010) Band 3 catalyzes sickle hemoglobin polymerization. *Biophysical Chemistry*, **146**, 55–59.

Schmugge, M., Speer, O., Ozsahin, A.H. & Martin, G. (2008) Die Sichelzellerkrankung in der Schweiz. Teil 1: pathophysiologie, Klinik. *Schweiz Med Forum*, **8**, 582–586.

Singh, P., Doshi, S., Spaethling, J.M., Hockenberry, A.J., Patel, T.P., Geddes-Klein, D.M., Lynch, D.R. & Meaney, D.F. (2012) N-methyl-D-aspartate receptor mechanosensitivity is governed by C terminus of NR2B subunit. *Journal of Biological Chemistry*, **287**, 4348–4359.

Swe, K.M., Abas, A.B., Bhardwaj, A., Barua, A. & Nair, N.S. (2013) Zinc supplements for treating thalassaemia and sickle cell disease. *Cochrane Database Systematic Review*, **6**, CD009415.

Tauskela, J.S., Mealing, G., Comas, T., Brunette, E., Monette, R., Small, D.L. & Morley, P. (2003) Protection of cortical neurons against oxygen-glucose deprivation and N-methyl-D-aspartate by DIDS and SITS. *European Journal of Pharmacology*, **464**, 17–25.

Tietze, F. (1969) Enzymic method for quantitative determination of nanogram amounts of total and oxidized glutathione: applications to mammalian blood and other tissues. *Analytical Biochemistry*, **27**, 502–522.

Tiffert, T., Bookchin, R.M. & Lew, W.L. (2003) Calcium homeostasis in normal and abnormal human red cells. In: Red Cell Membrane transport in Health and Disease (eds by Bernhardt, I. & Ellory, J.C.), pp. 373–405. Springer, Berlin.

Vandorpe, D.H., Xu, C., Shmukler, B.E., Otterbein, L.E., Trudel, M., Sachs, F., Gottlieb, P.A., Brugnara, C. & Alper, S.L. (2010) Hypoxia activates a $Ca2^{+}$-permeable cation conductance sensitive to carbon monoxide and to GsMTx-4 in human and mouse sickle erythrocytes. *PLoS ONE*, **5**, e8732.

6. Discussion

6.1. More than memory formation - Plasticity of NMDAR in erythroid cells

We have shown the expression of NMDARs in EPCs and their presence in RBCs of healthy human subjects. During erythropoietic maturation, the number of functional receptors decreased from several hundred thousand to 15-30 per cell in fully differentiated RBCs. [3] These findings strongly suggest that NMDARs are not only essential for memory formation and synaptic plasticity in neurons, but also important for hematopoietic cells, along with platelets, leucocytes, megakaryocytes, and osteoclasts. [172,174,274,275,348-350]

The data obtained for mRNA and protein expression of the different GluN subunits indicate that the subunit composition of the erythroid NMDAR differs strongly from that in neurons. The mRNA expression patterns showed the presence of *GRIN* genes` transcripts for each known NMDAR subunit, except for *GRIN2B.* Maximal expression levels were observed for the *GRIN2C* and *GRIN2D* transcripts. The expression of GluN1, GluN2C, GluN2D, GluN3A and GluN3B could be confirmed on protein level by means of flow cytometry and western blotting. The expression pattern suggests that the EPCs, from the stage of polychromatic erythroblasts, possess a slow deactivating receptor with low conductance. These characteristics would even be enhanced by the co-expression of the dominant negative subunits GluN3A and Glu3B. [215,219]

Nonetheless, the characterization at the molecular level is not sufficient to clarify the subunit composition and the functional properties of the NMDARs in erythroid cells. The relatively low expression levels of *GRIN1* and GluN1 respectively, indicates a structure with only one instead of the two “obligatory” GluN1 subunits. [196] Furthermore, the sensitivity to channel blockers, including magnesium, MK-801, and Memantine, is expected to be low compared to the “classic” neuronal NMDARs. [231] Therefore, studies on the functional level were required to investigate the properties of those receptors.

We were able to demonstrate the presence of functional receptors in EPCs and circulating RBC. Our studies showed that NMDAR activation caused enhanced Ca^{2+} influx in erythroid cells. Even more substantial was the finding of the functional plasticity of NMDAR during erythropoietic maturation. The alteration of the functional properties

(conductance, deactivation time, and Ca^{2+} uptake) reflected the changes in the mRNA expression pattern (**Figure 9**). [351]

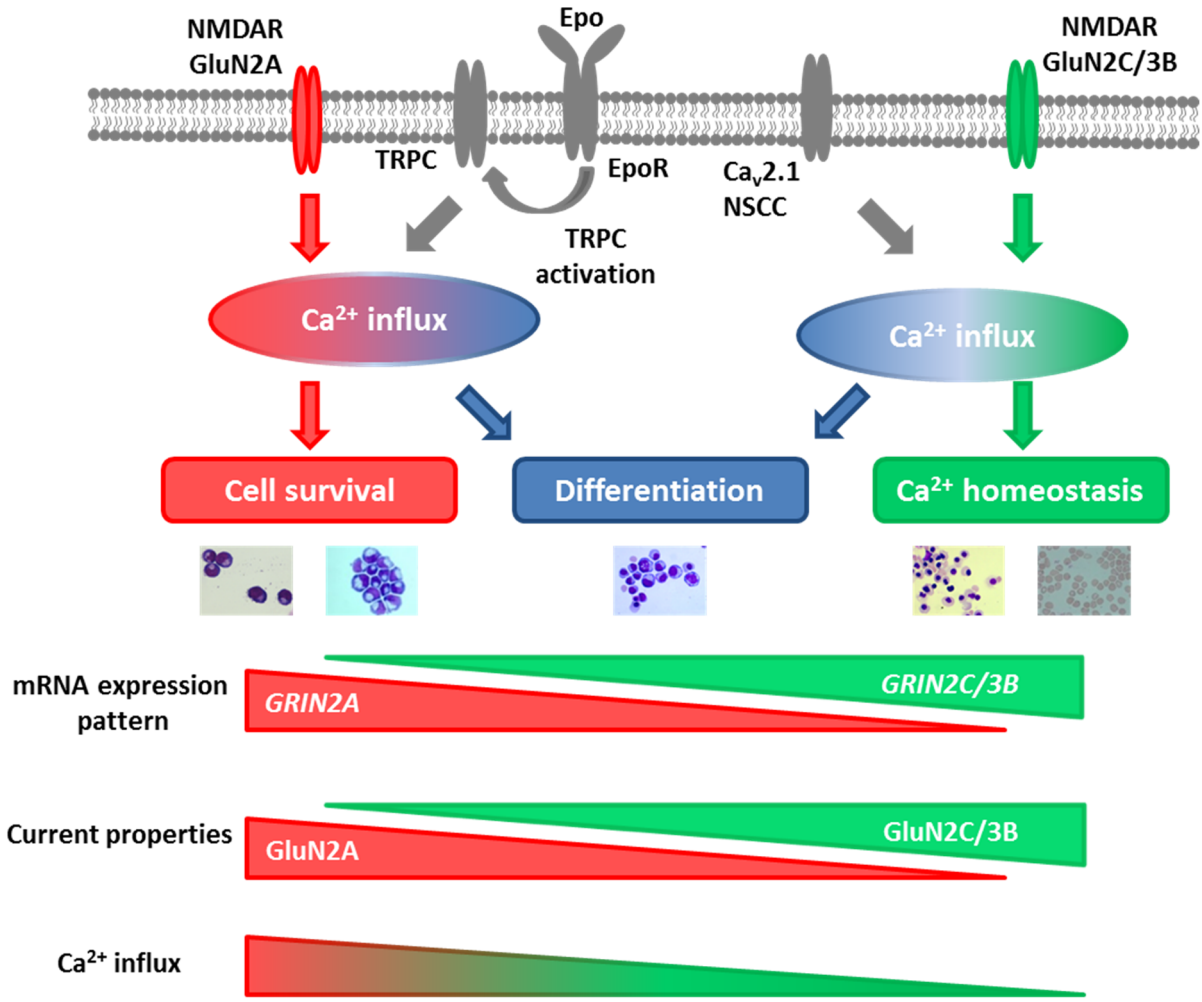

Figure 9: Schematic summary on the functional plasticity of the NMDAR during human erythropoietic maturation. GluN2A-containing NMDAR (red) is involved together with EpoR and TRPC in the regulation of cell survival and differentiation of early stage erythropoietic precursor cells (proerythroblasts and basophilic erythroblasts). During further maturation, the alteration of the expression pattern, the current properties and the reduced Ca^{2+} influx indicate a switch from a GluN2A-containing receptor to a GluN2C/3B-containing receptor (green). In orthochromatic erythroblasts and reticulocytes, GluN2C/3B-containing receptor is more likely to participate in the final part of differentiation and the regulation of Ca^{2+} homeostasis. [351]

Proerythroblasts and basophilic erythroblasts with the highest *GRIN2A* expression exhibited typical current properties of the GluN2A containing receptor. [221] At this stage of maturation, the Epo-driven Ca^{2+} signaling is essential for cell survival and differentiation. This suggests the existence of a complex interplay between EpoR, TRPC, and NMDAR for the mandatory enhanced Ca^{2+} influx in proerythroblasts and basophilic erythroblasts. [18,165,352] During ongoing differentiation with increasing

GRIN2C expression, the NMDA current properties changed to a GluN2C containing receptor. The switch to reduced conductance in polychromatic and orthochromatic erythroblasts correlated with the decrease in NMDA mediated Ca^{2+} influx, onset of hemoglobinization, iron kinetics, and the general remodeling of the membrane during differentiation. [201,353,354] Along the possible role of the NMDAR with low conductance in maturation, these receptors, together with VDACs, non-selective cation channel, and $Ca_V2.1$, presumably take part in the regulation of basal intracellular Ca^{2+}. Especially the presence and the contribution of these channels to the regulation of cell volume, proteolysis, and redox balance control in circulating RBCs supports this hypothesis. [3,5,351,355]

Furthermore, complete blocking of the NMDAR resulted in apoptosis of nearly all proerythroblasts and basophilic erythroblasts. Polychromatic erythroblasts and orthochromatic erythroblasts with the “slow” NMDAR subtypes were significantly less sensitive to the inhibition. This further supports the hypothesis that a “fast” GluN2A containing receptor is participating in the regulation of cell survival of CFU-e cells, proerythroblasts, and basophilic erythroblasts.

Experiments performed with erythroid cells of the same donor during repetitive blood sampling revealed a high degree of reproducibility in the expression patterns and functional properties of the erythroid NMDAR. However, within a group of donors, considerable inter-individual variability that presumably was driven by genetic and epigenetic variation was observed. Substantial inter-cellular heterogeneity was monitored in orthochromatic erythroblasts and reticulocytes. Inter-cellular and inter-individual heterogeneity persisted when an assessment of glutamate sensitivity was performed in the sub-populations of the circulating RBCs. [3,5,351] These observations are of potential clinical significance for the prediction of the quality of blood conserves and the outcome of blood transfusion, as well as for analysis of abnormalities in erythropoiesis and RBC clearance. [355] The molecular mechanisms and the consequences of the inter-cellular and inter-individual variability in RBCs require further investigations.

We have shown the presence of NMDARs in erythroid cells and their contribution to the regulation of intracellular Ca^{2+}. [351] The functional plasticity of NMDAR in erythroid cells and the alteration of passive electrophysiological properties imply that ion channels and ion homeostasis are very dynamic processes during erythropoietic maturation. The interplay of all the different receptors and ion channels during

differentiation is probably highly complex and more detailed studies are required. The change from prevalent chloride currents to potassium and calcium currents during enuclation would be of special interest. Two main questions that remained unanswered are (i) the role of NDMARs in the control of EPC proliferation, survival and differentiation, and (ii) the molecular mechanisms in control of *GRIN* genes' expression in these cells during their maturation into reticulocytes.

The observed alterations in the expression levels of the GluN2A and 2C subunits are a part of complex and precisely controlled changes occurring in EPCs during differentiation. Unfortunately, our knowledge of the mechanism in control of the protein expression in differentiating EPCs is incomplete. Little information is available in the literature on the possible involvement of the key regulators of erythropoiesis at the stages from BFU-e onward, such as GATA1, SCL and FOG, in management of *GRIN* genes expression in any cell type. [356,357] However, analysis of the promoter region of the *GRIN* genes (using TESS, Transcriptional Element Search System, Perelman School of Medicine, University of Pennsylvania, US) indicate the existence of potential binding sites for several transcription factors that are essential to the survival of EPCs and the differentiation, including GATA-2, GATA-1, LMO2, p300, Pu.1, Sp1, and STAT5. Further studies are needed to clarify the contribution of these transcription factors to the regulation of NMDAR subunits in erythroid cells.

Besides the transcriptional and posttranscriptional regulation, the detailed downstream signaling mechanisms of NMDAR activation was outside of the scope of this study. Nevertheless, independent from the cell type, EpoR and NMDAR have similar targets, including PLC and PKC. [358,359] The regulation of the survival of the EPCs at the early differentiation stages is mediated by ERK1/2, Bcl-xL, and Epo-driven signaling. [360] In neuronal cells, ERK1/2 are downstream targets of the NMDAR. [361] This suggests that the regulation of cell survival and apoptosis is co-regulated by Epo signaling and GluN2A containing NMDARs at the early stages EPC differentiation.

In addition to the regulation of the NMDARs and their downstream targets, another important aspect is the role of glutamate signaling for hematopoiesis. Glutamate is not only the most abundant excitatory neurotransmitter; it is also an important signaling molecule in the bone marrow. [173,174,274,362,363] This implies that transient fluctuation in serum glutamate levels influences erythropoiesis. We have shown that erythroid NMDAR gets deactivated after repetitive activation, and prolonged chronic activation did not induce apoptosis. The erythroid NMDAR is therefore protected against hyper-

activation under physiological conditions. In contrast to this, circulating RBCs of SCD patients responded to hyper-activation with transient increase in Ca^{2+}, cell shrinkage, and oxidative burst, which indicates the role of NMDAR in the pathophysiology of the anemic disorder. [5]

6.2. An old drug for young kids – the potential of Memantine for the treatment of sickle cell anemia

Our studies indicated that sickle cell anemia patients have an abnormally high abundance of functional NMDARs in circulating RBCs. [5] This higher abundance in circulating erythrocytes was associated with hemolytic events. Furthermore, we showed *ex vivo* that activation of NMDARs induces massive transient Ca^{2+} uptake into the SCD-RBCs. These enhanced intracellular Ca^{2+} levels trigger openings of the Gardos channels, the loss of K^+-Cl^-, and dehydration. Additionally, the inhibition of the NMDARs by Memantine suppressed the formation of terminally sickled cells upon deoxygenation. These findings suggest that the inhibition of NMDARs in RBCs has beneficial effects on the pathophysiology of SCD and indicate that the receptor is a promising novel target for the treatment of several other rare anemias.

We have shown that reticulocytes contain a higher number of NMDAR copies per cell and are more sensitive to the stimulation with agonists (NMDA or glutamate) than mature and senescent cells. These findings are consistent with higher susceptibility of young RBCs of SCD patients to dehydration. [3,364] The number of transcripts, the protein abundance of the GluN subunits, the conductance and the Ca^{2+} uptake mediated by the activation of the NMDARs decreased steadily during the final stages of EPC maturation. The higher number of functional receptor copies in reticulocytes and the disturbed clearance during differentiation might contribute to the predisposition of young cells and to premature removal from the circulation. [364] In all RBC fractions of SCD patients, the abundance and activity of the NMDARs was up-regulated. Particularly in the “light” fraction and within in hemolytic crises those parameters were further enhanced. This observation supports our hypothesis of the important role of NMDARs in the pathophysiology of sickle cell anemia.

Although *GRIN3B* mRNA expression was highly up-regulated in EPCs from SCD patients, this finding could not be confirmed on the protein level. However, SCD-EPCs exhibited lower sensitivity to the inhibition than EPCs from healthy subjects. An unpublished observation (Hänggi, 2014) indicates that higher abundance of the GluN3B rather than the number of receptor units per cell in EPCs of patients, may be the cause of this change in the receptors' pharmacological properties. The discrepancy between the higher abundance of NMDAR in SCD patients' RBCs, and the lack of difference in their abundance in the EPCs of healthy and diseased subjects is more likely to be attributed to the clearance of receptors than the higher number of receptors in EPCs. To clarify this hypothesis, voltage-clamp recordings are required.

Our studies strongly suggest that erythroid NMDARs are a promising novel target for pharmacological intervention. The inhibition of the ion channel hits multiple downstream Ca^{2+}-sensitive targets in RBCs. Due to the lack of any major side effects, low toxicity, and excellent pharmacological properties Memantine would be the best candidate for a first clinical trial, which is currently in preparation at the Clinic of Hematology at the University Hospital Zurich (USZ). The combination therapy of the non-competitive channel blocker with the allosteric modulator zinc might lead to significant improvements in the treatment of SCD progression. As evoked Ca^{2+} uptake in RBCs is one of the first and major steps in the pathophysiology, our new therapy approach is very promising (**Figure 10**).

Moreover, if the clinical trial is successful, Memantine has the potential to be a therapeutic option for several other rare hereditary forms of anemia, including thalassemia and spherocytosis, in which an abnormally high number of NMDAR copies per RBC was detected (Makhro, Hänggi, Bogdanova unpublished observations).

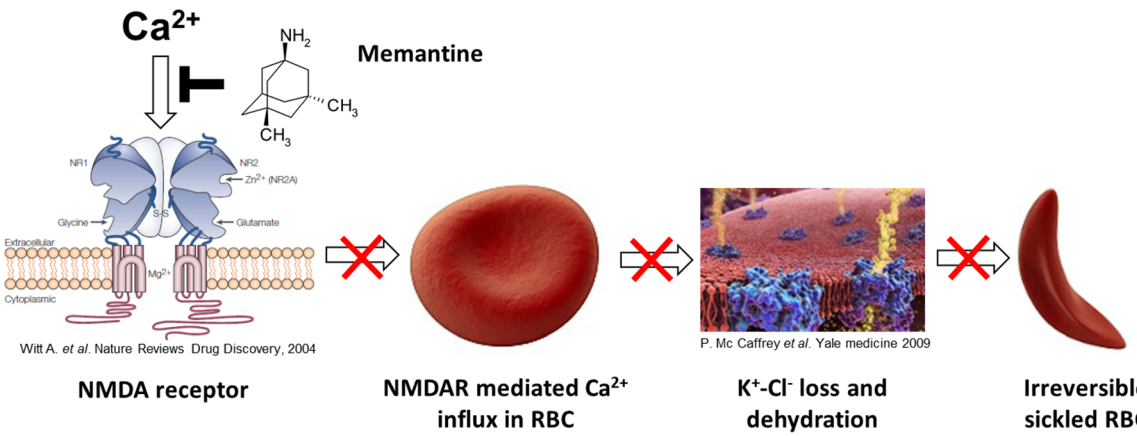

Figure 10: Hypothetical mechanism of Memantine for the treatment of sickle cell anemia (Copyright of RBC images by Georgia Regents University, 2013). The open-channel blocker Memantine binds to the transmembrane loop of the NMDAR in RBC. Thereby, enhanced and pathological Ca^{2+} influx should be avoided. Without the critically high intracellular Ca^{2+} levels, the loss of K^{+}-Cl^{-}, dehydration, and irreversible sickle would be reduced.

7. Outlook

The focus of the ongoing work will be on the approval of Memantine for the treatment of sickle cell anemia (**Figure 11**). We have shown the presence of NMDARs in circulating RBCs of healthy subjects and SCD patients and the clinical trial approval (CTA) was submitted to the Swiss health authorities (Swissmedic).

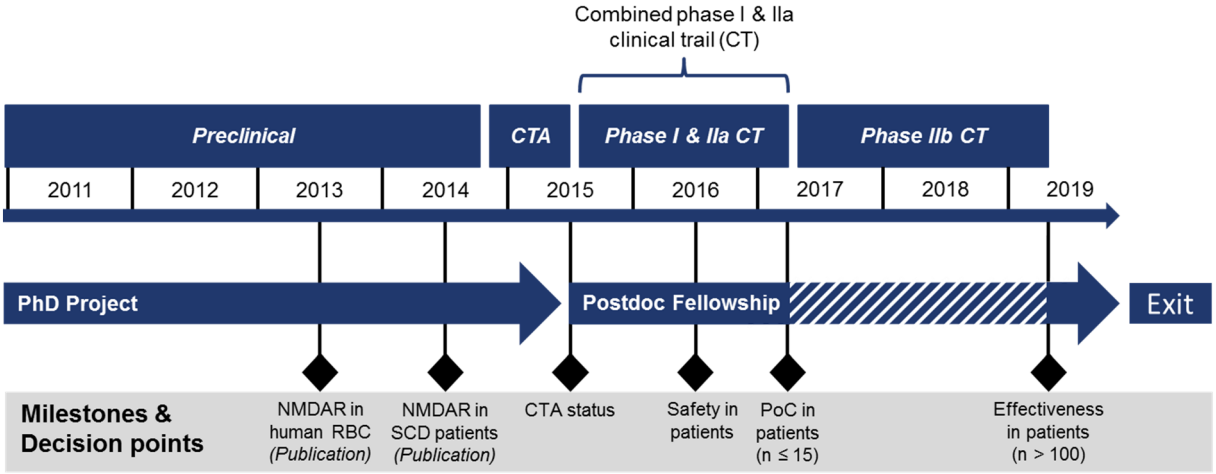

Figure 11: Development plan for Memantine. Schematic overview of the development plan for Memantine as a novel treatment for sickle cell anemia. After the proof of concept (PoC) in a small number of patients (n ≤ 15), the effectiveness will be evaluated in a higher number of patients (n > 100). Exit point would be the out-licensing of Memantine after the successful completion of clinical phase IIb.

After receiving the CTA for a combined CT phase I and IIa, we will evaluate the therapeutic potential of Memantine in a small number of patients (n ≤ 15 SCD patients). As the drug is already approved by Swissmedic for Alzheimer's disease, it is possible to combine clinical trial phase I (first use in man) and phase IIa (first use in patient). Depending on whether, the proof of concept (safe and efficient drug) was shown in the small SCD patient cohort; this could be a first exit point for out-licensing. Nevertheless, the preferred exit point would be after successful completion of clinical trial phase IIb with a higher number of patients (n > 100) and therefore a substantial derisk for possible investors and out-licensing. Independent from the exit point, we would plan and organize the proof of effectiveness in patients (CT phase IIb) in Europe, either Great Britain and/or France.

Besides the clinical trial, there are be several follow-up projects in the field of ion channels, hematopoiesis, and rare hereditary blood disorders. The focus of the first work package (listed in left panel of **Figure 12**) would be on NMDARs in erythroid cells.

To study the NMDARs on single channel level the replacement for several components of the patch clamp setup is required, including the air table, the microscope, and the pipette puller. The appropriate modifications allow detailed studies of the different NMDAR subtypes and their role in erythroid cells. Investigation of the downstream signaling cascade and the transcrtional regulation would be the part of the first work package as well. Furthermore, the validation of GluN2C/2D specific antagonist, might lead to a new therapeutic approach to target NMDRs highly specific in mature erythrocytes only.

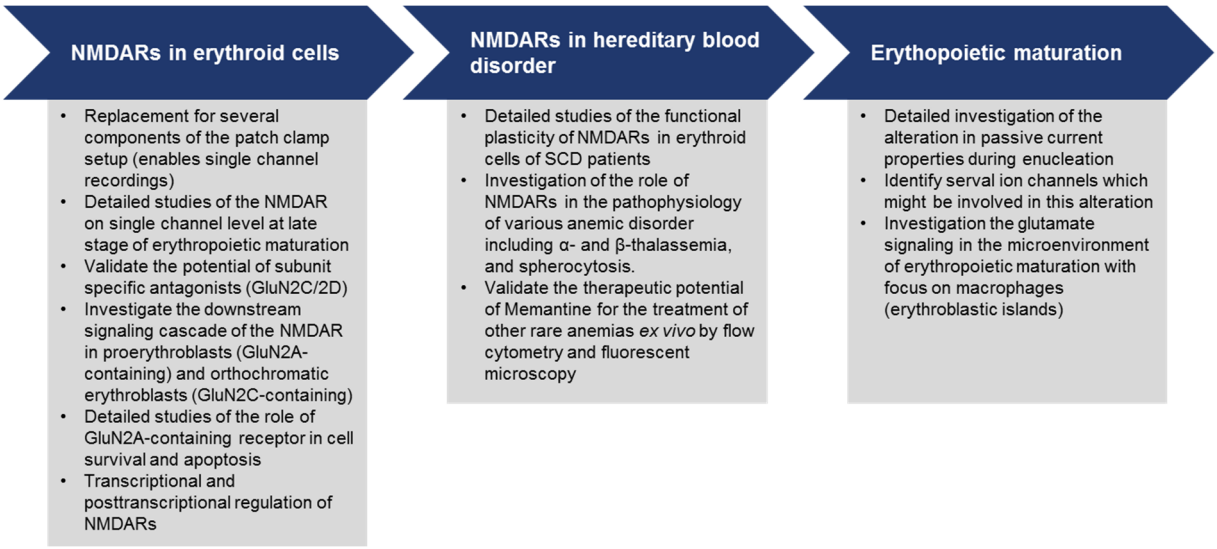

Figure 12: Work packages for follow-up studies. The follow-up studies/work packages of the PhD project would be in the field of NMDARs in erythroid cells, NMDARs in hereditary blood disorders, and erythropoietic maturation.

The second work package (listed in middle panel of **Figure 12**) would be more related to SCD and other rare anemic disorder including α- and β-Thalassemia, and spherocytosis. The main deliverable from the second work package would be the validation of Memantine as a treatment for other hereditary rare anemic disorders.
The third work package (listed in right panel of **Figure 12**) would focus on ion channels, the microenvironment of erythropoiesis, and their influence on hematopoiesis. Before the investigation of the glutamate signaling in *ex vivo* co-culture systems, the focus of this work package would be on the identification and role of the different ion channels during enucleation.

8. References

1. Weber RE, Vinogradov SN. Nonvertebrate hemoglobins: functions and molecular adaptations. *Physiol Rev*. 2001;81(2):569-628.
2. Cantor AB, Orkin SH. Transcriptional regulation of erythropoiesis: an affair involving multiple partners. *Oncogene*. 2002;21(21):3368-3376.
3. Makhro A, Hanggi P, Goede JS, et al. N-methyl D-aspartate (NMDA) receptors in human erythroid precursor cells and in circulating red blood cells contribute to the intracellular calcium regulation. *Am J Physiol Cell Physiol*. 2013.
4. Makhro A, Wang J, Vogel J, et al. Functional NMDA receptors in rat erythrocytes. *Am J Physiol Cell Physiol*. 2010;298(6):C1315-1325.
5. Hänggi P, Makhro A, Gassmann M, et al. Red blood cells of sickle cell disease patients exhibit abnormally high abundance of N-methyl D-aspartate receptors mediating excessive calcium uptake. *Br J Haematol*. 2014.
6. Komatsu N, Yamamoto M, Fujita H, et al. Establishment and characterization of an erythropoietin-dependent subline, UT-7/Epo, derived from human leukemia cell line, UT-7. *Blood*. 1993;82(2):456-464.
7. Steinberg MH, et al. Disorders of Hemoglobin: Cambridge University Press; 2009.
8. Fernández KS, de Alarcón PA. Development of the hematopoietic system and disorders of hematopoiesis that present during infancy and early childhood. *Pediatr Clin North Am*. 2013;60(6):1273-1289.
9. Migliaccio G, Sanchez M, Masiello F, et al. Humanized culture medium for clinical expansion of human erythroblasts. *Cell Transplant*. 2010;19(4):453-469.
10. Migliaccio G, Di Pietro R, di Giacomo V, et al. In vitro mass production of human erythroid cells from the blood of normal donors and of thalassemic patients. *Blood Cells Mol Dis*. 2002;28(2):169-180.
11. Masiello F, Tirelli V, Sanchez M, et al. Mononuclear cells from a rare blood donor, after freezing under good manufacturing practice conditions, generate red blood cells that recapitulate the rare blood phenotype. *Transfusion*. 2013.
12. Migliaccio AR. Erythroblast enucleation. *Haematologica*. 2010;95(12):1985-1988.
13. Hattangadi SM, Wong P, Zhang L, Flygare J, Lodish HF. From stem cell to red cell: regulation of erythropoiesis at multiple levels by multiple proteins, RNAs, and chromatin modifications. *Blood*. 2011;118(24):6258-6268.
14. Spivak JL. The anaemia of cancer: death by a thousand cuts. *Nat Rev Cancer*. 2005;5(7):543-555.
15. Hänggi P, Telezhkin V, Kemp PJ, et al. Functional plasticity of the N-methyl-D-aspartate receptor in differentiating human erythroid precursor cells. *Am J Physiol Cell Physiol*. 2015:(Epub ahead of print).
16. Walasek MA, van Os R, de Haan G. Hematopoietic stem cell expansion: challenges and opportunities. *Ann N Y Acad Sci*. 2012;1266:138-150.
17. Zhang CC, Lodish HF. Cytokines regulating hematopoietic stem cell function. *Curr Opin Hematol*. 2008;15(4):307-311.
18. Miller BA, Cheung JY, Tillotson DL, Hope SM, Scaduto RC. Erythropoietin stimulates a rise in intracellular-free calcium concentration in single BFU-E derived erythroblasts at specific stages of differentiation. *Blood*. 1989;73(5):1188-1194.
19. Miller BA, Scaduto RC, Tillotson DL, Botti JJ, Cheung JY. Erythropoietin stimulates a rise in intracellular free calcium concentration in single early human erythroid precursors. *J Clin Invest*. 1988;82(1):309-315.
20. Johnson GR, Pappas S. Hemopoietic progenitors, stimulating factors, and hemoglobin switching. *Prog Clin Biol Res*. 1983;134:399-410.

21. Wojchowski DM, Menon MP, Sathyanarayana P, et al. Erythropoietin-dependent erythropoiesis: New insights and questions. *Blood Cells Mol Dis*. 2006;36(2):232-238.
22. P C. Sur l'activite hemopoietique du serum au cours de la regeneration du sang. In: C D ed. Vol. 143: C R Acad. Sci Paris; 1906.
23. Ogunshola OO, Bogdanova AY. Epo and non-hematopoietic cells: what do we know? *Methods Mol Biol*. 2013;982:13-41.
24. Nathan DG. Amino acid uptake in erythropoiesis. *Sci Signal*. 2015;8(372):fs9.
25. Ihle JN, Witthuhn BA, Quelle FW, Yamamoto K, Silvennoinen O. Signaling through the hematopoietic cytokine receptors. *Annu Rev Immunol*. 1995;13:369-398.
26. Cheung JY, Miller BA. Molecular mechanisms of erythropoietin signaling. *Nephron*. 2001;87(3):215-222.
27. Broudy VC, Lin N, Brice M, Nakamoto B, Papayannopoulou T. Erythropoietin receptor characteristics on primary human erythroid cells. *Blood*. 1991;77(12):2583-2590.
28. Zhang J, Socolovsky M, Gross AW, Lodish HF. Role of Ras signaling in erythroid differentiation of mouse fetal liver cells: functional analysis by a flow cytometry-based novel culture system. *Blood*. 2003;102(12):3938-3946.
29. Mihov D, Vogel J, Gassmann M, Bogdanova A. Erythropoietin activates nitric oxide synthase in murine erythrocytes. *Am J Physiol Cell Physiol*. 2009;297(2):C378-388.
30. Risso A, Ciana A, Achilli C, Minetti G. Survival and senescence of human young red cells in vitro. *Cell Physiol Biochem*. 2014;34(4):1038-1049.
31. Risso A, Ciana A, Achilli C, Antonutto G, Minetti G. Neocytolysis: none, one or many? A reappraisal and future perspectives. *Front Physiol*. 2014;5:54.
32. Wang L, Di L, Noguchi CT. Erythropoietin, a novel versatile player regulating energy metabolism beyond the erythroid system. *Int J Biol Sci*. 2014;10(8):921-939.
33. Magócsi M, Apáti A, Gáti R, Kolonics A. Signalling mechanisms and the role of calcineurin in erythropoiesis. *Immunol Lett*. 1999;68(1):187-195.
34. Parkash J, Asotra K. Calcium wave signaling in cancer cells. *Life Sci*. 2010;87(19-22):587-595.
35. Sparatore B, Pessino A, Patrone M, Passalacqua M, Melloni E, Pontremoli S. Changes in calcium influx affect the differentiation of murine erythroleukaemia cells. *Biochem J*. 1995;305 (Pt 1):285-290.
36. Sparatore B, Passalacqua M, Pessino A, Melloni E, Patrone M, Pontremoli S. Modulation of the intracellular Ca(2+)-dependent proteolytic system is critically correlated with the kinetics of differentiation of murine erythroleukemia cells. *Eur J Biochem*. 1994;225(1):173-178.
37. Goll DE, Thompson VF, Li H, Wei W, Cong J. The calpain system. *Physiol Rev*. 2003;83(3):731-801.
38. Myklebust JH, Smeland EB, Josefsen D, Sioud M. Protein kinase C-alpha isoform is involved in erythropoietin-induced erythroid differentiation of CD34(+) progenitor cells from human bone marrow. *Blood*. 2000;95(2):510-518.
39. Hebbert D, Morgan EH. Calmodulin antagonists inhibit and phorbol esters enhance transferrin endocytosis and iron uptake by immature erythroid cells. *Blood*. 1985;65(3):758-763.
40. Neubauer H, Cumano A, Müller M, Wu H, Huffstadt U, Pfeffer K. Jak2 deficiency defines an essential developmental checkpoint in definitive hematopoiesis. *Cell*. 1998;93(3):397-409.
41. Damen JE, Liu L, Cutler RL, Krystal G. Erythropoietin stimulates the tyrosine phosphorylation of Shc and its association with Grb2 and a 145-Kd tyrosine phosphorylated protein. *Blood*. 1993;82(8):2296-2303.
42. Cutler RL, Liu L, Damen JE, Krystal G. Multiple cytokines induce the tyrosine phosphorylation of Shc and its association with Grb2 in hemopoietic cells. *J Biol Chem*. 1993;268(29):21463-21465.
43. Wood AD, Chen E, Donaldson IJ, et al. ID1 promotes expansion and survival of primary erythroid cells and is a target of JAK2V617F-STAT5 signaling. *Blood*. 2009;114(9):1820-1830.
44. Schaefer A, Magócsi M, Marquardt H. Signalling mechanisms in erythropoiesis: the enigmatic role of calcium. *Cell Signal*. 1997;9(7):483-495.
45. Divecha N, Irvine RF. Phospholipid signaling. *Cell*. 1995;80(2):269-278.

46. Calvo V, Wood M, Gjertson C, Vik T, Bierer BE. Activation of 70-kDa S6 kinase, induced by the cytokines interleukin-3 and erythropoietin and inhibited by rapamycin, is not an absolute requirement for cell proliferation. *Eur J Immunol*. 1994;24(11):2664-2671.
47. Franke TF, Kaplan DR, Cantley LC. PI3K: downstream AKTion blocks apoptosis. *Cell*. 1997;88(4):435-437.
48. Ren HY, Komatsu N, Shimizu R, Okada K, Miura Y. Erythropoietin induces tyrosine phosphorylation and activation of phospholipase C-gamma 1 in a human erythropoietin-dependent cell line. *J Biol Chem*. 1994;269(30):19633-19638.
49. Gyan E, Frisan E, Beyne-Rauzy O, et al. Spontaneous and Fas-induced apoptosis of low-grade MDS erythroid precursors involves the endoplasmic reticulum. *Leukemia*. 2008;22(10):1864-1873.
50. Nunomura W, Gascard P, Takakuwa Y. Insights into the Function of the Unstructured N-Terminal Domain of Proteins 4.1R and 4.1G in Erythropoiesis. *Int J Cell Biol*. 2011;2011:943272.
51. Pigozzi D, Ducret T, Tajeddine N, Gala JL, Tombal B, Gailly P. Calcium store contents control the expression of TRPC1, TRPC3 and TRPV6 proteins in LNCaP prostate cancer cell line. *Cell Calcium*. 2006;39(5):401-415.
52. Tong Q, Hirschler-Laszkiewicz I, Zhang W, et al. TRPC3 is the erythropoietin-regulated calcium channel in human erythroid cells. *J Biol Chem*. 2008;283(16):10385-10395.
53. Tong Q, Chu X, Cheung JY, et al. Erythropoietin-modulated calcium influx through TRPC2 is mediated by phospholipase Cgamma and IP3R. *Am J Physiol Cell Physiol*. 2004;287(6):C1667-1678.
54. Nielsen JS, McNagny KM. Novel functions of the CD34 family. *J Cell Sci*. 2008;121(Pt 22):3683-3692.
55. Munugalavadla V, Dore LC, Tan BL, et al. Repression of c-kit and its downstream substrates by GATA-1 inhibits cell proliferation during erythroid maturation. *Mol Cell Biol*. 2005;25(15):6747-6759.
56. Jayapal SR, Lee KL, Ji P, Kaldis P, Lim B, Lodish HF. Down-regulation of Myc is essential for terminal erythroid maturation. *J Biol Chem*. 2010;285(51):40252-40265.
57. Munugalavadla V, Kapur R. Role of c-Kit and erythropoietin receptor in erythropoiesis. *Crit Rev Oncol Hematol*. 2005;54(1):63-75.
58. Nocka K, Majumder S, Chabot B, et al. Expression of c-kit gene products in known cellular targets of W mutations in normal and W mutant mice--evidence for an impaired c-kit kinase in mutant mice. *Genes Dev*. 1989;3(6):816-826.
59. Wu H, Klingmüller U, Besmer P, Lodish HF. Interaction of the erythropoietin and stem-cell-factor receptors. *Nature*. 1995;377(6546):242-246.
60. Klingmüller U, Wu H, Hsiao JG, et al. Identification of a novel pathway important for proliferation and differentiation of primary erythroid progenitors. *Proc Natl Acad Sci U S A*. 1997;94(7):3016-3021.
61. Marsee DK, Pinkus GS, Yu H. CD71 (transferrin receptor): an effective marker for erythroid precursors in bone marrow biopsy specimens. *Am J Clin Pathol*. 2010;134(3):429-435.
62. Furthmayr H, Marchesi VT. Subunit structure of human erythrocyte glycophorin A. *Biochemistry*. 1976;15(5):1137-1144.
63. Böhmer RM. IL-3-dependent early erythropoiesis is stimulated by autocrine transforming growth factor beta. *Stem Cells*. 2004;22(2):216-224.
64. Goodman JW, Hall EA, Miller KL, Shinpock SG. Interleukin 3 promotes erythroid burst formation in "serum-free" cultures without detectable erythropoietin. *Proc Natl Acad Sci U S A*. 1985;82(10):3291-3295.
65. Fuchs O, Simakova O, Klener P, et al. Inhibition of Smad5 in human hematopoietic progenitors blocks erythroid differentiation induced by BMP4. *Blood Cells Mol Dis*. 2002;28(2):221-233.
66. Harandi OF, Hedge S, Wu DC, McKeone D, Paulson RF. Murine erythroid short-term radioprotection requires a BMP4-dependent, self-renewing population of stress erythroid progenitors. *J Clin Invest*. 2010;120(12):4507-4519.

67. Perry JM, Harandi OF, Porayette P, Hegde S, Kannan AK, Paulson RF. Maintenance of the BMP4-dependent stress erythropoiesis pathway in the murine spleen requires hedgehog signaling. *Blood*. 2009;113(4):911-918.
68. Kobayashi M, Laver JH, Lyman SD, Kato T, Miyazaki H, Ogawa M. Thrombopoietin, steel factor and the ligand for flt3/flk2 interact to stimulate the proliferation of human hematopoietic progenitors in culture. *Int J Hematol*. 1997;66(4):423-434.
69. Kaushansky K. Lineage-specific hematopoietic growth factors. *N Engl J Med*. 2006;354(19):2034-2045.
70. Lyman SD, Jacobsen SE. c-kit ligand and Flt3 ligand: stem/progenitor cell factors with overlapping yet distinct activities. *Blood*. 1998;91(4):1101-1134.
71. Tsapogas P, Swee LK, Nusser A, et al. In vivo evidence for an instructive role of fms-like tyrosine kinase-3 (FLT3) ligand in hematopoietic development. *Haematologica*. 2014;99(4):638-646.
72. Sawada K, Krantz SB, Dessypris EN, Koury ST, Sawyer ST. Human colony-forming units-erythroid do not require accessory cells, but do require direct interaction with insulin-like growth factor I and/or insulin for erythroid development. *J Clin Invest*. 1989;83(5):1701-1709.
73. Merchav S, Silvian-Drachsler I, Tatarsky I, Lake M, Skottner A. Comparative studies of the erythroid-potentiating effects of biosynthetic human insulin-like growth factors-I and -II. *J Clin Endocrinol Metab*. 1992;74(2):447-452.
74. Miyagawa S, Kobayashi M, Konishi N, Sato T, Ueda K. Insulin and insulin-like growth factor I support the proliferation of erythroid progenitor cells in bone marrow through the sharing of receptors. *Br J Haematol*. 2000;109(3):555-562.
75. Carlile GW, Smith DH, Wiedmann M. A non-apoptotic role for Fas/FasL in erythropoiesis. *FEBS Lett*. 2009;583(4):848-854.
76. Eshghi S, Vogelezang MG, Hynes RO, Griffith LG, Lodish HF. Alpha4beta1 integrin and erythropoietin mediate temporally distinct steps in erythropoiesis: integrins in red cell development. *J Cell Biol*. 2007;177(5):871-880.
77. Flygare J, Rayon Estrada V, Shin C, Gupta S, Lodish HF. HIF1alpha synergizes with glucocorticoids to promote BFU-E progenitor self-renewal. *Blood*. 2011;117(12):3435-3444.
78. Bauer A, Tronche F, Wessely O, et al. The glucocorticoid receptor is required for stress erythropoiesis. *Genes Dev*. 1999;13(22):2996-3002.
79. Perry C, Soreq H. Transcriptional regulation of erythropoiesis. Fine tuning of combinatorial multi-domain elements. *Eur J Biochem*. 2002;269(15):3607-3618.
80. Shivdasani RA, Orkin SH. The transcriptional control of hematopoiesis. *Blood*. 1996;87(10):4025-4039.
81. Scott EW, Simon MC, Anastasi J, Singh H. Requirement of transcription factor PU.1 in the development of multiple hematopoietic lineages. *Science*. 1994;265(5178):1573-1577.
82. Wong P, Hattangadi SM, Cheng AW, Frampton GM, Young RA, Lodish HF. Gene induction and repression during terminal erythropoiesis are mediated by distinct epigenetic changes. *Blood*. 2011;118(16):e128-138.
83. Miller IJ, Bieker JJ. A novel, erythroid cell-specific murine transcription factor that binds to the CACCC element and is related to the Krüppel family of nuclear proteins. *Mol Cell Biol*. 1993;13(5):2776-2786.
84. Merika M, Orkin SH. Functional synergy and physical interactions of the erythroid transcription factor GATA-1 with the Krüppel family proteins Sp1 and EKLF. *Mol Cell Biol*. 1995;15(5):2437-2447.
85. Perkins AC, Sharpe AH, Orkin SH. Lethal beta-thalassaemia in mice lacking the erythroid CACCC-transcription factor EKLF. *Nature*. 1995;375(6529):318-322.
86. Huisman TH. Levels of Hb A2 in heterozygotes and homozygotes for beta-thalassemia mutations: influence of mutations in the CACCC and ATAAA motifs of the beta-globin gene promoter. *Acta Haematol*. 1997;98(4):187-194.

87. Socolovsky M, Fallon AE, Wang S, Brugnara C, Lodish HF. Fetal anemia and apoptosis of red cell progenitors in Stat5a-/-5b-/- mice: a direct role for Stat5 in Bcl-X(L) induction. *Cell*. 1999;98(2):181-191.
88. Lu J, Guo S, Ebert BL, et al. MicroRNA-mediated control of cell fate in megakaryocyte-erythrocyte progenitors. *Dev Cell*. 2008;14(6):843-853.
89. Felli N, Pedini F, Romania P, et al. MicroRNA 223-dependent expression of LMO2 regulates normal erythropoiesis. *Haematologica*. 2009;94(4):479-486.
90. Dore LC, Amigo JD, Dos Santos CO, et al. A GATA-1-regulated microRNA locus essential for erythropoiesis. *Proc Natl Acad Sci U S A*. 2008;105(9):3333-3338.
91. Chasis JA, Mohandas N. Erythroblastic islands: niches for erythropoiesis. *Blood*. 2008;112(3):470-478.
92. Ji P, Murata-Hori M, Lodish HF. Formation of mammalian erythrocytes: chromatin condensation and enucleation. *Trends Cell Biol*. 2011;21(7):409-415.
93. Felsenfeld G, Groudine M. Controlling the double helix. *Nature*. 2003;421(6921):448-453.
94. Berridge MJ. Inositol trisphosphate and calcium signalling mechanisms. *Biochim Biophys Acta*. 2009;1793(6):933-940.
95. Miccio A, Wang Y, Hong W, et al. NuRD mediates activating and repressive functions of GATA-1 and FOG-1 during blood development. *EMBO J*. 2010;29(2):442-456.
96. Mankidy R, Faller DV, Mabaera R, et al. Short-chain fatty acids induce gamma-globin gene expression by displacement of a HDAC3-NCoR repressor complex. *Blood*. 2006;108(9):3179-3186.
97. Ji P, Yeh V, Ramirez T, Murata-Hori M, Lodish HF. Histone deacetylase 2 is required for chromatin condensation and subsequent enucleation of cultured mouse fetal erythroblasts. *Haematologica*. 2010;95(12):2013-2021.
98. Wu H, Liu X, Jaenisch R, Lodish HF. Generation of committed erythroid BFU-E and CFU-E progenitors does not require erythropoietin or the erythropoietin receptor. *Cell*. 1995;83(1):59-67.
99. Miller BA. Trpc2. *Handb Exp Pharmacol*. 2014;222:53-65.
100. Cheung JY, Elensky MB, Brauneis U, et al. Ion channels in human erythroblasts. Modulation by erythropoietin. *J Clin Invest*. 1992;90(5):1850-1856.
101. Thomas SL, Bouyer G, Cueff A, Egee S, Glogowska E, Ollivaux C. Ion channels in human red blood cell membrane: actors or relics? *Blood Cells Mol Dis*. 2011;46(4):261-265.
102. Browning JA, Ellory JC, Gibson JS. Pathophysiology of red cell volume. *Contrib Nephrol*. 2006;152:241-268.
103. Rinehart J, Gulcicek EE, Joiner CH, Lifton RP, Gallagher PG. Determinants of erythrocyte hydration. *Curr Opin Hematol*. 2010;17(3):191-197.
104. Bruce LJ. Hereditary stomatocytosis and cation-leaky red cells--recent developments. *Blood Cells Mol Dis*. 2009;42(3):216-222.
105. Bogdanova A, Goede JS, Weiss E, et al. Cryohydrocytosis: increased activity of cation carriers in red cells from a patient with a band 3 mutation. *Haematologica*. 2010;95(2):189-198.
106. Gallagher PG. Disorders of red cell volume regulation. *Curr Opin Hematol*. 2013;20(3):201-207.
107. Noguchi CT, Rodgers GP, Schechter AN. Intracellular polymerization. Disease severity and therapeutic predictions. *Ann N Y Acad Sci*. 1989;565:75-82.
108. Gallagher PG. Red cell membrane disorders. *Hematology Am Soc Hematol Educ Program*. 2005:13-18.
109. Kaul DK, Chen D, Zhan J. Adhesion of sickle cells to vascular endothelium is critically dependent on changes in density and shape of the cells. *Blood*. 1994;83(10):3006-3017.
110. Eaton WA, Hofrichter J. Sickle cell hemoglobin polymerization. *Adv Protein Chem*. 1990;40:63-279.
111. Pan D, Kalfa TA, Wang D, et al. K-Cl cotransporter gene expression during human and murine erythroid differentiation. *J Biol Chem*. 2011;286(35):30492-30503.
112. De Franceschi L, Ronzoni L, Cappellini MD, et al. K-CL co-transport plays an important role in normal and beta thalassemic erythropoiesis. *Haematologica*. 2007;92(10):1319-1326.

113. Clapham DE. Calcium signaling. *Cell*. 2007;131(6):1047-1058.
114. Berridge MJ. Calcium microdomains: organization and function. *Cell Calcium*. 2006;40(5-6):405-412.
115. Hoeflich KP, Ikura M. Calmodulin in action: diversity in target recognition and activation mechanisms. *Cell*. 2002;108(6):739-742.
116. Naraghi M, Neher E. Linearized buffered Ca2+ diffusion in microdomains and its implications for calculation of [Ca2+] at the mouth of a calcium channel. *J Neurosci*. 1997;17(18):6961-6973.
117. Long SB, Campbell EB, Mackinnon R. Voltage sensor of Kv1.2: structural basis of electromechanical coupling. *Science*. 2005;309(5736):903-908.
118. Sabatini BL, Oertner TG, Svoboda K. The life cycle of Ca(2+) ions in dendritic spines. *Neuron*. 2002;33(3):439-452.
119. Alvarez VA, Ridenour DA, Sabatini BL. Distinct structural and ionotropic roles of NMDA receptors in controlling spine and synapse stability. *J Neurosci*. 2007;27(28):7365-7376.
120. Alvarez VA, Sabatini BL. Anatomical and physiological plasticity of dendritic spines. *Annu Rev Neurosci*. 2007;30:79-97.
121. Wayman GA, Walters MJ, Kolibaba K, Soderling TR, Christian JL. CaM kinase IV regulates lineage commitment and survival of erythroid progenitors in a non-cell-autonomous manner. *J Cell Biol*. 2000;151(4):811-824.
122. Walters MJ, Wayman GA, Notis JC, Goodman RH, Soderling TR, Christian JL. Calmodulin-dependent protein kinase IV mediated antagonism of BMP signaling regulates lineage and survival of hematopoietic progenitors. *Development*. 2002;129(6):1455-1466.
123. Wayman GA, Wei J, Wong S, Storm DR. Regulation of type I adenylyl cyclase by calmodulin kinase IV in vivo. *Mol Cell Biol*. 1996;16(11):6075-6082.
124. Hayashi Y, Nishio M, Naito Y, et al. Regulation of neuronal nitric-oxide synthase by calmodulin kinases. *J Biol Chem*. 1999;274(29):20597-20602.
125. Garrahan PJ, Glynn IM. The behaviour of the sodium pump in red cells in the absence of external potassium. *J Physiol*. 1967;192(1):159-174.
126. Garrahan PJ, Glynn IM. The stoicheiometry of the sodium pump. *J Physiol*. 1967;192(1):217-235.
127. Kaestner L. Cation Channels in Erythrocytes - Historical and Future Perspetive. Calcium signalling: Spinger Berlin Heidelberg; 2012:223-233.
128. Kaestner L, Bernhardt I. Ion channels in the human red blood cell membrane: their further investigation and physiological relevance. *Bioelectrochemistry*. 2002;55(1-2):71-74.
129. Corry DB, Lee DB, Tuck ML. A kinetic study of cation transport in erythrocytes from uremic patients. *Kidney Int*. 1987;32(2):256-260.
130. Tuck ML, Corry DB, Maxwell M, Stern N. Kinetic analysis of erythrocyte Na+-K+ pump and cotransport in essential hypertension. *Hypertension*. 1987;10(2):204-211.
131. Lauf PK, Adragna NC. Functional evidence for a pH sensor of erythrocyte K-Cl cotransport through inhibition by internal protons and diethylpyrocarbonate. *Cell Physiol Biochem*. 1998;8(1-2):46-60.
132. Brugnara C, Bunn HF, Tosteson DC. Ion content and transport and the regulation of volume in sickle cells. *Ann N Y Acad Sci*. 1989;565:96-103.
133. Brugnara C, De Franceschi L, Bennekou P, Alper SL, Christophersen P. Novel therapies for prevention of erythrocyte dehydration in sickle cell anemia. *Drug News Perspect*. 2001;14(4):208-220.
134. Schwartz RS, Musto S, Fabry ME, Nagel RL. Two distinct pathways mediate the formation of intermediate density cells and hyperdense cells from normal density sickle red blood cells. *Blood*. 1998;92(12):4844-4855.
135. Maher AD, Kuchel PW. The Gardos channel: a review of the Ca2+-activated K+ channel in human erythrocytes. *Int J Biochem Cell Biol*. 2003;35(8):1182-1197.
136. Clark MR, Morrison CE, Unger RC, Shohet SB. Abnormal monovalent cation transport in irreversibly sickled cells. *Prog Clin Biol Res*. 1978;20:93-103.

137. Clark MR, Morrison CE, Shohet SB. Monovalent cation transport in irreversibly sickled cells. *J Clin Invest*. 1978;62(2):329-337.
138. Ortiz OE, Lew VL, Bookchin RM. Deoxygenation permeabilizes sickle cell anaemia red cells to magnesium and reverses its gradient in the dense cells. *J Physiol*. 1990;427:211-226.
139. Decherf G, Bouyer G, Egée S, Thomas SL. Chloride channels in normal and cystic fibrosis human erythrocyte membrane. *Blood Cells Mol Dis*. 2007;39(1):24-34.
140. Chu X, Tong Q, Cheung JY, et al. Interaction of TRPC2 and TRPC6 in erythropoietin modulation of calcium influx. *J Biol Chem*. 2004;279(11):10514-10522.
141. Bouyer G, Egée S, Thomas SL. Three types of spontaneously active anionic channels in malaria-infected human red blood cells. *Blood Cells Mol Dis*. 2006;36(2):248-254.
142. Dyrda A, Cytlak U, Ciuraszkiewicz A, et al. Local membrane deformations activate Ca2+-dependent K+ and anionic currents in intact human red blood cells. *PLoS One*. 2010;5(2):e9447.
143. Glogowska E, Dyrda A, Cueff A, et al. Anion conductance of the human red cell is carried by a maxi-anion channel. *Blood Cells Mol Dis*. 2010;44(4):243-251.
144. GARDOS G. The permeability of human erythrocytes to potassium. *Acta Physiol Hung*. 1956;10(2-4):185-189.
145. Schwarz W, Grygorczyk R, Hof D. Recording single-channel currents from human red cells. *Methods Enzymol*. 1989;173:112-121.
146. Staines HM, Powell T, Ellory JC, et al. Modulation of whole-cell currents in Plasmodium falciparum-infected human red blood cells by holding potential and serum. *J Physiol*. 2003;552(Pt 1):177-183.
147. Egée S, Lapaix F, Decherf G, et al. A stretch-activated anion channel is up-regulated by the malaria parasite Plasmodium falciparum. *J Physiol*. 2002;542(Pt 3):795-801.
148. Thomas SL, Bouyer G, Cueff A, Egée S, Glogowska E, Ollivaux C. Ion channels in human red blood cell membrane: actors or relics? *Blood Cells Mol Dis*. 2011;46(4):261-265.
149. Ataga KI, Stocker J. Senicapoc (ICA-17043): a potential therapy for the prevention and treatment of hemolysis-associated complications in sickle cell anemia. *Expert Opin Investig Drugs*. 2009;18(2):231-239.
150. De Franceschi L, Franco RS, Bertoldi M, et al. Pharmacological inhibition of calpain-1 prevents red cell dehydration and reduces Gardos channel activity in a mouse model of sickle cell disease. *FASEB J*. 2013;27(2):750-759.
151. Ataga KI. Novel therapies in sickle cell disease. *Hematology Am Soc Hematol Educ Program*. 2009:54-61.
152. Lew VL, Tiffert T, Etzion Z, et al. Distribution of dehydration rates generated by maximal Gardos-channel activation in normal and sickle red blood cells. *Blood*. 2005;105(1):361-367.
153. Tiffert T, Spivak JL, Lew VL. Magnitude of calcium influx required to induce dehydration of normal human red cells. *Biochim Biophys Acta*. 1988;943(2):157-165.
154. Shoshan-Barmatz V, De Pinto V, Zweckstetter M, Raviv Z, Keinan N, Arbel N. VDAC, a multi-functional mitochondrial protein regulating cell life and death. *Mol Aspects Med*. 2010;31(3):227-285.
155. Moran O, Sorgato MC. High-conductance pathways in mitochondrial membranes. *J Bioenerg Biomembr*. 1992;24(1):91-98.
156. Kayser H, Kratzin HD, Thinnes FP, et al. [Identification of human porins. II. Characterization and primary structure of a 31-lDa porin from human B lymphocytes (Porin 31HL)]. *Biol Chem Hoppe Seyler*. 1989;370(12):1265-1278.
157. Thinnes FP, Götz H, Kayser H, et al. [Identification of human porins. I. Purification of a porin from human B-lymphocytes (Porin 31HL) and the topochemical proof of its expression on the plasmalemma of the progenitor cell]. *Biol Chem Hoppe Seyler*. 1989;370(12):1253-1264.
158. Thinnes FP, Schmid A, Benz R, Hilschmann N. Studies on human porin. III. Does the voltage-dependent anion channel "Porin 31HL" form part of the chloride channel complex, which is observed in different cells and thought to be affected in cystic fibrosis? *Biol Chem Hoppe Seyler*. 1990;371(11):1047-1050.

159. Bouyer G, Cueff A, Egée S, et al. Erythrocyte peripheral type benzodiazepine receptor/voltage-dependent anion channels are upregulated by Plasmodium falciparum. *Blood*. 2011;118(8):2305-2312.
160. Veenman L, Shandalov Y, Gavish M. VDAC activation by the 18 kDa translocator protein (TSPO), implications for apoptosis. *J Bioenerg Biomembr*. 2008;40(3):199-205.
161. Cheung JY, Zhang XQ, Bokvist K, Tillotson DL, Miller BA. Modulation of calcium channels in human erythroblasts by erythropoietin. *Blood*. 1997;89(1):92-100.
162. Chu X, Cheung JY, Barber DL, et al. Erythropoietin modulates calcium influx through TRPC2. *J Biol Chem*. 2002;277(37):34375-34382.
163. Hirschler-Laszkiewicz I, Tong Q, Conrad K, et al. TRPC3 activation by erythropoietin is modulated by TRPC6. *J Biol Chem*. 2009;284(7):4567-4581.
164. Hirschler-Laszkiewicz I, Tong Q, Waybill K, et al. The transient receptor potential (TRP) channel TRPC3 TRP domain and AMP-activated protein kinase binding site are required for TRPC3 activation by erythropoietin. *J Biol Chem*. 2011;286(35):30636-30646.
165. Gillo B, Ma YS, Marks AR. Calcium influx in induced differentiation of murine erythroleukemia cells. *Blood*. 1993;81(3):783-792.
166. Huber SM, Duranton C, Henke G, et al. Plasmodium induces swelling-activated ClC-2 anion channels in the host erythrocyte. *J Biol Chem*. 2004;279(40):41444-41452.
167. Watkins JC, Davies J, Evans RH, Francis AA, Jones AW. Pharmacology of receptors for excitatory amino acids. *Adv Biochem Psychopharmacol*. 1981;27:263-273.
168. Evans RH, Francis AA, Watkins JC. Mg2+-like selective antagonism of excitatory amino acid-induced responses by alpha, epsilon-diaminopimelic acid, D-alpha-aminoadipate and HA-966 in isolated spinal cord of frog and immature rat. *Brain Res*. 1978;148(2):536-542.
169. Bozic M, Valdivielso JM. The potential of targeting NMDA receptors outside the CNS. *Expert Opin Ther Targets*. 2015;19(3):399-413.
170. Mashkina AP, Cizkova D, Vanicky I, Boldyrev AA. NMDA receptors are expressed in lymphocytes activated both in vitro and in vivo. *Cell Mol Neurobiol*. 2010;30(6):901-907.
171. Boldyrev AA, Kazey VI, Leinsoo TA, et al. Rodent lymphocytes express functionally active glutamate receptors. *Biochem Biophys Res Commun*. 2004;324(1):133-139.
172. Kalev-Zylinska ML, Green TN, Morel-Kopp MC, et al. N-methyl-D-aspartate receptors amplify activation and aggregation of human platelets. *Thromb Res*. 2014;133(5):837-847.
173. Lee YS, Lee SJ, Seo KW, Bae JU, Park SY, Kim CD. Homocysteine induces COX-2 expression in macrophages through ROS generated by NMDA receptor-calcium signaling pathways. *Free Radic Res*. 2013;47(5):422-431.
174. Hitchcock IS, Skerry TM, Howard MR, Genever PG. NMDA receptor-mediated regulation of human megakaryocytopoiesis. *Blood*. 2003;102(4):1254-1259.
175. .
176. Jahr CE, Stevens CF. Glutamate activates multiple single channel conductances in hippocampal neurons. *Nature*. 1987;325(6104):522-525.
177. Nowak L, Bregestovski P, Ascher P, Herbet A, Prochiantz A. Magnesium gates glutamate-activated channels in mouse central neurones. *Nature*. 1984;307(5950):462-465.
178. Ascher P, Nowak L. The role of divalent cations in the N-methyl-D-aspartate responses of mouse central neurones in culture. *J Physiol*. 1988;399:247-266.
179. Ascher P, Bregestovski P, Nowak L. N-methyl-D-aspartate-activated channels of mouse central neurones in magnesium-free solutions. *J Physiol*. 1988;399:207-226.
180. Jespersen A, Tajima N, Fernandez-Cuervo G, Garnier-Amblard EC, Furukawa H. Structural insights into competitive antagonism in NMDA receptors. *Neuron*. 2014;81(2):366-378.
181. Sommer B, Monyer H, Wisden W, et al. Glutamate-gated ion channels in the brain. Genetic mechanism for generating molecular and functional diversity. *Arzneimittelforschung*. 1992;42(2A):209-210.
182. Schoepfer R, Monyer H, Sommer B, et al. Molecular biology of glutamate receptors. *Prog Neurobiol*. 1994;42(2):353-357.

183. Witt A, Macdonald N, Kirkpatrick P. Memantine hydrochloride. *Nat Rev Drug Discov*. 2004;3(2):109-110.
184. Evans RH, Francis AA, Jones AW, Smith DA, Watkins JC. The effects of a series of omega-phosphonic alpha-carboxylic amino acids on electrically evoked and excitant amino acid-induced responses in isolated spinal cord preparations. *Br J Pharmacol*. 1982;75(1):65-75.
185. Johnson JW, Ascher P. Glycine potentiates the NMDA response in cultured mouse brain neurons. *Nature*. 1987;325(6104):529-531.
186. Benveniste M, Mayer ML. Kinetic analysis of antagonist action at N-methyl-D-aspartic acid receptors. Two binding sites each for glutamate and glycine. *Biophys J*. 1991;59(3):560-573.
187. Clements JD, Westbrook GL. Activation kinetics reveal the number of glutamate and glycine binding sites on the N-methyl-D-aspartate receptor. *Neuron*. 1991;7(4):605-613.
188. Cull-Candy S, Brickley S, Farrant M. NMDA receptor subunits: diversity, development and disease. *Curr Opin Neurobiol*. 2001;11(3):327-335.
189. Furukawa H, Singh SK, Mancusso R, Gouaux E. Subunit arrangement and function in NMDA receptors. *Nature*. 2005;438(7065):185-192.
190. Laube B, Kuhse J, Betz H. Evidence for a tetrameric structure of recombinant NMDA receptors. *J Neurosci*. 1998;18(8):2954-2961.
191. Monyer H, Sprengel R, Schoepfer R, et al. Heteromeric NMDA receptors: molecular and functional distinction of subtypes. *Science*. 1992;256(5060):1217-1221.
192. Cavara NA, Orth A, Hollmann M. Effects of NR1 splicing on NR1/NR3B-type excitatory glycine receptors. *BMC Neurosci*. 2009;10:32.
193. Holmes KD, Mattar PA, Marsh DR, Weaver LC, Dekaban GA. The N-methyl-D-aspartate receptor splice variant NR1-4 C-terminal domain. Deletion analysis and role in subcellular distribution. *J Biol Chem*. 2002;277(2):1457-1468.
194. Winkler A, Mahal B, Zieglgänsberger W, Spanagel R. Accurate quantification of the mRNA of NMDAR1 splice variants measured by competitive RT-PCR. *Brain Res Brain Res Protoc*. 1999;4(1):69-81.
195. Chatterton JE, Awobuluyi M, Premkumar LS, et al. Excitatory glycine receptors containing the NR3 family of NMDA receptor subunits. *Nature*. 2002;415(6873):793-798.
196. Ulbrich MH, Isacoff EY. Rules of engagement for NMDA receptor subunits. *Proc Natl Acad Sci U S A*. 2008;105(37):14163-14168.
197. Kemp JA, McKernan RM. NMDA receptor pathways as drug targets. *Nat Neurosci*. 2002;5 Suppl:1039-1042.
198. Vicini S, Wang JF, Li JH, et al. Functional and pharmacological differences between recombinant N-methyl-D-aspartate receptors. *J Neurophysiol*. 1998;79(2):555-566.
199. Traynelis SF, Wollmuth LP, McBain CJ, et al. Glutamate receptor ion channels: structure, regulation, and function. *Pharmacol Rev*. 2010;62(3):405-496.
200. Tong CK, Kaftan EJ, Macdermott AB. Functional identification of NR2 subunits contributing to NMDA receptors on substance P receptor-expressing dorsal horn neurons. *Mol Pain*. 2008;4:44.
201. Vicini S, Rumbaugh G. A slow NMDA channel: in search of a role. *J Physiol*. 2000;525 Pt 2:283.
202. Misra C, Brickley SG, Wyllie DJ, Cull-Candy SG. Slow deactivation kinetics of NMDA receptors containing NR1 and NR2D subunits in rat cerebellar Purkinje cells. *J Physiol*. 2000;525 Pt 2:299-305.
203. Mosley CA, Acker TM, Hansen KB, et al. Quinazolin-4-one derivatives: A novel class of noncompetitive NR2C/D subunit-selective N-methyl-D-aspartate receptor antagonists. *J Med Chem*. 2010;53(15):5476-5490.
204. Mullasseril P, Hansen KB, Vance KM, et al. A subunit-selective potentiator of NR2C- and NR2D-containing NMDA receptors. *Nat Commun*. 2010;1:90.
205. Auberson YP, Allgeier H, Bischoff S, Lingenhoehl K, Moretti R, Schmutz M. 5-Phosphonomethylquinoxalinediones as competitive NMDA receptor antagonists with a preference for the human 1A/2A, rather than 1A/2B receptor composition. *Bioorg Med Chem Lett*. 2002;12(7):1099-1102.

206. Gielen M, Siegler Retchless B, Mony L, Johnson JW, Paoletti P. Mechanism of differential control of NMDA receptor activity by NR2 subunits. *Nature*. 2009;459(7247):703-707.
207. Erreger K, Dravid SM, Banke TG, Wyllie DJ, Traynelis SF. Subunit-specific gating controls rat NR1/NR2A and NR1/NR2B NMDA channel kinetics and synaptic signalling profiles. *J Physiol*. 2005;563(Pt 2):345-358.
208. Erreger K, Traynelis SF. Allosteric interaction between zinc and glutamate binding domains on NR2A causes desensitization of NMDA receptors. *J Physiol*. 2005;569(Pt 2):381-393.
209. Wollmuth LP, Kuner T, Seeburg PH, Sakmann B. Differential contribution of the NR1- and NR2A-subunits to the selectivity filter of recombinant NMDA receptor channels. *J Physiol*. 1996;491 (Pt 3):779-797.
210. Dravid SM, Burger PB, Prakash A, et al. Structural determinants of D-cycloserine efficacy at the NR1/NR2C NMDA receptors. *J Neurosci*. 2010;30(7):2741-2754.
211. Qu XX, Cai J, Li MJ, et al. Role of the spinal cord NR2B-containing NMDA receptors in the development of neuropathic pain. *Exp Neurol*. 2009;215(2):298-307.
212. Cavara NA, Hollmann M. Shuffling the deck anew: how NR3 tweaks NMDA receptor function. *Mol Neurobiol*. 2008;38(1):16-26.
213. Low CM, Wee KS. New insights into the not-so-new NR3 subunits of N-methyl-D-aspartate receptor: localization, structure, and function. *Mol Pharmacol*. 2010;78(1):1-11.
214. Smothers CT, Woodward JJ. Pharmacological characterization of glycine-activated currents in HEK 293 cells expressing N-methyl-D-aspartate NR1 and NR3 subunits. *J Pharmacol Exp Ther*. 2007;322(2):739-748.
215. Nishi M, Hinds H, Lu HP, Kawata M, Hayashi Y. Motoneuron-specific expression of NR3B, a novel NMDA-type glutamate receptor subunit that works in a dominant-negative manner. *J Neurosci*. 2001;21(23):RC185.
216. Piña-Crespo JC, Talantova M, Micu I, et al. Excitatory glycine responses of CNS myelin mediated by NR1/NR3 "NMDA" receptor subunits. *J Neurosci*. 2010;30(34):11501-11505.
217. Andersson O, Stenqvist A, Attersand A, von Euler G. Nucleotide sequence, genomic organization, and chromosomal localization of genes encoding the human NMDA receptor subunits NR3A and NR3B. *Genomics*. 2001;78(3):178-184.
218. Fukumori R, Takarada T, Nakamichi N, et al. Requirement of both NR3A and NR3B subunits for dominant negative properties on Ca2+ mobilization mediated by acquired N-methyl-D-aspartate receptor channels into mitochondria. *Neurochem Int*. 2010;57(7):730-737.
219. Henson MA, Roberts AC, Perez-Otano I, Philpot BD. Influence of the NR3A subunit on NMDA receptor functions. *Prog Neurobiol*. 2010;91(1):23-37.
220. Wang H, Yan H, Zhang S, Wei X, Zheng J, Lee J. GluN3A subunit exerts a neuroprotective effect in brain ischemia and hypoxia process. *ASN Neuro*. 2013.
221. Paoletti P, Bellone C, Zhou Q. NMDA receptor subunit diversity: impact on receptor properties, synaptic plasticity and disease. *Nat Rev Neurosci*. 2013;14(6):383-400.
222. Wollmuth LP, Sakmann B. Different mechanisms of Ca2+ transport in NMDA and Ca2+-permeable AMPA glutamate receptor channels. *J Gen Physiol*. 1998;112(5):623-636.
223. Cull-Candy SG, Brickley SG, Misra C, Feldmeyer D, Momiyama A, Farrant M. NMDA receptor diversity in the cerebellum: identification of subunits contributing to functional receptors. *Neuropharmacology*. 1998;37(10-11):1369-1380.
224. Mayer ML. Emerging models of glutamate receptor ion channel structure and function. *Structure*. 2011;19(10):1370-1380.
225. Cao JY, Qiu S, Zhang J, Wang JJ, Zhang XM, Luo JH. Transmembrane region of N-methyl-D-aspartate receptor (NMDAR) subunit is required for receptor subunit assembly. *J Biol Chem*. 2011;286(31):27698-27705.
226. Ault B, Evans RH, Francis AA, Oakes DJ, Watkins JC. Selective depression of excitatory amino acid induced depolarizations by magnesium ions in isolated spinal cord preparations. *J Physiol*. 1980;307:413-428.

227. Honoré T, Drejer J, Nielsen M, Watkins JC, Olverman HJ. Molecular target size of NMDA antagonist binding sites. *Eur J Pharmacol*. 1987;136(1):137-138.
228. Kemp JA, Foster AC, Wong EHF. Non-competitive antagonists of excitatory amino acid receptors. Vol. 10: Trends in Neurosciences; 1987:294-298.
229. Siegler Retchless B, Gao W, Johnson JW. A single GluN2 subunit residue controls NMDA receptor channel properties via intersubunit interaction. *Nat Neurosci*. 2012;15(3):406-413, S401-402.
230. Banke TG, Dravid SM, Traynelis SF. Protons trap NR1/NR2B NMDA receptors in a nonconducting state. *J Neurosci*. 2005;25(1):42-51.
231. Cavara NA, Orth A, Hicking G, Seebohm G, Hollmann M. Residues at the tip of the pore loop of NR3B-containing NMDA receptors determine Ca2+ permeability and Mg2+ block. *BMC Neurosci*. 2010;11:133.
232. Chen L, Huang LY. Sustained potentiation of NMDA receptor-mediated glutamate responses through activation of protein kinase C by a mu opioid. *Neuron*. 1991;7(2):319-326.
233. Tingley WG, Roche KW, Thompson AK, Huganir RL. Regulation of NMDA receptor phosphorylation by alternative splicing of the C-terminal domain. *Nature*. 1993;364(6432):70-73.
234. Kelso SR, Nelson TE, Leonard JP. Protein kinase C-mediated enhancement of NMDA currents by metabotropic glutamate receptors in Xenopus oocytes. *J Physiol*. 1992;449:705-718.
235. Bayer KU, Schulman H. Regulation of signal transduction by protein targeting: the case for CaMKII. *Biochem Biophys Res Commun*. 2001;289(5):917-923.
236. Bayer KU, LeBel E, McDonald GL, O'Leary H, Schulman H, De Koninck P. Transition from reversible to persistent binding of CaMKII to postsynaptic sites and NR2B. *J Neurosci*. 2006;26(4):1164-1174.
237. Merrill MA, Chen Y, Strack S, Hell JW. Activity-driven postsynaptic translocation of CaMKII. *Trends Pharmacol Sci*. 2005;26(12):645-653.
238. Hardingham GE, Bading H. Synaptic versus extrasynaptic NMDA receptor signalling: implications for neurodegenerative disorders. *Nat Rev Neurosci*. 2010;11(10):682-696.
239. Monyer H, Burnashev N, Laurie DJ, Sakmann B, Seeburg PH. Developmental and regional expression in the rat brain and functional properties of four NMDA receptors. *Neuron*. 1994;12(3):529-540.
240. Watanabe M, Inoue Y, Sakimura K, Mishina M. Developmental changes in distribution of NMDA receptor channel subunit mRNAs. *Neuroreport*. 1992;3(12):1138-1140.
241. Sheng M, Cummings J, Roldan LA, Jan YN, Jan LY. Changing subunit composition of heteromeric NMDA receptors during development of rat cortex. *Nature*. 1994;368(6467):144-147.
242. Sanz-Clemente A, Nicoll RA, Roche KW. Diversity in NMDA receptor composition: many regulators, many consequences. *Neuroscientist*. 2013;19(1):62-75.
243. Snyder EM, Nong Y, Almeida CG, et al. Regulation of NMDA receptor trafficking by amyloid-beta. *Nat Neurosci*. 2005;8(8):1051-1058.
244. Rönicke R, Mikhaylova M, Rönicke S, et al. Early neuronal dysfunction by amyloid β oligomers depends on activation of NR2B-containing NMDA receptors. *Neurobiol Aging*. 2011;32(12):2219-2228.
245. Dunah AW, Wang Y, Yasuda RP, et al. Alterations in subunit expression, composition, and phosphorylation of striatal N-methyl-D-aspartate glutamate receptors in a rat 6-hydroxydopamine model of Parkinson's disease. *Mol Pharmacol*. 2000;57(2):342-352.
246. Gladding CM, Raymond LA. Mechanisms underlying NMDA receptor synaptic/extrasynaptic distribution and function. *Mol Cell Neurosci*. 2011;48(4):308-320.
247. Gaspar PA, Bustamante ML, Silva H, Aboitiz F. Molecular mechanisms underlying glutamatergic dysfunction in schizophrenia: therapeutic implications. *J Neurochem*. 2009;111(4):891-900.
248. Suvarna N, Borgland SL, Wang J, et al. Ethanol alters trafficking and functional N-methyl-D-aspartate receptor NR2 subunit ratio via H-Ras. *J Biol Chem*. 2005;280(36):31450-31459.

249. Borgland SL, Taha SA, Sarti F, Fields HL, Bonci A. Orexin A in the VTA is critical for the induction of synaptic plasticity and behavioral sensitization to cocaine. *Neuron*. 2006;49(4):589-601.
250. Carpenter-Hyland EP, Woodward JJ, Chandler LJ. Chronic ethanol induces synaptic but not extrasynaptic targeting of NMDA receptors. *J Neurosci*. 2004;24(36):7859-7868.
251. Gibert-Rahola J, Villena-Rodriguez A. Glutamatergic drugs for schizophrenia treatment. *Actas Esp Psiquiatr*. 2014;42(5):234-241.
252. Planells-Cases R, Lerma J, Ferrer-Montiel A. Pharmacological intervention at ionotropic glutamate receptor complexes. *Curr Pharm Des*. 2006;12(28):3583-3596.
253. Palmer GC. Neuroprotection by NMDA receptor antagonists in a variety of neuropathologies. *Curr Drug Targets*. 2001;2(3):241-271.
254. Johnson JW, Kotermanski SE. Mechanism of action of memantine. *Curr Opin Pharmacol*. 2006;6(1):61-67.
255. Parsons CG, Stoffler A, Danysz W. Memantine: a NMDA receptor antagonist that improves memory by restoration of homeostasis in the glutamatergic system--too little activation is bad, too much is even worse. *Neuropharmacology*. 2007;53(6):699-723.
256. Lipton SA. Paradigm shift in NMDA receptor antagonist drug development: molecular mechanism of uncompetitive inhibition by memantine in the treatment of Alzheimer's disease and other neurologic disorders. *J Alzheimers Dis*. 2004;6(6 Suppl):S61-74.
257. Lipton SA. Failures and successes of NMDA receptor antagonists: molecular basis for the use of open-channel blockers like memantine in the treatment of acute and chronic neurologic insults. *NeuroRx*. 2004;1(1):101-110.
258. Reisberg B, Doody R, Stöffler A, et al. Memantine in moderate-to-severe Alzheimer's disease. *N Engl J Med*. 2003;348(14):1333-1341.
259. Gerzon K, Krumkalns EV, Brindle RL, Marshall FJ, Root MA. The adamantyl group in medical agents. I. Hypoglycemic N-Arylsulfonyl-N'-Adamantylureas. *J Med Chem*. 1963;6:760-763.
260. Schneider E, Fischer PA, Clemens R, Balzereit F, Fünfgeld EW, Haase HJ. [Effects of oral memantine administration on Parkinson symptoms. Results of a placebo-controlled multicenter study]. *Dtsch Med Wochenschr*. 1984;109(25):987-990.
261. Grossmann W, Schütz W. [Memantine and neurogenic bladder disorders within the bounds of spastic conditions]. *Arzneimittelforschung*. 1982;32(10):1273-1276.
262. Parsons CG, Gruner R, Rozental J, Millar J, Lodge D. Patch clamp studies on the kinetics and selectivity of N-methyl-D-aspartate receptor antagonism by memantine (1-amino-3,5-dimethyladamantan). *Neuropharmacology*. 1993;32(12):1337-1350.
263. Kornhuber J, Bormann J, Retz W, Hübers M, Riederer P. Memantine displaces [3H]MK-801 at therapeutic concentrations in postmortem human frontal cortex. *Eur J Pharmacol*. 1989;166(3):589-590.
264. . Kornhuber J, Bormann J. Neuroprotective effects of memantine. *Neurology*. 1993; 43(5): 1054-5
265. Chen HS, Pellegrini JW, Aggarwal SK, et al. Open-channel block of N-methyl-D-aspartate (NMDA) responses by memantine: therapeutic advantage against NMDA receptor-mediated neurotoxicity. *J Neurosci*. 1992;12(11):4427-4436.
266. Bormann J. Memantine is a potent blocker of N-methyl-D-aspartate (NMDA) receptor channels. *Eur J Pharmacol*. 1989;166(3):591-592.
267. Wesemann W, Sontag KH, Maj J. [Pharmacodynamics and pharmacokinetics of memantine]. *Arzneimittelforschung*. 1983;33(8):1122-1134.
268. Lipton SA, Chen HS. Paradigm shift in neuroprotective drug development: clinically tolerated NMDA receptor inhibition by memantine. *Cell Death Differ*. 2004;11(1):18-20.
269. Kornhuber J, Quack G. Cerebrospinal fluid and serum concentrations of the N-methyl-D-aspartate (NMDA) receptor antagonist memantine in man. *Neurosci Lett*. 1995;195(2):137-139.
270. Schmitt HP. On the paradox of ion channel blockade and its benefits in the treatment of Alzheimer disease. *Med Hypotheses*. 2005;65(2):259-265.

271. Hosenbocus S, Chahal R. Memantine: a review of possible uses in child and adolescent psychiatry. *J Can Acad Child Adolesc Psychiatry*. 2013;22(2):166-171.
272. Ghaleiha A, Asadabadi M, Mohammadi MR, et al. Memantine as adjunctive treatment to risperidone in children with autistic disorder: a randomized, double-blind, placebo-controlled trial. *Int J Neuropsychopharmacol*. 2013;16(4):783-789.
273. Sproul A, Steele SL, Thai TL, et al. N-methyl-D-aspartate receptor subunit NR3a expression and function in principal cells of the collecting duct. *Am J Physiol Renal Physiol*. 2011;301(1):F44-54.
274. Merle B, Itzstein C, Delmas PD, Chenu C. NMDA glutamate receptors are expressed by osteoclast precursors and involved in the regulation of osteoclastogenesis. *J Cell Biochem*. 2003;90(2):424-436.
275. Miglio G, Varsaldi F, Lombardi G. Human T lymphocytes express N-methyl-D-aspartate receptors functionally active in controlling T cell activation. *Biochem Biophys Res Commun*. 2005;338(4):1875-1883.
276. Eaton JW, Skelton TD, Swofford HS, Kolpin CE, Jacob HS. Elevated erythrocyte calcium in sickle cell disease. *Nature*. 1973;246(5428):105-106.
277. Rees DC, Williams TN, Gladwin MT. Sickle-cell disease. *Lancet*. 2010;376(9757):2018-2031.
278. Herrick JB. Peculiar elongated and sickle-shaped red blood corpuscles in a case of severe anemia. 1910. *Yale J Biol Med*. 2001;74(3):179-184.
279. Pauling L, Itano HA, et al. Sickle cell anemia a molecular disease. *Science*. 1949;110(2865):543-548.
280. INGRAM VM. Gene mutations in human haemoglobin: the chemical difference between normal and sickle cell haemoglobin. *Nature*. 1957;180(4581):326-328.
281. Serjeant GR, Serjeant BE. Sickle Cell Disease. Vol. Third Edition. Oxford, UK: Oxford University Press; 2001.
282. Platt OS, Brambilla DJ, Rosse WF, et al. Mortality in sickle cell disease. Life expectancy and risk factors for early death. *N Engl J Med*. 1994;330(23):1639-1644.
283. Gilman JG, Huisman TH. A mutation associated with elevated G gamma chain in sickle cell anemia and hereditary persistence of fetal hemoglobin. *Prog Clin Biol Res*. 1985;191:141-149.
284. Lettre G, Sankaran VG, Bezerra MA, et al. DNA polymorphisms at the BCL11A, HBS1L-MYB, and beta-globin loci associate with fetal hemoglobin levels and pain crises in sickle cell disease. *Proc Natl Acad Sci U S A*. 2008;105(33):11869-11874.
285. Bunn HF. Pathogenesis and treatment of sickle cell disease. *N Engl J Med*. 1997;337(11):762-769.
286. Osarogiagbon UR, Choong S, Belcher JD, Vercellotti GM, Paller MS, Hebbel RP. Reperfusion injury pathophysiology in sickle transgenic mice. *Blood*. 2000;96(1):314-320.
287. Stuart MJ, Nagel RL. Sickle-cell disease. *Lancet*. 2004;364(9442):1343-1360.
288. Turhan A, Weiss LA, Mohandas N, Coller BS, Frenette PS. Primary role for adherent leukocytes in sickle cell vascular occlusion: a new paradigm. *Proc Natl Acad Sci U S A*. 2002;99(5):3047-3051.
289. Manwani D, Frenette PS. Vaso-occlusion in sickle cell disease: pathophysiology and novel targeted therapies. *Blood*. 2013;122(24):3892-3898.
290. Frenette PS. Sickle cell vaso-occlusion: multistep and multicellular paradigm. *Curr Opin Hematol*. 2002;9(2):101-106.
291. Nouraie M, Lee JS, Zhang Y, et al. The relationship between the severity of hemolysis, clinical manifestations and risk of death in 415 patients with sickle cell anemia in the US and Europe. *Haematologica*. 2013;98(3):464-472.
292. Gladwin MT, Barst RJ, Gibbs JS, et al. Risk factors for death in 632 patients with sickle cell disease in the United States and United kingdom. *PLoS One*. 2014;9(7):e99489.
293. Gladwin MT, Sachdev V. Cardiovascular abnormalities in sickle cell disease. *J Am Coll Cardiol*. 2012;59(13):1123-1133.
294. Repka T, Hebbel RP. Hydroxyl radical formation by sickle erythrocyte membranes: role of pathologic iron deposits and cytoplasmic reducing agents. *Blood*. 1991;78(10):2753-2758.

295. Reiter CD, Wang X, Tanus-Santos JE, et al. Cell-free hemoglobin limits nitric oxide bioavailability in sickle-cell disease. *Nat Med*. 2002;8(12):1383-1389.
296. Gladwin MT, Schechter AN, Ognibene FP, et al. Divergent nitric oxide bioavailability in men and women with sickle cell disease. *Circulation*. 2003;107(2):271-278.
297. Morris CR, Gladwin MT, Kato GJ. Nitric oxide and arginine dysregulation: a novel pathway to pulmonary hypertension in hemolytic disorders. *Curr Mol Med*. 2008;8(7):620-632.
298. De Caterina R, Libby P, Peng HB, et al. Nitric oxide decreases cytokine-induced endothelial activation. Nitric oxide selectively reduces endothelial expression of adhesion molecules and proinflammatory cytokines. *J Clin Invest*. 1995;96(1):60-68.
299. Shin WS, Hong YH, Peng HB, De Caterina R, Libby P, Liao JK. Nitric oxide attenuates vascular smooth muscle cell activation by interferon-gamma. The role of constitutive NF-kappa B activity. *J Biol Chem*. 1996;271(19):11317-11324.
300. Ataga KI, Moore CG, Hillery CA, et al. Coagulation activation and inflammation in sickle cell disease-associated pulmonary hypertension. *Haematologica*. 2008;93(1):20-26.
301. Fabry ME, Nagel RL. Heterogeneity of red cells in the sickler: a characteristic with practical clinical and pathophysiological implications. *Blood Cells*. 1982;8(1):9-15.
302. Canessa M, Fabry ME, Blumenfeld N, Nagel RL. Volume-stimulated, Cl(-)-dependent K+ efflux is highly expressed in young human red cells containing normal hemoglobin or HbS. *J Membr Biol*. 1987;97(2):97-105.
303. Franco RS, Puchulu-Campanella ME, Barber LA, et al. Changes in the properties of normal human red blood cells during in vivo aging. *Am J Hematol*. 2013;88(1):44-51.
304. Weatherall DJ, Clegg JB. Inherited haemoglobin disorders: an increasing global health problem. *Bull World Health Organ*. 2001;79(8):704-712.
305. Yusuf HR, Lloyd-Puryear MA, Grant AM, Parker CS, Creary MS, Atrash HK. Sickle cell disease: the need for a public health agenda. *Am J Prev Med*. 2011;41(6 Suppl 4):S376-383.
306. Modell B, Darlison M. Global epidemiology of haemoglobin disorders and derived service indicators. *Bull World Health Organ*. 2008;86(6):480-487.
307. Allison AC. Protection afforded by sickle-cell trait against subtertian malareal infection. *Br Med J*. 1954;1(4857):290-294.
308. Williams TN, Mwangi TW, Wambua S, et al. Sickle cell trait and the risk of Plasmodium falciparum malaria and other childhood diseases. *J Infect Dis*. 2005;192(1):178-186.
309. Williams TN, Mwangi TW, Roberts DJ, et al. An immune basis for malaria protection by the sickle cell trait. *PLoS Med*. 2005;2(5):e128.
310. Makani J, Komba AN, Cox SE, et al. Malaria in patients with sickle cell anemia: burden, risk factors, and outcome at the outpatient clinic and during hospitalization. *Blood*. 2010;115(2):215-220.
311. Serjeant GR. Mortality from sickle cell disease in Africa. *BMJ*. 2005;330(7489):432-433.
312. Darlison MW, Modell B. Sickle-cell disorders: limits of descriptive epidemiology. *Lancet*. 2013;381(9861):98-99.
313. Modell B, Darlison M, Birgens H, et al. Epidemiology of haemoglobin disorders in Europe: an overview. *Scand J Clin Lab Invest*. 2007;67(1):39-69.
314. Schmugge M, Speer O, Ozsahin AH, Martin G. Die Sichelzellerkrankung in der Schweiz. Teil 1: Pathophysiologie, Klinik. Vol. 8. Klinik. Schweiz Med Forum; 2008:582-586.
315. Piel FB, Patil AP, Howes RE, et al. Global epidemiology of sickle haemoglobin in neonates: a contemporary geostatistical model-based map and population estimates. *Lancet*. 2013;381(9861):142-151.
316. Chou ST. Transfusion therapy for sickle cell disease: a balancing act. *Hematology Am Soc Hematol Educ Program*. 2013;2013:439-446.
317. Koduri PR. Iron in sickle cell disease: a review why less is better. *Am J Hematol*. 2003;73(1):59-63.
318. Porter JB, Garbowski M. The Pathophysiology of Transfusional Iron Overload. *Hematol Oncol Clin North Am*. 2014;28(4):683-701.

319. Sears DA, Anderson PR, Foy AL, Williams HL, Crosby WH. Urinary iron excretion and renal metabolism of hemoglobin in hemolytic diseases. *Blood*. 1966;28(5):708-725.
320. Washington R, Boggs DR. Urinary iron in patients with sickle cell anamia. *J Lab Clin Med*. 1975;86(1):17-23.
321. Comer GM, Ozick LA, Sachdev RK, et al. Transfusion-related chronic liver disease in sickle cell anemia. *Am J Gastroenterol*. 1991;86(9):1232-1234.
322. Harmatz P, Butensky E, Quirolo K, et al. Severity of iron overload in patients with sickle cell disease receiving chronic red blood cell transfusion therapy. *Blood*. 2000;96(1):76-79.
323. Calvaruso G, Vitrano A, Di Maggio R, et al. Deferiprone versus Deferoxamine in Sickle Cell Disease: Results from a 5-year long-term Italian multi-center randomized clinical trial. *Blood Cells Mol Dis*. 2014.
324. Vichinsky EP. Current issues with blood transfusions in sickle cell disease. *Semin Hematol*. 2001;38(1 Suppl 1):14-22.
325. Chou ST, Jackson T, Vege S, Smith-Whitley K, Friedman DF, Westhoff CM. High prevalence of red blood cell alloimmunization in sickle cell disease despite transfusion from Rh-matched minority donors. *Blood*. 2013;122(6):1062-1071.
326. Ribeiro KR, Guarnieri MH, da Costa DC, Costa FF, Pellegrino J, Castilho L. DNA array analysis for red blood cell antigens facilitates the transfusion support with antigen-matched blood in patients with sickle cell disease. *Vox Sang*. 2009;97(2):147-152.
327. Wilkinson K, Harris S, Gaur P, et al. Molecular blood typing augments serologic testing and allows for enhanced matching of red blood cells for transfusion in patients with sickle cell disease. *Transfusion*. 2012;52(2):381-388.
328. Yarbro JW. Mechanism of action of hydroxyurea. *Semin Oncol*. 1992;19(3 Suppl 9):1-10.
329. de Lima PD, Cardoso PC, Khayat AS, Bahia MeO, Burbano RR. Evaluation of the mutagenic activity of hydroxyurea on the G1-S-G2 phases of the cell cycle: an in vitro study. *Genet Mol Res*. 2003;2(3):328-333.
330. Platt OS, Orkin SH, Dover G, Beardsley GP, Miller B, Nathan DG. Hydroxyurea enhances fetal hemoglobin production in sickle cell anemia. *J Clin Invest*. 1984;74(2):652-656.
331. Miller BA, Platt O, Hope S, Dover G, Nathan DG. Influence of hydroxyurea on fetal hemoglobin production in vitro. *Blood*. 1987;70(6):1824-1829.
332. Weiner DL, Brugnara C. Hydroxyurea and sickle cell disease: a chance for every patient. *JAMA*. 2003;289(13):1692-1694.
333. Goldberg MA, Brugnara C, Dover GJ, Schapira L, Charache S, Bunn HF. Treatment of sickle cell anemia with hydroxyurea and erythropoietin. *N Engl J Med*. 1990;323(6):366-372.
334. Elmariah H, Garrett ME, De Castro LM, et al. Factors associated with survival in a contemporary adult sickle cell disease cohort. *Am J Hematol*. 2014;89(5):530-535.
335. Platt OS, Thorington BD, Brambilla DJ, et al. Pain in sickle cell disease. Rates and risk factors. *N Engl J Med*. 1991;325(1):11-16.
336. Okam MM, Shaykevich S, Ebert BL, Zaslavsky AM, Ayanian JZ. National trends in hospitalizations for sickle cell disease in the United States following the FDA approval of hydroxyurea, 1998-2008. *Med Care*. 2014;52(7):612-618.
337. Smith WR, Penberthy LT, Bovbjerg VE, et al. Daily assessment of pain in adults with sickle cell disease. *Ann Intern Med*. 2008;148(2):94-101.
338. Weiss E, Cytlak UM, Rees DC, Osei A, Gibson JS. Deoxygenation-induced and Ca(2+) dependent phosphatidylserine externalisation in red blood cells from normal individuals and sickle cell patients. *Cell Calcium*. 2012;51(1):51-56.
339. Vichinsky EP, Neumayr LD, Earles AN, et al. Causes and outcomes of the acute chest syndrome in sickle cell disease. National Acute Chest Syndrome Study Group. *N Engl J Med*. 2000;342(25):1855-1865.
340. Gladwin MT, Vichinsky E. Pulmonary complications of sickle cell disease. *N Engl J Med*. 2008;359(21):2254-2265.

341. Machado RF, Farber HW. Pulmonary hypertension associated with chronic hemolytic anemia and other blood disorders. *Clin Chest Med*. 2013;34(4):739-752.
342. Sachdev V, Machado RF, Shizukuda Y, et al. Diastolic dysfunction is an independent risk factor for death in patients with sickle cell disease. *J Am Coll Cardiol*. 2007;49(4):472-479.
343. Gaston MH, Verter JI, Woods G, et al. Prophylaxis with oral penicillin in children with sickle cell anemia. A randomized trial. *N Engl J Med*. 1986;314(25):1593-1599.
344. Adams RJ, McKie VC, Brambilla D, et al. Stroke prevention trial in sickle cell anemia. *Control Clin Trials*. 1998;19(1):110-129.
345. Adams R, McKie V, Nichols F, et al. The use of transcranial ultrasonography to predict stroke in sickle cell disease. *N Engl J Med*. 1992;326(9):605-610.
346. Sharpe CC, Thein SL. How I treat renal complications in sickle cell disease. *Blood*. 2014;123(24):3720-3726.
347. Hagar W, Vichinsky E. Advances in clinical research in sickle cell disease. *Br J Haematol*. 2008;141(3):346-356.
348. Spencer GJ, McGrath CJ, Genever PG. Current perspectives on NMDA-type glutamate signalling in bone. *Int J Biochem Cell Biol*. 2007;39(6):1089-1104.
349. Skerry TM, Genever PG. Glutamate signalling in non-neuronal tissues. *Trends Pharmacol Sci*. 2001;22(4):174-181.
350. Genever PG, Wilkinson DJ, Patton AJ, et al. Expression of a functional N-methyl-D-aspartate-type glutamate receptor by bone marrow megakaryocytes. *Blood*. 1999;93(9):2876-2883.
351. Hanggi P, Telezhkin V, Kemp PJ, et al. Functional plasticity of the N-methyl-D-aspartate receptor in differentiating human erythroid precursor cells. *Am J Physiol Cell Physiol*. 2015:ajpcell.00395.02014.
352. Misiti J, Spivak JL. Erythropoiesis in vitro. Role of calcium. *J Clin Invest*. 1979;64(6):1573-1579.
353. Liu J, Guo X, Mohandas N, Chasis JA, An X. Membrane remodeling during reticulocyte maturation. *Blood*. 2010;115(10):2021-2027.
354. Grasso JA, Bruno M, Yates AA, Wei LT, Epstein PM. Calmodulin dependence of transferrin receptor recycling in rat reticulocytes. *Biochem J*. 1990;266(1):261-272.
355. Bogdanova A, Makhro A, Wang J, Lipp P, Kaestner L. Calcium in red blood cells-a perilous balance. *Int J Mol Sci*. 2013;14(5):9848-9872.
356. Herberth B, Minkó K, Csillag A, Jaffredo T, Madarász E. SCL, GATA-2 and Lmo2 expression in neurogenesis. *Int J Dev Neurosci*. 2005;23(5):449-463.
357. Hinks GL, Shah B, French SJ, et al. Expression of LIM protein genes Lmo1, Lmo2, and Lmo3 in adult mouse hippocampus and other forebrain regions: differential regulation by seizure activity. *J Neurosci*. 1997;17(14):5549-5559.
358. Xiao Z, Jaiswal MK, Deng PY, et al. Requirement of phospholipase C and protein kinase C in cholecystokinin-mediated facilitation of NMDA channel function and anxiety-like behavior. *Hippocampus*. 2012;22(6):1438-1450.
359. Mandal M, Yan Z. Phosphatidylinositol (4,5)-bisphosphate regulation of N-methyl-D-aspartate receptor channels in cortical neurons. *Mol Pharmacol*. 2009;76(6):1349-1359.
360. Mori M, Uchida M, Watanabe T, et al. Activation of extracellular signal-regulated kinases ERK1 and ERK2 induces Bcl-xL up-regulation via inhibition of caspase activities in erythropoietin signaling. *J Cell Physiol*. 2003;195(2):290-297.
361. Krapivinsky G, Krapivinsky L, Manasian Y, et al. The NMDA receptor is coupled to the ERK pathway by a direct interaction between NR2B and RasGRF1. *Neuron*. 2003;40(4):775-784.
362. Mason DJ, Huggett JF. Glutamate transporters in bone. *J Musculoskelet Neuronal Interact*. 2002;2(5):406-414.
363. Bhangu PS. 'Pre-synaptic' vesicular glutamate release mechanisms in osteoblasts. *J Musculoskelet Neuronal Interact*. 2003;3(1):17-29.
364. Bookchin RM, Ortiz OE, Lew VL. Evidence for a direct reticulocyte origin of dense red cells in sickle cell anemia. *J Clin Invest*. 1991;87(1):113-124.

9. Curriculum Vitae

CURRICULUM VITAE

Pascal Hänggi
Badenerstrasse 797
8048 Zürich

Tel. +41 (0)79 256 15 87
Pascalrhaenggi@gmail.com

Date of Birth: 11.10.1983
Nationality: Swiss

EDUCATION

06/2015
01/2011

PhD Thesis

- Integrative Molecular Medicine, University of Zurich, Switzerland

01/2011
08/2009

Master of Sciences, Pharmaceutical Sciences

- Department of Pharmaceutical Sciences, University of Basel, Switzerland

12/2009
08/2006

Bachelor of Sciences, Pharmaceutical Sciences

- Department of Pharmaceutical Sciences, University of Basel, Switzerland

08/2006
09/2004

Academic studies, Biology

- Department of Biology, University of Basel, Switzerland

08/2004
04/2004

Language Course, English

- Language International Auckland, New Zealand

12/2003
08/2000

Matura, Economy and Law

- Gymnasium Laufental-Thierstein, Laufen, Switzerland

Awards

09/2013

- Young Researcher Award, Oetliker Prize, Annual meeting of Swiss Physiology Society, Bern, Switzerland

08/2012

- Award for best poster, 8th ZHIP Symposium, University of Zurich, Switzerland

Grants

04/2014

- Postdoc Fellowship (Co-Applicant), Vontobel Stiftung (100,000 CHF), Switzerland

List of Publications

03/2015
- Hänggi P, Telezhkin V, et al. Functional plasticity of the N-methyl-D-aspartate receptors during erythropoietic maturation. Am J Physiol Cell Physio. 2015

05/2014
- Hänggi P, Makhro A, et al. Red blood cells of sickle cell disease patients exhibit abnormally high abundance of N-methyl D-aspartate receptors mediating excessive calcium uptake. Br J Haematol. 2014

09/2013
- Makhro A, Hänggi P, et al. N-methyl D-aspartate (NMDA) receptors in human erythroid precursor cells and in circulating red blood cells contribute to the intracellular calcium regulation. Am J Physiol Cell Physio. 2013

Academic Work

06/2015
01/2011

PhD Thesis

- "Keep dementia in mind, but forget memory formation: Plasticity of the N-methyl-D-aspartate receptor in erythroid cells and its potential for the treatment of sickle cell anemia"

  The study investigates the role of the NMDA receptor during erythropoietic maturation and in red blood cells. Furthermore more it examines the potential of the ion channel as a new drug target for the treatment of sickle cell anemia.

  Cooperative project of Children's University Hospital, University Hospital, Veterinary Physiology and Center for Integrative Human Physiology, University of Zurich, Switzerland

01/2011
03/2010

Master's Thesis

- "Regulation of the human 17β-hydroxysteroid dehydrogenase type 3 gene: Cloning analysis of the promoter region"

  Study of 17βHSD type 3 gen regulation in human leydig cells and analysis of various endogenous and exogenous factors on expression and function of the enzyme.

  Molecular and Systems Toxicology, Department of Pharmaceutical Sciences, University of Basel, Switzerland

Meetings and Seminars, Selection

06/2014
- Talk: Integrative molecular medicine PhD Program retreat 2014, Magglingen, Switzerland

10/2013
- Talk: European Red Cell Society Meeting 2013, Forteiland, Netherlands

01/2013
- Talk: Rigi Workshop 2013 "Thinking Big in a Small World: Creativity in the Molecular Sciences", Swiss Academy of Science (SCNAT), Switzerland

10/2012
- Talk: Children's Research Centre retreat 2012, Halbinsel Au, Switzerland

11/2010
- Talk: Seminar on Molecular Toxicology 2010, University of Basel

10. Acknowledgments

First of all, sincere thanks are given to all of the healthy and sickle cell anemia patients who donate blood for the study. I would like to also thank as well to all of my supervisors Dr. Jeroen Goede, Dr. Oliver Speer, and Dr. Anna Bogdanova for their invaluable help und critical input during my four years of PhD. I am very grateful to Prof. Dr. Max Gassmann, Prof Dr. David Nadal and all members of my PhD thesis committee for their support and their invaluable inputs during the entire PhD project at the University of Zurich. I could greatly improve my technical, hard, and soft skills during my PhD and get an excellent preparation for future scientific research.

Special thanks goes to Prof. Dr. Paul J Kemp, Dr. Seva Telezhkin, and the entire research group at the Division of Pathophysiology and Repair, School of Biosciences, Cardiff University, UK, for assisting me in learning and preforming electrophysiological experiments. I am appreciative to Dr Dipak Ramji at the University of Cardiff, UK, for his valuable help by organizing blood samples for my study. Furthermore, I want to thank all the members and technical assistant in the group of Prof. Dr. Max Gassmann at the Institute of Veterinary Physiology, Vetsuisse Faculty and as well to the Dr. Markus Schmugge-Liner for his critical input and whole team of the Erythrozyten Labor, at Children's Hospital Zurich for their helpful support.

The study was funded a by cooperative grant from ZIHP, University of Zurich (J. Goede, O. Speer, and A. Bogdanova) supported by the Swiss National Science Foundation (No. 112 449 and 310030 124970/1 to A. Bogdanova), the Vontobel Foundation (A. Bogdanova), the Hartmann Müller Stiftung (J .Goede and O.Speer), and received funding from the European Community's Seventh Framework Programme (FP7/2007-2013) under grant agreement 602121 (CoMMiTMenT project) to A. Bogdanova.